

CHARLES UNIVERSITY in PRAGUE

Faculty of Science

Study programme:

Molecular and Cellular Biology, Genetics and Virology



Mgr. Jakub Masaryk

Trk1 potassium importers, key transport systems for yeast cell fitness and stress tolerance

Doctoral Thesis

Supervisor: RNDr. Hana Sychrová, DrSc.

Laboratory of Membrane Transport, Institute of Physiology, Czech Academy of Sciences

Prague, 2022

Declaration

I hereby declare that the doctoral thesis presented here is my own, conducted under the supervision of RNDr. Hana Sychrová, DrSc. and that I have properly listed all literary sources. This thesis has not been submitted, in whole or in part, to obtain any other academic degree.

Prague, November 2022

.....

Acknowledgements

I would like to express my gratitude to my supervisor RNDr, Hana Sychrová, DrSc. for advice, support and help throughout my PhD study. I would also like to acknowledge all the members of the Laboratory of Membrane Transport, Czech Academy of Sciences for their help, which contributed invaluable to this work. Additionally, I would like to acknowledge Dr. Francisco J. Ruiz-Castilla and Prof. José Ramos from the Department of Microbiology, University of Córdoba and also Joel Abidemi Akinola and Prof. John Morrissey from the School of Microbiology, University College Cork for their help during internships in their respective departments.

This work was supported by the following research projects:

Czech Science Foundation

20-04420S (2020-2022) Trk1 potassium importers - key transport systems for yeast cell fitness and multiple-stress tolerance

21-08985S (2021-2024) Eukaryotic Na⁺/H⁺ antiporters – key elements in their structure determining activity, biogenesis and physiological functions

Ministry of Education, Youth and Sports of the Czech Republic

National Sustainability Program II BIOCEV-FAR LQ1604 (2016-2020) Transporters of potassium in the regulation of the cellular cycle, pH and response to the stress of lower eukaryotes

Inter-Excellence LTC20006 (2020-2023) Transport systems involved in intracellular pH homeostasis and yeast tolerance to low external pH

Inter-Excellence LTC20005 (2020-2023) Specific transporters of non-conventional yeasts

COST Actions

CA18113 (2019-2023) Understanding and exploiting the impacts of low pH on microorganisms

CA18229 (2019-2024) Nonconventional yeast for the production of bioproducts

Abstract

One of the key prerequisites for yeast cell growth is the uptake of essential compounds, such as potassium. Potassium is a vital monovalent cation and its sufficient intracellular concentration is crucial for various processes, for instance: regulation of membrane potential and cell turgor, enzymatic activity, and protein synthesis. A sufficient internal concentration of potassium is also one of the pivotal signals for cell division. However, as also excess of potassium might lead to unfavourable physiological consequences in yeast, such as deacidification of vacuoles and depolarization of plasma membrane, it is imperative for the yeast cells that the whole process of potassium acquisition is a tightly regulated affair, in order to maintain proper potassium homeostasis. In yeast *Saccharomyces cerevisiae*, uniporter Trk1 is considered a key player in potassium uptake. The presented thesis aimed to provide novel knowledge regarding Trk1, more specifically to study its ability to modify its capacity for potassium uptake, putative regulation by phosphorylation, and involvement in the survival of glucose-induced cell death (GICD). Additionally, potassium-uptake systems in selected non-conventional species were characterized as well.

The most distinctive feature of Trk1 is its alleged ability to switch between two affinity modes: low- and high-affinity mode, as a response to changes in external potassium concentration. We performed a detailed characterization of the process of 'affinity-switch' and found that rather than switching between two modes, Trk1 was able to adjust both its affinity and maximum velocity precisely in accordance with the availability of potassium. Additionally, we identified novel signals presumably driving the aforementioned changes in the capacity of Trk1-mediated uptake: internal potassium content and membrane potential. Our results also suggested the involvement of specific subdomains of Trk1, P-helices, in processes of adjustments of affinity.

Despite the indispensable role of Trk1 in yeast physiology, there is a substantial scarcity of detailed knowledge regarding its regulation. Transporter Trk1 has been previously shown to be expressed on a low level regardless of external conditions and its regulation is therefore thought to occur on a posttranslational level, mainly in form of phosphorylation. We identified two novel putative phosphorylation sites: Ser882 and Thr900 within the highly conserved intracellular subdomain of Trk1. Moreover, the involvement of small, regulatory 14-3-3 proteins in the orchestration of the activity of Trk1 was established, as well as their specific binding sites within Trk1.

In addition to Trk1, the genome of *S. cerevisiae* also encodes the second Trk-transporter and paralog of Trk1, Trk2. Despite the high degree of homology between the two, the role of Trk2 in potassium uptake is considered marginal and its precise physiological role remains obscure. We

studied the role of Trk-transporters in connection to GICD and found both Trk1 and Trk2 to be important for the survival of GICD with Trk2 fulfilling a major role. Additionally, a functional connection between Trk2 and H⁺-ATPase Pma1 was established unravelling putative, novel physiological roles of transporter Trk2.

Sufficient uptake of potassium and improved function of Trk1 has been shown multiple times to enhance the survival and performance of yeast during biotechnological production. It is therefore highly desirable to study processes of potassium acquisition and homeostasis also in biotechnologically relevant, often non-conventional species. We performed the initial characterization of two potassium uptake systems: Trk1 and Hak1 in the species *Kluyveromyces marxianus*. We found Hak1 to be a major player under low external potassium concentrations and Trk1 to presumably function under potassium non-limiting conditions. The individual contribution of both transporters to the survival of various stresses was studied as well.

Taken all together, the presented thesis provides novel results regarding Trk1 and its ability to react to changes in the availability of substrate by changing the overall capacity for uptake and its regulation by phosphorylation and association with 14-3-3 proteins. Presented results also point to the novel, previously uncharacterised physiological roles of transporter Trk2. Additionally, potassium uptake systems were also studied in non-conventional, biotechnologically relevant species *K. marxianus*.

Keywords: *Saccharomyces cerevisiae*, potassium homeostasis, Trk1, Trk2, regulation, affinity, phosphorylation, 14-3-3 proteins, *Kluyveromyces marxianus*, Hak1

Abstrakt

Jedním z klíčových předpokladů pro dělení kvasinkových buněk je příjem základních živin a iontů, jako je draslík. Draslík je důležitý, monovalentní kation a jeho dostatečná intracelulární koncentrace je rozhodující pro různé procesy, například regulaci membránového potenciálu a buněčného turgoru, enzymatickou aktivitu a syntézu proteinů. Dostatečná vnitřní koncentrace draslíku je také jedním z klíčových signálů pro buněčné dělení. Nicméně, protože také přebytek draslíku může vést k nepříznivým fyziologickým důsledkům v kvasinkách, jako jsou deacidifikace vakuol a depolarizace plazmatické membrány, je pro kvasinkové buňky nezbytné, aby celý proces získávání draslíku byl přísně regulován, aby se udržela jeho správná homeostáze. V kvasinkách *Saccharomyces cerevisiae* je za klíčového hráče v příjmu draslíku považován uniportér Trk1. Cílem předkládané disertační práce bylo získat nové poznatky týkající se proteinu Trk1, konkrétněji studovat jeho schopnost modifikovat vlastní kapacitu pro příjem draslíku, regulaci pomocí fosforylace a také zapojení do přežití buněčné smrti vyvolané glukózou (GICD). Dále byly také charakterizovány systémy příjmu draslíku u vybraných nekonvenčních, kvasinkových druhů.

Nejvýraznějším rysem Trk1 je jeho schopnost přepínat mezi dvěma afinitními stavy, nízko- a vysoce-afinitní stav, jako reakce na změny vnější koncentrace draslíku. V naší práci jsme provedli podrobnou charakterizaci procesu "afinitního přepínání" a zjistili jsme, že spíše, než přepínání mezi dvěma stavy byl Trk1 schopen přesně upravit jak svou afinitu, tak maximální rychlost transportu v závislosti od dostupnosti draslíku. Kromě toho jsme také identifikovali nové signály, které pravděpodobně řídí výše uvedené změny v kapacitě transportu zprostředkovaném proteinem Trk1: vnitřní obsah draslíku a membránový potenciál. Naše výsledky také naznačily zapojení specifických subdomén Trk1, P-helixů, do procesů modifikace afinity proteinu Trk1.

Navzdory nepostradatelné roli proteinu Trk1 ve fyziologii kvasinek, existuje značný nedostatek detailních znalostí o jeho regulaci. Již dříve bylo prokázáno, že transportér Trk1 je exprimován na nízké úrovni bez ohledu na vnější podmínky, a proto se předpokládá, že jeho regulace probíhá na post translační úrovni, zejména ve formě fosforylace. V naší práci jsme identifikovali dvě nová potenciální fosforylační místa: Ser882 a Thr900, obě lokalizované rámci vysoce konzervované, intracelulární subdomény proteinu Trk1. Kromě toho bylo také studováno zapojení malých, regulačních proteinů 14-3-3 do regulace aktivity Trk1, stejně tak jako jejich specifická vazební místa v rámci sekvence proteinu Trk1.

Kromě proteinu Trk1, genom *S. cerevisiae* také kóduje druhý Trk-transportér a paralog Trk1, Trk2. Navzdory vysokému stupni homologie mezi těmito dvěma transportéry je role Trk2 v příjmu

draslíku považována za okrajovou a jeho přesná fyziologická role zůstává nejasná. Studium role Trk-transportérů v souvislosti s GICD jsme zjistili, že Trk1 i Trk2 byli důležité pro přežití GICD, přičemž hlavní roli plnil právě transportér Trk2. Navíc bylo také pozorováno funkční spojení mezi Trk2 a H⁺-ATPázou Pma1. Tyto výsledky poukázali na potenciální, nové fyziologické role transportéru Trk2.

Již několikrát bylo prokázáno, že dostatečný příjem draslíku a také zlepšená funkce transportéru Trk1, vede ke zlepšení přežití a výkonnosti kvasinek během biotechnologické produkce. Je proto velmi žádoucí studovat procesy získávání draslíku a draslíkové homeostázy také u biotechnologicky významných, často nekonvenčních druhů. V naší práci jsme se proto zabývali také základní charakterizací dvou systémů importu draslíku u druhu *Kluyveromyces marxianus*: Trk1 a Hak1. Zjistili jsme, že Hak1 je hlavním přenašečem při nízkých vnějších koncentracích draslíku a Trk1 pravděpodobně funguje za podmínek, kdy externí koncentrace draslíku není omezující. Dále byl také studován individuální přínos obou transportérů k přežití různých typů externích stresů.

Celkově vzato, prezentovaná práce poskytuje nové znalosti týkající se transportéru Trk1, a to jeho schopnosti reagovat na změny v dostupnosti substrátu změnou celkové kapacity pro příjem draslíku a také možností regulace pomocí fosforylací a asociací s proteiny 14-3-3. Prezentované výsledky také poukazují na nové, dříve necharakterizované fyziologické role transportéru Trk2. Kromě toho byly systémy příjmu draslíku studovány také u nekonvenčního, biotechnologicky relevantního druhu *K. marxianus*.

Klíčová slova: *Saccharomyces cerevisiae*, draslíková homeostáze, Trk1, Trk2, regulace, afinita, fosforylace, 14-3-3 proteiny, *Kluyveromyces marxianus*, Hak1

Table of contents

Abstract	5
Abstrakt	7
1. Introduction.....	11
1.1 Yeast as a model organism.....	11
1.2 Roles of potassium in yeasts	11
1.3 SKT proteins and evolution of potassium-uptake systems from bacteria to plants and yeasts .	12
1.4 Trk1.....	16
1.4.1 Discovery and basic features.....	16
1.4.2 Structure of Trk1	18
1.4.3 Affinity switch.....	20
1.4.4 Regulation of the activity of Trk1	21
1.4.5 Trk1 in biotechnology and potential antifungal therapy	22
1.5 Other potassium-uptake systems in yeasts	23
1.6 Potassium homeostasis in <i>S. cerevisiae</i>	24
1.6.1 Intracellular potassium-transporting systems	26
1.6.2 Nha1	28
1.6.3 Ena1.....	29
1.6.4 Tok1	30
1.6.5 Pma1.....	31
1.6.6 Intracellular V-ATPase	32
1.7 14-3-3 proteins.....	32
1.8 <i>Kluyveromyces marxianus</i>	35
2. Aims of the thesis	37
3. Results	38
3.1 Yeast Trk1 Potassium Transporter Gradually Changes Its Affinity in Response to Both External and Internal Signals	38
3.2 Putative role of phosphorylation and interaction with 14-3-3 proteins in the regulation of activity of Trk1.....	68
3.3 Minority potassium-uptake system Trk2 has a crucial role in yeast survival of glucose-induced cell death	122
3.4 Potassium-uptake systems in <i>Kluyveromyces marxianus</i>	133
3.4.1 Introduction.....	134
3.4.2 Material and methods.....	134
3.4.3 Results	136
4. Discussion.....	144

4.1 Regulation and putative mechanism of changes in affinity and maximum velocity of Trk1-mediated uptake	144
4.2 Putative role of phosphorylation and interaction with 14-3-3 proteins in the regulation of activity of Trk1.....	150
4.3 Role of Trk-transporters in the survival of glucose-induced cell death and high-temperature	153
4.4 Potassium-uptake systems in <i>Kluyveromyces marxianus</i>	154
5. Conclusions.....	158
6. References	159

1. Introduction

1.1 Yeast as a model organism

Yeast *Saccharomyces cerevisiae* has, for a long time, been one of the most popular model organisms for basic biological research, due to various characteristics such as the early availability of genome sequences, a wide array of microbiological and biochemical tools and, as importantly, easy and low-cost manipulation. Even though, it is one of the simplest eukaryotic organisms, the rudimentary cellular and metabolic processes in this yeast do not differ significantly from those occurring in other organisms, such as plants or even animals, including humans. Since the essence of many human diseases lies in disruptions of very fundamental cellular mechanisms, such as cell division, DNA repair etc., the results from yeast-based studies can be easily extrapolated and serve as a base for crucial biomedical research. The power of yeasts in biomedical research is also supported by a number of Nobel Prizes in Physiology or Medicine awarded for research including yeast as a model organism.

In addition to basic, often biomedical research, yeasts, including *S. cerevisiae*, have an invaluable place in biotechnology, the role, they have likely been fulfilling for several millennia since fermentation is one of the oldest practices in human history. Nowadays, yeast cells are being employed in more sophisticated biotechnological fields, ranging from the production of biofuels through the synthesis of high-value compounds to the design of yeast-based vaccines.

The presented thesis exploits the above-mentioned advantages of the yeast *S. cerevisiae*, as a model organism, in the study of one of the key cellular mechanisms, potassium homeostasis. Additionally, this work also aims to extrapolate the results from the basic research to the potential use in biotechnologically-attractive yeast species.

1.2 Roles of potassium in yeasts

Due to its various indispensable roles, potassium is considered one of, if not the most important intracellular cation. The essentiality of potassium is illustrated by its intracellular concentration in yeast, ranging from 200-300 mM, the highest of all intracellular ions [1], and also by the amount of energy, in form of ATP, the yeast cells expend on maintenance of its sufficient intracellular levels. Even though uptake of potassium, in *Saccharomyces cerevisiae*, is not facilitated by primary active transport and thus does not consume ATP directly, it is thought to be energized by

membrane potential, which is determined mainly by the export of protons through specific ATPase, shown to consume up to 25% of total cellular ATP [2]. This mechanism is discussed, in more detail, below.

Intracellular potassium levels have been directly connected to the regulation of several physiological parameters, mainly the membrane potential, intracellular pH and also cellular size. A decrease in internal potassium has been shown to lead to the hyperpolarized plasma membrane [3], acidification of cytoplasm [4] and an overall decrease in the size of the cells [4]. Additionally, intracellular potassium has also been shown to be important for the structure of ribosomes and protein synthesis [5]. Activation of certain enzymes is also thought to be dependent on the presence of potassium [6] and finally, sufficient intracellular potassium concentration and consequently critical cell size, is one of the pivotal signals for cellular division [7]. Due to the involvement of potassium in these essential processes, its sufficient intracellular concentration has been tied to the survival of various external stresses, including those encountered during biotechnological production, for instance, low external pH and high external concentrations of ethanol [8,9], making the potassium homeostasis an attractive target for studying in biotechnologically relevant yeast species.

Apart from the main functions, potential novel roles of potassium in yeast cells have been suggested by studies focused on cellular response to potassium starvation. Lack of available potassium leads to various physiological changes, including changes in mRNA levels of hundreds of genes, alternations in various metabolic traits and also triggering of oxidative stress response pathway and autophagy [10,11]. Whether these effects can be connected to the above-mentioned roles of potassium or they represent a set of novel functions, should be subjected to further study.

Due to these essential roles of potassium, all living cells, including yeast, developed an array of effective mechanisms responsible for its accumulation.

1.3 SKT proteins and evolution of potassium-uptake systems from bacteria to plants and yeasts

Even though the presented thesis focuses on Trk potassium-uptake systems in yeast, in order to properly perceive the evolutionary origin of its function and structure and also the structural nature of the evolutionary transition from highly selective channels to transporters and channels with a somewhat lesser degree of selectivity, one must look at the evolution of a whole group of, so-called, SKT proteins.

The superfamily of K⁺ transporters (SKT) is a large group of K⁺ transporters and channels found in all kingdoms of life, except animals [12]. This group comprises bacterial channels TrkH and KtrB, bacterial ATPase KdpA, plant transporters HKT1 and HKT2 and fungi transporters Trk1 and Trk2 [13]. Even though, bacterial SKT proteins TrkH, KtrB and KdpA share common structural features (section 1.3, Fig. 1), their general mechanism of potassium uptake and overall contribution to potassium homeostasis in bacteria, differs significantly. Proteins TrkH and KtrB were originally considered transporters, however, recent studies suggest that they function as channels, facilitating the uptake of potassium driven by its concentration gradient [13]. At low external potassium concentrations, however, KtrB and TrkH fail to maintain sufficient internal concentrations of potassium and bacterial cells, thus, have to resort to the uptake of potassium against its concentration gradient. This uptake is facilitated by P-type ATPase KdpA, which couples the uptake of potassium to the hydrolysis of ATP [14]. Expression profiles of these three proteins in bacteria showed TrkH and KtrB being expressed at stable levels, thus maintaining sufficient internal potassium concentration under normal conditions and KdpA to be strongly induced under osmotic stress and potassium limitations, making it a sort of emergency potassium-uptake system [15]. It is also important to note that both TrkH and KtrB interact with additional subunits, TrkA and KtrA respectively, with these interactions presumably having regulatory effects [16,17]. ATPase KdpA is a part of a large protein complex, jointly called KdpFABC [18]. Unlike remaining members of the SKT family, plant transporters HKT1 and HKT2 are not considered potassium-specific transporters, but rather sodium-specific transporters or transporters of both potassium and sodium [19]. In general, HKT1 is responsible for the transport of sodium, while HKT2 is considered a potassium-sodium symporter [20]. The main role of HKT-transporters in plants is the maintenance of an ion balance in various tissues, making them, i. a., the key determinants of resistance to the high concentration of salts in soil [21]. And finally, having been identified in genomes of all sequenced yeast species, Trk-transporters are considered key potassium-uptake systems in yeast [1].

The large degree of conservation between 2TM-K⁺ channels, such as KcsA and SKT proteins led to a proposition of a hypothetical scheme of the evolution of SKT proteins, depicted in Figure 1 (section 1.3). SKT proteins are thought to have evolved from a simple KcsA-like 2TM-K⁺ channel, by multiple gene duplications and fusion resulting in four covalently linked, so-called, MPM-domains [15,22]. In this scheme, a single subunit of KcsA corresponds to one MPM domain of respective SKT proteins [15].

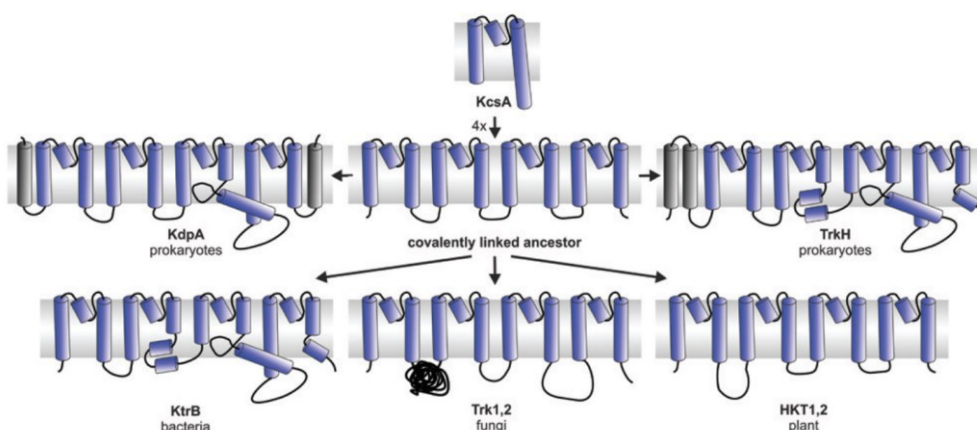


Figure. 1. Hypothetical scheme of evolution of SKT proteins from the ancestral 2TM-K⁺ channel (KcsA). Evolution most likely occurred by multiple gene duplication and fusion. Analogous subunits are shown in blue, and segments specific to KdpA or TrkH are shown in grey colour (adapted from [15]).

One subunit of the typical 2TM-K⁺ channel, such as KcsA, and consequently, each MPM domain of SKT proteins, consists of two transmembrane helices, M1 and M2, connected by short pore-loop, also called P-loop [23,24]. The P-loop contains a short P-helix and also harbours a sequence of the selectivity filter [15,24]. Four separate subunits of KcsA are assembled around a central axis, thus creating a pore for the uptake of potassium [25,26] (section 1.3, Fig. 2). Selectivity filter, responsible for binding and entrance of potassium into the channel, is located in the upper part of the pore. In KcsA, the selectivity filter is formed by canonical TVGYG sequence on each subunit, together creating four potential binding positions for potassium [23] (section 1.3, Fig. 3). Conformation of the selectivity filter is to a large degree dependent on non-covalent interactions with P-helices [23]. Transmembrane helices M1 and M2 serve as a sort of anchor, holding the entire channel in the plasma membrane [23]. The basic structure of the SKT proteins to a large degree copies the structure of the KcsA channel, recently confirmed by a resolved crystal structure for bacterial channels KtrB and TrkH as well as ATPase KdpA [16-18]. The sequence of subunits of the KcsA channel is to a large degree homologous to individual MPM domains of Trk1 protein, so much so that the initial and also recent models of Trk1, are both largely based on the resolved structures of KcsA and other SKT proteins [22,27]. However, some deviations from this basic structural paradigm arose throughout the evolution, most notably, as mentioned above, the SKT proteins do not consist of four separate subunits, but rather are single polypeptides, containing four MPM segments, each corresponding to a single subunit of KcsA channel [15]. There are some additional structural differences, such as additional transmembrane elements on the N-terminal end in TrkH [16] and both N- and C-terminal ends in KdpA [18], or in the case of yeast Trk1, unusually long first intracellular loop [28]. And finally, some transmembrane helices in KtrB, TrkH and KdpA are broken into two helices,

connected by loops (section 1.3, Fig. 1) with this loop thought to be involved in the gating mechanism [17].

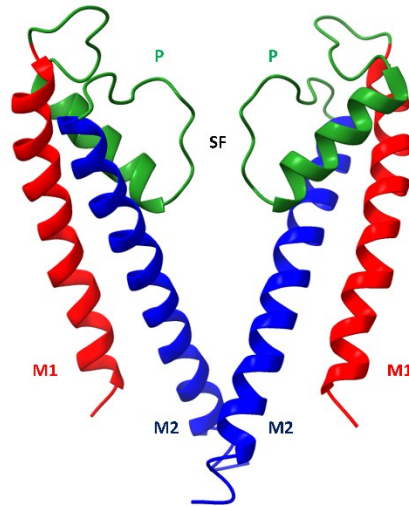


Figure. 2. Structure of the typical bacterial 2TM-K⁺ channel KcsA. M1 helices are labelled in red colour, M2 helices are labelled in blue colour and P-loops are labelled in green colour. The approximate position of the selectivity filter is highlighted by 'SF'. For better clarity, only two opposing subunits, out of four total, are shown. 3D model was obtained from PDB database, entry code 1J95 [25] and visualised in ChimeraX v1.1.

An additional difference between KcsA and SKT proteins is in the structure of the selectivity filter and this difference is, likely, the essence of divergence in selectivity between 2TM-K⁺ channels and SKT proteins. The sequence of the selectivity filter of SKT proteins significantly differs from the canonical TVGYG present in KcsA and also exhibits a low degree of conservation, with only the first glycine being conserved [15,29]. This difference presumably leads to an alternation in the overall conformation of the selectivity filter, as well as the reduction in the number of potential binding positions for potassium and consequently to decreased selectivity [29] (section 1.3, Fig. 3). Unlike KcsA, which has been observed to be highly selective for potassium [26], SKT proteins have been shown to also transport other ions, such as sodium, rubidium, caesium and lithium [1,20,29,30]. The reduction of a number of potassium-binding positions leading to a reduced selectivity has also been confirmed by the artificial alternation of a number of binding positions in a different bacterial channel, NaK, which resulted in a transition from a highly K⁺-selective channel to a channel able to also transport Na⁺ [31,32]. Additionally, this structural alternation in SKT proteins also likely leads to increase structural flexibility of the whole region, as well as a decreased overall capacity for transport, compared to 2TM-K⁺ channels [13,15].

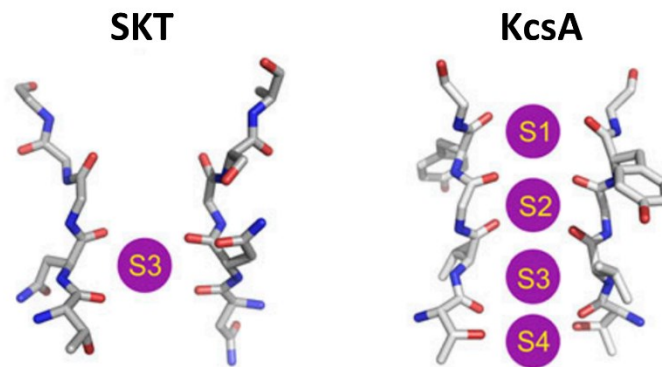


Figure. 3. Comparison of the structures of the selectivity filters of 2TM-K⁺ channel KcsA and typical SKT protein, represented by KdpA. Potassium binding positions are highlighted by purple circles labelled S1-S4 (adapted from [29]).

To summarise the evolution of the potassium-uptake systems from ancestral 2TM-K⁺ bacterial channel to bacterial, plant and yeast channels and transporters, it is important to keep in mind a set of structural changes, mainly creation of covalently linked MPM domains, alternations of the sequence and consequently structure of the selectivity filter and also structural alternations specific for certain members of the SKT family. All of these changes led to the transition from highly selective potassium channels in bacteria to significantly less selective channels and transporters in bacteria, plants and yeast.

1.4 Trk1

1.4.1 Discovery and basic features

Trk1, as a key potassium uptake system in yeast, was initially identified and characterised in various studies dating back to the early and late 80s. Deletion of part of the genome of *S. cerevisiae* containing *TRK1* led to a substantial decrease in kinetic parameters for potassium uptake estimated in mutant cells [33] and also to a sharp increase in external potassium, required for survival of the mutants [34]. Gene *TRK1*, even though crucial for yeast survival on external potassium concentrations in micromolar and low millimolar ranges, has, at the same time, been shown to be non-essential [34].

Besides *S. cerevisiae*, the *TRK1* gene has been identified and subsequently studied in many other yeast species with sequenced genomes, including a number of non-conventional species, such as *Hansenula polymorpha* and *Debaryomyces hansenii* [35,36] or pathogenic species *Candida glabrata* and *Candida albicans* [37,38]. Genomes of many other species, which have become available in recent years, such as the genome of *Kluyveromyces marxianus* [39] also contain ORFs corresponding to the Trk transporter.

In *S. cerevisiae*, *TRK1* (*ScTRK1*) is located on chromosome X and bears a systematic name YJL129C. *ScTRK1* encodes 180 kDa plasma-membrane protein, containing 1235 amino acids, responsible for the uptake of potassium into cells [40]. Originally thought to operate either as a channel, K^+H^+ or K^+Na^+ symporter, it has later been proposed to function as a uniport with uptake, often against the concentration gradient, being energized by a membrane potential [1]. Trk1 has been shown to be localized, primarily, into plasma membrane lipid rafts [41] and is thought to function as a dimer [28] or even tetramer [42].

As mentioned above, the main role of Trk1 is the uptake of potassium, however, as is typical for the SKT proteins, Trk1 has also been shown to be able to facilitate the uptake of other ions, such as sodium and rubidium and is also, presumably able to transport ammonium [43-45]. It is important to note, however, that Trk1 likely facilitates the uptake of sodium with substantially lower affinity, compared to potassium [43,45]. On the other hand, kinetic parameters of the uptake of potassium and rubidium in *S. cerevisiae*, are to a large degree comparable, thus most measurements of uptake capacity of Trk1 are, in fact, performed using rubidium as a substrate, rather than radioactively-labelled potassium [44].

Besides the already mentioned alternations in potassium requirements, the deletion of *TRK1* and *TRK2* has various other effects on cellular physiology, suggesting several putative secondary functions of the Trk1 transporter. Most notably, the deletion of *TRK1* and *TRK2* leads to hyperpolarization of the membrane and acidification of cytoplasm, with these effects detectable even in the cells exhibiting normal intracellular potassium concentrations [4,46]. Additionally, *trk1trk2* mutants are also substantially more susceptible to high external concentrations of salts, such as sodium chloride and lithium chloride and also to the presence of the cationic drug Hygromycin B, although both of these effects are likely a consequence of hyperpolarization of the plasma membrane, leading to increased uptake of both Hygromycin B and toxic cations [4,47].

Trk1 proteins, in *S. cerevisiae*, have also been proposed to be able to form tetramers in the plasma membrane with a single central pore, in the centre of this putative tetramer, being able to facilitate the efflux of various anions, such as chloride, bromide and iodide anions [42,48].

Additionally, so far, an undisclosed role in the survival of glucose-induced cell death has also been assigned to Trk proteins [49].

Apart from Trk1, genome *S. cerevisiae* also encodes a second Trk-transporter, paralog Trk2 [40]. *ScTRK2*, the systematic name YKR050W, is localized on chromosome XI. Trk1 and Trk2 share up to 55% of sequence identity, with Trk2 being shorter by a little over 300 amino acids, although, the majority of this difference lies in the length of the second intracellular loop (see below). Deletion of *TRK2* has no detectable effect on the growth of yeast cells at low potassium concentrations, however, double mutant *trk1trk2* exhibits substantially increased potassium requirements compared to mutant *trk1TRK2*, leading to the notion of marginal, yet existing, the role of this transporter in the uptake of potassium [40]. Originally, though to mediate a low-affinity uptake of potassium [50], it has later been shown to be equally capable of supplementing cells with potassium, when expressed on the same level as Trk1 [51]. Even though, there is no data available concerning the differences in expression profiles of Trk1 and Trk2 in *S. cerevisiae*, growth defects of cells expressing only Trk2, seen on low potassium, are currently hypothesized to be a consequence of its low level of expression in exponentially growing cells. However, Trk2 has been later shown to be crucial in the survival of dehydration/rehydration treatments [52].

1.4.2 Structure of Trk1

Unlike in the case of bacterial members of the SKT family, the structure of Trk1 has not been resolved so far, and thus, our knowledge of its topology and 3D structure relies exclusively on models. The initial model of the 3D structure of Trk1 was proposed by Durell et. al. [22] and was based on, at the time, the recently resolved crystal structure of the KcsA from *Streptomyces lividans* [23]. Another 3D model was published much later, in 2015, by Zayats et. al. [27], although in this paper, Trk1 was modelled without its intracellular segments, thus only the presumed structure of the MPM domains was provided. And finally, the complete model was also recently provided by the AlphaFold database (discussed in more detail in section 3.2). Additionally, also the general topological model of Trk1 based on sequences from various species was proposed in 2009, however, this model considers the conformation of neither individual intracellular loops nor transmembrane segments [53].

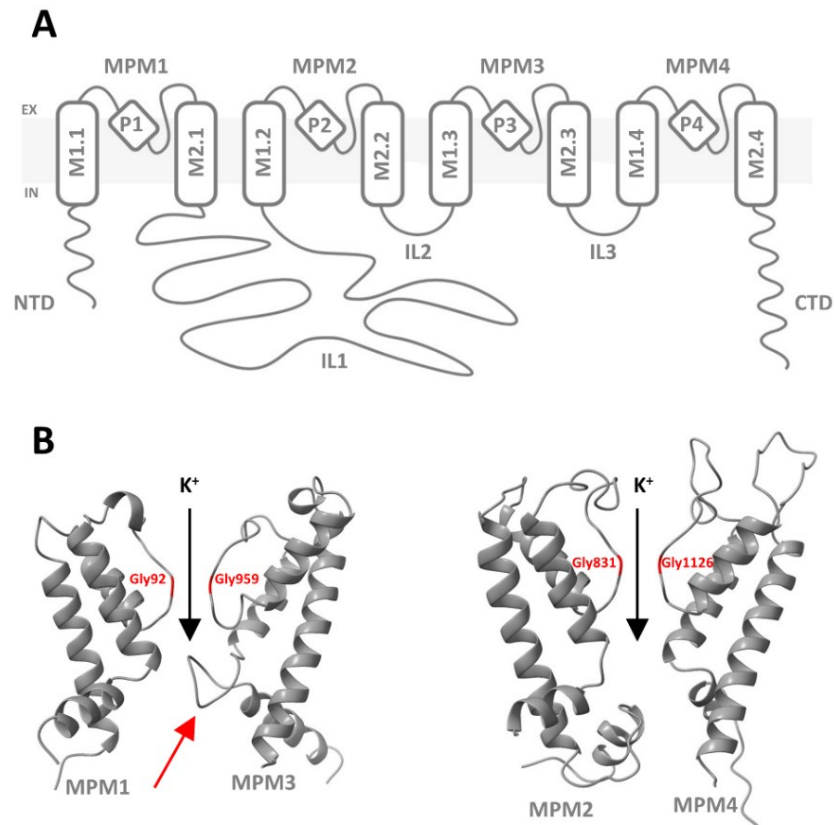


Figure 4. Topological and 3D models of a structure of Trk1. **(A)** Scheme of a topological model of Trk1 [53]. MPM domains labelled MPM1-4. Intracellular loops labelled IL1-3, N-terminal, and C-terminal domains labelled NTD and CTD, respectively. The extracellular and intracellular sides of the plasma membrane are labelled with EX and IN, respectively. **(B)** 3D model of a structure of Trk1 according to Zayats et. al. [27]. Individual MPM domains are labelled MPM1-4. For better clarity, two pairs of opposing MPM domains are shown separately. Conserved glycines of the selectivity filter are marked by a red colour. A large intramembrane loop within the M2 helix of the third MPM domain is marked with the red arrow. The direction of potassium transport is highlighted by black arrows. Visualization and graphical modification were performed in ChimeraX v1.1.

Taken altogether, the structure of Trk1 is in line with the structural paradigm of a typical SKT protein. Trk1 contains 4 MPM domains connected by intracellular loops of various lengths. The MPM domains are assembled around the central axis, thus creating a pore through which potassium is transported (section 1.4.2, Fig. 4) [22,27]. Potassium-binding site, within the selectivity filter, is presumably made up of four conserved glycine residues: Gly92, Gly831, Gly959 and Gly1126, each located within a P-loop of its respective MPM domain [27] (section 1.4.2, Fig. 4). A distinctive feature of Trk1, not present in other SKT proteins, is its unusually long first intracellular loop. Even though its function has been analysed, and a certain role in the selectivity of Trk1 was proposed, its precise

function remains, largely, unclear [28]. Additionally, according to a model by Zayats et. al. (2015), the M2 helix of each of the MPM domains is broken and consists of 2 smaller helices (section 1.4.2, Fig. 4). In the third MPM domain, a break in the M2 helix creates a large intramembrane loop, similar to intramembrane loop observed in the channel KtrB [17] (section 1.4.2, Fig. 4). Interestingly, M2 helix of the last MPM domain contains an unusually large number of a positively charged residues [54]. These positively charged residues are thought to interact with various residues of the first MPM domain, thus stabilizing the overall conformation of the Trk1 [27].

1.4.3 Affinity switch

Likely the most intriguing and distinctive feature of Trk1 is its ability to perform, so called, affinity switch. The affinity switch includes a rapid and substantial increase in both affinity and maximum velocity of Trk1-mediated uptake of potassium, as a reaction to exposure to environments with significant potassium limitations. According to this concept, Trk1 can thus exist in, either a low-affinity state, when the external potassium concentration is high or in a high-affinity state, when the external potassium is scarce [33]. This ability has been initially described concurrently with the identification of the Trk1 as a key player in potassium uptake, in various studies dating back early and late 80s [33,34,55,56]. Even though the precise values of both K_T and V_{max} in low- and high-affinity states tend to differ from study to study, the general pattern seems to be a K_T in millimolar ranges in low-affinity state and low micromolar ranges, approximately 100 μ M, in the high-affinity state, with V_{max} increasing from 3 to 5 times during the transition to high-affinity state [33,43,55,56].

Even though this basic concept has been proven many times in various *S. cerevisiae* strains and under diverse experimental conditions [43,55], and also for the Trk1 transporters from other yeast species (e.g., [57]), the exact mechanism, regulation or even the specific signal promoting these changes, remain unknown. According to the currently accepted model, it is the external potassium concentration, more specifically, its significant decrease that promotes the affinity switch [43]. However, also internal potassium content [56] and the presence of a toxic concentration of sodium ions [43], have both been suggested to stimulate the transition to the high-affinity state.

Surprisingly, in *Neurospora crassa*, the Trk1 transporter has been shown to be unable to react to changes in external potassium by performing the affinity switch, instead the expression of the second high-affinity potassium-uptake system, Hak1 (discussed in section 1.5), was shown to be stimulated by potassium starvation [58,59]. These results point to the existence of an alternative strategy for dealing with the lack of the availability of external potassium.

So far, only one amino-acid residue has been shown to participate in the process of affinity switch. Identified by random mutagenesis and selection of strains unable to grow specifically under low external potassium concentrations, Trk1 with substitution L949P has been shown to undergo an incomplete switch to the high-affinity state, upon potassium starvation [60]. According to the available model (section 1.4.2, Fig. 4; discussed in more detail in section 3.1), amino acid residue Leu949 is located approximately in the middle of the third P-helix. No additional data regarding this substitution and its connection to the affinity switch are currently available.

Additionally, also Trk2 has been shown to be able to perform affinity switch, albeit with the two specifics. First, kinetic parameters of Trk2-mediated potassium uptake in the *trk1TRK2* mutant in the low-affinity state were indistinguishable from the *trk1trk2* mutant and secondly, both affinity and maximum velocity of the Trk2-mediated uptake, in the high-affinity state, seemed to be substantially lower, compared to Trk1 [50].

1.4.4 Regulation of the activity of Trk1

As mentioned above, there is a scarcity of data regarding specifically the expression of both Trk1 and Trk2 in *S. cerevisiae* under various conditions. However, by extrapolating the result from various non-conventional or pathogenic species, in which the expression of Trk1 has been analysed, we can assume that the Trk1 proteins are, in general, expressed on low and stable levels, regardless of the external conditions [36,57,59], thus the regulation of the activity of Trk1 likely does not occur at the transcriptional level.

There are, however, data supporting the possibility of post-translational modifications, more specifically phosphorylation, being involved in governing the activity of Trk1. Several kinases and phosphatases have been suggested to be involved, albeit most of them probably indirectly, in this process. Kinase Hal5 has been extensively studied in connection to Trk1-mediated potassium uptake as its deletion has various effects comparable to the lack of *TRK1*, such as diminished growth on low potassium, increased susceptibility to high concentrations of salts and also decrease in Trk1-mediated uptake. On the other hand, overexpression of this kinase has been shown to lead to an increase in Trk1-mediated uptake [61]. Upon closer inspection of the potential role of Hal5 in the regulation of Trk1, it seems that this kinase might be responsible for the stabilisation of Trk1 in the plasma membrane by phosphorylating its C-terminal end [62]. Additionally, Sky1 kinase has been suggested as involved in the negative regulation of Trk1. Its deletion presumably leads to the up-regulated activity of Trk1. This kinase was proposed to be involved in the regulation of the nuclear

export of mRNA, including the mRNA of the Trk1 protein [63]. Kinase Snf1 was also suggested as a positive regulator of Trk1, with the possibility of its functioning upstream of the kinase Hal5, thus being a part of a larger signalling cascade resulting in alternations of the activity of Trk1 [64]. Besides kinases, also phosphatases have been shown to have a role in the regulation of Trk1. Most notably, phosphatase calcineurin was proposed as a positive regulator of Trk1 [65,66]. As in the case of the kinase Snf1, also calcineurin is thought to not regulate the Trk1 directly, but rather function upstream of the kinase Hal5, by stimulating its expression [67]. And finally, Ppz1 phosphatase has been shown to be a negative regulator of Trk1, with also colocalization and physical interaction between Ppz1 and Trk1 observed [41].

Several putative phosphorylation sites, coming from various phosphoproteomic studies, have been identified in Trk1 (discussed in more detail in section 3.2). However, none of the putative phosphorylation sites has been analysed individually, nor has any study connecting them to specific kinases or conditions upon which the phosphorylation might occur, have been performed so far.

1.4.5 Trk1 in biotechnology and potential antifungal therapy

Several recent studies focused on the improvement of biotechnological productions, mainly through the construction of yeast strains more suitable for withstanding stresses, encountered during the various biotechnological processes, have revolved around the Trk1 protein. Most notably, overexpression of Trk1 in *S. cerevisiae* led to increased alcohol tolerance and consequently to the elevated yield of ethanol during fermentation [8]. Trk1 has also been suggested to play a substantial role in resistance to another common ‘biotechnological’ stress, low pH [68]. The specific set of substitutions within the Trk1, obtained by adaptive laboratory evolution, also resulted in increased resistance to low pH and the presence of high external concentrations of propionic acid [9]. And finally, by comparing Trk1 sequences from several dozens of *S. cerevisiae* strains, several substitutions within Trk1, leading to an increased cell tolerance to the high external concentration of ammonium, have been identified [45].

Additionally, the deletion of *TRK1* in the pathogenic species *Candida glabrata* was shown to lead to decreased cell virulence and also increased elimination of mutant cells by macrophages [69]. Since *C. glabrata* encodes Trk1 as its only potassium-uptake system, this effect of the *TRK1* deletion, combined with the fact, that neither Trk1 nor any other member of the SKT family, occurs in animals [15], makes Trk1 transporter a potentially promising target for future development of novel antifungal agents.

1.5 Other potassium-uptake systems in yeasts

Apart from Trk-proteins, two additional potassium-uptake systems have been identified and characterised in yeasts, K^+ - H^+ symporter Hak1 and ATPase Acu1. Unlike Trk-proteins, which have been identified in all, hitherto, sequenced genomes, the presence of *HAK1* and *ACU1* genes seems to be specific only for a certain species, with none of these genes being present in the genome of *S. cerevisiae*.

Transporter Hak1 has been, so far, characterised in several non-conventional species, such as *Schwanniomyces occidentalis* [70], *Hansenula polymorpha* [36] or *Debaryomyces hansenii* [35] as well as in pathogenic *Candida albicans* [57] and mycelial fungi *Neurospora crassa* [59]. Due to its very high affinity for potassium uptake [36] and functional dependence on low external pH [71], this transporter is thought to operate as a K^+ - H^+ . Unlike Trk1, which has been shown to be expressed constitutively, expression of Hak1 is substantially stimulated specifically under low external concentrations of potassium and repressed when external potassium concentration is high [59]. Additionally, under high external potassium concentrations, the Hak1 protein is endocytosed [36]. Taken altogether, data regarding the potassium-uptake system Hak1 suggest its importance in supporting the Trk1-mediated uptake of potassium, especially under severe potassium limitations.

Hitherto most obscure system for potassium uptake in yeast is the P-type ATPase Acu1. So far, it has been identified in only few species, such as fungi *Ustilago maydis* and yeast *Pichia sorbitophila* [72] and *Candida albicans* [38]. Acu1 is thought to be able to facilitate high-affinity uptake of both potassium and sodium [72], however, *C. albicans* Acu1 presumably lost the ability to transport sodium [38]. When the expression profile was analysed, the *CaACU1* gene seemed to be stimulated under low external potassium concentration and both low and high external pH. On the other hand, the expression of *CaACU1* was substantially repressed when cells were exposed to a high external concentration of sodium [57]. Additionally, heterologous expression of CaAcu1 in *S. cerevisiae* led to increased resistance to toxic concentrations of lithium [38].

As a potassium uptake through plasma membrane has also been detected in *S. cerevisiae* mutants lacking both *TRK1* and *TRK2* [73], it is also important to note the so-called, 'non-specific' uptake of potassium, or uptake not mediated by either of the Trk-transporters. So far only amino-acid permeases and sugar transporters have been shown to be able to facilitate the uptake of potassium in absence of Trk-transporters, albeit this uptake exhibited very low affinity [73,74]. Additionally, the non-specific uptake has been shown to be stimulated by hyperpolarization of the plasma membrane [46]. NSC1, a non-specific cation channel, has also been suggested to play a role in

the low-affinity uptake of potassium, however, very little information is available regarding this protein, including the precise ORF by which it is encoded [1,75].

1.6 Potassium homeostasis in *S. cerevisiae*

Even though, in *S. cerevisiae*, Trk1 fulfils an irreplaceable role in the uptake of potassium and consequently in its homeostasis, also intracellular redistribution, export and energizing of the uptake are imperative processes for the maintenance of proper overall homeostasis of potassium. As seen in Figure 5 (section 1.6), the whole process depends on the precisely orchestrated interplay among a number of proteins, embedded not only in the plasma membrane but also in membranes of various organelles [1].

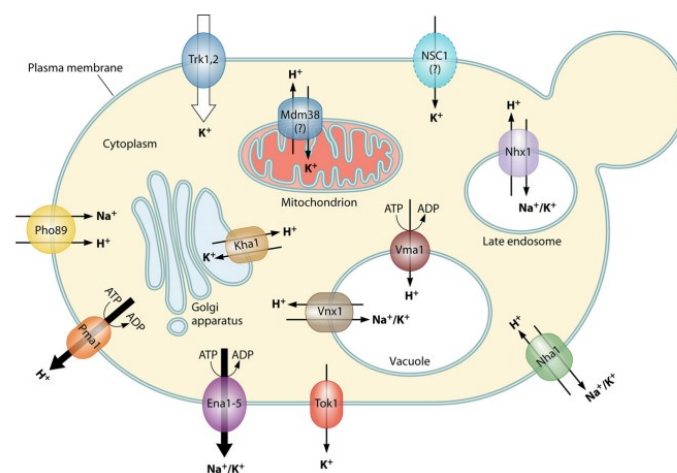


Figure. 5. Overview of transport proteins involved in cation transport in yeast *Saccharomyces cerevisiae* (adapted from [1]).

Apart from previously discussed general functions of potassium in yeast, this cation also fulfils several roles specific to particular organelles and thus intracellular redistribution of potassium is an essential aspect of its overall homeostasis. Since most, if not all, transport of potassium into organelles is mediated by H⁺/K⁺ antiporters, redistribution of potassium is dependent on the existence of stable, close to neutral, pH in the cytoplasm and relatively acidic pH within organelles, since this combination creates a proton gradient that energizes the actual transport of potassium across the membranes of the organelles [1]. In general, vacuoles serve mostly as storage of excess ions, including potassium [76], however, the amount of potassium stored within vacuoles also substantially affects the pH of the vacuoles and consequently its ability to properly fulfil its function

[77]. The main antiporter responsible for the transport of potassium from the cytoplasm to vacuoles is Vnx1 [78]. In mitochondria, to which potassium is presumably transported by a complex system, including protein Mdm38 [79], potassium has been shown to be involved in the regulation of matrix volume, mitochondrial membrane potential, redox signalling, and thus inevitably also respiratory rate [80]. Additionally, storage of potassium in the Golgi apparatus, through antiporter Kha1 and in late endosome, facilitated by antiporter Nhx1, has been connected to the absorption and metabolism of both iron and copper with consequences on respiratory metabolism [79]. And finally, a substantial portion of intracellular potassium is also stored in the nucleus, where it might serve as a balance of the negative charge of the DNA and RNA and has been also shown to interact with various proteins, including histones [81,82]. Additionally, nuclear ions, including potassium, have also been shown to participate in the higher order structure of chromosomes by interacting with nonhistone proteins [83].

As mentioned before, under standard laboratory conditions, the intracellular concentration of potassium is maintained within a range of 200-300 mM [1]. Concerning the relative redistribution of potassium within cells, surprisingly, only approximately 15% of total intracellular potassium is kept in the cytoplasm and roughly 5% of the total potassium is transported each to mitochondria, Golgi apparatus and endoplasmic reticulum, where potassium presumably fulfils its actual functions [81]. A large portion of 30% of internal potassium is also kept in the nucleus and the majority of internal potassium, approximately 40%, is stored within vacuoles [81]. It is important to note, that, unlike other discussed organelles, the membrane of the nucleus does not contain any cation-transporting systems and potassium likely enters the nucleus non-specifically, through the nuclear pores [83]. Upon prolonged potassium starvation, which inevitably leads to a loss of intracellular potassium [4,81], potassium stored in vacuoles is promptly transported into cytoplasm, presumably by a channel Yvc1, to ensure stable levels of potassium in both cytoplasm and all of the organelles, thus allowing essential potassium-dependent processes to be carried on, even under severe potassium limitations [76]. This ability of vacuoles, to store such large amounts of potassium, allows cells to survive and proliferate on a wide range of external potassium concentrations [1].

In addition to redistribution, also export of surplus potassium is an important cellular tool in the maintenance of proper potassium homeostasis since it has been previously shown, that excess of potassium might lead to few unfavourable physiological consequences, including deacidification of vacuoles and loss of membrane potential [77,84]. In *S. cerevisiae*, the export of excess potassium is ensured by three types of transport proteins: antiporter Nha1, ATPase Ena1 and channel Tok1 [1].

And finally, as Trk1-mediated uptake of potassium is thought to be energized by membrane potential [1], the main creator of membrane potential in *S. cerevisiae*, H⁺-ATPase Pma1, also fulfils an invaluable role in potassium homeostasis by both energizing the potassium uptake and balancing uptake of potassium by efflux of protons to ensure a stable membrane potential [85].

It is also important to emphasize the interplay between the homeostasis of potassium and sodium. Unlike potassium, which fulfils several essential functions in yeast cells, the sodium ions, in higher concentrations, are toxic for the cells and it is, thus, of the highest priority for the yeast cells to accumulate high internal concentrations of potassium, while keeping the internal levels of sodium at a bare minimum or, alternatively, sequester the sodium and limit its toxic effects. The main reason why homeostases of potassium and sodium are connected is the fact, that they share, to various degrees, most of the major transporters discussed in this work, that being a Trk1, shown to be able to facilitate non-specific and low-affinity uptake of sodium [43], but also exporting systems Nha1 and Ena1, as well as the intracellular transport systems Vnx1 and Nhx1 [1,84]. In order to maintain the above-mentioned high intracellular potassium-sodium ratio, the yeast cells employ two main strategies. First, yeast cells employ discriminatory uptake, having a much higher affinity for potassium compared to sodium [43]. However, when the external sodium-potassium ratio is very high, above 700:1 [44], a substantial amount of sodium still enters the cells, forcing the cells to employ the second main strategy, sodium efflux or sequestration.

The following sections provide a brief overview of the function, structure and regulation of all the major players involved in the above-mentioned processes of redistribution and export of potassium and sodium, as well as the generation of the energy needed for potassium uptake.

1.6.1 Intracellular potassium-transporting systems

As mentioned above, the intracellular redistribution of potassium is one of the key elements of its overall homeostasis. *S. cerevisiae* cells employ several cation-translocating systems, in order to facilitate the transport of cations across the membrane of organelles (section 1.6, Fig. 5). As all of these transporters, presumably, function as H⁺/cation antiporters, their common feature is the dependence on the existence of strong proton gradients, across the membrane of the particular organelle. With exception of mitochondria, in which the proton gradient is dependent on the electron transport chain, this proton gradient, across the membranes of the organelles, is generated and maintained by the intracellular V-ATPase (see below).

Antiporter Vnx1 is considered the main player in the uptake of both potassium and sodium into vacuoles [78]. This protein contains 908 amino acids, according to prediction software, forming 13 transmembrane domains [84]. The main physiological role of Vnx1 is the sequestration of excess potassium and toxic sodium into vacuoles, however, in this process, also the pH of the cytoplasm is affected [78]. Surprisingly, even in a strain lacking the *VNX1* gene, certain potassium transport activity across the vacuolar membrane has been detected, leading to the establishment of the second transporter, Vcx1, in this process [86]. Containing 411 amino acids, and forming 11 transmembrane segments, the main role of this antiporter has been shown to be the facilitation of the H^+/Ca^{2+} antiport across the vacuolar membrane, thus the transport of potassium into vacuoles is considered a mere secondary function [86]. Additionally, Vhc1 a K^+-Cl^- symporter, has been also shown to participate in the uptake of potassium into vacuoles [87].

In addition to transport into vacuoles, also export of potassium from vacuoles into the cytoplasm, is an essential aspect of potassium homeostasis, especially under conditions of potassium starvation. Even though the data regarding the export of potassium from vacuoles are scarce, the voltage-gated ion channel Yvc1 has been suggested to be engaged in this process. The presumed main role of Yvc1 is participation in calcium signalling, by mediating the export of calcium cations from vacuoles into the cytoplasm [88], however, also export of both potassium and sodium through Yvc1 has been observed [76], Yvc1 channel is thought to be activated by various stresses, including hyperosmotic shock [89], however, the precise regulatory connection to the homeostasis of potassium remains to be thoroughly studied.

In a pre-vacuolar late endosome, the uptake of potassium into its lumen is mediated by the Nhx1 antiporter [90]. In addition to the late endosome, this transporter has also been observed to be present in the trans-Golgi network [91]. Nhx1 is 633 amino acids long, assembled into 12 transmembrane domains [84]. Nhx1 fulfils several physiological roles, mainly sequestration of excess potassium and toxic sodium, regulation of pH of cytoplasm and vesicles, but also involvement in vesicle fusion [92].

Finally, membranes of the Golgi apparatus contain protein Kha1, containing 873 amino acids and 12 transmembrane domains, this protein's presumed main function is the transport of potassium into the lumen of the Golgi apparatus [93]. In addition to potassium, this protein is also thought to be able to mediate the transport of sodium and lithium [94]. Apart from ensuring sufficient concentration of potassium within the Golgi apparatus, this transporter also substantially affects its luminal pH [84].

Potassium-proton exchange (KHE) across the membranes of mitochondria is an essential prerequisite for the maintenance of mitochondrial osmotic balance and membrane potential [95]. Despite its essentiality, out of all processes discussed in this section of the thesis, KHE remains the most enigmatic. Three genes have been identified to be involved in process of KHE in *S. cerevisiae*: *MDM38*, *YLH47* and *YDL183c* [1,84]. All three proteins are predicted to form a transmembrane domain, although, due to their rather small size, they are unlikely to facilitate KHE by themselves [96]. As all of these proteins have been shown to oligomerize, it is conceivable, that all of them are mere co-factors of, so far, unidentified transport proteins responsible for KHE [96].

1.6.2 Nha1

Yeast Nha1 transporter belongs to a large group of proton/alkali metal cation antiporters conserved in all organisms, from bacteria to mammals. Even though the structure of these transporters is conserved, the actual physiological function diverged throughout the evolution [97]. In *S. cerevisiae*, this transporter consists of 985 amino acids predicted to form 12 transmembrane segments and a large C-terminal domain [98] although an AlphaFold model predicts 13 transmembrane segments.

Nha1, in yeast, functions as a H^+/Na^+-K^+ antiporter, consuming the proton gradient created by Pma1 (see below) and exporting sodium or potassium, thus its main function is the detoxification of surplus alkali metal cations [99]. Nha1 transporters are also able to facilitate the export of lithium and rubidium, albeit with lower capacity compared to potassium and sodium [98,100]. A concomitant occurrence of this transport process has a substantial impact on intracellular pH and membrane potential, with the regulation of both being considered a secondary function of Nha1 [99,101].

NHA1 is thought to be expressed constitutively, on low levels, hence belonging to, so-called, housekeeping genes [102]. Thus, the majority of its regulation likely occurs on a post-translational level. Nha1 has been shown to be phosphorylated under osmotic, salt stress, by Hog1 on two residues located within the C-terminal domain, Thr765 and Thr876, leading to its activation [103]. Under osmotic stress caused by nonsalt solutes, the activity of Nha1 is suppressed, in order to sustain intracellular potassium and consequently intracellular water [104]. Negative regulation of Nha1 is thought to be mediated by association with small, regulatory 14-3-3 proteins [105,106] (discussed in more detail in sections 1.7 and 3.2). Additionally, the potential for regulation of Nha1 on the level of transition through the secretory pathway has been suggested, since proper membrane expression of this protein is dependent on the presence of the Erv14 cargo receptor [107].

Despite its proven importance in the export of surplus alkali-metal cations, Nha1 is not the only transporter, in yeast, capable of fulfilling this function and its likely main role is to ensure this process until the second, more potent cation-exporter, Ena1, is expressed.

1.6.3 Ena1

Another major player, facilitating the export of alkali metal cations, is the P-type ATPase Ena1. Ena1 couples hydrolysis of ATP with the export of either sodium, potassium or lithium against their respective concentration gradients [108]. Ena proteins are present in most fungi and are the key determinants of resistance to high external concentrations of salts [108]. In *S. cerevisiae*, multiple *ENA* genes are present, on chromosome IV, usually in tandems with the precise number being strain-specific and ranging from 3 to 5 [84]. All *ENA* genes encode highly similar proteins, however, concerning the level of expression, *ENA1* seems to be the dominant *ENA* gene. *ENA1* encodes a protein containing 1095 amino acids with predicted 10 transmembrane segments [1].

In contrast to the Nha1 antiporter, the essence of the regulation of Ena transporters lies in the precise orchestration of their expression, in accordance with external conditions. Under normal conditions, *S. cerevisiae* cells, contain a small number of Ena proteins, however, under high external concentrations of salt or high external pH, expression of *ENA* genes is significantly induced through multiple signalling pathways. Presumably, the main signalling pathway, stimulating the expression of *ENA* genes, is the calcineurin pathway [109]. Upon increased external concentration of salts or in case of alkalization of the environment, the calcineurin pathway is triggered, resulting in dephosphorylation of transcription factor Crz1 by phosphatase calcineurin. Upon dephosphorylation, Crz1 is able to enter the nucleus and stimulate the expression of a great number of genes, including *ENA* genes, which contain two Crz1-binding sites within their promoters [110]. Alternatively, the Rim101 pathway, initiated by high external pH and salt stress, has also been shown to stimulate the expression of *ENA* genes by repression of the expression of Nrg1, a protein responsible for suppressing the expression of *ENA* genes [111]. Additionally, the Rim101 pathway also likely regulates the transition of Ena protein through the secretory pathway [84]. And finally, phosphatase Ppz1 has been suggested to negatively regulate the expression of *ENA* genes, as elevated levels of *ENA1* mRNA have been documented in the *ppz1* mutant strain [112].

Expression of *ENA* genes has also been observed to be regulated by the availability of certain nutrients, such as glucose and sources of nitrogen. Upon limited availability of glucose, Snf1 kinase inhibits transcription repressors Mig1 and Mig2, consequently leading to elevated expression of *ENA*

genes [113]. Lack of an appropriate source of nitrogen also leads to the stimulation of the expression of ENA genes, presumably through the TOR signalling pathway [114].

To summarise the putative interplay between Nha1 and Ena1, it seems to be dependent on the constant level of expression of Nha1 and very low basal expression of Ena1. Upon external stimulus, in form of salt stress, Nha1 is presumably rapidly activated by phosphorylation and ensures a certain degree of export of toxic cations, until the external signal is transferred, through multiple signalling pathways, into stimulation of expression of the Ena1. It is also important to note the presumed stimulation of expression of Ena1 by high pH, which is probably crucial, for under such circumstances, ergo absence of proper proton gradient, Nha1 is likely unable to fulfil its role effectively and therefore the expression of Ena1 is necessary.

1.6.4 Tok1

Another system participating in the maintenance of potassium homeostasis, by mediating its export, is the Tok1 channel. Unlike Nha1 and Ena1 however, Tok1 appears to be specific for potassium, making it the only potassium-specific transport system in *S. cerevisiae* [115]. *TOK1*, in *S. cerevisiae*, encodes a protein containing 691 amino acids assembled into, predicted, 8 transmembrane domains, four of which are transmembrane helices and the remaining four are contained within two MPM domains [84].

The primary function of Tok1 is the export of potassium, however, this channel appears to be open predominantly in case of depolarization of plasma membrane and therefore the main physiological role of Tok1 is the maintenance of proper membrane potential, rather than export of surplus potassium, as is the case of Nha1 and Ena1 [116]. This channel is likely also able to facilitate the uptake of potassium, as its overexpression in the *S. cerevisiae* strain lacking both Trk1 and Trk2 led to a partial rescue of the diminished growth of this mutant strain on limiting external potassium concentrations [117].

The gating of the Tok1 channel is presumably regulated by its C-terminal domain [118]. Additionally, external potassium concentration has also been shown to regulate the activity of Tok1, as well as, the high external concentration of salt, which might lead to Hog1-mediated phosphorylation of Tok1 with unknown consequences [103].

1.6.5 Pma1

Representing approximately 15% of the total amount of plasma membrane proteins and consuming up to 25 % of total cellular ATP [1], ATPase Pma1, responsible for the efflux of protons, is considered one of, if not the key transporter in yeasts. Pma1 belongs to the family of P-type ATPases and consumes ATP in order to facilitate the efflux of protons [119]. *PMA1* encodes a protein with a length of 918 amino acids, assembled into 10 transmembrane segments. The intracellular loop, between transmembrane segments 4 and 5 is phosphorylated during the cycle of proton export [120]. The genome of *S. cerevisiae* also contains the gene *PMA2*. Even though Pma2 is highly identical to Pma1 and is also able to export protons, the basal level of expression of this *PMA2* gene is very low and consequently, Pma2 has little effect on overall proton export [121].

The main function of Pma1 is an efflux of protons out of the cells and consequently regulation of both intracellular pH and membrane potential, but also the creation of an electrochemical proton gradient across the plasma membrane [1]. Both H⁺-gradient and proper membrane potential are essential for the uptake of the majority of nutrients, such as amino acids and phosphate, the uptake of which is mediated by H⁺-nutrient symporters [122,123] and ions, such as potassium, the uptake of which is presumably energized by the membrane potential [1].

The activity of Pma1 has been shown to be regulated by the presence of glucose through phosphorylation-dependent suppression of C-terminal domain-mediated autoinhibition. Upon elevation of external glucose concentration, Pma1 is phosphorylated by kinases Ptk2 or Hrk1 on its C-terminal end, disrupting the interaction of the C-terminal domain with the catalytic site of Pma1, thus stimulating the Pma1-mediated efflux of protons [124]. Several putative phosphorylation sites on the C-terminal end have been suggested, including Ser899, Ser911 and Thr912 [125,126]. Pma1 is also thought to be activated by low intracellular pH, however, the precise mechanism remains unclear [127].

It is important to note here, the previously documented substantial interdependence between the simultaneous activation of Pma1 and Trk1. The likely physiological nature of this functional connection is the need for balancing the increased uptake of potassium by elevated efflux of protons and vice versa, in order to maintain proper membrane potential [85]. The precise nature of this functional interplay or the existence of a signal triggering a similar regulatory effect on Pma1 and Trk1 is, hitherto, unknown.

1.6.6 Intracellular V-ATPase

Another crucial player in overall potassium homeostasis is an intracellular V-ATPase, responsible for the transport of protons from cytoplasm to vacuoles, Golgi apparatus and endosomes and consequently for acidification of their lumens [128]. Contrastingly to Pma1, V-ATPase is not a single polypeptide, but a rather large complex of proteins assembled into two main domains, the V_1 catalytic domain and the V_0 membrane-embedded domain [129].

Regulation of the activity of V-ATPase is dependent on reversible assembly, leading to activation and disassembly, resulting in the inactivation, of V_0 and V_1 domains [130]. This cycle has been shown to respond to the external concentration of glucose, external pH and also to salt stress [130], although much is to be discovered in order to unravel the precise regulatory process.

By facilitating the transport of protons into specific organelles, intracellular V-ATPase fulfils three main physiological roles. First, this ATPase participates in the regulation of cytosol pH by sequestering the protons into organelles [1]. Second, acidifying the lumen of organelles, enables the existence of pH-dependent processes within the vacuoles, for instance, enzymatic degradation of biological polymers [131]. And finally, the transport of protons into the lumen of organelles creates a proton gradient essential for the transport of various compounds, including potassium, from the cytoplasm into organelles via H^+/K^+ antiporters.

Similarly, as in the case of Trk1, also V-ATPase has been shown to exhibit coordinated activity with Pma1, a process most likely essential for maintaining proper pH in the cytoplasm. One could hypothesize, however, that this interdependence might also serve the overall homeostasis of potassium, for the elevated activity of Pma1 presumably leads to an increase Trk1-mediated potassium uptake and simultaneous stimulation of the activity of V-ATPase could, in theory, lead to stronger proton gradient across the membrane of vacuole and consequently increased capacity for storage of potassium.

1.7 14-3-3 proteins

According to a prediction software 14-3-3-Pred [132], the sequence of Trk1, in *S. cerevisiae*, contains a number of putative binding sites for interaction with a special group of regulatory proteins, the 14-3-3 proteins. Part of section 3.2 is therefore dedicated to the putative involvement of 14-3-3 proteins in the regulation of the activity of Trk1.

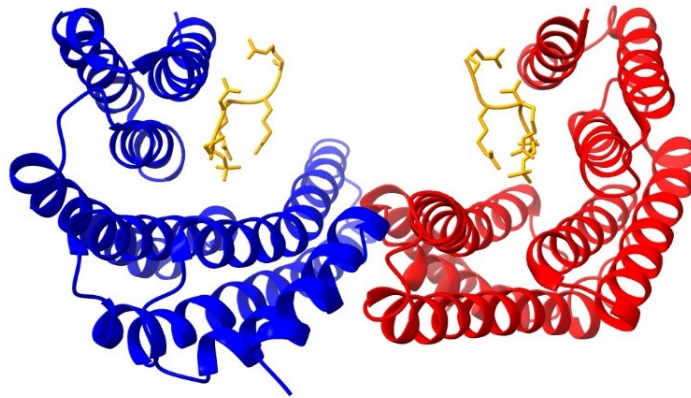


Figure 6. 3D structure of homodimer of human 14-3-3 isoform epsilon. Respective monomers are distinguished by red and blue colours. Peptides interacting with the binding site of each monomer are highlighted in orange. 3D structure was obtained from PDB-database, entry code 7C8E [133] and visualized using ChimeraX v1.1.

The 14-3-3 proteins are a family of highly conserved, regulatory proteins ubiquitously expressed in all eukaryotes, with a number of isoforms ranging from 2 in yeast [134] to 7 in mammals [135] and up to 12-15 in higher plants [136]. These proteins are acidic, small in mass, app. 30 kDa for a monomer, and able to form both homo- and heterodimers. Each respective monomer is capable of binding peptides containing phosphorylated serine or threonine within specific recognition motifs [137], although binding to non-phosphorylated peptides has been reported as well [138]. 14-3-3 proteins also exhibit a remarkable and distinctive degree of conservation, with over 50 % of sequence identity, not only across the species but also across the kingdoms of life [139]. Apart from the sequence, also functional conservation has been established in yeast, in which the lack of both native isoforms was successfully complemented by isoforms from higher plants [139].

Crystal structures of human isoforms revealed, in more detail, a general pattern of structure and function of 14-3-3 proteins [133,140,141]. Individual monomeric isoforms have a characteristic helical structure, consisting of 9 antiparallel α -helices, usually labelled H1-H9 [142]. As seen in Figure 6 (section 1.7), when forming a dimer, the orientation of monomers creates a typical cup-like shape, with a large central channel, in which both peptide-binding sites, one on each monomer, are located [133]. Binding sites are formed by helices H3, H5, H7 and H9, consequently, these helices exhibit the highest degree of conservation [142]. Several co-crystal structures of 14-3-3 proteins, interacting with synthetic phosphopeptides, are also available, revealing putative ionic interactions or formation of

hydrogen bonds between the phosphate group of a target protein and several highly conserved positively charged amino acids of a respective 14-3-3 monomer [142].

Lacking catalytic activity, the regulatory function of 14-3-3 proteins relies exclusively on the binding of the target, typically phosphorylated proteins. Consequences of this binding vary and define the precise mechanism by which 14-3-3 proteins regulate their specific target. First, the binding of 14-3-3 proteins to a target protein might lead to a conformational change in the target protein and consequently to an alternation in activity [142]. Alternatively, the interaction between 14-3-3 proteins and target proteins might lead to an occlusion of specific regulatory sequences within the target protein and in turn to either prevention of interaction of target protein with other proteins or DNA, alternations in activity or subcellular localization of target protein [143,144]). And finally, the interaction of each monomer of 14-3-3 dimer might facilitate protein-protein interaction of a specific tandem of partners [145].

14-3-3 proteins themselves are also subject to strict regulation by multiple distinct mechanisms. Even though most of the 14-3-3 proteins are being expressed constitutively, the expression of certain isoform in mammals and plants have been shown to be tissue-specific [146]. Additionally, the phosphorylation of 14-3-3 proteins has been established as an important mechanism governing dimerization, with phosphorylated monomers being substantially less prone to the formation of dimers [147]. Interaction with cofactors, such as AMP has been also suggested to regulate the 14-3-3 proteins by blocking their ability to bind their target proteins [148].

As several hundred interaction partners have been identified so far [149,150], the 14-3-3 proteins are involved in the regulation of essentially all types of cellular processes, ranging from metabolism [151] through cell division [152], tissue development and differentiation [153] to apoptosis [154] etc.

S. cerevisiae possesses two isoforms of 14-3-3 proteins, encoded by open reading frames *BMH1* and *BMH2*, with *BMH1* accounting for approximately 80 % of a total 14-3-3-expression [134]. Even though mutants with a deletion in either *BMH1* or *BMH2* are viable, suggesting an overlap in the function of individual isoforms, their combined deletion is lethal in most strains [155]. Similarly, as in the case of human and plant 14-3-3 proteins, several hundred interaction partners for both Bmh1 and Bmh2 have been identified [156] and consequently, their involvement in the regulation of essentially every major cellular process has been established [157].

1.8 *Kluyveromyces marxianus*

Historically, a dominant position in the fields of yeast microbiology and biotechnology has, undoubtedly, been occupied by the species *S. cerevisiae*, providing not only an effective model organism for research but being also suitable for use in fermentation and various other branches of biotechnology. However, with the availability of novel tools of microbiology and molecular biology and with the vast diversification of processes of biotechnological production, that goes way beyond simple beverage fermentation, there is a substantial need for the exploitation of yeast biodiversity in search of new biotechnologically-relevant species. Diverting the focus of biotechnological research from *S. cerevisiae* to other species led to the emergence of, so-called, non-conventional yeast species, including *Kluyveromyces marxianus*.

K. marxianus is a hemiascomycetous yeast, belonging to the family Saccharomycetaceae, closely phylogenetically related to both *S. cerevisiae* and *Kluyveromyces lactis*, however, both *K. lactis* and *K. marxianus* belong to a group of pre-WGD yeast, as opposed to post-WGD *S. cerevisiae* [158]. It is considered a homothallic yeast, existing as either mating type *MATa* or *MAT α* with the possibility of switching between these two types. This yeast is, likely, able to exist in both haploid and diploid forms, with preference seemingly being strain-specific [159].

As *K. marxianus* is closely related to *S. cerevisiae*, there is a propensity for extrapolation of knowledge from the study of the metabolism of *S. cerevisiae*, to predict analogous processes in *K. marxianus*, however, as proved by several studies, there are several specifics. *K. marxianus* is a respiro-fermentative yeast, able to employ both oxidative phosphorylation and fermentation in order to generate energy [160]. The balance between oxidative phosphorylation and fermentation seems to be strain-specific with some strains being able to perform these two processes simultaneously [161]. Unlike *S. cerevisiae*, however, this species is considered Crabtree negative, meaning that even under aerobic conditions and high external concentrations of glucose, *K. marxianus* does not necessarily resort to fermentation [162]. Nonetheless, as *K. marxianus* possesses genes necessary for fermentation, it is important to note an ongoing debate regarding the Crabtree status of *K. marxianus* and the possibility of this effect, again, being strain-specific [158].

What makes *K. marxianus* a particularly attractive organism is a variety of traits considered highly advantageous for utilization in many biotechnological processes. It is currently considered the fastest-growing eukaryotic organism, with a generation time being approximately 70 minutes [163]. Additionally, *K. marxianus* is highly thermotolerant, being able to grow at temperatures as high as 52 °C and survive in high-temperature bioreactors [164]. Another particularly favourable trait is the

ability to utilize a wide range of carbon sources, including i. a. glucose, raffinose, sucrose and lactose [165]. And finally, *K. marxianus* is capable of secretion of lytic enzymes, thus greatly expanding a portfolio of potential substrates used throughout biotechnological production [166].

All the above-mentioned characteristics led to the successful employment of *K. marxianus* in various subfields of biotechnology, from basic fermentation to more advanced high-value products. Concerning fermentation, *K. marxianus* has been widely used for the production of bioethanol [167], however, this process has been, to a large degree, limited by its relatively low ethanol tolerance, prompting several studies aimed at increase of ethanol tolerance through adaptive laboratory evolution [168,169]. Commercially most relevant current use of *K. marxianus* is the production of native enzymes, such as inulinase, β -galactosidases and pectinases, with inulinase being the most attractive of the three, as it commonly does not occur in other yeast species [158]. Additionally, this species is also applied in the food industry, for the production of cell wall mannoproteins, as natural emulsifiers [170], or various natural flavours and fragrance compounds [171]. Biosorption and bioaccumulative properties of *K. marxianus* are being utilized in environmental biotechnology and bioremediation, more specifically, biosorption of textile dyes [172], recovery and removal of heavy metals [173] and various sugars [174] from wastewater and also for the treatment of paper waste a sludge [175].

Since the majority of the research concerning *K. marxianus* has been, hitherto, driven by its potential for use in biotechnology, there is a noticeable contrast between its biotechnological potential and use and the actual knowledge regarding fundamental physiological processes occurring in this yeast species. The availability of a number of biochemical and microbiological tools applicable to *K. marxianus* (reviewed in [158]), opens up the possibility of redirecting part of the focus of applied to more basic research, with the aim of thorough characterisation of physiology and metabolism of species *K. marxianus*.

2. Aims of the thesis

Trk1, as a key player in yeast potassium homeostasis, has been extensively studied for a little over three decades. Even though a considerable amount of data has been collected regarding its role in yeast physiology, role in potassium uptake, secondary functions and even relevance regarding yeast biotechnology and antifungal therapy, there are still many aspects of Trk1's functionality that remain obscure or completely unknown. The presented dissertation thesis aimed to extend the knowledge about the transporter Trk1 from *S. cerevisiae* in three separate areas. Additionally, potassium-uptake systems in *K. marxianus* were studied as well.

Experimental aims were divided into sections, as follows:

- **Detailed characterisation of the ability of Trk1 to switch its affinity and maximum velocity as a reaction to changes in the availability of external potassium.**
- **Elucidation of the putative mechanism of regulation of Trk1 through phosphorylation.**
- **Study of the role of Trk1 and Trk2 in the survival of glucose-induced cell death and high temperature.**
- **Characterization of potassium-uptake systems in non-conventional species *Kluyveromyces marxianus*.**

3. Results

3.1 Yeast Trk1 Potassium Transporter Gradually Changes Its Affinity in Response to Both External and Internal Signals

Reference: Masaryk, J.; Sychrova, H. Yeast Trk1 Potassium Transporter Gradually Changes Its Affinity in Response to Both External and Internal Signals. *J. Fungi* **2022**, *8*, doi:10.3390/jof8050432. IF₂₀₂₂=5.266

Summary: One of the most intriguing abilities of Trk1 protein is the ability to modify its kinetic parameters for uptake based on the availability of external potassium. According to current literature, this process, often called affinity-switch, includes the transition from a low- to high-affinity state when cells are transferred from an environment with high external potassium concentration to an environment with severe potassium limitations. This transition includes a substantial increase in both affinity and maximum velocity of Trk1-mediated uptake. Even though this basic concept has been known for many years, there is a considerable lack of additional data regarding time course, precise dependence on external potassium concentration and the dominant signal driving the changes in kinetic parameters. Additionally, putative structural changes underlying the affinity switch are also unclear. The presented part of the dissertation thesis aimed to answer the aforementioned ambiguities, expand the knowledge about Trk1-mediated cellular reaction to potassium limitations and establish a putative mechanism that goes beyond simple switching between two affinity states.

Contrary to previously published data, we did not observe switching between low- and high-affinity states, but rather precise and gradual increase in both affinity and maximum velocity of Trk1-mediated uptake in accordance with the decrease in external potassium concentration, thus expanding the original 'affinity-switch' concept to a concept of 'affinity-adjustment'. This adjustment was fast and correlated with changes in both internal potassium concentration and membrane potential that accompany changes in external potassium levels, suggesting the involvement of additional signals in the regulation of kinetic parameters of Trk1. Additionally, we analysed a specific set of substitutions that prevented the complete increase in Trk1-mediated uptake upon exposure to potassium limitation. Substituted amino acids were localized within specific regions of Trk1 (P-helices) with the putative direct effect on the conformation of potassium binding site and region of the selectivity filter, suggesting the importance of this region in process of increase of affinity of the Trk1.



Even though a lot remains to be discovered about the role of Trk1 in cellular adaptation to potassium limitations, this work provided novel and valuable knowledge regarding the phenomenon of Trk1-mediated affinity-switch and allowed us to expand previously known concepts. Results were published in 2022 in the *Journal of Fungi*.

Essential practical and theoretical skills regarding measurements of Trk1-mediated uptake and calculation of kinetic parameters were obtained during my internship at the University of Córdoba in the laboratory of José Ramos.

Author's contribution: conceptualization, experimental work, data collection and analysis and writing of the original draft of the manuscript were all performed by the author of the thesis.

Article

Yeast Trk1 Potassium Transporter Gradually Changes Its Affinity in Response to Both External and Internal Signals

Jakub Masaryk  and Hana Sychrová *

Laboratory of Membrane Transport, Institute of Physiology, Czech Academy of Sciences,
142 20 Prague, Czech Republic; jakub.masaryk@fgu.cas.cz

* Correspondence: hana.sychrova@fgu.cas.cz

Abstract: Yeasts need a high intracellular concentration of potassium to grow. The main K^+ uptake system in *Saccharomyces cerevisiae* is the Trk1 transporter, a complex protein with four MPM helical membrane motifs. Trk1 has been shown to exist in low- or high-affinity modes, which reflect the availability of potassium in the environment. However, when and how the affinity changes, and whether the potassium availability is the only signal for the affinity switch, remains unknown. Here, we characterize the Trk1 kinetic parameters under various conditions and find that Trk1's K_T and V_{max} change gradually. This gliding adjustment is rapid and precisely reflects the changes in the intracellular potassium content and membrane potential. A detailed characterization of the specific mutations in the P-helices of the MPM segments reveals that the presence of proline in the P-helix of the second and third MPM domain (F820P and L949P) does not affect the function of Trk1 in general, but rather specifically prevents the transporter's transition to a high-affinity state. The analogous mutations in the two remaining MPM domains (L81P and L1115P) result in a mislocalized and inactive protein, highlighting the importance of the first and fourth P-helices in proper Trk1 folding and activity at the plasma membrane.

Keywords: cation homeostasis; *Saccharomyces cerevisiae*; potassium uptake; membrane potential



Citation: Masaryk, J.; Sychrová, H. Yeast Trk1 Potassium Transporter Gradually Changes Its Affinity in Response to Both External and Internal Signals. *J. Fungi* **2022**, *8*, 432. <https://doi.org/10.3390/jof8050432>

Academic Editors: Margarida Casal, Sandra Paiva and Isabel Soares-Silva

Received: 24 March 2022

Accepted: 20 April 2022

Published: 22 April 2022

Publisher's Note: MDPI stays neutral with regard to jurisdictional claims in published maps and institutional affiliations.



Copyright: © 2022 by the authors. Licensee MDPI, Basel, Switzerland. This article is an open access article distributed under the terms and conditions of the Creative Commons Attribution (CC BY) license (<https://creativecommons.org/licenses/by/4.0/>).

1. Introduction

A sufficient amount of intracellular potassium is a key prerequisite for yeast survival and growth. Due to its essential role in many cell processes, yeast cells accumulate potassium at an intracellular concentration of 200–300 mM, the highest of all cellular ions [1]. Since yeast cells are able to grow in a wide range of concentrations of external potassium (from a few μ M to more than 2.5 M), it is highly important that the capacity for the import and export of potassium is precisely adjusted, to maintain the internal potassium levels within optimal ranges. At their plasma membrane, yeast species employ an array of potassium uptake systems, differing in their structure and mode of action (uniporters Trk, K^+ -H⁺ symporter Hak1 and ATPase Acu1). Based on the genome sequencing of various yeasts, Trk uniporters seem to be the only transporters that exist in all species [2].

The genome of *S. cerevisiae* encodes two potassium transporters, Trk1 and Trk2. The gene encoding the Trk1 protein was first characterized by Gaber et al. [3]. Even though *TRK1* is a non-essential gene, its deletion leads to a sharp increase in potassium requirements and renders cells unable to grow in a low external potassium concentration. Therefore, Trk1 is considered the key player in potassium uptake in *S. cerevisiae*, and the highly similar Trk2 only plays a marginal role in potassium acquisition [4,5]. Trk1 is an integral plasma membrane protein consisting of 1235 amino acids and, based on its primary structure and function, it is ranked among the superfamily of K^+ transporters (SKT proteins), a conserved group of potassium and sodium transporters in yeast, bacteria and plants [6,7]. Trk1 is specific for potassium and rubidium; nevertheless, it has been shown that some sodium ions may enter via the Trk1 system, if the ratio between potassium and sodium cations in

the environment is higher than 1:700 [8]. Moreover, although Trk1 transports cations as a monomer, the protein is also believed to form tetramers in the yeast plasma membrane, and to mediate the efflux of chloride anions via the central pore of the tetramer [9].

While the structure of Trk1 remains experimentally unresolved, several Trk1 models based on the structures of KcsA potassium channel and other members of the SKT-proteins are available [10,11]. According to these models, Trk1 consists of four membrane-pore-membrane (MPM) motifs, each MPM motif includes two transmembrane helices connected by a short pore helix (P-helix), cf. Figure S1. The four MPM motifs are presumably assembled around the central axis, thus, creating a pore for the transport of potassium. In such an arrangement, P-helices are responsible for the structural integrity of the pore region and selectivity filter [11,12].

The most striking feature of Trk1 is the ability to modify its affinity for potassium according to the external availability of this cation. The potential of *S. cerevisiae* cells to quickly modify their capacity for potassium uptake has been known for many years [13]. This feature was assigned to Trk1 shortly after its identification as a key player in potassium uptake [3]. The original 'dual affinity' concept presumed a switching between low and high-affinity states as a reaction to transfer from an environment with high potassium concentration to an environment with severe potassium limitations [14]. Though the dominant regulatory role has been always attributed to the external potassium concentration, other regulatory signals, such as the depletion of internal potassium [15] or excess of external sodium [16], have also been suggested to play a role in Trk1's switching to a high-affinity state. Nonetheless, there is a considerable lack of knowledge beyond these simple concepts, regarding the precise mechanism and regulation of the affinity switch of the Trk1 protein.

So far, only one amino-acid residue has been suggested to play a significant role in the switching of Trk1 to its high-affinity state. Identified by random mutagenesis, the substitution L949P led to an incomplete increase in the affinity, as a response to the potassium limitations [17]. According to the latest Trk1 model [11], Leu949 is localized to the third P-helix. Neither additional data from follow-up experiments, nor any further information about the actual effect of the L949P substitution on Trk1's performance is available.

Due to the high internal concentration of potassium maintained in yeast cells, in most environments, potassium is imported against a concentration gradient and the uptake is thought to be energized by the plasma-membrane potential [18]. P-type H⁺-ATPase Pma1 is responsible for the extrusion of protons; thus, it plays a crucial role in the regulation of the internal pH and the creation of membrane potential [19]. Apart from enabling the energization of potassium uptake, additional levels of functional connection between Pma1 and Trk1 have been reported [20–23]. Their nature may be summarized as an interdependence of Pma1 and Trk1 activities and, more specifically, as a need to balance the export of protons by importing potassium and vice versa to maintain an appropriate membrane potential. The precise nature of the signal leading to the parallel increase or attenuation of the activities of Pma1 and Trk1 is currently unknown.

This study focuses on Trk1's ability to modify its affinity in accordance with the requirements of cells for potassium acquisition. As mentioned above, the basic knowledge of Trk1 existing in two affinity modes has been known for many years. However, it is almost impossible to extract a single concept of a mechanism of the changes in Trk1 affinity from all the published data, as strains with different genetic backgrounds and with various combinations of mutations were used in previous studies, as well as multiple types of growth media or substrates (K⁺, Rb⁺) and diverse experimental procedures. We, therefore, decided to focus our study on a detailed characterization of the changes in the affinity of Trk1 and its regulation and, more specifically, the time course of these changes, the role of external and internal potassium concentrations, as well as the possible involvement of membrane potential. Additionally, in order to unravel the effective mechanism of the affinity changes, we characterized in more detail the effect of L949P and analogous substitutions on the functionality of Trk1.

2. Materials and Methods

2.1. Strains and Growth Conditions

All strains used in this study are listed in Table S1. The yeast cultures were routinely grown at 30 °C in a standard YNB (0.67% YNB, 2% glucose) or a YNB-F (0.17% YNB-F, 2% glucose, 0.4% ammonium sulphate), which only contained 15 µM K⁺. The desired amount of KCl was added to the media, and the pH was adjusted to 5.8 using NH₄OH, before autoclaving. A mixture of auxotrophic supplements was added after autoclaving. For Rb⁺ uptake, intracellular K⁺ content and membrane potential measurements, yeast cells were grown overnight in a YNB, supplemented with 100 mM KCl to OD₆₀₀ 0.3–0.4, then harvested and used for measurements, or additionally incubated for various times in a YNB-F supplemented with the indicated concentrations of KCl.

2.2. Plasmids

The plasmids used in this study are listed in Table S2 and the oligonucleotides used for their construction and verification are listed in Table S3. To construct centromeric plasmids, the *CEN6ARS4* fragment from pRS316 was amplified by PCR, using the oligonucleotides 2µ-CEN6ARS4_for and 2µ-CEN6ARS4_rev. The resulting DNA fragment was used to replace the 2µ sequence in the linearized YE_p352- or pGRU1-derived plasmids via homologous recombination. Proper insertion was confirmed by diagnostic PCR. The plasmids that expressed Trk1 with amino-acid substitutions were constructed by site-directed mutagenesis (QuikChange II Site-Directed Mutagenesis Kit, Agilent Technologies, Santa Clara, CA, USA), using pCScTRK1 or pCScTRK1-GFP as templates. All substitutions were confirmed by sequencing.

2.3. Growth Assay

The growth of yeast cells was tested on solid media supplemented with 2% agar. The cells were pre-grown on YNB plates, supplemented with 100 mM KCl, and resuspended in sterile water to OD₆₀₀ 0.6. Serial 10-fold dilutions were prepared and 3 µL aliquots were spotted on YNB-F plates, supplemented with the indicated concentrations of alkali-metal-cation salts, and incubated at 30 °C. The representative results of at least three independent repetitions are shown.

2.4. Estimation of Kinetic Parameters for Rb⁺ Uptake

The yeast cells were grown and incubated as described above, collected, washed with sterile water and resuspended in 50 mL of MES buffer (20 mM MES, 2% glucose, 0.1 mM MgCl₂; pH adjusted to 5.8 with Ca(OH)₂) to OD₆₀₀ ~0.25. To measure the Rb⁺ uptake, RbCl was added to the cell suspension at time 0, and 5-mL samples were collected at 1 min intervals over 5 min. The samples were filtered through Millipore filters (0.8 µm pore size) and washed with 20 mM MgCl₂. The cells on filters were subsequently extracted overnight in an extraction buffer (0.2 M HCl, 10 mM MgCl₂, 0.2% KCl). The extracts were analyzed by atomic absorption spectrometry, and the initial rate of Rb⁺ uptake in nmoles per mg of dry weight of cells per minute was calculated [24]. Six different RbCl concentrations, ranging from 50 µM to 5 mM, were used for the potassium-starved cells, and six concentrations, ranging from 1 mM to 20 mM, for non-starved cells. For the estimation of the K_T and V_{max} kinetic parameters, the values corresponding to the initial rate of Rb⁺ uptake obtained for individual external Rb⁺ concentrations were plotted on a Lineweaver–Burk plot. For rough estimates of the kinetic parameters, only the 50 µM and 5 mM concentrations were used.

2.5. Measurements of K⁺ Content

The yeast cells were grown and incubated as described above, collected, washed with sterile water and resuspended in an MES buffer (20 mM MES, 2% glucose, 0.1 mM MgCl₂; pH adjusted to 5.8 with Ca(OH)₂) to OD₆₀₀ ~0.4. Three 1-mL samples were immediately withdrawn, filtered through Millipore filters (0.8 µm pore size), washed with 20 mM MgCl₂ and extracted overnight in a K⁺-free extraction buffer (0.2 M HCl, 10 mM MgCl₂). The

extracts were analyzed by atomic absorption spectrometry and the total K^+ content in nmoles per mg of dry weight of cells was calculated, as previously described [25].

2.6. Estimation of Relative Membrane Potential

A fluorescence assay, based on the potential-dependent redistribution of the probe diS-C3(3) (3,3'-dipropylthiacarbocyanine iodide), was used for the estimation of the relative membrane potential, as previously described [26]. Cells were grown and incubated as described above, washed with sterile water and resuspended in an MES buffer (20 mM MES, 0.1 mM $MgCl_2$; pH adjusted to 5.8 with $Ca(OH)_2$) to OD_{600} 0.2. The probe was added to a 2×10^{-8} M final concentration from a 10^{-4} M stock solution in ethanol. The fluorescence emission spectra ($\lambda_{ex} = 531$ nm and $\lambda_{em} = 560$ –590 nm) of the cell suspensions were measured in a Fluoromax 4 spectrofluorometer equipped with a Xenon lamp. The staining curves are presented as the time-dependent spectral shift of the wavelength maximum (λ_{max}) of diS-C3(3) fluorescence emission. Three independent measurements were performed for each strain and condition; either representative staining curves or mean values of λ_{max} reached after 50 min of staining are shown.

2.7. Fluorescence Microscopy

The yeast expressing GFP-tagged Trk1 versions were used for visualizing the subcellular localization of Trk1. Cells were either grown in a YNB supplemented with 100 mM KCl or in a YNB-F supplemented with various KCl concentrations to $OD_{600} \sim 1$, and visualized using an Olympus Bx53 microscope (Olympus, Hamburg, Germany) and captured with an Olympus DP73 camera (Olympus, Hamburg, Germany). The excitation of 460 nm and emission of 515 nm was used to visualize the GFP-tagged Trk1 proteins. Differential interference contrast (DIC) was used for the visualization of whole yeast cells.

2.8. Bioinformatics

Sequence alignment was performed using the multiple sequence alignment tool MUSCLE (EMBL-EBI, HINXTON, UK) with the default parameters. For the visualization of the positions of the substituted amino acids, the 3D atomic-scale model of *S. cerevisiae* Trk1 from reference [11] was used. The visualization was obtained using USFC ChimeraX version 1.1 (University of California, San Francisco, CA, USA) [27].

2.9. Statistics

All data were analyzed in Microsoft Excel 2010 (Microsoft, Prague, Czech Republic) or GraphPad Prism version 9.1.0. (GraphPad Software, San Diego, CA, USA), and *p*-values were calculated using the two-tailed Student's T-test. All experiments were performed at least three times and the mean values with standard deviation are shown.

3. Results

3.1. Role of Extracellular and Intracellular K^+ Content in Changes in Trk1 Affinity

To select the appropriate strain for the characterization of Trk1's kinetic parameters, we first compared the growth of five strains. The wild-type BY4741, which possesses chromosomally encoded *TRK1* and *TRK2* genes, and the BYT12 strain, which lacks both these genes, were transformed with the empty vector YCp352. The other three strains lacked the *TRK2* gene and expressed *TRK1*, either from its original chromosomal locus (BYT2 with the empty plasmid YCp352) or from centromeric (BYT12[pCScTRK1]) or multicopy (BYT12[pScTRK1]) plasmids, respectively. As shown in Figure 1A, the lack of both *TRK* genes rendered the cells unable to grow in media with low KCl concentrations. In addition, surprisingly, the expression of Trk1 from a multicopy plasmid (BYT12[pScTRK1]) resulted in significantly worse growth on limiting K^+ concentrations, compared to the other strains possessing *TRK1* genes. It is worth noting that most of the published results dealing with the characterization of Trk1 properties have so far been obtained with cells expressing Trk1 from various multicopy plasmids. As chromosomal *TRK1* is thought to be expressed at

a low and constitutive level, we decided to use the BYT12 strain (lacking chromosomal copies of both *TRK* genes), transformed with a centromeric plasmid containing the *TRK1* gene behind a well-characterized, weak and constitutive *NHA1* promoter. We believed that this approach would prevent possible changes in *TRK1* expression in a varying potassium environment and, thus, changes in Trk1 transport capacity.

Next, we confirmed that we could detect the dual affinity of Trk1, i.e., a much higher affinity in potassium-starved cells than in cells growing at high potassium concentrations (a YNB supplemented with 100 mM KCl). To estimate the kinetics of transport via Trk1, we employed the usually used potassium analogue rubidium ([8], cf. Materials and Methods). Figure 1B summarizes the obtained results and shows that starving cells for potassium in the YNB-F (with only 15 μ M KCl) for 3 h increased the affinity of Trk1 almost 10-fold, compared to non-starved cells (K_T ~290 and 2500 μ M, respectively), while the maximum velocity increased from 23.3 to 37.7 nmoles.mg⁻¹ min⁻¹.

To elucidate how the affinity changes with the length of potassium starvation, we estimated the kinetic parameters after 1 and 5 h of starvation. We found that the highest affinity was observed after only 1 h, and with prolonged incubation at low potassium conditions, it surprisingly slightly decreased, while the V_{max} increased over time, being about twice as large after 5 h as after 1 h (Figure 1C). To observe in more detail how quick the affinity change is, we measured the initial uptake of 50 μ M Rb⁺ immediately after transferring the cells to a starvation medium, and also after 5, 15, 30, 45 and 60 min. As shown in Figure 1D, the uptake of Rb⁺ was clearly measurable after only 5 min, which suggested that the lack of potassium is quickly sensed by the cell, and the affinity of Trk1 rapidly adapts to the new potassium conditions. The majority of previous studies that focused on the Trk1 affinity switch were performed after 3 h of potassium starvation; however, taking into account the results we obtained (Figure 1C,D), we decided to starve the cells for only 1 h in most of the following experiments.

Our first experiments confirmed the role of external potassium in the regulation of the kinetic parameters of Trk1. Whether directly or indirectly, the low concentration of external potassium upregulates Trk1's capacity to import potassium/rubidium. However, the exact dynamics of the dependence of the Trk1 transport capacity on the changes in the amount of external potassium is unclear. Considering the 'dual affinity' model, ergo, switching between low and high-affinity states, we assumed the existence of a threshold amount of external potassium above (or below), which the Trk1 protein would switch to one of the two states. In order to identify this threshold concentration, we measured the initial rates of either 50 μ M or 5 mM Rb⁺ uptake after 1 h of incubation in a YNB-F supplemented with 11 different concentrations of potassium, up to 100 mM. The obtained results are summarized in Figure 1E,F, respectively. Interestingly, we did not observe a sharp increase/decrease in the initial rates of Rb⁺ uptake upon incubation, in media supplemented with a specific concentration of potassium, i.e., a threshold concentration for the affinity switch, which we had expected according to the 'dual affinity' model. We instead detected a gradual change in the initial uptake rate depending on the availability of external potassium. The same course of gradual change of uptake was observed for both the low (50 μ M) and high (5 mM) concentrations of the substrate (Figure 1E,F). When the rough estimates of the kinetic parameters were calculated (Table 1), it was evident that both affinity and maximum velocity increased gradually, with the decrease in external potassium concentration. Trk1 exhibited its maximum capacity to import Rb⁺ after the incubation of cells in media supplemented with ≤ 0.1 mM KCl, and minimal capacity after incubation in media supplemented with ≥ 10 mM KCl. As a negative control, we used the same cells transformed with an empty vector, and the obtained results showed that the significant uptake of Rb⁺ was only observed in cells expressing Trk1 (Figure 1E,F).

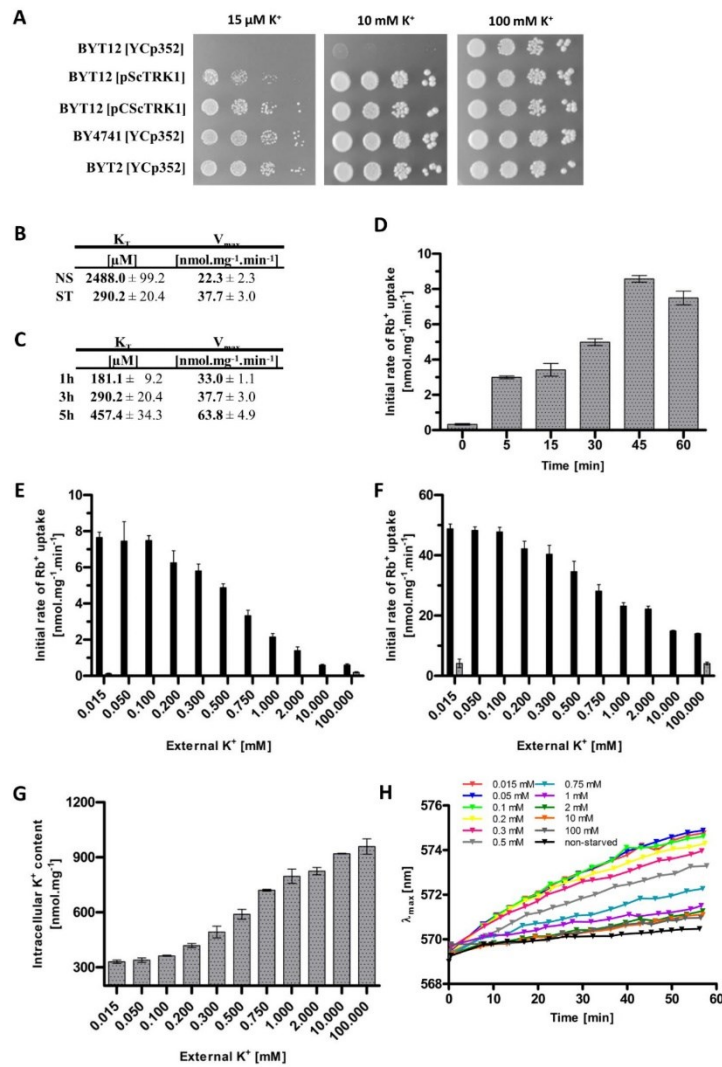


Figure 1. Changes in Trk1’s transport capacity, intracellular K^+ content and membrane potential upon shifts in external K^+ concentration. (A) Growth of strains BYT12 ($\text{trk1}\Delta \text{trk2}\Delta$), BY4741 wt and BYT2 ($\text{trk2}\Delta$), transformed either with the YCp352 empty vector, pScTRK1 multicopy vector or pCScTRK1 centromeric vector, on YNB-F plates supplemented with indicated concentrations of K^+ . Pictures were captured after 3 days of incubation at 30°C . (B) Kinetic parameters of rubidium uptake in potassium non-starved (NS) and starved (ST) cells. BYT12[pCScTRK1] cells were grown as described in Section 2. ST-cells were further incubated in a YNB-F ($15 \mu\text{M} \text{K}^+$, conditions of potassium starvation) for an additional 3 h. Rb^+ uptake was measured and kinetic parameters calculated as described in Section 2. (C) Time course of the changes in kinetic parameters of rubidium uptake. BYT12[pCScTRK1] cells were grown as in (B) and starved of potassium in YNB-F for 1, 3 and 5 h. The estimation of kinetic parameters was the same as in (B). (D) Initial rates of $50 \mu\text{M} \text{Rb}^+$ uptake in BYT12[pCScTRK1] cells within the first hour of K^+ starvation. Cells were grown overnight as in (B),

transferred to a YNB-F, and the uptake of Rb^+ was measured immediately and after 5, 15, 30, 45 and 60 min. (E) Initial rates of 50 μM Rb^+ uptake in BYT12[pCScTRK1] (black columns) and BYT12[YCp352] (grey columns) cells incubated in media with various K^+ concentrations for 1 h. Cells were grown as in (B) and then incubated in a YNB-F supplemented with the indicated concentrations of K^+ . (F) Initial rates of 5 mM Rb^+ uptake in BYT12 [pCScTRK1] (black columns) and BYT12 [YCp352] (grey columns). The experiment was performed as in (E). (G) Intracellular K^+ content in BYT12[pCScTRK1] cells after incubation for 1 h in YNB-F media with various K^+ concentrations. Cells were incubated as in (E), 3 aliquots of cell suspension were withdrawn immediately, and the concentration of K^+ was estimated as described in Section 2. (H) Relative membrane potential of BYT12[pCScTRK1] cells after incubation for 1 h in YNB-F media with various K^+ concentrations. Cells were grown overnight and incubated as in (E), then resuspended in an MES buffer, diS-C3(3) probe was added and the fluorescence emission spectra were measured. Staining curves are presented as the time-dependent spectral shift of the wavelength maximum (λ_{max}) of diS-C3(3) fluorescence emission. Non-starved cells (black curve) are cells probed without 1-h incubation in a YNB-F.

Table 1. Correlations among external K^+ concentration, intracellular K^+ content, membrane potential and kinetic parameters.

External K^+ [mM]	Intracellular K^+ [nmoles mg^{-1}]	λ_{max} [nm]	K_T [μM]	V_{max} [nmoles mg^{-1} min^{-1}]
0.015	330 ± 9	574.43	288.7	51.6
0.05	339 ± 12	574.59	290.8	51.0
0.1	363 ± 3	574.33	287.9	50.5
0.2	418 ± 11	574.05	309.4	44.8
0.3	492 ± 32	573.61	317.6	42.9
0.5	589 ± 26	572.94	328.4	36.9
0.75	720 ± 5	571.95	407.3	30.4
1	796 ± 39	571.22	547.6	25.7
2	824 ± 19	571.03	860.1	26.1
10	919 ± 2	570.92	1590.6	19.7
100	958 ± 41	570.85	1439.4	18.1

Summary of intracellular potassium concentrations, relative membrane potential (λ_{max} from curves in Figure 1H), and rough estimates of kinetic parameters K_T and V_{max} of Rb^+ uptake, obtained for cells incubated at external potassium concentrations, ranging from 15 μM to 100 mM.

Next, we wanted to estimate whether and how much the changes in the external potassium concentration affect the intracellular potassium content, and whether the changes in the intracellular potassium are reflected in the changes in the kinetic parameters. These experiments were based on the observation that the depletion of external potassium leads to a gradual loss of intracellular potassium content [28]. Figure 1G shows that the incubation of cells (pre-grown in the presence of 100 mM KCl) in a YNB-F supplemented with various external concentrations of potassium, for 1 hour, dramatically changed their intracellular potassium content; the lower the external concentration, the deeper the observed decrease in intracellular potassium content. By extrapolating the associations between the decrease in external potassium concentration and increase in Trk1 affinity on one hand, and the dependency of intracellular K^+ content on the extracellular potassium conditions on the other, we were able to highlight a possible relation between the intracellular potassium concentration and the regulation of Trk1 affinity. The external K^+ concentrations, at which we observed approximate maximal and minimal concentrations of intracellular potassium, closely correlated with the external K^+ concentrations, at which we detected the lowest and highest initial rates of Rb^+ uptake, respectively. After incubation in the presence of ≥ 10 mM KCl, we observed the maximum intracellular potassium content and minimal initial rate of Rb^+ uptake. Vice versa, after incubation in ≤ 0.1 mM KCl, we detected the lowest intracellular potassium content and measured the maximal initial rates of Rb^+ uptake (Figure 1E–G).

As Trk1 contributes to the maintenance of appropriate potential across the plasma membrane, changes in K^+ transport across the plasma membrane, and consequently potassium content, should be reflected in the changes in cell membrane potential. To confirm this presumption, we estimated the differences in relative membrane potential of cells pre-grown with 100 mM KCl and then incubated in a YNB-F supplemented with various KCl concentrations for 1 hour, similarly for the experiments summarized in Figure 1E–G. We monitored the changes in relative membrane potential with a potentiometric fluorescence probe and the obtained results (Figure 1H) confirmed our presumption. The incubation of cells in the presence of low KCl concentrations (15–100 μ M) led to the highest relative hyperpolarization, whereas increasing the external KCl concentrations (above 100 μ M) resulted in a more and more pronounced decrease in the relative membrane potential. We also observed a small difference in the relative membrane potential between the cells pre-grown in 100 mM KCl and probed directly, and the cells pre-grown in 100 mM KCl and transferred to a fresh YNB-F supplemented with 100 mM KCl for 1 h (black and dark grey curves in Figure 1H, respectively). This difference may serve as a positive control of our method, as it has been repeatedly shown that the transfer of cells to fresh media (with a higher concentration of glucose) leads to an immediate activation of Pma1, measurable as both an alkalization of the cytosol and as an increase in the relative membrane potential (e.g., references [29,30]). In summary, the use of a potentiometric probe confirmed our assumption that a change in the external/internal concentration of potassium, reflected in the changes in Trk1 affinity, correlates with the changes in the membrane potential.

According to all the results summarized in Table 1, Trk1 does not, in fact, switch between low- and high-affinity states, but rather the kinetic parameters slide along with the changes in the external and internal potassium concentrations and follow the changes in membrane potential, suggesting the possibility of up to three signals being involved in the regulation of Trk1's transport capacity.

Apart from the limitations in external potassium concentration, an elevated external concentration of sodium has also been suggested to provoke a high-affinity state of Trk1 [16]. To verify whether we could observe a change in Trk1 affinity upon the addition of salt, we measured the uptake of Rb^+ (50 μ M or 5 mM, respectively) in the presence/absence of NaCl. The cells were pre-grown with 100 mM KCl and incubated in a YNB-F supplemented with 1 mM KCl (to ensure a medium-affinity state of Trk1 in conditions w/o NaCl) and with/without 0.5 M NaCl for 1 hour. In contrast to previously published data [16], we detected no significant difference in the initial rates of 50 μ M Rb^+ uptake, and only a very small difference in the 5 mM Rb^+ uptake between cells incubated with and without NaCl (Figure 2). When we used the measured initial rates to calculate the rough estimates of K_T , the obtained values were very similar (approx. 550 μ M after incubation in 1 mM potassium and 630 μ M after incubation in 1 mM potassium + 0.5 M sodium). Our results did not confirm the increase in Trk1 affinity because of the exposure to a high concentration of toxic sodium in cells with the BY4741 genetic background.

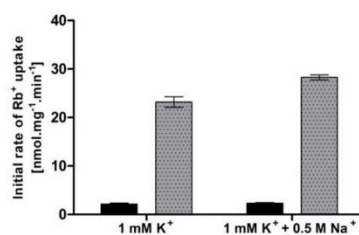


Figure 2. Effect of high external Na^+ concentration on Trk1-mediated Rb^+ uptake. BYT12 [pCScTRK1] cells were grown overnight as described in Section 2, and then incubated in a YNB-F supplemented with either 1 mM K^+ or 1 mM K^+ and 0.5 M Na^+ for 1 h. Initial rates of 50 μ M (black columns) and 5 mM (grey columns) Rb^+ uptake were measured, as described in Section 2.

3.2. *Trk1* Affinity Is Directly Proportional to the Level of Plasma-Membrane Potential

To characterize in more detail the regulatory signal for the aforementioned changes in *Trk1* capacity to import potassium, we decided to compare the kinetic parameters, intracellular potassium content and relative membrane potential of four strains, expressing *TRK1* under different conditions. These were BY4741[YCp352], BYT2[YCp352] with chromosomal copies of *TRK1*, and two BYT12 strains lacking chromosomal copies of both *TRK* genes and transformed with a centromeric (pCScTRK1) or multicopy (pScTRK1) plasmids, respectively. Although these strains exhibit differences in the ability to grow on low potassium (Figure 1A) and in some physiological parameters [25], we presumed that the fundamental mechanism of *Trk1* regulation should be similar; therefore, by extracting a common pattern of the correlation of the changes in the *Trk1* kinetic parameters and changes in either the intracellular potassium content or relative membrane potential, the dominant regulatory force could be identified.

The comparison of kinetic parameters yielded an unexpected degree of variety in *Trk1*'s affinity in both potassium non-starved cells and starved cells (Figure 3A). In non-starved cells (NS), the strains expressing *TRK1* from the chromosome (BY4741 and BYT2) exhibited a significantly higher affinity (K_T values $\sim 1000 \mu\text{M}$) than the strains expressing *TRK1* from plasmids (K_T around $2000 \mu\text{M}$ for the multicopy and around $2500 \mu\text{M}$ for the centromeric plasmids, respectively). The maximum velocity of rubidium uptake was similar in all four strains ($\sim 17\text{--}22 \text{ nmol}\cdot\text{mg}^{-1}\cdot\text{min}^{-1}$). In cells starved of potassium for 1 h (ST), we observed a similar K_T for cells expressing *TRK1* from the centromeric plasmid or chromosome (approx. $200 \mu\text{M}$), and a strikingly high affinity ($38 \mu\text{M}$) of *Trk1* in cells transformed with the multicopy pScTRK1 plasmid. In addition, we detected comparable V_{max} values, which were also surprising, as the V_{max} is predominantly determined by the total number of active transporters in the membrane. According to this principle, we would expect the V_{max} to be highest in the strain BYT12[pScTRK1]. We only observed an increase in the V_{max} of BY4741 cells, which could be attributed to a more pronounced contribution of the *Trk2* system under starvation conditions. The discrepancy between the observed changes in affinity and changes in maximum velocity suggested that these two parameters are regulated differently. In summary, our results clearly showed a difference in the intensity of the response to potassium starvation, mediated by an increase in the affinity of *Trk1*. While both strains expressing *Trk1* from a chromosome exhibited a comparable increase in affinity upon potassium starvation (5.0-fold for BY4741 and 5.2-fold for BYT2), in the BYT12[pCScTRK1] strain the *Trk1*'s affinity increased 13.7-fold, and *Trk1* in the BYT12[pScTRK1] strain exhibited a 51.5-fold increased affinity for Rb^+ (Figure 3A). The above-mentioned differences also contradicted the direct role of external potassium in the regulation of the affinity of *Trk1*. For all four strains, the external concentration of potassium was identical throughout the experiments (both overnight cultivation and the subsequent starvation period), but the values of K_T before and after potassium starvation were vastly different.

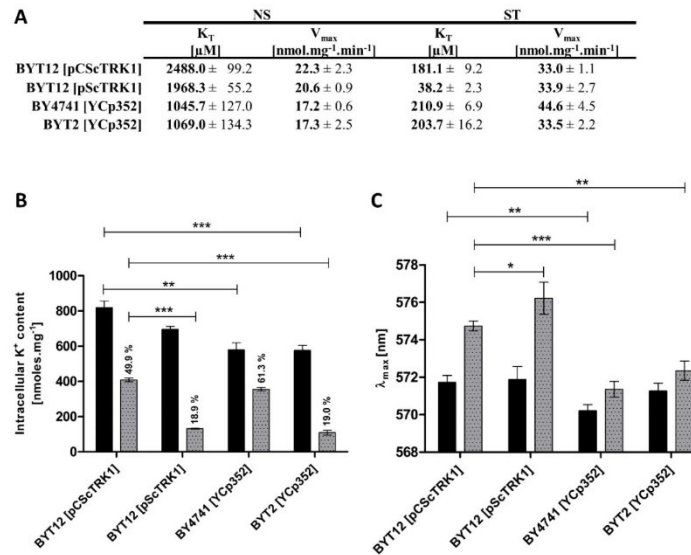


Figure 3. Differences in kinetic parameters, intracellular K^+ content and membrane potential among strains. Cells expressing *TRK1* either from chromosome (BY4741[YCp352] and BYT2 (*trk2Δ*)[YCp352]) or from centromeric (BYT12[pCScTRK1]) and multicopy plasmids (BYT12[pScTRK1]), respectively, were grown as described in Section 2, and used directly (non-starved (NS) cells) or first incubated in a YNB-F (15 μ M K^+ , conditions of potassium starvation) for 1 h (starved (ST) cells). (A) Differences in kinetic parameters of Rb^+ uptake. Initial uptake rates and kinetic parameters were estimated as in Figure 1B. (B) Intracellular K^+ content. Three aliquots of NS (black columns) or ST (grey columns) cell suspension were withdrawn and the concentration of K^+ in cells was estimated as described in Section 2. (C) Relative membrane potential. The membrane-potential measurement was performed as in Figure 1G with NS (black columns) and ST (grey columns) cells. The λ_{max} reached after 50 min of staining is shown for each strain. Significant differences in (B,C) are indicated with asterisks (* $p < 0.05$; ** $p < 0.01$; *** $p < 0.001$).

To distinguish whether the dominant role in the affinity level is played by the intracellular potassium content or membrane potential, we tested the correlation between the degree of changes in affinity and the degree of changes in intracellular potassium content and membrane potential in the four strains, after 1 h of potassium starvation. As shown in Figure 3B, the intracellular potassium content already exhibited some differences in non-starved cells, i.e., cells grown in the presence of 100 mM KCl (conditions under which the activity of Trk1 is dispensable; cf. Figure 1A, strain BYT12[YCp352]). The cells expressing Trk1 from plasmids (BYT12 [pCScTRK1] or [pScTRK1]) accumulated a higher amount of potassium (820 and 700 nmol/mg, respectively), compared to the 580 nmol/mg in strains BY4741 and BYT2 with chromosomal copies of *TRK1*.

Considering the possibility of the internal potassium content being the main determinant of the affinity of Trk1, the observed differences between the internal potassium content were in line with the differences in the affinity of non-starved cells (Figure 3A). Thus, the higher affinity detected in BY4741 and BYT2 strains could be a consequence of the accumulation of a lower amount of potassium in these cells. Nevertheless, the results obtained after one hour of potassium starvation disproved the general validity of this conclusion. Upon starvation, these were the cells expressing *TRK1*, either from a multicopy plasmid or cells with chromosomally encoded *TRK1* and lacking the *TRK2* gene, which similarly lost more than 80% of their intracellular potassium content (Figure 3B), but whose

affinity did not increase in a similar way (Figure 3A). This result contradicted the presumed major role of internal potassium in the regulation of the affinity of Trk1, but simultaneously revealed a novel observation that Trk2 contributes significantly to potassium acquisition in starving cells, plays a role in the regulation of intracellular potassium content (cf. V_{max} and K^+ content of BY4741 and BYT2 cells in Figure 3A,B, respectively), and its absence leads to a relative hyperpolarization of both non-starved and starved cells (Figure 3C).

Furthermore, we measured the changes in relative membrane potential in non-starved and starved cells. As shown in Figure 3C, the changes in λ_{max} (as an indicator of the level of the relative values of plasma-membrane potential) fully corresponded to the K_T changes during potassium starvation. Table 2 summarizes all the obtained results and shows a good correlation between the level of increase in membrane potential and the level of increase in Trk1's affinity.

Table 2. Correlation of changes in kinetic parameters and relative membrane potential upon 1 h of K^+ starvation.

	K_m [μ M]		
	NS	ST	K_T^{NS}/K_T^{ST}
BYT12 [pCScTRK1]	2488.0	181.1	13.7
BYT12 [pScTRK1]	1968.3	38.2	51.5
BY4741 [Y Cp352]	1045.7	210.9	5.0
BYT2 [Y Cp352]	1069.0	203.7	5.2
	λ_{max} [nm]		
	NS	ST	$\Delta\lambda_{max}^{ST-NS}$ [nm]
BYT12 [pCScTRK1]	571.73	574.74	3.01
BYT12 [pScTRK1]	571.89	576.22	4.33
BY4741 [Y Cp352]	570.21	571.36	1.15
BYT2 [Y Cp352]	571.27	572.35	1.08

In summary, the increase in membrane potential upon potassium starvation seems to play a dominant role in the regulation of changes in Trk1's affinity, and not the external or internal potassium content.

3.3. Role of Short P-Helices in Trk1 Activity and Affinity Adjustment

In the experiments described above, we focused on finding the potential regulator of Trk1's affinity at the cellular level. To further elucidate how the changes in affinity are interconnected with protein structure, we focused on characterizing the role of one of the Trk1 amino-acid residues (Leu949) in the affinity changes.

According to a 3D model of *S. cerevisiae* Trk1, Leu949 is localized approximately in the middle of a short P-helix (P3) of the third MPM motif, and is, thus, situated close to the region of the selective filter (SF) and potassium binding site (Figure 4A and reference [11]). We, therefore, assumed that the substitutions of Leu949 could have a significant effect on the conformation of helix P3 and consequently on the structure of the entire region of the selectivity filter, which could presumably affect potassium uptake as such. To more closely characterize not only the mutation L949P, but also the importance of leucine at this position, we performed site-directed mutagenesis replacing Leu949 with proline, alanine, glutamic acid, arginine, and serine. The BYT12 cells were transformed with the resulting plasmids (cf. Table S2), and the effects of these substitutions on the functionality, subcellular localization and kinetic parameters of Trk1 were studied.

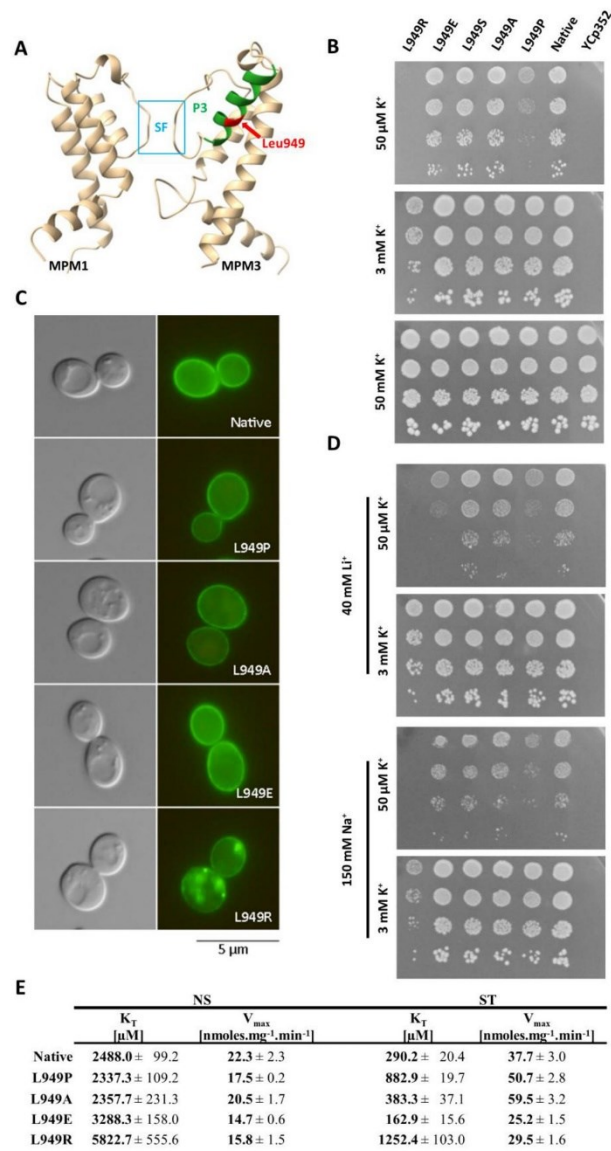


Figure 4. Effects of Leu 949 substitution. (A) Localization of Leu949 within a 3D model of Trk1 protein. P-helix 3 is shown in green, the position of Leu949 in P3 is highlighted in red, and the part of the selectivity filter (SF) in blue. For better clarity, only MPM domains 1 and 3 are shown. (B) Growth of BYT12 cells without *TRK1* (BYT12[YCp352]) or with centromeric vector harbouring *TRK1* (native) and its mutated versions on YNB-F plates supplemented with K⁺, as indicated. Images were captured after 5 days of incubation at 30 °C. (C) Localization of GFP-tagged Trk1 and its mutated versions in BYT12 cells. Cells were grown and viewed as described in Section 2. (D) Growth of cells on YNB-F plates supplemented with indicated concentrations of K⁺, Na⁺ and Li⁺. The order of strains and length of incubation were the same as in (B). (E) Kinetic parameters of native Trk1 and its mutated

versions after 3 h of K⁺ starvation. Cells were grown as described in Section 2. ST cells were incubated in a YNB-F for an additional 3 h. Rb⁺ uptake was measured and kinetic parameters were estimated as described in Materials and Methods.

The tests on the plates supplemented with various concentrations of potassium (Figure 4B) revealed that the growth of cells expressing the L949P version of Trk1 was significantly diminished at low potassium concentrations (50 μM; native Trk1 in high-affinity state), but not on plates supplemented with 3 mM KCl (native Trk1 with the affinity close to low-affinity state). This result was in line with the assumption that the substitution L949P specifically affected the increase in Trk1's affinity upon potassium limitations. We detected no or minimal changes in growth on 50 μM KCl for substitutions L949A, L949S and L949E, which led to the conclusion that the effect of L949P substitution is, in fact, caused by the introduction of proline, rather than the absence of leucine at position 949. Finally, the introduction of a positively charged Arg residue into position 949 led to a complete inhibition of growth on low potassium and significantly diminished growth on the plates supplemented with 3 mM KCl (Figure 4B).

As shown in Figure 4C, native Trk1-GFP together with the mutated versions L949P, L949A and L949E were localized primarily in the plasma membrane; therefore, the effects of these mutations could be attributed to the altered functionality of Trk1, rather than to the changes in subcellular localization. On the other hand, the introduction of positively charged arginine into position 949 led to a substantial alteration in Trk1's subcellular localization (Figure 4C). This effect was most likely due to defects in the folding of Trk1 and the subsequent partial retention within the secretory pathway, which in turn resulted in diminished Trk1 activity observed on a whole-cell level.

Some members of the SKT family of potassium transporters were shown to also transport small monovalent cations [31]. Thus, we further tested whether the introduced mutations could affect the size of the binding site and thereby change Trk1's strict substrate specificity, e.g., allowing the binding and transport of smaller Na⁺ and Li⁺ cations. Even though we detected a slight overall negative effect of the high external concentrations of Na⁺ and Li⁺ in the presence of low concentrations of potassium (50 μM) on the growth of all the tested strains (Figure 4D), the growth pattern was, in fact, similar to the pattern observed for the strains grown only in the presence of 50 μM KCl (Figure 4B,D). The apparent exceptions were cells expressing the Trk1 mutant L949E. The introduction of a negative charge led to an increased sensitivity to Li⁺ in the presence of low KCl (but not with 3 mM KCl), suggesting that when there is a sufficiently high ratio of external concentrations of Li⁺ and K⁺, the L949E version could possess an increased capacity to transport lithium, but not sodium (Figure 4D).

Finally, to complete the characterization of the Leu949 mutants and to confirm the effect of L949P substitution on Trk1 affinity, we estimated the kinetic parameters of the non-starved and starved cells (summarized in Figure 4E). The obtained results confirmed the inability of the L949P mutant to properly increase its affinity, since this version of Trk1 exhibited approximately three-fold higher K_T than the native form after starvation. Interestingly, in non-starved cells, the K_T values for the native and L949P versions were similar, showing that the substitution L949P did not disrupt the functionality of Trk1 as such, but rather specifically the ability to shift to a higher affinity upon potassium starvation. The kinetic parameters of the L949A mutant confirmed the negligible effect of this mutation observed in the drop tests. These results attributed all the negative effects of the L949P substitution to the introduction of a proline, rather than to the loss of a leucine in the 949 position. The results obtained for the L949R version also fully corresponded to the results of the drop tests. We detected a substantial decrease in the affinity of the mutated Trk1 in both non-starved and starved cells, suggesting that the introduction of a positive charge into position 949 has a generally negative effect on Trk1 activity (Figure 4E). We observed surprising effects on Trk1 affinity with the mutation L949E. Whereas the affinity of this mutant was significantly lower than that of the native Trk1 in non-starved cells

(K_T approx. 3300 vs. 2500 μM , respectively; Figure 4E), we detected the opposite effect of this mutation in starved cells, in which the affinity was approx. 160 μM , i.e., the highest of all experiments performed with Trk1 expressed from a centromeric plasmid (compare Figure 1B,C, 2B and 4E).

Our results confirmed that the introduction of proline in the P3-helix at position 949 negatively affects the proper increase in affinity as a response to potassium starvation, and showed that the introduction of charged amino acids in this position also changes the transport properties of Trk1.

As Trk1 contains four MPM domains, we decided to test the effects of similar mutations (the introduction of a prolyl residue) in the other three P-helices. The amino-acid residues for substitution were selected according to a sequence alignment of all four MPM domains (Figure 5A). The amino-acid residues corresponding to Leu949 were Leu81, Phe820 and Leu1115 (Figure 5B), and their replacement with proline was performed by site-directed mutagenesis of the *TRK1* gene in the pCScTRK1 and pCScTRK1-GFP plasmids, respectively (Table S2).

By testing the growth of the cells expressing mutated *TRK1* versions on plates supplemented with various concentrations of potassium, and by observing the subcellular localisation of GFP-tagged Trk proteins, we detected two distinct effects of proline introduction into P-helices. The introduction into P-helices number 1 and 4 (L81P and L1115P) led to a complete loss of cell ability to grow at low potassium concentrations (50 μM and 3 mM; Figure 5C). This growth inhibition was most likely due to an almost complete mislocalisation of these mutated versions of Trk1 (Figure 5D).

For the substitution F820P (MPM2), we observed effects similar to L949P. The cells expressing the F820P version were relatively sensitive to low potassium concentrations (Figure 5C), but the subcellular localization of this mutated Trk1 version remained unaltered (Figure 5D). The kinetic parameters of the F820P version in non-starved cells were comparable to those of the native and L949P versions, respectively (Figure 5E). For potassium-starved cells expressing Trk1 F820P, we observed a slightly higher inability to reach the maximum affinity than for the L949 version (Figure 5E). As the growth of cells expressing this version on low potassium was also slightly more inhibited than the growth of cells with the L949P version (Figure 5C), we concluded that the introduction of proline into P-helix 2 has an even more significant effect on Trk1's ability to increase its affinity, than the introduction of proline into P-helix 3.

As mentioned in previous sections, intracellular potassium content and membrane potential might play a role in the regulation of the changes in Trk1 kinetic parameters. To distinguish whether the mutations F820P and L949P prevent the increase in Trk1 affinity due to alterations in the transporter's functionality, or whether they disrupt overall potassium homeostasis, thus, affecting the regulatory signal for an increase in affinity, we estimated both the intracellular potassium content and relative membrane potential in non-starved and starved cells expressing the native and mutated versions, respectively. As shown in Figure 6, both the intracellular potassium content and accumulation of the potentiometric probe were almost the same in cells expressing either the native or F820P or L949P versions of Trk1. These results led us to conclude that the inability of Trk1, with the substitutions F820P and L949P, to properly increase its affinity upon potassium starvation is a consequence of the alterations in protein structure and functionality, rather than the absence of a regulatory signal.

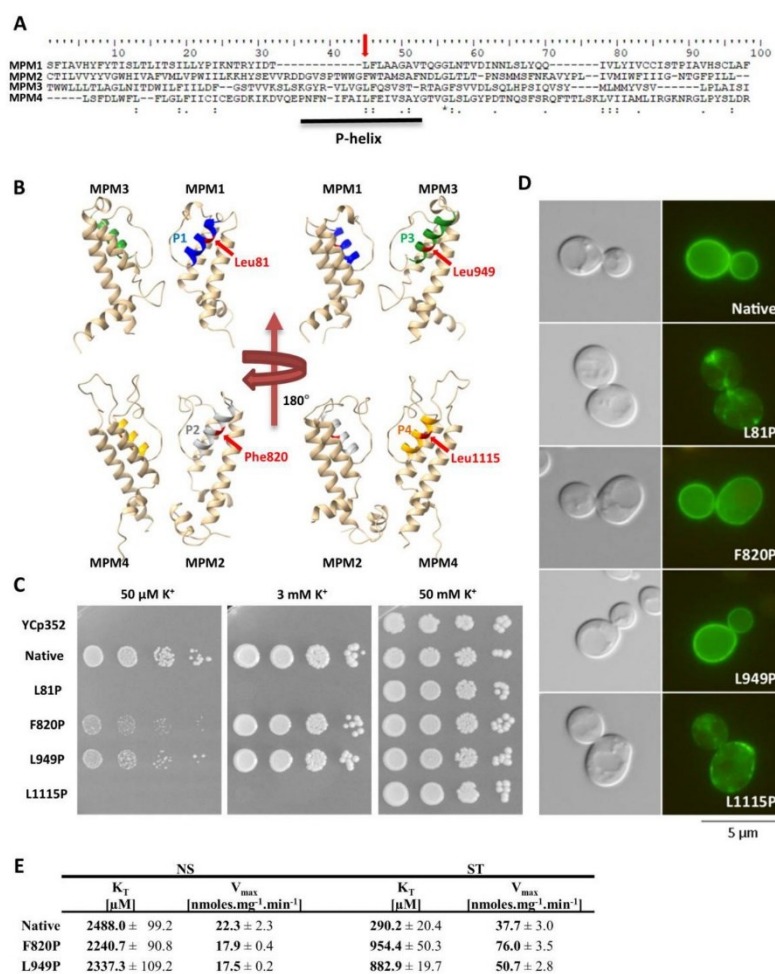


Figure 5. Effects of introduction of proline into P-helices. (A) Sequence alignment of Trk1’s MPM domains 1–4. Leu949 and corresponding amino acids in MPM 1, 2 and 4 are indicated with red arrows. P-helices within MPM domains are underlined. (B) Positions of amino acids Leu81, Phe820, Leu949 and Leu1115 within 3D model of Trk1 protein. P-helix 1 is highlighted in blue, 2 in grey, 3 in green and 4 in orange. Studied amino-acid residues are shown in red. For better clarity, only two opposing MPM domains are shown. (C) Growth of BYT12 cells without *TRK1* (BYT12 [YcP352]) or with centromeric vector harbouring *TRK1* (native) and its mutated versions on YNB-F plates supplemented with K^+ as indicated. Images were captured after 5 days of incubation at 30 °C. (D) Localisation of GFP-tagged Trk1 and its mutated versions in BYT12 cells. Cells were grown and viewed as described in Section 2. (E) Kinetic parameters of native Trk1 and its mutated versions after 3 h of K^+ starvation. Both non-starved (NS) and starved (ST) cells were grown as described in Section 2. ST cells were incubated in a YNB-F for an additional 3 h. Rb^+ uptake was measured and kinetic parameters were estimated as described in Section 2.

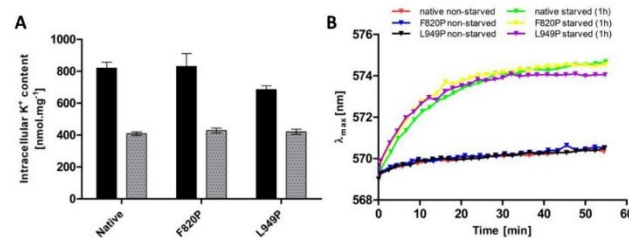


Figure 6. Intracellular K⁺ content and relative membrane potential in BYT12 cells with native, L949P and F820P Trk1 versions. Cells were grown as described in Materials and Methods, and used directly (non-starved cells), or first incubated in a YNB-F for 1h (starved cells). (A) Intracellular K⁺ content was estimated in non-starved (black columns) and starved (grey columns) cells as described in Section 2. (B) Relative membrane potential was estimated as described in Section 2.

4. Discussion

The central role of Trk1 in yeast potassium uptake has been known for many years, and its ability to switch its affinity according to the available potassium has been demonstrated many times. Even though a considerable amount of data has been generated in previous studies, a comprehensive picture of the regulation and mechanism of the affinity changes remains unavailable.

There are a few examples of transporters with the ability to switch their affinity for substrates. The most thoroughly described is the plant nitrate importer Nrt1.1. Upon a sharp decrease in external nitrate concentration, Nrt1.1 switches to a high-affinity state, simultaneously decreasing its K_T and V_{max} [32]. It is the phosphorylation of one threonyl residue (Thr101) that leads to a dissociation of the Nrt1.1 dimers with elevated structural flexibility and increased affinity of monomers for nitrate uptake [33–35]. While the common pattern, i.e., an increase in affinity as a result of the limited availability of substrate, seems to be similar between Nrt1.1 and Trk1, there are a couple of notable differences. First, the most significant difference between Nrt1.1 and Trk1 are the dynamics of the K_T changes. Nrt1.1 switches between only two affinity states, which has also been originally presumed for Trk1 [13,15]. However, according to our results, Trk1 does not switch between only two states, but rather gradually adjusts its affinity according to the availability of external potassium (Figure 1E,F and Table 1).

Second, in contrast to Nrt1.1, the Trk1's affinity change is accompanied by a significant increase in V_{max} . We observed the V_{max} in the high-affinity state to be almost double that of the V_{max} in the low-affinity state (Figure 1B). In addition, the time course of the V_{max} increase differs from the time course of the increase in affinity (Figure 1C), suggesting that the two processes are, at least, partially independent. The relative independence of the observed changes in both kinetic parameters is in contrast to the documented cases of the affinity switch of other transporters, in which the increase in affinity is accompanied by a significant decrease in maximum velocity [33,36,37]. The explanation of this phenomenon is that the high-affinity state leads to a stronger bond between the binding site and substrate, which in turn leads to an overall decrease in transport velocity. We cannot exclude the possibility that a similar phenomenon exists for Trk1, and that the high-affinity-induced decrease in maximum velocity is masked by the elevation in the number of active transporters in the membrane, as a reaction to potassium starvation. There are a few potential mechanisms for an increase in the number of active transporters—increased gene expression, stimulation of the Trk1 molecule passage from later stages of the secretory pathway to the plasma membrane, or the activation of previously inactive plasma-membrane transporters. The stimulation of gene expression is an unlikely explanation, as *TRK1* was expressed from a constitutive promoter. Additionally, the expression of chromosomally-encoded *TRK1* is not responsive to changes in external potassium levels [2,38]. The stimulation of the secretion

of transporters from the later stages of the secretory pathway [39] is again unlikely, as we did not observe a significant proportion of GFP-tagged Trk1 proteins to be retained in the secretory pathway in the high-potassium environment (Figure S2). Thus, the most likely explanation is the inactivity of a significant portion of proteins under high-potassium conditions and their gradual activation as a response to prolonged potassium starvation.

Taken together, our data demonstrate that the observed changes in whole-cell capacity to transport potassium, under conditions with a limited amount of this cation, consists of at least two partially independent events reflecting the availability of potassium, a gradual increase in Trk1's substrate affinity, and a gradual elevation of the number of active transporters in the plasma membrane. This is in sharp contrast with the simple Nrt1.1 switching between a low- V_{\max} -low- K_T and a high- V_{\max} -high- K_T state. As a consequence, the excessive increase in the uptake of nitrate via a high-affinity Nrt1.1 is prevented by a substantial decrease in V_{\max} . A similar regulation for Trk1, i.e., existence in only two states (either high affinity and high velocity or low affinity and low velocity) would only be favourable in environments with either extremely high or extremely low concentrations of potassium. In environments with a potassium concentration close to the presumed threshold for the affinity switch, sudden and small shifts in the availability of potassium would lead to a substantial increase or decrease in potassium uptake, and inevitably, to momentous disturbances in potassium homeostasis. The precise adjustment of both kinetic parameters of Trk1 described here would render yeast cells viable over a broad range of external potassium concentrations, and enable them, to a certain extent, to compensate for rapid changes in environmental potassium, without significant disturbances to their internal potassium balance.

The external potassium concentration has been considered to be a pivotal signal in the regulation of Trk1's affinity for a long time [13]. We confirmed this premise by observing a substantial decrease in K_T in cells starved of potassium, compared to non-starved cells (Figure 1B). The observed gradual increase in both the affinity and maximum velocity precisely copied the decrease in external potassium concentration (Figure 1E,F, Table 1). However, the assumption that Trk1 reacts exclusively and directly to the changes in the external potassium levels was contradicted by a comparison of the kinetic parameters and their changes in four strains cultivated and subsequently starved under the same conditions. The affinities and also the degree of changes in their Trk1 systems were vastly different (Figure 3A). We, therefore, conclude that, while the external potassium has an apparent effect on the uptake capacity of Trk1, this effect is indirect. Interestingly, in contrast to the values of K_T , the values of V_{\max} seemed to be mostly comparable among the four strains, supporting the hypothesis that the regulation of K_T and V_{\max} upon potassium starvation is separate (Figure 3A).

Another potential signal initiating the transition of Trk1 to the high-affinity state could be a decrease in the internal potassium concentration [15]. Our results, which exhibit a connection between a gradual loss of potassium and an increase in both the affinity and maximum velocity, support this presumption (Figure 1G and Table 1). The potential mechanism of such regulation of Trk1 should involve protein(s) with intracellular potassium-binding domains (possibly Trk1 itself), which would bind intracellular potassium with a frequency proportional to its internal concentration. The binding of potassium would lead to conformational changes that result in activity alterations. Potassium-sensing proteins have been reported, e.g., a small cytosolic protein in *E. coli* [40]. However, this mechanism of Trk1's affinity regulation is unlikely. Although potassium starvation leads to a loss of internal potassium in *S. cerevisiae*, presumably by export from the cytoplasm, the actual levels of potassium in the cytoplasm remain relatively stable, because they are constantly supplemented from potassium stocks in vacuoles [41]. Consequently, the intracellular domains of Trk1 are probably exposed to relatively constant amounts of cytosolic potassium; thus, the direct regulation of Trk1's affinity by the amount of potassium in the cytosol seems unlikely. In addition, more data that contradict the regulatory role of internal potassium came from the comparison of the four strains. Even though we detected

a comparable loss of internal potassium in strains BYT12[pScTRK1] and BYT2 [YCP352] upon potassium starvation (approx. 80%, Figure 3B), the values of K_T and their change also differed significantly (Figure 3A). Taken altogether, in addition to external potassium, our results also contradicted a direct role of internal potassium in the regulation of Trk1 affinity.

Finally, our data suggested another physiological parameter, membrane potential, as a regulator of Trk1's capacity to import potassium. As with internal potassium, we detected a substantial correlation between the increase in affinity and the maximum velocity of Trk1 and the relative hyperpolarization (Figure 1H and Table 1). The increase in membrane potential was not a mere consequence of potassium loss, but rather the regulatory force, as evidenced by the data obtained for the BYT2[YCP352] strain. Although this strain lost a comparable amount of potassium to BYT12[pScTRK1] (approx. 80%, Figure 3B) upon potassium starvation, it was, at the same time, significantly less hyperpolarized (Figure 3C, Table 2) and the increase in affinity of its Trk1 was much less pronounced than in the BYT12[pScTRK1] strain (approx. 5-fold compared to more than 50-fold, Table 2). The correlation between the affinity and membrane potential seems to be the only common pattern of regulation of Trk1's affinity among the four compared strains. As summarized in Table 2, the increase in affinity closely correlates with the degree of relative hyperpolarization upon potassium starvation. Thus, the dominant signal for increasing the affinity seems to be the level of plasma-membrane hyperpolarization.

The role of membrane potential in the Trk1's affinity confirms the possibility of a direct functional connection between Pma1 and Trk1. The interdependence of the export of protons and import of potassium on the whole-cell level has been known for a number of years [20–22], as well as the mutual dependence of Pma1 and Trk1 transport activities, e.g., reference [23]. Since Pma1 is the main creator of membrane potential in yeast cells, and its increased activity leads to the hyperpolarization of their plasma membranes, it is likely that Trk1 reacts directly to an increase in membrane potential, by increasing its capacity to import potassium, thus, balancing the export of protons. The elevated uptake of potassium could, at the same time, lead to a partial depolarization of the plasma membrane, thus, creating a negative feedback loop that would result in a gradual decrease in the uptake capacity of Trk1.

In the last part of our work, we focused on the putative structural changes that Trk1 undergoes during switching to the high-affinity state. As was mentioned in the Introduction, substitution L949P is the only mutation known to abolish Trk1's switch to the high-affinity state [17]. In accordance with the published information, our cells expressing the L949P version of Trk1 were specifically susceptible to a very low external concentration of potassium (Figure 4B), and exhibited a severe impairment in switching to the high-affinity state (Figure 4E). To distinguish between the effects of the absence of leucine in position 949 and the introduction of proline, we constructed several additional Trk1 versions. The mutations L949A and L949S had almost no effect on cell growth and kinetic parameters (Figure 4B,E for L949A). These data led us to believe that the effects of the L949P mutation are caused by the introduction of proline, rather than the absence of leucine. Prolines induce distortion in α -helices, as their cyclic side chains introduce a local break (Pro kink). Thus, a prolyl residue introduces a flexible point in the P-helix, which seems to be of both structural and functional importance. The Leu949 residue is located within the P-helix of the third MPM Trk1 domain. The P-helices of the four MPM domains are thought to have a substantial effect on the conformation of the pore and selectivity filter in models of Trk1, other SKT proteins and the KcsA channel [11,12,42]. The introduction of proline into this short helix in Trk1 might potentially lead to a disruption of the conformation of the helix, and consequently to a disruption of the entire pore region. It is, however, striking how this putative local structural change only affects Trk1's performance in the high-affinity state and has little to no effect on the low-affinity state (Figure 4E). This discrepancy strongly suggests that the entire region, presumably affected by this substitution, might be in a substantially different conformation in the low- and high-affinity states. It is also interesting that this mutation has no effect on the growth of cells on the plates supplemented with

high concentrations of lithium and sodium (Figure 4D) and, therefore, probably no effect on the selectivity of Trk1.

The replacement of Leu949 with charged amino-acid residues also gave interesting results. The introduction of a negative charge led to a decrease in affinity in the low-affinity state, but also surprisingly to an increase in affinity and decrease in V_{\max} in the high-affinity state, and to diminished growth in the presence of a high external Li^+/K^+ ratio, compared to cells with native Trk1 (Figure 4D,E). The lower K_T upon potassium starvation can be explained by an elevated local concentration of potassium, due to the presence of a negatively charged glutamic acid in proximity to the pore, and the decrease in V_{\max} by a stronger bond between the substrate and high-affinity binding site, similarly described for Nrt1.1 (cf. above and [33]). There could be a similar explanation for the diminished growth upon a high external concentration of lithium. The elevated local concentration increases the chance of lithium being imported non-specifically through Trk1. It is, however, unclear why we have not detected a similar effect for a high external concentration of sodium. The opposite effects of glutamic acid at position 949 on affinity in the low- and high-affinity states again point to the possibility of this region adopting different conformations when in one of the states, as opposed to the other. The negative effect on affinity in the low-affinity state might possibly be caused by the structural impairment of the pore region in this conformational state.

The replacement of Leu949 with positively charged arginine led to significantly diminished growth under all the tested conditions, accompanied by a decrease in affinity in both states. The presence of a positive charge in proximity to the pore region might create an electrostatic barrier to the entrance of potassium ions. Moreover, the observed mislocalization of the L949R version suggests that this mutation also prevents the proper folding and targeting of Trk1 to the plasma membrane (Figure 4C).

When similar mutations were introduced to the other three P-helices (Figure 5), the substitutions L81P and L1115P led to the almost complete abolishment of Trk1's functionality (Figure 5C), most likely as a consequence of a severe mislocalization of these Trk1 versions (Figure 5D). A number of putative interactions between the amino-acid residues located within the first and fourth MPM domains exist according to the Trk1 model, some of them in the vicinity of L81 and L1115 residues [11]. It is likely that these interactions are disrupted upon the introduction of the proline, and consequently the Trk1 protein is not properly folded. On the other hand, we detected effects similar to the L949P substitution for the F820P substitution in the second MPM domain (Figure 5)—diminished growth on low potassium, an incomplete switch to a high-affinity state and proper localization. As no substantial differences were observed in potassium content or relative membrane potential between the cells expressing the two mutants and the native Trk1 (Figure 6), the signal for a proper affinity switch is similar in all of them, and the observed incomplete switch of the mutated variants to the high-affinity state is most likely a consequence of the structural changes to Trk1.

5. Conclusions

In conclusion, our study disproved the concept of a dual-affinity mode of Trk1, and demonstrated that *S. cerevisiae* cells react to potassium conditions by a rapid, continuous and precise adjustment of both the affinity and maximum velocity of their Trk1 proteins. Additionally, we identified a novel important player that participates in the regulation of Trk1's affinity, membrane potential. The characterization of Trk1 variants with specific mutations suggested structural changes in its pore region, during the transition to the high-affinity state. As the uptake of potassium via Trk1 is involved in yeast cell tolerance to various stresses, e.g., ethanol [43], acidic pH [44,45] or high ammonium [46], and in the virulence of pathogenic yeasts [47], a thorough description of the mechanism and regulation of the changes in Trk1's uptake capacity is an important step towards understanding the complex mechanisms underlying yeast performance in various biotechnological (often adverse) processes, and also towards the development of new antifungal drugs.

Supplementary Materials: The following supporting information can be downloaded at: <https://www.mdpi.com/article/10.3390/jof8050432/s1>. Table S1: list of yeast strains; Table S2: list of plasmids; Table S3: list of used oligonucleotides; Figure S1: schematic representation of the predicted transmembrane topology of ScTrk1; Figure S2: localization of GFP-tagged Trk1. References [48–50] are cited in the Supplementary Materials.

Author Contributions: Conceptualization, J.M. and H.S.; methodology, J.M.; formal analysis, H.S.; investigation, J.M.; resources, H.S.; writing—original draft preparation, J.M.; writing—review and editing, H.S.; supervision, H.S.; project administration, H.S.; funding acquisition, H.S. All authors have read and agreed to the published version of the manuscript.

Funding: This research was funded by the Czech Science Foundation, grant number 20-04420S.

Institutional Review Board Statement: Not applicable.

Informed Consent Statement: Not applicable.

Data Availability Statement: Not applicable.

Acknowledgments: We thank Olga Zimmermannová for the critical reading of the manuscript, Marie Kodedová for the advices on the membrane-potential measurements, Klára Papoušková for pScTRK1 and Jost Ludwig for the PDB-file of the Trk1 model.

Conflicts of Interest: The authors declare no conflict of interest. The funders had no role in the design of the study; in the collection, analyses, or interpretation of data; in the writing of the manuscript, or in the decision to publish the results.

References

- Arino, J.; Ramos, J.; Sychrova, H. Alkali metal cation transport and homeostasis in yeasts. *Microbiol. Mol. Biol. Rev.* **2010**, *74*, 95–120. [[CrossRef](#)] [[PubMed](#)]
- Arino, J.; Ramos, J.; Sychrova, H. Monovalent cation transporters at the plasma membrane in yeasts. *Yeast* **2019**, *36*, 177–193. [[CrossRef](#)] [[PubMed](#)]
- Gaber, R.; Styles, C.; Fink, G. *TRK1* encodes a plasma membrane protein required for high-affinity potassium transport in *Saccharomyces cerevisiae*. *Mol. Cell. Biol.* **1988**, *8*, 2848–2859. [[CrossRef](#)] [[PubMed](#)]
- Ko, C.; Gaber, R. *TRK1* and *TRK2* encode structurally related K⁺ transporters in *Saccharomyces cerevisiae*. *Mol. Cell. Biol.* **1991**, *11*, 4266–4273. [[CrossRef](#)] [[PubMed](#)]
- Bertl, A.; Ramos, J.; Ludwig, J.; Lichtenberg-Frate, H.; Reid, J.; Bihler, H.; Calero, F.; Martinez, P.; Ljungdahl, P. Characterization of potassium transport in wild-type and isogenic yeast strains carrying all combinations of *trk1*, *trk2* and *tok1* null mutations. *Mol. Microbiol.* **2003**, *47*, 767–780. [[CrossRef](#)]
- Durell, S.; Hao, Y.; Nakamura, T.; Bakker, E.; Guy, H. Evolutionary relationship between K⁺ channels and symporters. *Biophys. J.* **1999**, *77*, 775–788. [[CrossRef](#)]
- Diskowski, M.; Mikusevic, V.; Stock, C.; Hanelt, I. Functional diversity of the superfamily of K⁺ transporters to meet various requirements. *Biol. Chem.* **2015**, *396*, 1003–1014. [[CrossRef](#)]
- Rodriguez-Navarro, A. Potassium transport in fungi and plants. *Biochim. Biophys. Acta* **2000**, *1469*, 1–30. [[CrossRef](#)]
- Rivetta, A.; Slayman, C.; Kuroda, T. Quantitative Modeling of chloride conductance in yeast TRK potassium transporters. *Biophys. J.* **2005**, *89*, 2412–2426. [[CrossRef](#)]
- Durell, S.; Guy, H. Structural models of the KtrB, TrkH, and Trk1,2 symporters based on the structure of the KcsA K⁺ channel. *Biophys. J.* **1999**, *77*, 789–807. [[CrossRef](#)]
- Zayats, V.; Stockner, T.; Pandey, S.; Wortz, K.; Etrich, R.; Ludwig, J. A refined atomic scale model of the *Saccharomyces cerevisiae* K⁺-translocation protein Trk1p combined with experimental evidence confirms the role of selectivity filter glycines and other key residues. *Biochim. Biophys. Acta* **2015**, *1848*, 1183–1195. [[CrossRef](#)] [[PubMed](#)]
- Doyle, D.; Morais, C.; Pfuetzner, R.; Kuo, A.; Gulbis, J.; Cohen, S.; Chait, B.; MacKinnon, R. The structure of the potassium channel: Molecular basis of K⁺ conduction and selectivity. *Science* **1998**, *280*, 69–77. [[CrossRef](#)] [[PubMed](#)]
- Rodriguez-Navarro, A.; Ramos, J. Dual system for potassium transport in *Saccharomyces cerevisiae*. *J. Bacteriol.* **1984**, *159*, 940–945. [[CrossRef](#)] [[PubMed](#)]
- Ramos, J.; Contreras, P.; Rodriguez-Navarro, A. A potassium transport mutant of *Saccharomyces cerevisiae*. *Arch. Microbiol.* **1985**, *143*, 88–93. [[CrossRef](#)]
- Ramos, J.; Rodriguez-Navarro, A. Regulation and interconversion of the potassium transport systems of *Saccharomyces cerevisiae* as revealed by rubidium transport. *Eur. J. Biochem.* **1986**, *154*, 307–311. [[CrossRef](#)]
- Ramos, J.; Haro, R.; Rodriguez-Navarro, A. Regulation of potassium fluxes in *Saccharomyces cerevisiae*. *Biochim. Biophys. Acta* **1990**, *1029*, 211–217. [[CrossRef](#)]

17. Haro, R.; Rodriguez-Navarro, A. Molecular analysis of the mechanism of potassium uptake through the Trk1 transporter of *Saccharomyces cerevisiae*. *Biochim. Biophys. Acta* **2002**, *1564*, 114–122. [[CrossRef](#)]
18. Cyert, M.; Philpott, C. Regulation of cation balance in *Saccharomyces cerevisiae*. *Genetics* **2013**, *193*, 677–713. [[CrossRef](#)]
19. Zhao, P.; Zhao, C.; Chen, D.; Yun, C.; Li, H.; Bai, L. Structure and activation mechanism of the hexameric plasma membrane H⁺-ATPase. *Nat. Commun.* **2021**, *12*, 6439. [[CrossRef](#)]
20. Yenush, L.; Mulet, J.; Arino, J.; Serrano, R. The Ppz protein phosphatases are key regulators of K⁺ and pH homeostasis: Implications for salt tolerance, cell wall integrity and cell cycle progression. *EMBO J.* **2002**, *21*, 920–929. [[CrossRef](#)]
21. Yenush, L.; Merchan, S.; Holmes, J.; Serrano, R. pH-Responsive, Posttranslational Regulation of the Trk1 Potassium Transporter by the Type 1-Related Ppz1 Phosphatase. *Mol. Cell. Biol.* **2005**, *25*, 8683–8692. [[CrossRef](#)] [[PubMed](#)]
22. Martinez-Munoz, G.; Kane, P. Vacuolar and plasma membrane proton pumps collaborate to achieve cytosolic pH homeostasis in yeast. *J. Biol. Chem.* **2008**, *283*, 20309–20319. [[CrossRef](#)] [[PubMed](#)]
23. Navarrete, C.; Petrezselyova, S.; Barreto, L.; Martinez, J.; Zahradka, J.; Arino, J.; Sychrova, H.; Ramos, J. Lack of main K⁺ uptake systems in *Saccharomyces cerevisiae* cells affects yeast performance in both potassium-sufficient and potassium-limiting conditions. *FEMS Yeast Res.* **2010**, *10*, 508–517. [[CrossRef](#)] [[PubMed](#)]
24. Zimmermannova, O.; Felcmanova, K.; Rosas-Santiago, P.; Papouskova, K.; Pantoja, O.; Sychrova, H. Erv14 cargo receptor participates in regulation of plasma-membrane potential, intracellular pH and potassium homeostasis via its interaction with K⁺-specific transporters Trk1 and Tok1. *Biochim. Biophys. Acta* **2019**, *1866*, 1376–1388. [[CrossRef](#)]
25. Petrezselyova, S.; Ramos, J.; Sychrova, H. Trk2 transporter is a relevant player in K⁺ supply and plasma-membrane potential control in *Saccharomyces cerevisiae*. *Folia Microbiol.* **2011**, *56*, 23–28. [[CrossRef](#)]
26. Kodedova, M.; Sychrova, H. Changes in the sterol composition of the plasma membrane affect membrane potential, salt tolerance and the activity of multidrug resistance pumps in *Saccharomyces cerevisiae*. *PLoS ONE* **2015**, *10*, e0139306. [[CrossRef](#)]
27. Goddard, T.; Huang, C.; Meng, E.; Pettersen, E.; Couch, G.; Morris, J.; Ferrin, T. UCSF ChimeraX: Meeting modern challenges in visualization and analysis. *Protein Sci.* **2018**, *27*, 14–25. [[CrossRef](#)]
28. Herrera, R.; Alvarez, M.; Gelis, S.; Kodedova, M.; Sychrova, H.; Kschischo, M.; Ramos, J. Role of *Saccharomyces cerevisiae* Trk1 in stabilization of intracellular potassium content upon changes in external potassium levels. *Biochim. Biophys. Acta* **2014**, *1838*, 127–133. [[CrossRef](#)]
29. Orij, R.; Bruhl, S.; Smits, G. Intracellular pH is a tightly controlled signal in yeast. *Biochim. Biophys. Acta* **2011**, *1810*, 933–944. [[CrossRef](#)]
30. Zahumensky, J.; Janickova, I.; Drietomska, A.; Svenkrtova, A.; Hlavacek, O.; Hendrych, T.; Plasek, J.; Sigler, K.; Gaskova, D. Yeast Tok1p channel is a major contributor to membrane potential maintenance under chemical stress. *Biochim. Biophys. Acta* **2017**, *1859*, 1974–1985. [[CrossRef](#)]
31. Hanelt, I.; Tholema, N.; Kroning, N.; Vor der Bruggen, M.; Wunnicke, D.; Bakker, E. KtrB, a member of the superfamily of K⁺ transporters. *Eur. J. Cell. Biol.* **2011**, *90*, 696–704. [[CrossRef](#)] [[PubMed](#)]
32. Parker, J.; Newstead, S. Molecular basis of nitrate uptake by the plant nitrate transporter NRT1.1. *Nature* **2014**, *507*, 68–72. [[CrossRef](#)] [[PubMed](#)]
33. Liu, K.; Tsay, Y. Switching between the two action modes of the dual-affinity nitrate transporter Chl1 by phosphorylation. *EMBO J.* **2003**, *22*, 1005–1013. [[CrossRef](#)] [[PubMed](#)]
34. Tsay, Y. How to switch affinity. *Nature* **2014**, *507*, 44–45. [[CrossRef](#)]
35. Sun, J.; Zheng, N. Molecular mechanism underlying the plant Nrt1.1 dual-affinity nitrate transporter. *Front. Physiol.* **2015**, *6*, 386. [[CrossRef](#)]
36. Reifenberger, E.; Boles, E.; Ciriacy, M. Kinetic characterization of individual hexose transporters of *Saccharomyces cerevisiae* and their relation to the triggering mechanisms of glucose repression. *Eur. J. Biochem.* **1997**, *245*, 324–333. [[CrossRef](#)]
37. Fu, H.; Luan, S. AtKUP1: A dual-affinity K⁺ transporter from *Arabidopsis*. *Plant Cell.* **1998**, *10*, 63–73. [[CrossRef](#)]
38. Ruiz-Castilla, F.; Bieber, J.; Caro, G.; Michan, C.; Sychrova, H.; Ramos, J. Regulation and activity of CaTrk1, CaAcu1 and CaHak1, the three plasma membrane potassium transporters in *Candida albicans*. *Biochim. Biophys. Acta* **2021**, *1863*, 183486. [[CrossRef](#)]
39. Capera, J.; Serrano-Novillo, C.; Navarro-Pérez, M.; Cassinelli, S.; Felipe, A. The potassium channel odyssey: Mechanisms of traffic and membrane arrangement. *Int. J. Mol. Sci.* **2019**, *20*, 734. [[CrossRef](#)]
40. Ashraf, K.; Josts, I.; Moshbahi, K.; Kelly, S.; Byron, O.; Smith, B.; Walker, D. The potassium binding protein Kbp is a cytoplasmic potassium sensor. *Structure* **2016**, *24*, 741–749. [[CrossRef](#)]
41. Herrera, R.; Alvarez, M.; Gelis, S.; Ramos, J. Subcellular potassium and sodium distribution in *Saccharomyces cerevisiae* wild-type and vacuolar mutants. *Biochem. J.* **2013**, *454*, 525–532. [[CrossRef](#)] [[PubMed](#)]
42. Levin, E.; Zhiu, M. Recent progress on the structure and function of the TrkH/KtrB ion channel. *Curr. Opin. Struct. Biol.* **2014**, *27*, 95–101. [[CrossRef](#)] [[PubMed](#)]
43. Lam, F.; Ghaderi, A.; Fink, G.; Stephanopoulos, G. Engineering alcohol tolerance in yeast. *Science* **2014**, *346*, 71–75. [[CrossRef](#)]
44. Henriques, S.; Mira, N.; Sa-Correia, I. Genome-wide search for candidate genes for yeast robustness improvement against formic acid reveals novel susceptibility (Trk1 and positive regulators) and resistance (Haa1-regulon) determinants. *Biotechnol. Biofuels* **2017**, *10*, 96. [[CrossRef](#)] [[PubMed](#)]
45. Xu, X.; Williams, T.; Divne, C.; Pretorius, I.; Paulsen, I. Evolutionary engineering in *Saccharomyces cerevisiae* a TRK1-dependent potassium influx mechanism for propionic acid tolerance. *Biotechnol. Biofuels* **2019**, *12*, 97. [[CrossRef](#)]

46. Reisser, C.; Dick, C.; Kruglyak, L.; Botstein, D.; Schacherer, J.; Hess, D. Genetic basis of ammonium toxicity resistance in a sake strain of yeast: A mendelian case. *G3 Genes Genomes Genet.* **2013**, *3*, 733–740. [[CrossRef](#)]
47. Llopis-Torregrosa, V.; Vaz, C.; Monteoliva, R.; Ryman, K.; Engstrom, Y.; Gacser, A.; Gil, C.; Lungdahl, P.; Sychrova, H. Trk1-mediated potassium uptake contributes to cell-surface properties and virulence of *Candida glabrata*. *Sci. Rep.* **2019**, *9*, 7529. [[CrossRef](#)]
48. Petrezselyova, S.; Zahradka, J.; Sychrova, H. *Saccharomyces cerevisiae* BY4741 and W303-1A laboratory strains differ in salt tolerance. *Fungal Biol.* **2010**, *114*, 144–150. [[CrossRef](#)]
49. Sikorski, R.; Hieter, P. A system of shuttle vectors and yeast host strains designed for efficient anipulation of DNA in *Saccharomyces cerevisiae*. *Genetics* **1989**, *122*, 19–27. [[CrossRef](#)]
50. Hill, J.; Myers, A.; Koerner, T.; Tzagoloff, A. Yeast/*E. coli* shuttle vectors with multiple unique restriction sites. *Yeast* **1986**, *2*, 163–167. [[CrossRef](#)]

Yeast Trk1 potassium transporter gradually changes its affinity in response to both external and internal signals

Jakub Masaryk, Hana Sychrová*

Laboratory of Membrane Transport, Institute of Physiology, Czech Academy of Sciences,
Prague, Czech Republic

Supplementary material

Table S1. List of yeast strains

Name	Genotype	Reference
BY4741	<i>MATa his3Δ1 leu2Δ0 met15Δ0 ura3Δ0</i>	EUROSCARF
BYT2	<i>trk2Δ::loxP</i> , derived from BY4741	[25]
BYT12	<i>trk1Δ::loxP trk2Δ::loxP</i> , derived from BY4741	[48]

[25] Petrezselyova, S.; Ramos, J.; Sychrova, H. Trk2 transporter is a relevant player in K⁺ supply and plasma-membrane potential control in *Saccharomyces cerevisiae*. *Folia Microbiol.* **2011**, *56*, 23-28.

[48] Petrezselyova, S.; Zahradka, J.; Sychrova, H. *Saccharomyces cerevisiae* BY4741 and W303-1A laboratory strains differ in salt tolerance. *Fungal Biol.* **2010**, *114*, 144-150.

Table S2. List of plasmids

Plasmid	Relevant features	Reference
<i>Empty multicopy plasmids</i>		
pRS316	<i>URA3</i> , CEN6ARS4	[49]
YEp352	<i>URA3</i> , 2 μ origin	[50]
<i>Empty centromeric plasmid</i>		
YCp352	YEp352-CEN6ARS4 <i>URA3</i> ,	This study
<i>Multicopy plasmids with TRK1*</i>		
pScTRK1	<i>ScTRK1</i> in YEp352	Papouskova (unpublished)
pGRU1ScTRK1	GFP-tagged <i>ScTRK1</i> <i>URA3</i> , 2 μ origin	[24]
<i>Centromeric plasmids with TRK1*</i>		
pCScTRK1	pScTRK1-CEN6ARS4	This study
pCScTRK1-GFP	pGRU1ScTRK1-CEN6ARS4	This study
<i>Centromeric plasmids pCScTRK1 and pCSTRK1-GFP bearing indicated mutations in TRK1*</i>		
pCScTRK1_L949P		This study
pCScTRK1_L949A		This study
pCScTRK1_L949E		This study
pCScTRK1_L949R		This study
pCScTRK1_L949S		This study
pCScTRK1_L81P		This study
pCScTRK1_F820P		This study
pCScTRK1_L1115P		This study
pCScTRK1-GFP_L949P		This study
pCScTRK1-GFP_L949A		This study
pCScTRK1-GFP_L949E		This study
pCScTRK1-GFP_L949R		This study
pCScTRK1-GFP_L81P		This study
pCScTRK1-GFP_F820P		This study
pCScTRK1-GFP_L1115P		This study

**TRK1* expressed under the control of weak and constitutive *S. cerevisiae NIIA1* promoter

- [49] Sikorski, R.; Hieter, P. A system of shuttle vectors and yeast host strains designed for efficient manipulation of DNA in *Saccharomyces cerevisiae*. *Genetics* **1989**, *122*, 19-27.
- [50] Hill, J.; Myers, A.; Koerner, T.; Tzagoloff, A. Yeast/*E. coli* shuttle vectors with multiple unique restriction sites. *Yeast* **1986**, *2*, 163-167.
- [24] Zimmermannova, O.; Felcmanova, K.; Rosas-Santiago, P.; Papouskova, K.; Pantoja, O.; Sychrova, H., Erv14 cargo receptor participates in regulation of plasma-membrane potential, intracellular pH and potassium homeostasis via its interaction with K⁺-specific transporters Trk1 and Tok1. *Biochim. Biophys. Acta* **2019**, *1866*, 1376-1388.

Table S3. List of used oligonucleotides

Oligonucleotide	Sequence (5'-3')
2μ-CEN6ARS4 exchange	
2 μ -CEN6ARS4_for	cggcatcagagcagattgactgagagtgaccataacgcGGGTCCTTTTCATCACGTGC
2 μ -CEN6ARS4_rev	tgctccttcctctgcttctctctctgctcgagattaccgCTTAGGACGGATCGCTTGCC
URA3_for	GTATATTCTCCAGTAGATAGG
CEN6ARS4_rev	GTAAGTTACAGGCAAGCGATCCG
Site-directed mutagenesis	
ScTRK1_L949P_for	GCTATAGAGTCCTTGTTCGGCCCGTTTCAATCTGTTAGCACAAAG
ScTRK1_L949P_rev	CTTGTGCTAACAGATTGAAACGGGCCGACAAGGACTCTATAGC
ScTRK1_L949A_for	GCTATAGAGTCCTTGTTCGGCCCGTTTCAATCTGTTAGCACAAAG
ScTRK1_L949A_rev	CTTGTGCTAACAGATTGAAACGGGCCGACAAGGACTCTATAGC
ScTRK1_L949E_for	GCTATAGAGTCCTTGTTCGGCCGAGTTTCAATCTGTTAGCACAAAG
ScTRK1_L949E_rev	CTTGTGCTAACAGATTGAAACTCGGCCGACAAGGACTCTATAGC
ScTRK1_L949R_for	GCTATAGAGTCCTTGTTCGGCCCGTTTCAATCTGTTAGCACAAAG
ScTRK1_L949R_rev	CTTGTGCTAACAGATTGAAACCGGCCGACAAGGACTCTATAGC
ScTRK1_L949S_for	GCTATAGAGTCCTTGTTCGGCTCGTTTCAATCTGTTAGCACAAAG
ScTRK1_L949S_rev	CTTGTGCTAACAGATTGAAACGAGCCGACAAGGACTCTATAGC
ScTRK1_L81P_for	GATACATTGATACACCGTTTTTAGCAGCGGG
ScTRK1_L81P_rev	CCCGCTGCTAAAAACGGTGTATCAATGTATC
ScTRK1_F820P_for	CTACATGGTGGGGACCTTGGACAGCAATGAG
ScTRK1_F820P_rev	CTCATGTGTCCAAGGTCCCCACCATGTAG
ScTRK1_L1115P_for	CAAACTTAATATATTTGCAATTCCITTTGAAATTGTTAGCGCTTACGG
ScTRK1_L1115P_rev	CCGTAAGCGCTAACCAATTTCAAAAAGGAATTGCAAATATATATAAAGTTTG

*underlined: codon for substituting amino acid

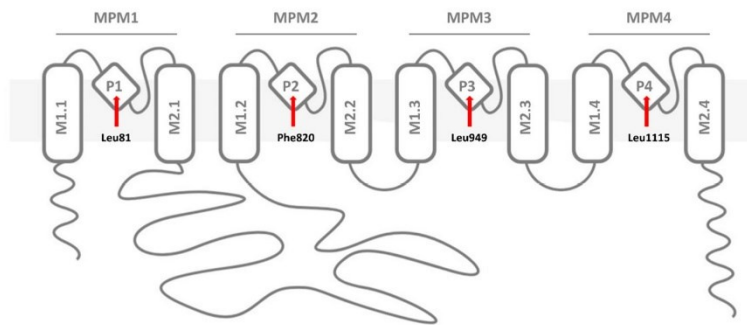


Figure S1: Schematic representation of the predicted transmembrane topology of *ScTRK1*. Highlighted are positions of residues studied in this work.

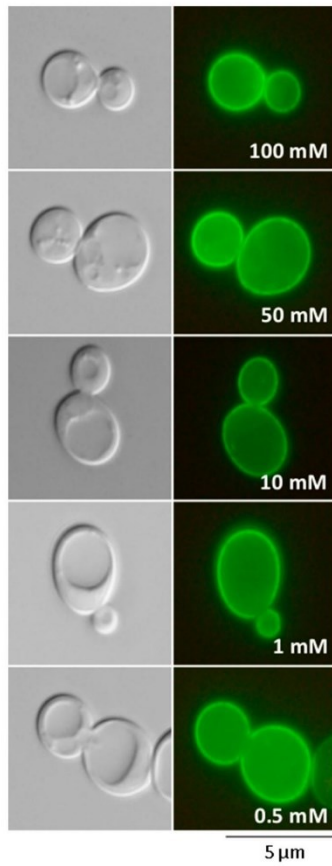


Figure S1. Localization of GFP-tagged Trk1. Cells were grown in YNB-F supplemented with indicated KCl concentrations to $OD_{600} \sim 1$, and visualized using Olympus Bx53 microscope and captured by Olympus DP73 camera.

3.2 Putative role of phosphorylation and interaction with 14-3-3 proteins in the regulation of activity of Trk1

Summary: In the second section of the dissertation thesis, we focused on another, so far not thoroughly studied aspect of the Trk1's functionality, its regulation. According to the results available, the Trk1 is expressed on the low and steady level and this expression is utterly independent of external conditions, including changes in external potassium concentrations. In order to fulfil the intrinsic need of yeast cells to appropriately react to changes in the availability of potassium, by modifying the activity of its main uptake system, the Trk1 protein is thought to be regulated on a post-translational level, mainly in form of phosphorylation. Several phosphoproteomic studies have been performed identifying putative phosphorylation sites within the sequence of Trk1 protein and involvement of a number of kinases has been suggested, however, the coherent mechanism connecting specific conditions to a single phosphorylation site through particular kinase or thorough analysis targeting individual identified phosphorylation sites are hitherto missing.

Using a combined approach of prediction software, site-directed mutagenesis and phenotype analysis, we were able to identify two novel putative phosphorylation sites, Ser882 and Thr900, both located within the highly conserved region of a second intracellular loop of the Trk1. Both sites could presumably be phosphorylated under conditions of potassium limitations and their phosphorylation would have a stimulatory effect on the Trk1. The structural importance of the second intracellular loop and both Ser882 and Thr900 was also examined and confirmed using a 3D model of Trk1 predicted by AlphaFold. Additionally, we studied the possible involvement of small, regulatory 14-3-3 proteins in the regulation of both potassium homeostasis and the function of the Trk1. We identified three putative phosphorylation sites with potential for interaction with 14-3-3 proteins within the sequence of the Trk1: Thr155, Ser414 and aforementioned Thr900. Physical interaction between 14-3-3 proteins and Thr900 was also confirmed by *in vitro* studies.

Results presented in this part of the dissertation thesis added to our, so far scarce knowledge about the orchestration of the activity of the Trk1, by identifying novel potential phosphorylation sites. Moreover, the putative structural importance of the entire second intracellular loop was discussed. Additionally, as 14-3-3 proteins have been previously shown to be involved in the regulation of other ion transporters, proof of their connection to the regulation of the Trk1 could help us place the Trk1 in the broader context of cellular synchronisation of overall ion homeostasis.

This part of the dissertation thesis is included in form of a near-final version of the manuscript expected to be submitted before the end of the year 2022.

Author's contribution: conceptualization, experimental work, data collection and analysis and writing of the original draft of the manuscript were performed by the author of the thesis. Initial measurements of Trk1-mediated uptake and optimization of the method were performed during an internship at the University of Córdoba by the author of the thesis under the supervision of Francisco J. Ruiz-Castilla and José Ramos. *S. cerevisiae* strains lacking genes for selected kinases were constructed by Deepika Kale from the Laboratory of Membrane Transport, Institute of Physiology. A fluorescence polarization assay was performed and data were collected and analysed by Pavel Pohl and Veronika Obšilová from the Laboratory of Structural Biology of Signalling Proteins, Institute of Physiology.

Putative role of phosphorylation and interaction with 14-3-3 proteins in the regulation of activity of Trk1

Jakub Masaryk¹, Deepika Kale¹, Pavel Pohl³, Francisco J. Ruiz-Castilla², Veronika Obšilová³, José Ramos², Hana Sychrová¹

¹*Laboratory of Membrane Transport, Institute of Physiology, Czech Academy of Sciences, 142 20 Prague 4, Czech Republic*

²*Department of Microbiology, University of Córdoba, 140 71 Córdoba, Spain*

³*Laboratory of Structural Biology of Signaling Proteins, Institute of Physiology- Division BIOCEV, Czech Academy of Sciences, 252 50 Vestec, Czech Republic*

Abstract

Potassium is an essential intracellular ion, and its sufficient internal concentration is crucial for many cellular processes and is also a pivotal signal for division. At the same time, however, excess internal potassium might have a negative effect on yeast survival and it is therefore fundamental for the cells to precisely regulate potassium acquisition through the plasma membrane. Uniporter Trk1 is a key player in potassium acquisition in yeast. Trk1 has been shown to be expressed on the low and stable level and orchestration of its activity is therefore thought to occur on a post-translational level, mainly in form of phosphorylation. Even though based mostly on global phosphoproteomic studies, several putative phosphorylation sites have been proposed to play a role in the stimulation or attenuation of activity of Trk1, the comprehensive picture of the regulation of Trk1 is up to this time missing. The first part of the presented study focuses on the identification of putative phosphorylation sites contained within a highly conserved second intracellular loop. We identified two potential phosphorylation sites within this region: Ser882 and Thr900 phosphorylation of which might stimulate the activity of Trk1. Additionally, the presented study also aims to identify putative residues with the potential for interaction with 14-3-3 proteins Bmh1 and Bmh2, small regulatory proteins involved in the regulation of a large number of cellular processes in *S. cerevisiae*. Based on prediction software and experimental analysis, we identified, in addition to Thr900, Thr155 and Ser414 as residues with potential for interaction with 14-3-3 proteins. Interaction of all three residues with either Bmh1 or Bmh2 could potentially lead to stimulation of the activity of Trk1.

Moreover, we confirmed *in vitro* physical interaction between short peptide containing phosphorylated Thr900 and both Bmh1 and Bmh2.

Introduction

Potassium as an indispensable intracellular ion fulfils many essential roles in cells, such as regulation of cell volume and internal pH, stabilization of membrane potential, balancing of negative charge of macromolecules, protein synthesis and enzyme activation. Additionally, sufficient internal potassium content is a pivotal signal for cellular division and also imperative for resistance to various stresses [1,2]. Nonetheless, excess internal potassium leads to the deacidification of vacuoles and consequently to a shortened lifespan of yeast [3]. It is therefore of the highest importance for the yeast cells to tightly regulate the transport of potassium across the plasma membrane in order to maintain its intracellular level within optimal ranges of 200-300 mM [1].

Yeast cells employ a variety of potassium uptake systems with distinct structures and modes of action: K^+ - H^+ symporters Hak1, ATPases Acu1 and uniporters Trk1. Acu1 and Hak1 only occur in certain species and are expressed under specific conditions, mainly external potassium limitations [4,5]. The Trk1 on the other hand has been identified in genomes of all sequence yeast species so far, with a characteristic stable level of expression and is therefore considered an overall key player in potassium acquisition in yeast cells [2].

The genome of *Saccharomyces cerevisiae* encodes two Trk-proteins: Trk1 and Trk2. The dominant role in potassium uptake is fulfilled by Trk1, as its deletion leads to a substantial increase in potassium requirements and abolishes the growth of yeast cells on low external potassium [6]. Even though paralog Trk2 most likely fulfils certain, so far undisclosed role in overall potassium homeostasis and is capable of providing yeast cells with a sufficient amount of potassium [7,8], when Trk1 is present, its contribution to potassium uptake is only marginal [9,10]. The Trk1 of *S. cerevisiae* is an integral membrane protein consisting of 1235 amino acids. According to a recent model, the Trk1 polypeptide chain contains four MPM subdomains, each consisting of two transmembrane M-helices connected by short pore P-helix. MPM subdomains are assembled around the central axis thus creating a pore for the transport of substrate [11]. MPM domains are connected by intracellular loops of various lengths. Trk1 of *S. cerevisiae* contains a distinctively long intracellular loop connecting the first and second MPM subdomains, however, its precise functions remain unclear [12]. Apart from potassium, Trk1 has been shown to also transport rubidium and sodium [1].

Moreover, the Trk1 is thought to form tetramers in plasma membrane capable of facilitating an efflux of chloride anions [13]. The most distinct feature of Trk1 is its ability to adjust its kinetic parameters precisely according to the availability of potassium, increasing the overall capacity for uptake with the decrease in external potassium concentration [8], although precise regulation and effective mechanism of this process remain unknown.

The Trk1 has been shown to be expressed on stable and low-level and its expression is presumably irresponsive to alternations in external conditions including changes in external potassium concentration [4,5]. The regulation of Trk1 is therefore thought to occur on a post-translational level, mainly in form of phosphorylation. Various phosphoproteomic studies led to the identification of multiple residues as potential targets for phosphorylation (all residues identified so far are listed in Figure S1). According to these studies, conditions upon which Trk1 is presumably phosphorylated include loss of one of the main N-acetyl transferases [14], exposure to alpha factor [15] and DNA damage [16]. Additionally, crosstalk between phosphorylation and ubiquitination has been suggested to play a role in the degradation of Trk1 [17] and finally, Trk1 has been indicated as a potential substrate for phosphorylation by kinase Cdk1 [18]. Apart from phosphoproteomic studies, several studies focusing on the involvement of specific kinases and phosphatases in the regulation of Trk1 have been performed. Kinases Hal5 [19], and Snf1 [20] together with phosphatase calcineurin [21] have been shown to play a stimulatory role in the regulation of Trk1. On the contrary, phosphatase Ppz1 [22] and kinase Sky1 [23] have been suggested to be involved in the down-regulation of Trk1.

14-3-3 proteins are a family of small, highly conserved, regulatory proteins expressed in all eukaryotes usually as multiple isoforms, ranging from at least twelve in plants and seven in mammals to two isoforms in yeast [24]. Forming dimers, each monomer is able to bind phosphorylated serine or threonine contained within specific consensus sequences [25], although binding to non-phosphorylated proteins has been reported as well [26]. 14-3-3 proteins do not possess the catalytic activity and their regulatory role relies solely on binding to various, functionally diverse proteins. The binding of 14-3-3 proteins leads to alternations of a function of target proteins by various mechanisms, mainly: alternation of conformation leading to either activation or inactivation [24] or blocking of specific regulatory sequences within target proteins and consequently altering either function or localization [27,28]. Additionally, the binding of proteins to each individual monomer might facilitate protein-protein interaction [24]. In *S. cerevisiae*, 14-3-3 proteins are encoded by two reading frames: *BMH1* and *BMH2*, where *BMH1* accounts for approximately 80% of total 14-3-3-expression [29]. Even though cells are able to withstand individual deletions, suggesting an overlap in the function of individual isoforms, combined deletion of both *BMH1* and *BMH2* is lethal in most

laboratory strains [30]. With up to hundreds of interaction partners identified so far in *S. cerevisiae* [31], 14-3-3 proteins are involved in the regulation of essentially every cellular process [32]. Additionally, 14-3-3 proteins have been previously shown to regulate both the activity [33-35] and subcellular localization of membrane transport proteins [36].

In order to add to existing data regarding the regulation of Trk1, the presented study focuses on the identification of putative phosphorylation sites and their possible contribution to the regulation of the uptake of potassium through Trk1. Additionally, connection to a specific set of kinases and possible involvement of 14-3-3 proteins are discussed as well.

Results

The putative role of the second intracellular loop in the regulation and structural integrity of Trk1

In order to elucidate a potential regulatory mechanism governing the activity of the Trk1 we decided to centre our study around the identification of putative phosphorylation sites. To narrow down the number of potential residues we initially focused exclusively on the second intracellular loop, IL2 (Fig. 1A). To our knowledge, this internal segment in Trk1 protein is yet to be studied. When we compared amino acid sequences of Trk1 proteins from *S. cerevisiae*, *C. albicans*, *C. glabrata*, *C. dubiliensis*, *C. parapsilosis*, *Z. rouxii* and Trk2 protein from *S. cerevisiae* we observed remarkable degree of amino acid conservation within IL2, with the majority of residues being 100% identical (Fig. 1B and Fig. S2). Such a degree of conservation is uncommon in intracellular segments of membrane proteins as they are, in general, substantially more prone to polymorphisms compared to their transmembrane counterparts [37] suggesting the significant function of IL2 in the overall activity of Trk1. In Trk1 from *S. cerevisiae*, IL2 contains 4 prospective phosphorylation sites: Ser878, Ser882, Ser887 and Thr900 (Fig. 1B). Three of the aforementioned residues, Ser882, Ser887 and Thr900 are 100% identical among compared sequences, residue Ser878 showed app. 57% of identity, with Trk1-sequences from *C. albicans*, *C. parapsilosis* and *C. dubiliensis* harbouring alanine in an analogous position instead of serine. (Fig. 1B and Fig. S2). We also employed prediction software NetPhos 3.1 [38] designed to predict and evaluate potential phosphorylation sites. As seen in Figure 1C, we obtained substantially high scores for two out of four selected sites (Ser882 and Ser887 with scores of 0.975 and 0.949 respectively). Additionally, Thr900 was identified by 14-3-3 Pred [39], by three separate algorithms, as a potential site for interaction with 14-3-3 proteins (Fig. 1C). To unravel, in

more detail, their possible contribution to the regulation of Trk1, selected residues were individually mutated for alanine and these versions of Trk1 were expressed from a centromeric plasmid (behind constitutive promotor *NHA1*) in *S. cerevisiae* strain BYT12 (lacking both *TRK1* and *TRK2* genes).

When growth on various external concentrations of potassium was tested, we detected substantially diminished growth on low potassium (50 μ M KCl) in BYT12 cells expressing S882A- and T900A-versions of Trk1 (Fig. 2A). Surprisingly, growth on plates with external KCl of 3mM seemed unaffected (Fig. 2A), suggesting, that these residues might play a role in upregulating the activity of Trk1 specifically under potassium limitations. We also tested growth in presence of high concentrations of sodium, lithium, ammonium and on media with low (4.0) and high (7.2) pH and while we detected the overall negative effect of high concentrations of Na^+ , Li^+ and NH_4^+ on the growth of BYT12 cells, the general growth pattern was similar to growth observed on various concentrations of potassium (Fig. S3). The negative effect of low pH appeared to be exclusive for mutants S882A and T900A as cells expressing these two versions of Trk1 had slightly slower growth rates compared to their growth on pH 5.8 as opposed to cells expressing native Trk1 growth of which seemed to be unaffected by low pH (Fig. S3). Surprisingly, high external pH improved the overall growth of BYT12 cells to the degree of partially suppressing the differences between cells expressing native Trk1 and mutated versions S882A and T900A, however, since we observed similar improvement on BYT12 cells carrying an empty plasmid, we consider this to be a general effect unrelated to the function of Trk1 (Fig. S3). Additionally, we estimated the initial rate of uptake of potassium analogue rubidium (Rb^+) as described in [40]. Prior to uptake measurements, the cells were starved for potassium for 1 hour, to ensure the Trk1's highest possible uptake capacity [8]. Due to negligible Rb^+ -uptake in BYT12 cells carrying an empty vector (Fig. 2B), we attributed all uptake measured in the remaining strains to Trk1 and its mutated versions. As seen in Figure 2B, Rb^+ uptake was affected in all mutated versions of Trk1, including versions S878A and S887A even though cells expressing these two versions grew similarly to cells expressing the native version of Trk1 protein (Fig. 2A). Nonetheless, the decrease in uptake capacity was significantly more pronounced in BYT12 cells expressing version S882A and T900A compared to S878A and S887A (approximately 35-50% decrease compared to approximately 15% decrease, respectively) (Fig. 2B). Due to stronger effect on uptake capacity and affected growth on low potassium we decided to focus subsequent experiments on cells expressing Trk1 with substitutions S882A and T900A. When subcellular localization of GFP-tagged Trk1 was tested, we observed a remarkable degree of mis localization of Trk1 with substitutions S882A and T900A (Fig. 2C) suggesting a possibility of the contribution of residues Ser882 and Thr900 to proper folding and structure of Trk1 protein. And finally, kinetic parameters for both nonstarved (NS) and starved (ST) cells were estimated. As seen in Figure 2D, in nonstarved cells

affinities of native and T900A versions were comparable while S882A had affinity decreased by approximately 20%. In starved cells, in which Trk1 proteins presumably are in the high-affinity state, we detected decreased affinity for both S882A and T900A mutated version compared to native Trk1 (Fig. 2D). Altogether, these results suggest a potential, albeit minor role of residue Thr900 in the transition of Trk1 to high-affinity state while in case of Ser882, the role is most likely general as we detected the negative effect of S882A-substitution on affinity in both low- and high-affinity state. Additionally, maximum velocities of S882A and T900A mutants were consistently decreased in both low- and high-affinity states by approximately 20-25% (Fig. 2D). Since the maximum velocity presumably directly correlates with the number of active transporters in the plasma membrane, these results are, in fact in line with previously observed mis localization (Fig. 2C).

To establish a possible connection between identified putative phosphorylation sites (Ser882 and Thr900) and specific kinases, we decided to express both native Trk1 and mutant-version in BYT12 cells with deletion of open reading frames for kinases Hog1, Snf1, Sky1, Ptk2 and Hal5. As previously mentioned, kinases Snf1, Sky1 and Hal5 have been suggested to play a role in the regulation of Trk1. Kinase Ptk2 was included as it has been shown to activate H⁺-ATPase Pma1 [41] and could thus play an important part in the interplay between the function of Pma1 and Trk1. Finally, as the Hog1 pathway is involved in the regulation of multiple diverse cellular processes including stress response [42], we hypothesised that Hog1 kinase could have a stimulatory effect on the function of Trk1 as well. As seen in Figure S4, we detected the overall negative effect of deletion of *HOG1* and *SNF1* on the growth of BYT12 cells expressing native Trk1 and both mutant-version while deletion of *SKY1*, *PTK2* and *HAL5* had no observable effect (Fig. S4). Moreover, as differences in growth between cells expressing native Trk1 and both mutant-version were similar in BYT12 and all mutant strains, no connection between selected kinases and identified phosphorylation sites could be conclusively established (Fig. S4).

To elucidate, whether amino acid residue Ser882 and Thr900 contribute to the function of Trk1 by shared or separate mechanisms, we constructed Trk1 containing both S882A and T900A substitutions. As seen in Figures 2 A, B and D (and Fig. S3), the double mutation leads to additive negative effects observed for individual substitutions S882A and T900A and while we are not able to quantify the degree of mis localization (Fig. 2C), based on the effect on maximum velocity as seen in Figure 2D, we presumed the additive effect also applied for subcellular localization of double mutant. Based on these results, we concluded that these two residues contribute to the function of Trk1 by separate mechanisms.

Due to mis localisation caused by mutations of both Ser882 and Thr900, we hypothesized, that these two residues might not participate in the function of Trk1 by being phosphorylated but rather fulfil a crucial structural function. To distinguish between these two potential roles (phosphorylation or structural function) we constructed two additional substitutions for each residue. Substitution for aspartic acid, with its negatively charged side chain presumably able to mimic phosphorylated residues (approach previously applied in [43,44]) and substitution for cysteine, the side chain of which is structurally highly similar to both serine and threonine and at the same time can not be phosphorylated. We presumed that if substitution for aspartic acid could reverse the negative effect of substitution for alanine, then residues would most likely be targets for phosphorylation, on the other hand, if the reversal was brought by cysteine-substitution, residues could possibly fulfil the structural function.

As seen in Figure 3A, substitution for cysteine completely reversed the negative effect of alanine-substitution on growth on low external potassium concentration as opposed to substitution for aspartic acid, which arguably led to a slightly more pronounced decrease in growth rate in both S882D- and T900D-mutants on low potassium compared to alanine-versions. We did not detect any additional differences when growth under stress conditions was tested apart from mutants S882D and T900D being, analogously to mutants S882A and T900A, slightly sensitive to low pH (Fig. S5). Additionally, subcellular localization of cysteine-versions was similar to the localization of native Trk1 with the vast majority of Trk1 proteins residing in the plasma membrane (Fig. 3C). Subcellular localization of S882D- and T900D-mutants was comparable to versions with alanine-substitutions with a large portion of Trk1 proteins being mis localized (Fig. 3C). Unexpectedly, we did not detect statistically significant reversal of the negative effect of alanine-substitutions when uptake-capacity was measured, and mutants S882A to S882C and T900A to T900C were compared (Fig. 3B) showing that while substitution for cysteine had a positive effect on localization and thus presumably on the structure and proper folding of Trk1, at the same time it did not rectify decrease in uptake capacity caused by the absence of serine or threonine in positions 882 and 900 respectively. In line with the additional decrease in growth rates (Fig. 3A), the uptake capacities of mutants S882D and T900D were lower than that of the S882A- and T900A-versions respectively (Fig. 3B). Lastly, we estimated kinetic parameters for Rb⁺-uptake after a starvation period of 1h. As seen in Figure 3D, in mutants S882D and T900D we detected an additional decrease in affinity compared to alanine-mutants, in the case of mutant T900D we also noted the additional reduction of maximum velocity (Fig. 3D). And while we detected an increase in affinity of mutants S882C and T900C compared to alanine-versions, albeit very marginal in case of T900C, the K_T values did not reach those of native Trk1 (Fig. 3D), confirming the assumption that cysteine-mutants did not have the capacity for Rb⁺ uptake similar to

that of native Trk1. Surprisingly, even though subcellular localization of both S882C and T900C was similar to the localization of native Trk1, we measured maximum velocity comparable to that of a native Trk1 only in the case of mutant S882C, while mutant T900C had maximum velocity decreased by app. 25% compared to native Trk1 (an effect similar to alanine-mutants) (Fig. 3D).

To address the discrepancy between the cultivation of cells used for fluorescent microscopy and measurements of uptake capacity (see Material and Methods) we also observed cells expressing GFP-tagged Trk1 and selected mutated versions in both nonstarved (NS) cells and cells starved for potassium for 1 hour (ST cells) (cultivation similar to cells used for measurements of Rb⁺ uptake and kinetic parameters). As seen in Figure S6, the results were similar to those shown in Figures 2C and 3C, moreover, there was no difference in localization of Trk1 between nonstarved cells and cells additionally starved for potassium for 1 hour (Fig. S6).

We also tested the growth of cells expressing GFP-tagged Trk1 and its mutated versions. We detected the overall negative effect of the GFP-tag on the growth of cells on low potassium and therefore presumably on the function of Trk1 compared to cells expressing a non-tagged native version of Trk1 (Fig S7 and 2A). This negative effect of GFP was likely a consequence of structural alternations brought by the presence of GFP. Surprisingly, GFP-tagged Trk1 with substitutions S882A, S882D, T900A, T900D, T900C and even double mutant S882+T900A grew better on low potassium concentrations compared to native GFP-tagged native Trk1 (Fig. S7). These results are contrary to the results obtained on strains expressing Trk1 and its mutated version without GFP, suggesting that the combination of GFP with the above-mentioned substitutions brought significant changes in the functionality of Trk1 most likely due to conformational changes. However, as GFP alone did not alter the subcellular localization of Trk1 (Fig. 2C), the mis localization observed in certain mutants (Fig. 2C and 3C) is, therefore, most likely a consequence of a given mutation, thus supporting the notion that these substitutions led to structural changes in Trk1. Additionally, these results also confirmed that GFP-tagged Trk1 with the above-mentioned substitutions was still able to facilitate the uptake of potassium, even though the majority of proteins were mis localized.

To supplement the characterization of the second intracellular loop (IL2) we obtained a 3D model of Trk1 from *S. cerevisiae* from the AlphaFold protein structure database [45]. We decided not to use the latest published model [11] for this prediction lacks internal segments of Trk1 protein and focuses exclusively on MPM domains. As seen in Figure 4, according to the AlphaFold prediction algorithm, the IL2 is, in fact surprisingly highly ordered segment with two helical regions (the first containing residues 869-877, the second containing residues 883-893) connected by a short turn (residues 878-882). These two helical regions could potentially explain the remarkable degree of

conservation observed upon the comparison of Trk1 sequences from various species (Fig. 1B) and also point to the potentially crucial function of this segment for the function of Trk1. We also observed very similar conformation of IL2 in models of Trk2 from *S. cerevisiae* and Trk1 from *C. albicans* (Fig. S8). The proper conformation of the two helices and the entire region is presumably maintained by a number of non-covalent interactions including hydrogen bonds. Figure 5 shows the participation of selected residues: Ser878, Ser882, Ser887 and Thr900 in the formation of such hydrogen bonds and potentially explains the distinct effects of substitution for alanine for residues 878 and 887 compared to 882 and 900. As seen in Figures 5A and 5C, both Ser878 and Ser887 participate in the creation of hydrogen bonds, however only with their main chains and not the side chains as opposed to Ser882 and Thr900 side chains which both participate in the formation of hydrogen bonds. The fact that the side chain of alanine is unable to form hydrogen bonds could explain the negative effect of the introduction of alanine into positions 882 and 900 and the marginal effects of alanine in positions 878 and 887 (Fig. 2) by a simple lack of crucial non-covalent interaction that includes positions 882 and 900 in mutants S882A and T900A. As seen in Figure 5B, the side chain of Ser882 forms a hydrogen bond with Glu886 from the very beginning of the second helical region of IL2 suggesting the importance of this interaction in the stabilization of orientation of the second IL2-helix with respect to the short turn connecting it to the first helical region. Residue Thr900 on the other hand forms a hydrogen bond with His122, part of the second transmembrane helix (M2) of domain MPM1. This interaction could potentially participate in the stabilization of not only local but rather overall conformation of Trk1 protein (Fig. 5D). Ability of the side chain of cysteine to form hydrogen bonds combined with high structural similarity could thus explain the reversal of the negative effect of alanine substitutions in positions 882 and 900 on growth on low potassium and subcellular localization upon substitution for cysteine (Fig. 3A and 3C). The structural importance of residues Ser882 and Thr900 might also explain the failure of mimicking putative phosphorylation by substitution for aspartic acid for the presence of a large negative charge in structurally important regions of Trk1 during folding of the protein might lead to structural impairments and thus again to mis localization of the nascent protein. The side chain of aspartic acid presumably is able to form hydrogen bonds, however, it also contains a large negative charge, and we hypothesize that this negative charge disrupts the local structure during the folding of a protein and prevents the formation of crucial non-covalent interactions. To confirm this hypothesis, we introduced a negative charge, in form of aspartic acid to position 881, the side chain of which according to the model is oriented outward from the turn of IL2 and does not participate in the formation of non-covalent interaction (Fig. S9B). As seen in Figure S9A, this substitution has no effect on the growth of cells on any of the tested concentrations of potassium thus indirectly confirming our hypothesis that

negatively charged residue in position 882 most likely disrupts structurally crucial non-covalent interactions and consequently leads to improper folding and mis localization of the protein.

Taken all together, obtained results suggest the potential dual function of residues Ser882 and Thr900. The structural function of residues Ser882 and Thr900, ergo importance for proper folding and conformation of Trk1 supported by a substantial degree of mis localization upon substitution for alanine and reversal of this mis localization by substitution for structurally similar cysteine (Fig. 2C and 3C) and also by presumably important non-covalent interactions of their side chains with other residues (Fig. 5B and 5D). Nonetheless, with decreased uptake capacity of cysteine-mutants, the side chain of which presumably can in certain cases be phosphorylated, however, which substantially lower frequency compared to serine or threonine [46] it is possible that residues Ser882 and Thr900 are, in addition to structural function, targets for phosphorylation that would up-regulate the function of Trk1. Since the decreased uptake was detected mainly in starved cells, this phosphorylation would most likely occur during potassium limitations (Fig. 3B and 3D). Additionally comparable capacity for uptake between alanine- and cysteine-version and at the same time substantially diminished growth on low potassium observed for S882A and T900A mutants offers a possibility of diminished growth being a consequence of mis localization of Trk1 with substitutions S882A or T900A, rather than decrease in overall import of potassium (Fig. 2 and 3).

Involvement of 14-3-3 proteins in the regulation of Trk1

In addition to being a putative phosphorylation site, residue Thr900 was also predicted by 14-3-3-Pred software as a potential site for interaction with 14-3-3 proteins (Fig. 1C). Moreover, as 14-3-3 proteins have been previously shown to negatively regulate potassium exporter Nha1 [33] association with these proteins could, in fact, represent a regulatory interplay between transporters Trk1 and Nha1. Simultaneous activity of both Trk1 and Nha1 under potassium limitations could potentially lead to a futile cycle of Trk1-mediated potassium uptake and concurrent loss of potassium through Nha1. However, the coordinated association of these transporters with 14-3-3 proteins leading to presumed upregulation of Trk1 and previously shown downregulation of Nha1 could ensure not only sufficient uptake but also retainment of internal potassium. This prompted us to investigate the possibility of the involvement of 14-3-3 proteins in the regulation of the uptake of potassium through Trk1.

To first determine the possible involvement of 14-3-3 proteins in the regulation of potassium homeostasis, we employed the BYT12 strain with deletion of *BMH1* expressing native Trk1 from the centromeric plasmid. As mentioned in the introduction chapter, *BMH1* accounts for approximately 80 % of total 14-3-3 expression and thus in this strain, expression of 14-3-3 proteins was significantly reduced, yet not completely abolished as the *BMH2* is still present. As seen in Figure 6A, deletion of *BMH1* in fact leads to slightly diminished growth specifically on low potassium, suggesting the role of 14-3-3 proteins in partial upregulation of uptake of potassium in case of external potassium limitations. This difference in growth was detected after 5 days of cultivation at 30 °C, after 7 days we observed no differences between the two strains (Fig. S10) pointing to the possibility that the absence of Bmh1 substantially affects early stages of cellular growth under potassium limiting conditions. Surprising was also an absence of the general effect of deletion of *BMH1* on 3mM and 50 mM KCl in BYT12 strains carrying both empty vector and vector expressing Trk1 (Fig. 6A) indicating a possibility that if the stress conditions, such as potassium limitations are absent, the activity of Bmh2 is sufficient for the growth of BYT12 cells. When growth under various stress conditions was tested, we noted improvement in the growth of BYT12 Δ *bmh1* compared to BYT12 (both expressing Trk1 from centromeric plasmid) strain in presence of both high external Na⁺ and Li⁺ (Fig. S10). However, as we noted the same effect for high external Na⁺ comparing BYT12 Δ *bmh1* and BYT12 strains carrying an empty vector (Fig. S10), we consider this to be a general effect of deletion of *BMH1* unrelated to the function of Trk1 and more likely connected to the upregulated activity of Nha1 as a consequence of absence of negative regulator Bmh1 [33]. Previously observed improvement of growth of BYT12 cells carrying an empty vector on high external pH (compared to pH 5.8) was also seen in strain BYT12 Δ *bmh1*[YCp352], however, this improvement was much less pronounced compared to strain BYT12[YCp2352] which again, due to absence of Trk1 in these strains, could be considered a general effect of lack of protein Bmh1 (Fig.S10). Additionally, the absence of Bmh1 also led to a slight decrease in uptake of Rb⁺ (Fig. 6B) and affinity without significant alternations to maximum velocity in starved cells (Fig. 6D). In non-starved cells which were only exposed to an environment with high external potassium, deletion of *BMH1* significantly increased the affinity of Trk1 and at the same time led to reduction of maximum velocity (Fig. 6D). As 14-3-3 proteins had been previously proposed to play a role in the regulation of transition through later stages of secretory pathway [36] we also tested subcellular localization of GFP-tagged Trk1 in both BYT12 and BYT12 Δ *bmh1* strains. As seen in Figure 6C, the subcellular localization of Trk1 in both strains was comparable, thus disproving the aforementioned type of regulation of Trk1 by 14-3-3 proteins. Surprisingly, as seen in Figure S7, the BYT12 strain with a deletion in *BMH1*, expressing GFP-tagged Trk1, exhibited significantly diminished growth on plates supplemented with low potassium compared to BYT12 Δ *bmh1* strain expressing non-tagged native Trk1 (Fig. 6A). As mentioned above, we presumed that the presence of

GFP to a certain degree altered the function of Trk1 and this alternation seemed to have a more substantial effect in absence of Bmh1, further supporting the notion of involvement of 14-3-3 proteins in the regulation of Trk1.

Taken all together, results obtained from strain *BYT12Δbmh1* suggested putative involvement of 14-3-3 proteins in the regulation of potassium homeostasis most likely under conditions of potassium limitations, presumably during early phases of cellular growth. However, whether this involvement includes direct binding to Trk1 or is mediated by additional proteins remains unclear. To elucidate, in more detail, a possible connection between Trk1 and 14-3-3 proteins we next focused on the identification of putative binding sites for interaction between Trk1 and Bmh1/Bmh2. To predict potential sites for binding of 14-3-3 proteins we employed 14-3-3-Pred software and focused on residues highly scored by all three prediction algorithms (all such residues listed in Figure S11). For further analysis, however, we selected residues by two additional parameters: NetPhos 3.1 score above 0.6 and percent of identity among compared sequences above 40%. The final set of residues is listed in Figure S11 and highlighted in red. The one residue, Thr491, even though not fulfilling the requirements, was nonetheless included due to close proximity to residue Ser490. All selected residues were mutated to alanine and expressed in the *BYT12* strain from the centromeric plasmid.

When growth on plates supplemented with various concentrations of KCl was tested, we did not observe any differences between cells expressing native Trk1 and mutated version, with exception of the previously discussed T900A-mutant (Fig. 7A). However, when uptake of Rb^+ was measured, we noted three mutants with a significant decrease in uptake- capacity. In addition to T900A, also mutants T155A and S414A showed reduced uptake by approximately 25% compared to native Trk1 (Fig. 7B). Unlike T900A-mutant, both T155- and S414A-versions of Trk1 protein were localized in the plasma membrane (Fig. 7C) and thus decrease in uptake was most likely caused by alternation in the activity of the protein rather than its mis localization. And finally, kinetic parameters for starved *BYT12* cells expressing both T155A- and S414A-versions of Trk1 were estimated. As shown in Figure 7D, both substitutions led to a decrease in affinity, while maximum velocity remained without significant alternations. It is important to note the parallels between the comparison of T900A to T900C and S414A. Similarly, as in comparison of T900A to T900C, both T900A and S414A showed a similar degree of uptake of Rb^+ (Fig. 7B) and thus presumably comparable capacity for uptake of potassium and yet unlike S414A, substitution T900A was also reflected in diminished growth on low potassium (Fig. 7A). This result again suggested that the negative effect of substitution T900A on cellular growth-rate is most likely brought by mis localization of protein rather than decrease in uptake for both T900C and S414A were localized

primarily in the plasma membrane (Fig. 3C and 7C) and showed no effect on the growth of the BYT12 cells (Fig. 3A and 7A).

To support previous results, we also aimed to determine the possibility of physical interaction between 14-3-3 proteins and Trk1. First, a short peptide containing phosphorylated Thr900 and surrounding residues (RRCFpTLLFP) was synthesized. The peptide was labelled on N-terminus by fluorescein isothio-cyanate (FITC) and a fluorescence polarization assay was performed to determine binding affinities to both Bmh1 and Bmh2. As shown in Figure 8A, phosphopeptide RRCFpTLLFP interacts with both Bmh1 and Bmh2 in a dose-dependent manner. Binding affinities for interaction with Bmh1 and Bmh2 were determined to be 4.0 and 3.4 μM respectively (Fig. 8B). These results combined with the prediction by three separate algorithms of 14-3-3-Pred strongly indicate the possibility of binding of both Bmh1 and Bmh2 to Thr900.

Altogether, obtained results supported the putative involvement of 14-3-3 proteins in the regulation of the activity of Trk1 as we detected a number of effects of the absence of Bmh1 on potassium homeostasis. Moreover, in addition to the previously discussed Thr900, we identified two new residues, Thr155 and Ser414, potentially involved in both regulation of Trk1 and interaction with 14-3-3 proteins. Finally, we confirmed the interaction between phosphorylated Thr900 and both Bmh1 and Bmh2 *in vitro*.

Discussion

Due to the essential roles of potassium in yeast cell physiology its sufficient internal level is a pivotal prerequisite for yeast proliferation and survival of exposure to stress conditions [1]. However, as not only the lack but also the excess uptake of potassium have a negative effect on yeast cells [3] the entire process of acquisition of potassium needs to be tightly regulated affair. Even though Trk1 is considered a key player in potassium uptake there is a significant scarcity of data regarding its regulation. Trk1 protein has been shown to be expressed on a low degree independent of external conditions [4] and its regulation is thought to occur on a post-translational level. As phosphorylation is the dominant posttranslational modification of eukaryotic cells [47] with various regulatory consequences, we presumed that Trk1 might also be subject to a similar type of regulation. The presented study focuses on the identification of putative phosphorylation sites and the disclosure of their putative involvement in the regulation of Trk1 protein.

Due to intracellular segments making up a large portion of Trk1 in *S. cerevisiae*, mainly on account of the first intracellular loop, this protein contains a large abundance of potential phosphorylation sites. We, therefore, decided to limit our study to a specific subset of these sites: putative phosphorylation sites located within the highly conserved second intracellular loop (IL2) and phosphorylation sites with the potential for interaction with 14-3-3 proteins.

Apart from harbouring four potential phosphorylation sites, according to a model acquired from the AlphaFold database, IL2 of Trk1 is a highly structured domain with two helical subdomains (Fig. 4). The structural definition combined with a high degree of conservation of this domain strongly suggests its functional importance. Internal domains of transport proteins have been shown to be involved in the regulation of the function of these proteins in various ways, most notably by interaction with either ATP [48] or other proteins with regulatory effects on given transporter [49]. Moreover, the structurally similar element has been proposed to be involved in gating by creating an intramembrane loop in KtrB, a protein belonging to the same group of SKT-proteins as Trk1 [49]. It is also possible that IL2 is important for interaction with various proteins encountered throughout the secretory pathway [36] and its impaired conformation could potentially lead to misfolding and mislocalization of a nascent protein. In addition to potential importance for presumed interaction with other proteins, IL2 most likely also fulfils imperative structural function as a number of residues of IL2, including residue Thr900 closely analysed in this study, were predicted to participate in the formation of noncovalent interactions with other MPM domains or intracellular segments of Trk1 (Fig. 5D and S12). These interactions could potentially define and stabilize the overall conformation of the Trk1 protein. Our results from analysis of the negative effect of substitution of Ser882 and Thr900 for alanine also indirectly confirmed at least a partial accuracy of the Trk1-model obtained from the AlphaFold database in both presumed localization of these two residues and their participation in the creation of hydrogen bonds.

Analysis of potential phosphorylation sites contained within IL2 pointed to a possibility of dual function of residues Ser882 and Thr900. First, both residues presumably fulfil crucial structural functions as according to a model, both participate in the formation of hydrogen bonds and their substitutions likely lead to misfolded and mislocalized Trk1 proteins. Apart from 3D-model, the structural function is also supported by the negative effects of the introduction of alanine and the lack of effect of the introduction of structurally similar cysteine into positions 882 and 900 on localization of Trk1 (Fig. 3). These noncovalent interactions might be especially imperative for proper folding during synthesis of a nascent protein as indirectly demonstrated by the failure of mimicking phosphorylation by the introduction of negatively charged aspartic acid for large negative charge present already during synthesis of a protein might lead to folding impairments and consequent mis

localization [50]. In fully folded protein, a change in the phosphorylation status of residues Ser882 and Thr900 might lead to alternations of existing hydrogen bonds in their vicinity or alternatively to the creation of new ionic interactions [51] with a significant effect on the conformation of IL2. Additionally, as Thr900 is a potential site for interaction with 14-3-3 proteins, confirmed by both prediction software and *in vitro* experiments, phosphorylation of this residue might potentially lead to interaction with either Bmh1 or Bmh2. The precise consequence of this presumed interaction is presently unclear. As discussed above, IL2 most likely to a certain extent defines the overall conformation of Trk1 and structural changes of IL2 as a result of the addition of phosphate groups to specific residues or interaction with 14-3-3 proteins could bring on substantial variations in the overall conformation of Trk1 and consequently an alternation of a function. As the substitution of both Ser882 and Thr900 for cysteine has a negative effect on the uptake capacity of Trk1, putative phosphorylation of these residues would most likely have a stimulative effect on the function of Trk1. We also could not exclude a possibility of residues Ser878 and Ser887 being involved in the regulation of Trk1 by phosphorylation, however, compared to Ser882 and Thr900 presumed lack of phosphorylation in these two positions seemed to have a marginal effect on the functionality of Trk1.

Our results also showed a certain degree of discrepancy between differences in subcellular localization and maximum velocity of Rb^+ uptake when native Trk1 and some mutated versions were compared. For instance, Trk1 with substitutions S882A and T900A showed significant, yet not complete mislocalization and only approximately a 25 % decrease in maximum velocity (Fig. 2C and 2D). As V_{max} is presumably directly connected to a number of active transporters in the membrane, we would, based on results from fluorescent microscopy, expect the difference in V_{max} between native Trk1 and mutants S882A and T900A to be substantially more pronounced. According to Masaryk et. al. [8], the majority of Trk1 proteins residing in the plasma membrane might be inactive after 1 hour of potassium starvation and being continuously activated during a time period of up to 5 hours of exposure to potassium-limiting conditions. As our experiments of both measurements of kinetic parameters and fluorescent microscopy (Fig. 2C and S6) were performed after the maximum period of 1 hour of potassium starvation, it is possible that even though a large part of S882A- and T900A-versions are mislocalized, the actual number of active proteins in the membrane is not substantially different when compared to native Trk1.

Growth experiments using strains with deletions in selected kinases failed to provide any clear connection to identified, putative phosphorylation sites. However, the conclusion about the lack of participation of these kinases in the regulation of Trk1 would be premature as there is still a possibility of both presumed phosphorylation sites being phosphorylated by more than one of the selected kinases. In such case, strains with a deletion in any of these kinases would still exhibit

diminished growth when expressing Trk1 lacking phosphorylation sites Ser882 and Thr900 compared to native Trk1, for native Trk1 could still be phosphorylated at these residues by remaining kinases.

Results from the study of a combined substitution S882A+T900A clearly showed an additive negative effect (Fig. 2) and therefore presumably two separate mechanisms of the contribution of these residues to the functionality of Trk1, however as the introduction of alanine into both positions likely resulted in structural impairments of Trk1 the additive negative effect was not unexpected and should not necessarily lead to a conclusion about separate regulatory contributions of Ser882 and Thr900. The more reliable result concerning the connection between putative phosphorylation of residues Ser882 and Thr900 could be obtained by combined substitutions S882C+T900C as we would expect this version of Trk1 to have unaltered structure and at the same time lacking the possibility of phosphorylation on neither Ser882 nor Thr900.

Intriguing is also the actual cause of the diminished growth of cells expressing Trk1 with substitutions S882A and T900A. According to our results, it is not the decrease in uptake capacity, but rather presumed improper folding and consequently a mis localization of Trk1 protein that leads to slower growth rates. Misfolded proteins are prone to the formation of insoluble aggregates in various cells, including yeast [52] and these aggregates tend to have a cytotoxic effect [53,54]. It is therefore possible that protein aggregate-induced stress and cytotoxicity is the actual effect of substitutions S882A and T900A. Nonetheless, this did not explain the lack of effect of substitutions S882A and T900A on growth on higher concentrations of potassium (Fig. 2A). Alternatively, it is possible that protein Trk1, in addition to potassium uptake, fulfils a secondary function in the plasma membrane and its aggregation and mis localization caused by substitutions S882A and T900A leads to a partial loss of this function and consequently to limited growth under low potassium. The potential alternative function of transporters in yeast is represented by the concept of transceptors [55,56]. According to this concept, transporter proteins, in addition to the uptake of nutrients, also participate in their sensing and by triggering various signalling pathways alternate their overall homeostasis. In the case of Trk1 being the transceptor protein, its absence in the membrane could lead to impaired sensing, and improper signalling of external potassium conditions and thus to limited growth, especially on low potassium.

As previously mentioned, both Bmh1 and Bmh2 have been shown to be involved in numerous cellular processes and therefore we had expected various effects of deletion of Bmh1 in BYT12 cells. Nonetheless, as we also detected a few effects of deletion of Bmh1 directly related to potassium homeostasis, mostly a decrease in growth on low potassium and alternations in kinetic parameters of Trk1, we presumed that the 14-3-3 proteins were likely involved in the regulation of

potassium homeostasis as well. However, the effect of deletion of Bmh1 on potassium homeostasis seemed to be dependent on external potassium concentration as we detected slightly diminished affinity of Trk1-mediated uptake in potassium-starved cells as opposed to significantly increased affinity for uptake and decreased V_{\max} in nonstarved cells. Limited uptake in starved cells could be presumably explained by the stimulatory effect of Bmh1 on Trk1 upon these conditions, however, the substantial increase in affinity combined with a decrease in maximum velocity in nonstarved cells was difficult to explain. As the uptake capacity of Trk1 has been previously shown to be regulated by either internal potassium content or membrane potential [8], it is possible that the absence of Bmh1 which has a number of general effects on yeast physiology leads to alternation in one of these physiological parameters and consequently to substantial changes in both K_T and V_{\max} of Trk1 detected in nonstarved cells.

Additionally, based on prediction software, we identified three residues with potential for interaction with 14-3-3 proteins: in addition to previously discussed Thr900, Thr155 and Ser414. Both Thr155 and Ser414 have been previously suggested as potential targets for phosphorylation [15,17,18]. Both residues could presumably be phosphorylated under conditions of stress, either exposure to alpha factor [15] or defective protein-degradation machinery [17]. In general, under stress, increased uptake of potassium is favourable for cell survival indicating that the phosphorylation of both Thr155 and Ser414 and consequent interaction with 14-3-3 proteins could have a stimulatory effect on the function of Trk1. The potential stimulatory effect of presumed phosphorylation of Thr155 and Ser414 was also supported by our results.

As mentioned above, the study of the connection between Trk1 and 14-3-3 proteins was partially aimed at the identification of a regulatory link connecting the attenuation of activity of Nha1 [33] and the simultaneous stimulation of Trk1. Our results supported the notion of the stimulatory effect of 14-3-3 proteins on the activity of Trk1, thus supporting the hypothesis about the 14-3-3-mediated interplay between Nha1 and Trk1. In addition to Nha1, 14-3-3 proteins could in theory also represent a regulatory connection between Trk1 and H^+ -ATPase Pma1 responsible for the export of protons. As previously shown, there is a crucial interdependence between the simultaneous activation of Trk1 and Pma1 as the import of potassium needs to be balanced by the export of protons in order to maintain proper membrane potential [57,58]. Pma1 ATPase has been shown to be regulated by C-terminal end-mediated autoinhibition suppressed by phosphorylation [59]. A strikingly similar mechanism has been described for plant H^+ -ATPase, although in the case of plant-ATPase involvement of 14-3-3 proteins in the suppression of autoinhibition has been confirmed [34,60]. Even though the association of yeast H^+ -ATPase Pma1 with 14-3-3 proteins has not been established yet, according to 14-3-3-Pred software, this protein contains a putative site for interaction with Bmh-

proteins (Thr912) on its C-terminal end, albeit predicted only by one out of three algorithms. However, plant H⁺-ATPase does not contain a canonical recognition sequence for interaction with 14-3-3 proteins on its C-terminal end at all and yet, this section of protein is able to interact with 14-3-3 proteins [60]. It is therefore possible that 14-3-3 proteins upregulate the activity of yeast H⁺-ATPase Pma1 by suppressing the autoinhibition as well. Bmh1 and Bmh2 proteins could thus represent a regulatory link connecting these three major players responsible for potassium homeostasis. For instance, under conditions of potassium limitation, association with 14-3-3 proteins could presumably lead to stimulation of acquisition of potassium through Trk1, balancing of membrane potential by activating Pma1 and retainment of acquired potassium through inactivation of Nha1.

The presented study achieved to identify two novel potential phosphorylation sites: Ser882 and Thr900, in addition to confirming two previously published sites: Thr155 and Ser414. Additionally, the involvement of small regulatory proteins Bmh1 and Bmh2 was also studied. Even though, the results presented here add to our knowledge regarding the regulation of Trk1, both precise signalling pathway leading to phosphorylation and functional consequence of the addition of phosphate group and putative interaction with 14-3-3 proteins remain unknown and should be a subject to further study.

Material and Methods

Strain and growth conditions

Yeast strains used in this study are listed in Table S1. BYT12 strains with a deletion in kinases *PTK2* (YJR059W), *SKY1* (YMR216C), *SNF1* (YDR477W), *HAL5* (YJL165C), *HOG1* (YLR113W) were constructed by homologous recombination with KanMX cassette and Cre-loxP system as described in Guldener et. al. [61] using oligonucleotides listed in Table S3. Successful deletions were confirmed by diagnostic PCR using oligonucleotides listed in Table S3. The yeast cultures were routinely grown at 30 °C in a YNB (0.67% YNB, 2% glucose) or for starvation experiments in a YNB-F (0.17% YNB-F, 2% glucose and 0.4% ammonium sulphate; containing approximately 15 μM KCl). The desired amount of KCl was added to the media and the pH was adjusted to 5.8 by NH₄OH. Media were sterilized by autoclaving. A mixture of auxotrophic supplements was added after autoclaving. Prior to uptake and kinetic parameters measurements, the yeast cells were grown on YNB supplemented with 100 mM KCl to OD₆₀₀ approximately 0.3-0.4 and used directly for measurements (non-starved cells) or additionally incubated for 1 hour on YNB-F media without added KCl (starved cells).

Plasmids

All plasmids used in this study are listed in Table S2. Single amino acid substitutions were performed by site-directed mutagenesis using QuikChange II Site-Directed Mutagenesis Kit (Agilent Technologies, Santa Clara, CA, USA) with oligonucleotides listed in Table S4. Plasmids pCScTRK1, pGRU1ScTRK1 or pCScTRK1-GFP were used as templates. All substitutions were confirmed by sequencing.

Growth tests

The growth of yeast cells was tested on solid media supplemented with 2% agar. Yeast cells were pre-grown on YNB plates supplemented with 100 mM KCl, collected and resuspended in sterile water to OD₆₀₀ 0.6. Three additional 10-fold dilutions were prepared and 3 μ L were spotted on YNB-F plates. The plates were supplemented with indicated concentrations of KCl, NaCl, LiCl or (NH₄)₂SO₄. The pH of the plates was adjusted with either NH₄OH (plates with pH 5.8 or 7.2) or diluted HCl (plates with pH 4.0). Plates with pH 7.2 were buffered with 20 mM MOPS buffer. Yeast cells were incubated at 30 °C, photos were captured after indicated time periods. Representative results of at least three repetitions are shown.

Fluorescence microscopy

For visualization of the subcellular localization of Trk1 and its mutated version, cells expressing GFP-tagged Trk1 from either a multicopy or centromeric plasmid were used. Cells were grown overnight on YNB supplemented with 100 mM KCl to OD₆₀₀ approximately 1, harvested and visualized using Olympus Bx53 fluorescent microscope and captured with Olympus D73 camera. Excitation light of wavelength 460 nm was used and emission light of wavelength 515 nm was captured to visualize GFP-tagged Trk1. Differential interference contrast (DIC) was used for the visualization of whole cells.

Rb⁺ uptake measurements and estimation of kinetic parameters

For Rb⁺ uptake measurements, yeast cells were grown and starved for potassium as described above, collected, washed with sterile water and resuspended in MES buffer (20 mM MES, 2% glucose, 0.1 mM MgCl₂; pH adjusted to 5.8 with Ca(OH)₂) to OD₆₀₀ approximately 0.2. At time 0, RbCl was added to a final concentration of 100 μ M. 5-mL samples were collected at 1-minute

intervals over the 5-minute time period, filtered through Millipore filters (0.8 μm pore size) and washed with 20 mM MgCl_2 . Filters with cells were then extracted overnight in an extraction buffer (0.2 M HCl, 10 mM MgCl_2 , 0.2% KCl). Obtained extracts were analysed by atomic absorption spectrometry and initial rates of Rb^+ uptake in nmoles per mg of the dry weight of cells per minute were calculated [40]. For the estimation of kinetic parameters of Rb^+ uptake, four different concentrations of RbCl were used ranging from 50 μM to 1 mM for starved cells and from 1mM to 10 mM for non-starved cells. Measurements of initial rates of Rb^+ uptake were obtained for each concentration as described above, respective values were plotted on a Lineweaver-Burke plot and K_T and V_{max} were calculated.

Bioinformatics

The sequence alignment was performed using the Geneious alignment function (Global Alignment with Cost Matrix Blosum90) from Geneious prime software version 2022.1.1 (Biomatters, Inc., San Diego, CA, USA) and the sequence logo was created using WebLogo version 2.8.2 [62]. For the prediction and scoring of putative phosphorylation sites, NetPhos 3.1 server was used [38]. For the evaluation of potential sites for interaction with 14-3-3 proteins, a 14-3-3-Pred server was employed [39]. The PDB-files of 3D models of Trk1 proteins from *S. cerevisiae* and *C. albicans* and Trk2 protein from *S. cerevisiae* were obtained from the AlphaFold database [45,63]), database numbers: P12685, A0A1D8PTL7 and P28584 respectively. Visualization of 3D models and prediction of hydrogen bonds was performed in USFC ChimeraX version 1.1 [64].

Fluorescence polarization assay

Both 14-3-3 isoforms (Bmh1 and Bmh2) from *S. cerevisiae* were expressed and purified as described previously [65,66]. The N-terminal 6 \times His-tag was removed using TEV protease, and final size-exclusion chromatography was performed in a HiLoad Superdex 75 column (GE Healthcare, Chicago, IL, USA). Bmh1 and Bmh2 were dialyzed overnight into a buffer containing 10 mM HEPES (pH 7.4) and 150 mM NaCl. Proteins at an initial concentration of 160 μM , followed by binary dilution series, were incubated for 1 h with 50 nM of FITC-labeled synthetic Trk1 peptide (FITC-RRCFpTLLFP), where pT denotes phosphothreonine (Pepscan Presto BV, Lelystad, Netherlands). Dilution series were performed in 384-well black low-volume flat-bottom plates (Corning, NY, USA) in a buffer containing 10 mM HEPES (pH 7.4), 150 mM NaCl, 0.1% (v/v) Tween 20 and 0.1% (w/v) BSA, using pipetting robot epMotion P5073 (Eppendorf, Hamburg, Germany). Fluorescence polarization assay

was measured using a CLARIOstar microplate reader (BMG Labtech, Thermo Fisher Scientific, Waltham, MA, USA). The excitation and emission wavelengths were 482 nm and 530 nm, respectively. The K_D values were determined as the mean of four independent measurements.

Statistics

All data were analysed in Microsoft Excel 2010 or GraphPad Prism version 9.1.0. (for fluorescence polarization assay, version 8.3.0 was used) (GraphPad Software, San Diego, CA, USA). P-values were calculated using the two-tailed Student's T-test in Microsoft Excel 2010. All measurements were repeated at least three times and the mean values with standard deviations are presented.

Figure Legends

Figure 1. Highly conserved internal segment: Intracellular loop 2 (IL2). (A) Topological model of protein Trk1 from *Saccharomyces cerevisiae* with the number of the initial and terminal residues of each internal segment labelled. Internal segments are defined according to Miranda et. al. [37]. Intracellular loop 2 (IL2) is highlighted in red. (B) WebLogo analysis of Trk1-IL2 sequences from *S. cerevisiae*, *Candida albicans*, *C. glabrata*, *C. parapsilosis*, *C. dubiliensis*, *Zygosaccharomyces rouxii* and Trk2-IL2 sequence from *S. cerevisiae*. Putative phosphorylation sites contained within IL2 from *S. cerevisiae* Trk1 are highlighted with grey arrows. (C) List of potential phosphorylation sites from IL2 with their respective NetPhos 3.1 score, percent of identity and results of 14-3-3-Pred analysis (+++ residue predicted by three algorithms as a potential binding site for 14-3-3 proteins, - residue not predicted by any algorithm).

Figure 2. Substitutions of Ser878, Ser882, Ser887 and Thr900 for alanine affect the activity of Trk1. (A) Growth of BYT12 cells carrying an empty vector (YCp352) or pCScTRK1 expressing a native Trk1 and its mutated version on YNB-F plates supplemented with indicated concentrations of KCl. Pictures were captured after 7 days of incubation at 30 °C. (B) Initial rates of Rb⁺ uptake in MES supplemented with 100 μM RbCl. Cells were grown overnight on YNB supplemented with 100 mM KCl and subsequently starved for potassium for 1 hour on YNB-F. Cells were thereafter processed and Rb⁺ uptake was measured and calculated as described in Material and methods (* p<0.05; ** p<0.01; ***

p<0.001). **(C)** Subcellular localization of GFP-tagged native Trk1 and mutated versions S882A and T900A. **(D)** Kinetic parameters of native Trk1 and mutated versions S882A, T900A and S882A+T900A. Cells were grown overnight on YNB supplemented with 100 mM KCl (non-starved cells, NS) or additionally incubated on YNB-F for 1 hour (starved cells, ST). Kinetic parameters were estimated as described in the Material and methods.

Figure 3. Partial reversal of negative effects of mutants S882A and T900A by the introduction of cysteine. (A) Growth of BYT12 cells carrying an empty vector (YCp352) or pCSCTRK1 expressing a native Trk1 or alanine-, aspartic acid- and cysteine-versions of residues Ser882 and Thr900. Pictures captured after 7 days of incubation at 30 °C. **(B)** Initial rates of Rb⁺ uptake in MES supplemented with 100 μM RbCl. Cells were processed and the initial rate of Rb⁺ uptake was calculated as in 2B (* p<0.05; ** p<0.01; *** p<0.001; n-no significant difference). **(C)** Subcellular localization of GFP-tagged native Trk1 and selected mutated versions. **(D)** Kinetic parameters of starved cells expressing native Trk1 and selected mutated versions. Cells were grown on YNB supplemented with 100 mM KCl and subsequently incubated on YNB-F for 1 hour. Kinetic parameters were estimated as described in the Material and methods.

Figure 4. 3D model of Trk1 from *S. cerevisiae* depicting the structure of MPM domains and IL2. PDB file was obtained from the AlphaFold database (database number: P12685) and visualized in ChimeraX version 1.1. For better clarity, only MPM domains and IL2 are shown. Putative phosphorylation sites from IL2 are highlighted with blue arrows.

Figure 5. Predicted hydrogen bonds among selected amino acid residues of the IL2 segment. Residues and hydrogen bonds were visualized using ChimeraX version 1.1 in the 3D model of Trk1 from *S. cerevisiae* (AlphaFold database number: P12685). **(A)** Hydrogen bonds of Ser878 with Met874 and Arg885. **(B)** Hydrogen bonds of Ser882 with Pro879, Met884 and Glu886. **(C)** Hydrogen bonds of Ser887 with Gln883 and Leu891. **(D)** The hydrogen bond between Thr900 and His122.

Figure 6. Possible involvement of Bmh1 in the regulation of potassium homeostasis. (A) Growth of BYT12 and BYT12Δ*bmh1* carrying an empty vector (YCp352) or pCScTRK1 on YNB-F plates supplemented with various concentrations of KCl. Pictures were captured after 5 days of incubation

at 30 °C. **(B)** Initial rates of Rb^+ uptake in MES supplemented with 100 μM RbCl . Cells were grown overnight in YNB supplemented with 100 mM KCl and starved for potassium for 1 hour in YNB-F. Rb^+ uptake was measured as described in Material and methods (* $p < 0.05$; ** $p < 0.01$; *** $p < 0.001$). **(C)** Subcellular localization of GFP-tagged Trk1 in BYT12 and BYT12 Δbmh1 cells. **(D)** Kinetic parameters of Trk1 protein in BYT12 and BYT12 Δbmh1 cells. Cells were grown overnight on YNB supplemented with 100 mM KCl (non-starved cells, NS) or additionally incubated on YNB-F for 1 hour (starved cells, ST). Kinetic parameters were estimated as described in the Material and methods.

Figure 7. Identification of putative sites for interaction with 14-3-3 proteins. (A) Growth of BYT12 cells carrying an empty vector (YcP352) or pCScTRK1 expressing a native Trk1 and its mutated version on YNB-F plates supplemented with indicated concentrations of KCl . Pictures were captured after 7 days of incubation at 30 °C. **(B)** Initial rates of Rb^+ uptake in MES supplemented with 100 μM RbCl . Cells were grown overnight on YNB supplemented with 100 mM KCl and subsequently starved for potassium for 1 hour on YNB-F. Cells were thereafter processed and Rb^+ uptake was measured and calculated as described in Material and methods (* $p < 0.05$; ** $p < 0.01$; *** $p < 0.001$; n-no significant difference). **(C)** Subcellular localization of GFP-tagged native Trk1 and mutated version T155A, S414A and T900A. **(D)** Kinetic parameters of native Trk1 and mutated versions T155A, S414A and T900A. Cells were grown overnight on YNB supplemented with 100 mM KCl and starved for potassium on YNB-F for 1 hour. Kinetic parameters were estimated as described in the Material and methods.

Figure 8. *In vitro* interaction between pThr900 and proteins Bmh1 and Bmh2. (A) Fluorescence polarization (FP) assay showing the interaction between peptide RRCFpTLLFP with phosphorylated residue Thr900 (Trk1_pT900) and proteins Bmh1 and Bmh2. FP assay was performed as described in Material and methods **(B)** Kinetic parameters (K_D and B_{max}) of binding between Trk1_pT900 peptide and Bmh1 (Trk1_pT900+Bmh1) and Bmh2 (Trk1_pT900+Bmh2).

Figure 1

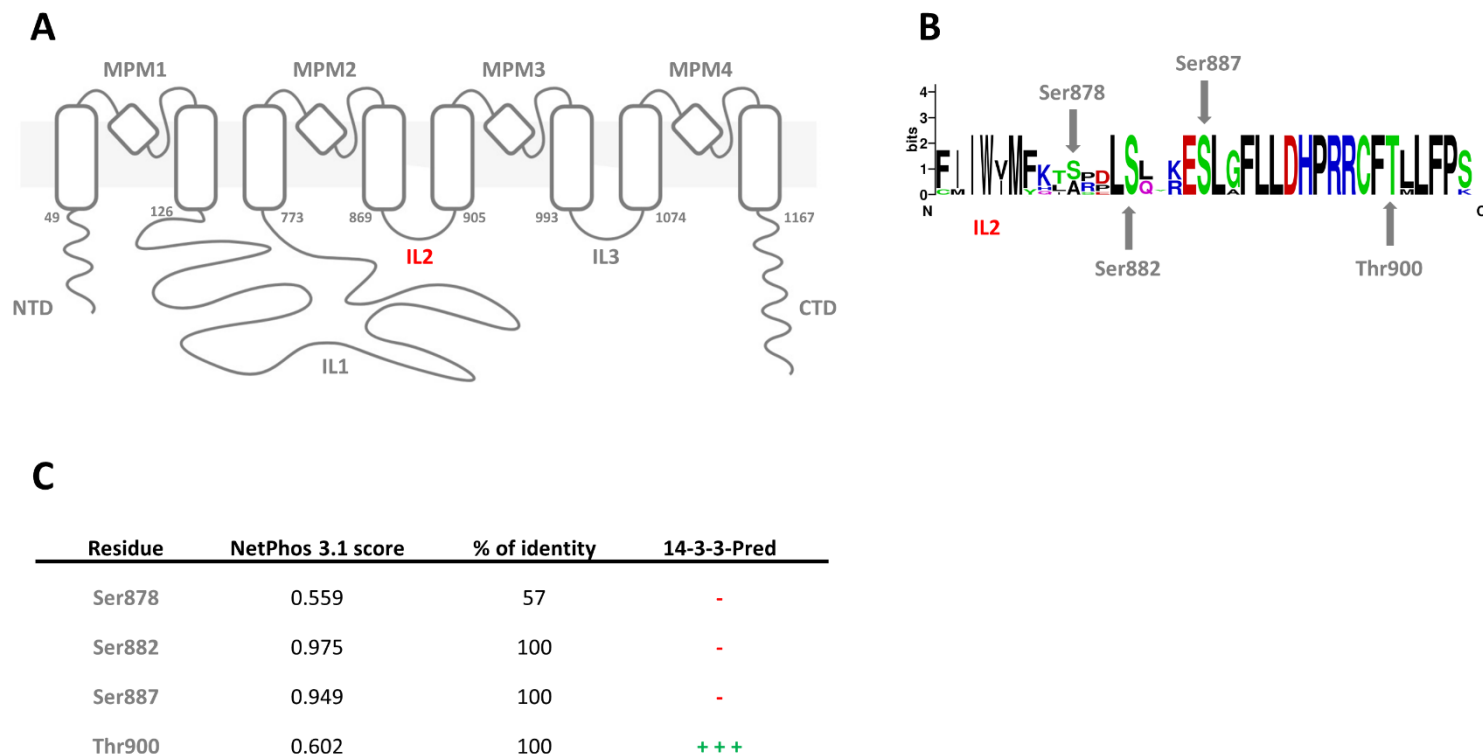


Figure 2

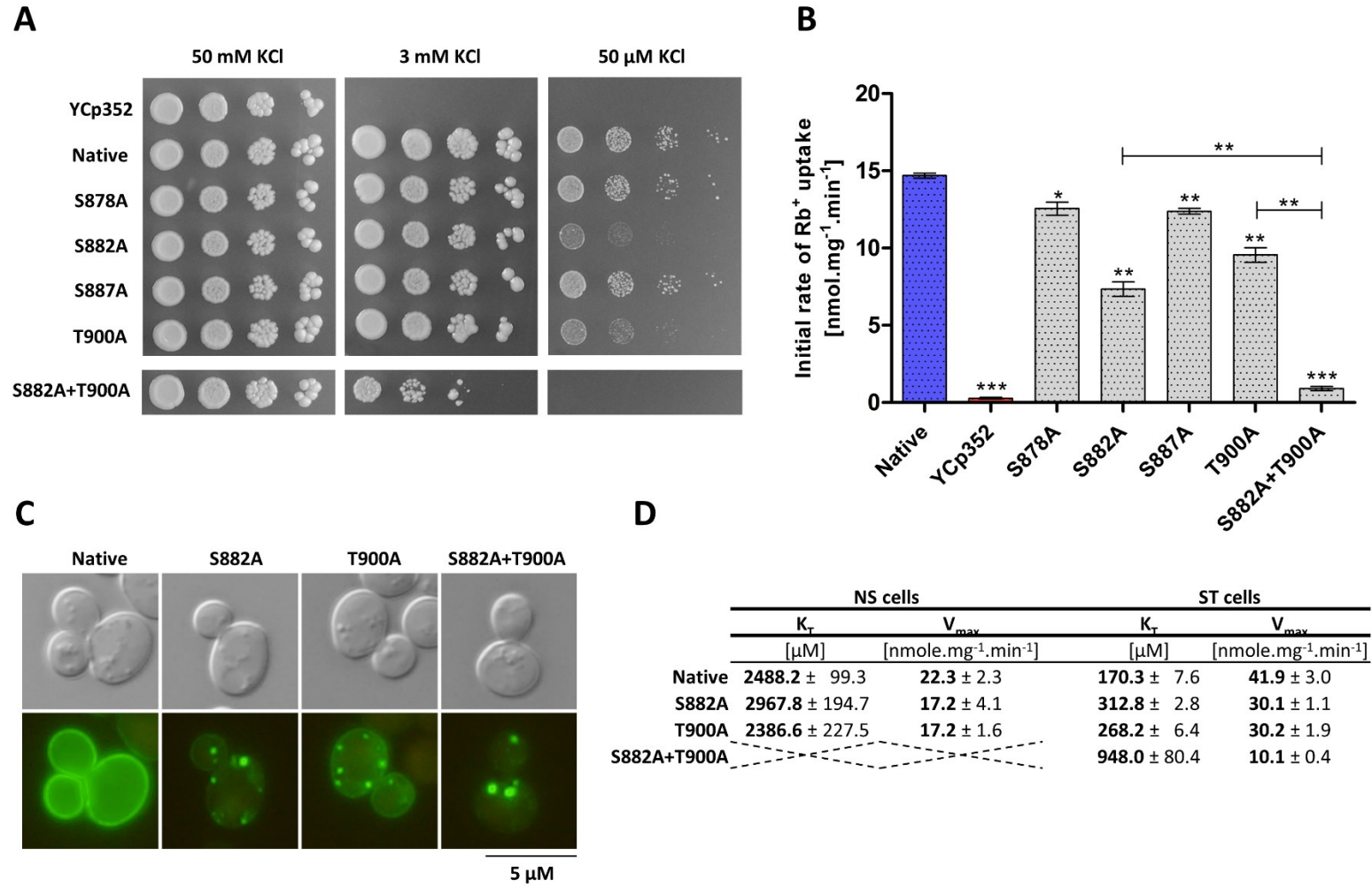


Figure 3

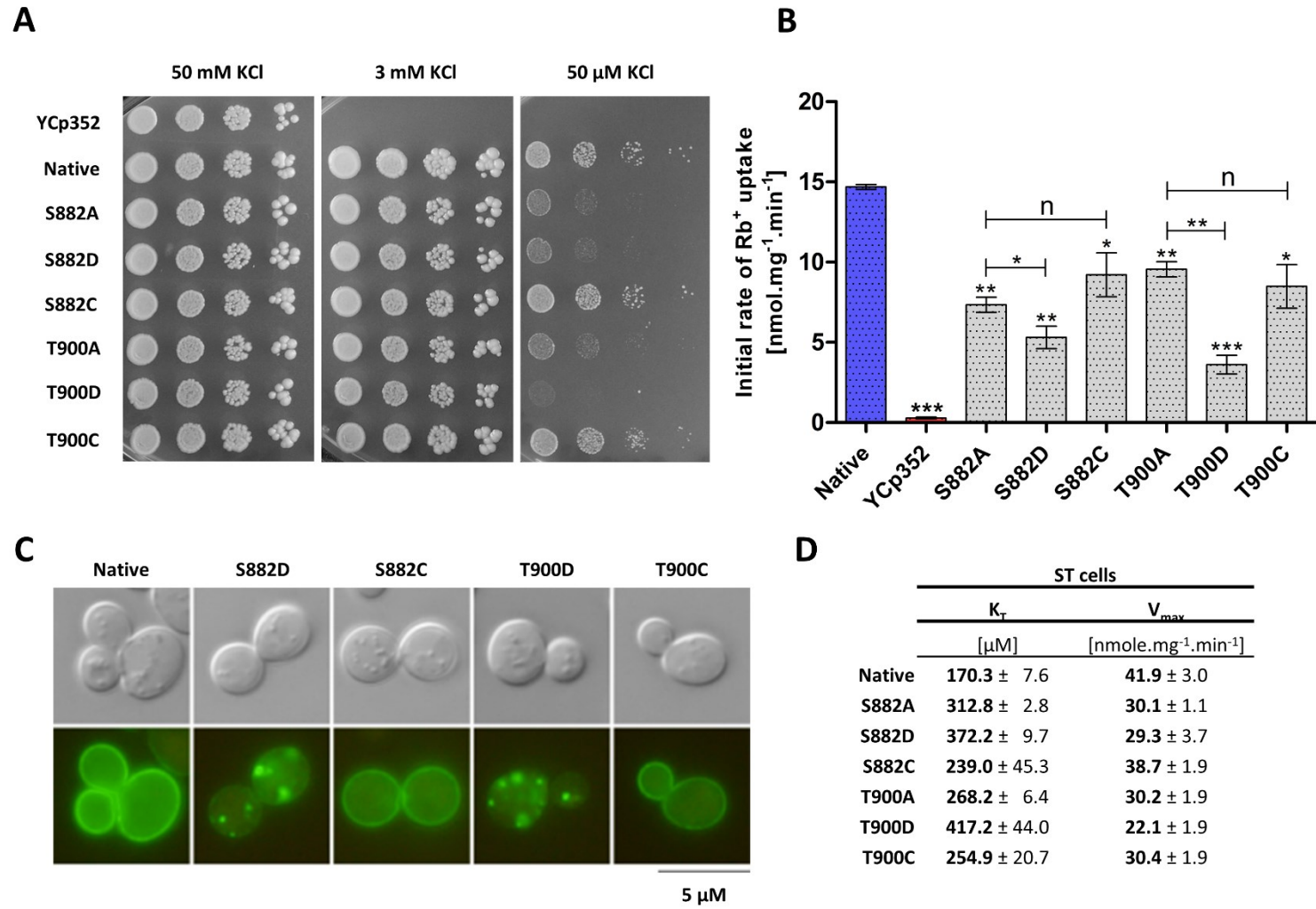


Figure 4

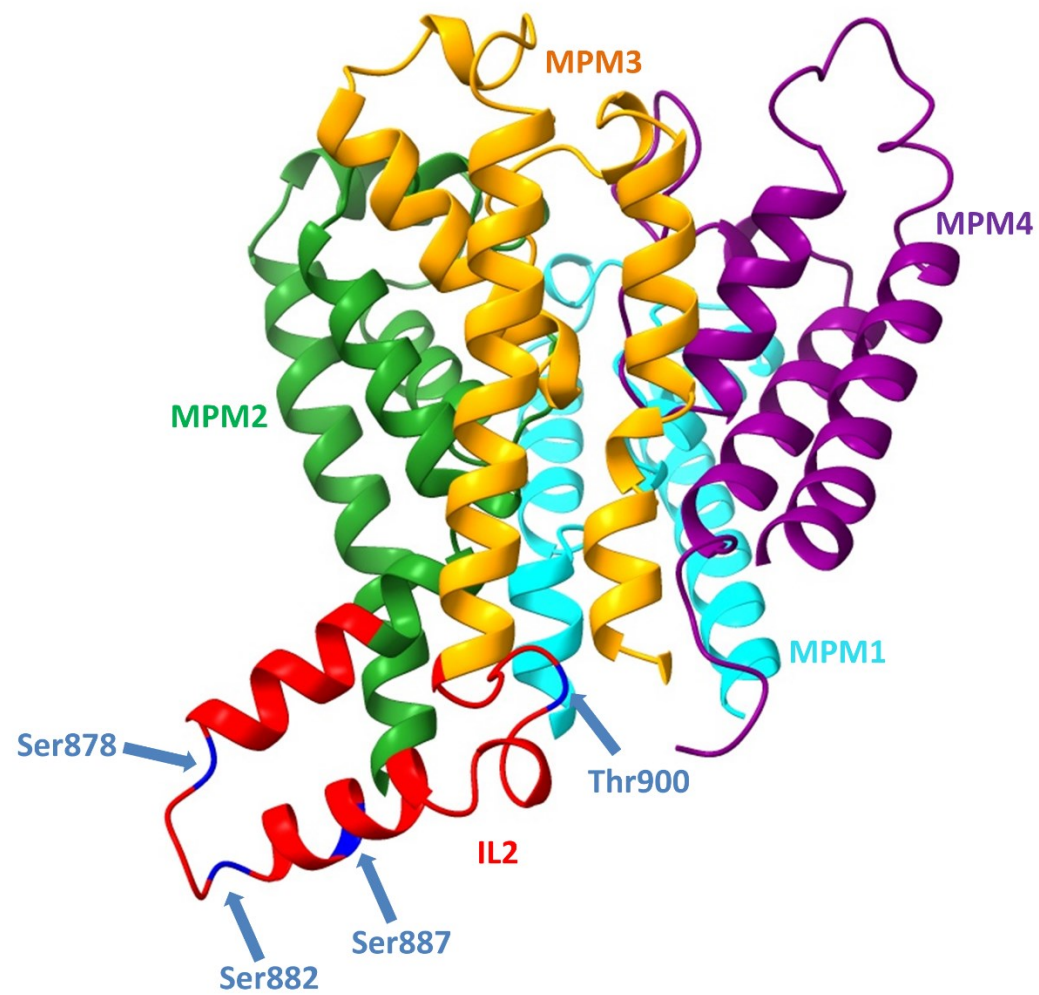


Figure 5

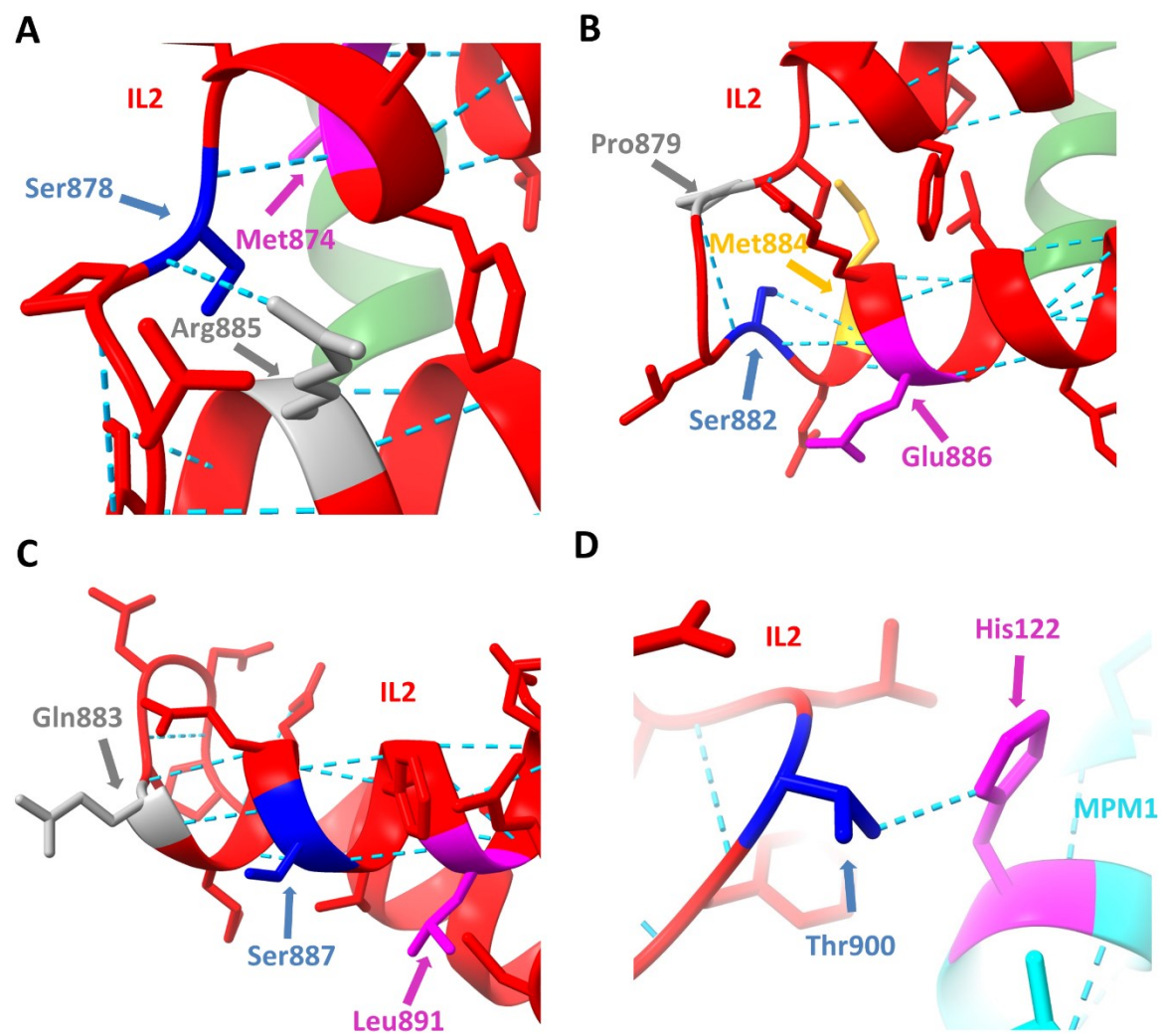


Figure 6

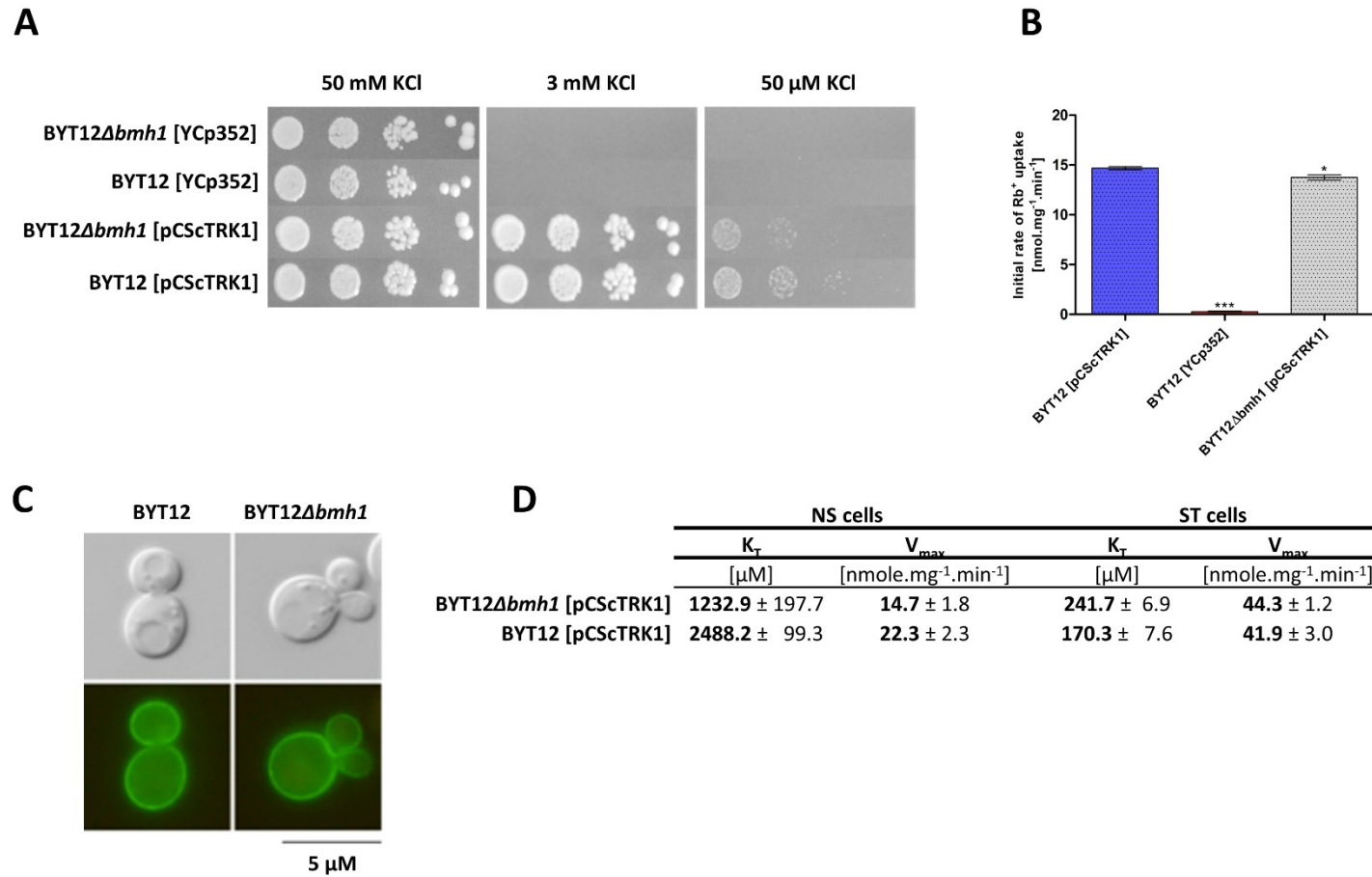


Figure 7

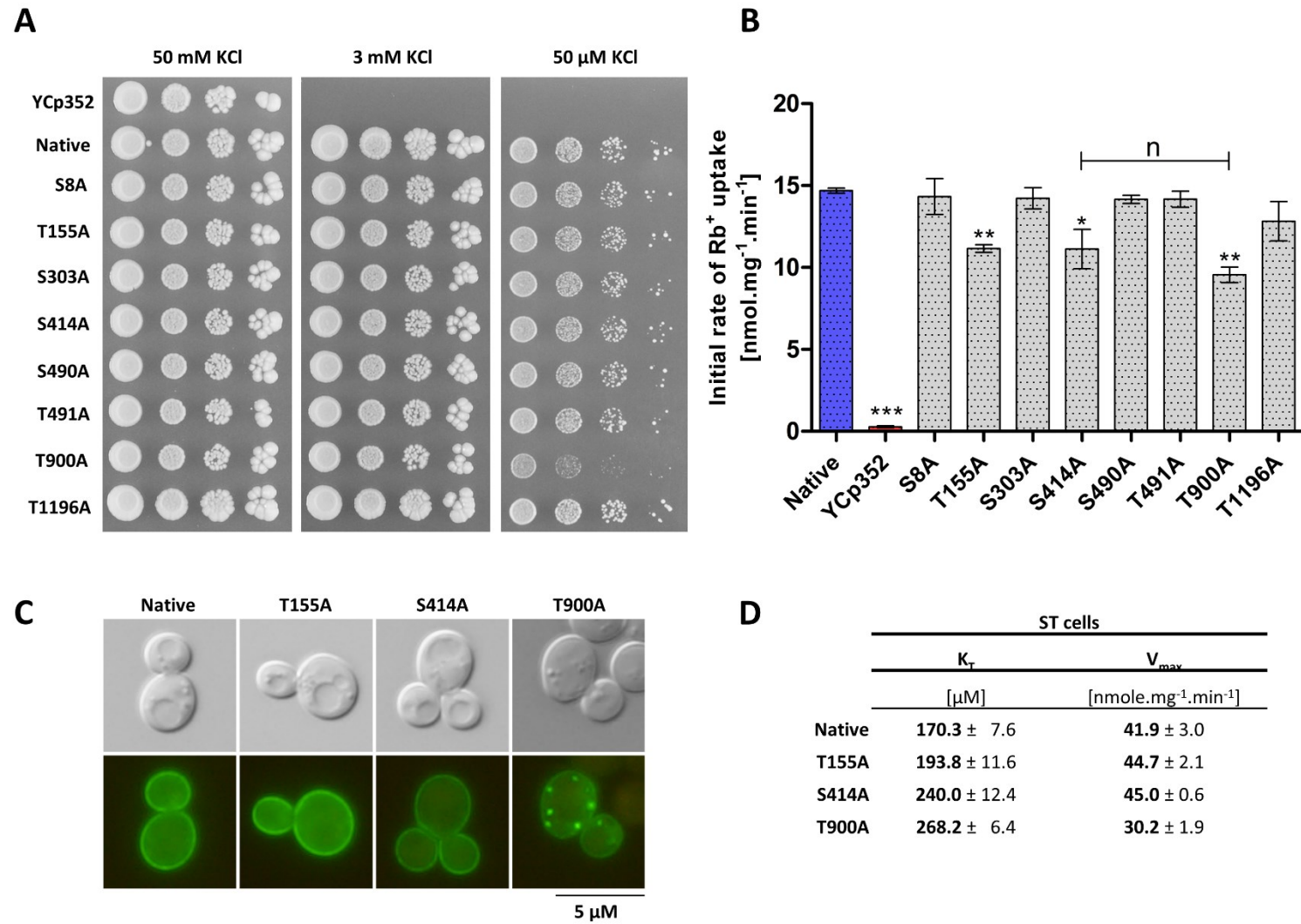
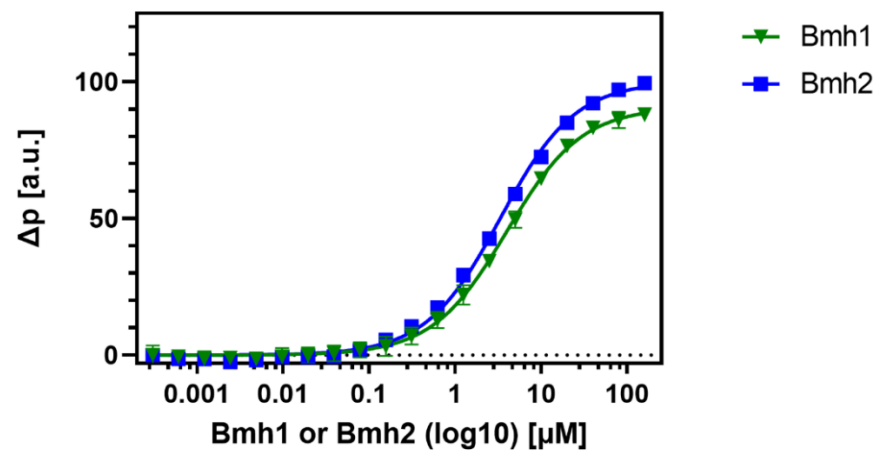


Figure 8

A



B

	Trk1_pT900+Bmh1	Trk1_pT900+Bmh2
B_{\max} [a.u.]	90.7 ± 0.8	100.1 ± 0.6
K_D [μM]	4.0 ± 0.2	3.4 ± 0.1

References

1. Arino, J.; Ramos, J.; Sychrova, H. Alkali Metal Cation Transport and Homeostasis in Yeasts. *Microbiol. Mol. Biol. Rev.* **2010**, *74*, 95-120, doi:10.1128/MMBR.00042-09.
2. Arino, J.; Ramos, J.; Sychrova, H. Monovalent Cation Transporters at the Plasma Membrane in Yeasts. *Yeast* **2019**, *36*, 177-193, doi:10.1002/yea.3355.
3. Sasikumar, A.; Killiea, D.; Kennedy, B.; Brem, R. Potassium Restriction Boosts Vacuolar Acidity and Extends Lifespan in Yeast. *Exp. Gerontol.* **2019**, *120*, 101-106, doi:10.1016/j.exger.2019.02.001.
4. Ruiz-Castilla, F.; Bieber, J.; Caro, G.; Michan, C.; Sychrova, H.; Ramos, J. Regulation and Activity of CaTrk1, CaAcu1 and CaHak1, the Three Plasma Membrane Potassium Transporters in *Candida albicans*. *Biochim. Biophys. Acta* **2021**, *1863*, doi:10.1016/j.bbamem.2020.183486.
5. Rivetta, A.; Allen, K.; Slayman, C.; Slayman, C. Coordination of K⁺ Transporters in Neurospora: *TRK1* Is Scarce and Constitutive, while *HAK1* Is Abundant and Highly Regulated. *Eukaryot. Cell* **2013**, *12*, 684-696, doi:10.1128/EC.00017-13.
6. Gaber, R.; Styles, C.; Fink, G. *TRK1* Encodes a Plasma Membrane Protein Required for High-affinity Potassium Transport in *Saccharomyces cerevisiae*. *Mol. Cell. Biol.* **1988**, *8*, 2848-2859, doi:10.1128/mcb.8.7.2848-2859.1988.
7. Petrezselyova, S.; Ramos, J.; Sychrova, H. Trk2 Transporter is a Relevant Player in K⁺ Supply and Plasma-membrane Potential Control in *Saccharomyces cerevisiae*. *Folia Microbiol.* **2011**, *56*, 23-28, doi:10.1007/s12223-011-0009-1.
8. Masaryk, J.; Sychrova, H. Yeast Trk1 Potassium Transporter Gradually Changes Its Affinity in Response to Both External and Internal Signals. *J. Fungi* **2022**, *8*, doi:10.3390/jof8050432.
9. Ko, C.; Gaber, R. *TRK1* and *TRK2* Encode Structurally Related K⁺ Transporters in *Saccharomyces cerevisiae*. *Mol. Cell. Biol.* **1991**, *11*, 4266-4273, doi:10.1128/mcb.11.8.4266.
10. Bertl, A.; Ramos, J.; Ludwig, J.; Lichtenberg-Frate, H.; Reid, J.; Bihler, H.; Calero, F.; Martinez, P.; Ljungdahl, P. Characterization of Potassium Transport in Wild-type and Isogenic Yeast Strains Carrying All Combinations of *trk1*, *trk2* and *tok1* Null Mutations. *Mol. Microbiol.* **2003**, *47*, 767-780, doi:10.1046/j.1365-2958.2003.03335.x.
11. Zayats, V.; Stockner, T.; Pandey, S.; Wortz, K.; Ettrich, R.; Ludwig, J. A Refined Atomic Scale Model of the *Saccharomyces cerevisiae* K⁺-translocation Protein Trk1p Combined With Experimental Evidence Confirms the Role of Selectivity Filter Glycines and Other Key Residues. *Biochim. Biophys. Acta* **2015**, *1848*, 1183-1195, doi:10.1016/j.bbamem.2015.02.007.
12. Kale, D.; Spurny, P.; Shamayeva, K.; Spurna, K.; Kahoun, D.; Ganser, D.; Zayats, V.; Ludwig, J. The *S. cerevisiae* Cation Translocation Protein Trk1 is Functional Without Its “Long Hydrophilic Loop” But LHL Regulates Cation Translocation Activity and Selectivity. *Biochim. Biophys. Acta* **2019**, *1861*, 1476-1488, doi:10.1016/j.bbamem.2019.06.010.
13. Rivetta, A.; Slayman, C.; Kuroda, T. Quantitative Modeling of Chloride Conductance in Yeast TRK Potassium Transporters. *Biophys. J.* **2005**, *89*, 2412-2426, doi:10.1529/biophysj.105.066712.
14. Helbig, A.; Rosati, S.; Pijnappel, P.; van Breukelen, B.; Timmers, M.; Mohammed, S.; Slijper, M.; Heck, A. Perturbation of the Yeast N-acetyltransferase NatB Induces Elevation of Protein Phosphorylation Levels. *BMC Genomics* **2010**, *11*, doi:10.1186/1471-2164-11-685.
15. Li, X.; Gerber, S.; Rudner, A.; Beausoleil, S.; Haas, W.; Villén, J.; Elias, J.; Gygi, S. Large-scale Phosphorylation Analysis of Alpha-factor-arrested *Saccharomyces cerevisiae*. *J. Proteome Res.* **2007**, *6*, 1190-1197, doi:10.1021/pr060559j.
16. Albuquerque, C.; Smolka, M.; Payne, S.; Bafna, V.; Eng, J.; Zhou, H. A Multidimensional Chromatography Technology For In-depth Phosphoproteome Analysis. *Mol. Cell. Proteomics* **2008**, *7*, 1389-1396, doi:10.1074/mcp.M700468-MCP200.

17. Swaney, D.; Beltrao, P.; Starita, L.; Guo, A.; Rush, J.; Fields, S.; Krogan, L.; Vilén, J. Global Analysis of Phosphorylation and Ubiquitylation Cross-talk in Protein Degradation. *Nat. Methods* **2013**, *10*, 676-682, doi:10.1038/nmeth.2519.
18. Holt, L.; Tuch, B.; Vilén, J.; Johnson, A.; Gygi, S.; Morgan, D. Global Analysis of Cdk1 Substrate Phosphorylation Sites Provides Insights Into Evolution. *Science* **2009**, *325*, 1682-1686, doi:10.1126/science.1172867.
19. Perez-Valle, J.; Jenkins, H.; Merchan, S.; Montiel, V.; Ramos, J.; Sharma, S.; Serrano, S.; Yenush, L. Key Role for Intracellular K⁺ and Protein Kinases Sat4/Hal4 and Hal5 in the Plasma Membrane Stabilization of Yeast Nutrient Transporters. *Mol. Cell. Biol.* **2007**, *27*, 5725-5736, doi:10.1128/MCB.01375-06.
20. Portillo, F.; Mulet, J.; Serrano, R. A Role for the Non-phosphorylated Form of Yeast Snf1: Tolerance to Toxic Cations and Activation of Potassium Transport. *FEBS Lett.* **2005**, *579*, 512-516, doi:10.1016/j.febslet.2004.12.019.
21. Casado, C.; Yenush, L.; Melero, C.; Ruiz Mdel, C.; Serrano, R.; Perez-Valle, J.; Arino, J.; Ramos, J. Regulation of Trk-Dependent Potassium Transport by the Calcineurin Pathway Involves the Hal5 Kinase. *FEBS Lett.* **2010**, *584*, 2415-2420, doi:10.1016/j.febslet.2010.04.042.
22. Yenush, L.; Merchan, S.; Holmes, J.; Serrano, R. pH-Responsive, Posttranslational Regulation of the Trk1 Potassium Transporter by the Type 1-Related Ppz1 Phosphatase. *Mol. Cell. Biol.* **2005**, *25*, 8683-8692, doi:10.1128/MCB.25.19.8683-8692.2005.
23. Forment, J.; Mulet, J.; Vicente, O.; Serrano, R. The Yeast SR Protein Kinase Sky1p Modulates Salt Tolerance, Membrane Potential and the Trk1,2 Potassium Transporter. *Biochim. Biophys. Acta* **2002**, *1565*, 36-40, doi:10.1016/s0005-2736(02)00503-5.
24. Bridges, D.; Moorhead, G. 14-3-3 Proteins: a Number of Functions For a Numbered Protein. *Sci. STKE* **2004**, doi:10.1126/stke.2962005re10.
25. Shi, L.; Ren, A.; Zhu, J.; Yu, H.; Jiang, A.; Zheng, H.; Zhao, M. 14-3-3 Proteins: A Window For a Deeper Understanding of Fungal Metabolism and Development. *World J. Microbiol. Biotechnol.* **2019**, *35*, doi:10.1007/s11274-019-2597-x.
26. Douherty, M.; Morrison, M. Unlocking The Code of 14-3-3. *J. Cell Sci.* **2004**, *117*, 1875-1884, doi:10.1242/jcs.01171.
27. Smidova, A.; Alblova, M.; Kalabova, D.; Psenakova, K.; Rosulek, M.; Herman, P.; Obsil, T.; Obsilova, V. 14-3-3 Protein Masks the Nuclear Localization Sequence of Caspase-2. *FEBS J.* **2018**, *285*, 4196-4213, doi:10.1111/febs.14670.
28. Kalabova, D.; Filandr, F.; Alblova, M.; Petrvalska, O.; Horvath, M.; Man, P.; Obsil, T.; Obsilova, V. 14-3-3 Protein Binding Blocks the Dimerization Interface of Caspase-2. *FEBS J.* **2020**, *287*, 3494-3510, doi:10.1111/febs.15215.
29. van Heusden, G. 14-3-3 Proteins: Insights From Genome-wide Studies in Yeast. *Genomics* **2009**, *94*, 287-293, doi:10.1016/j.ygeno.2009.07.004.
30. Bruckmann, A.; Steensma, H.; de Mattos, M.; van Heusden, G. Regulation of Transcription by *Saccharomyces cerevisiae* 14-3-3 Proteins. *Biochem. J.* **2004**, *382*, 867-875, doi:10.1042/BJ20031885.
31. Kakiuchi, K.; Yamauchi, Y.; Taoka, M.; Iwago, M.; Fujita, T.; Ito, T.; Song, S.; Isobe, T.; Ichimura, T. Proteomic Analysis of in Vivo 14-3-3 Interactions in the Yeast *Saccharomyces cerevisiae*. *Biochemistry* **2007**, *46*, 7781-7792, doi:10.1021/bi700501t.
32. van Heusden, G.; Steensma, H. Yeast 14-3-3 Proteins. *Yeast* **2006**, *23*, 159-171, doi:10.1002/yea.1338.
33. Smidova, A.; Stankova, K.; Petrvalska, O.; Lazar, J.; Sychrova, H.; Obsil, T.; Zimmermannova, O.; Obsilova, V. The Activity of *Saccharomyces cerevisiae* Na⁺, K⁺/H⁺ Antiporter Nha1 Is Negatively Regulated by 14-3-3 Protein Binding at Serine 481. *Biochim. Biophys. Acta* **2019**, *1866*, doi:10.1016/j.bbamcr.2019.118534.
34. Duby, G.; Poreba, W.; Piotrowiak, D.; Bobik, K.; Derua, R.; Waelkens, E.; Boutry, M. Activation of Plant Plasma Membrane H⁺-ATPase by 14-3-3 Proteins Is Negatively Controlled by Two

- Phosphorylation Sites Within the H⁺-ATPase C-terminal Region. *J. Biol. Chem.* **2009**, *284*, 4213-4221, doi:10.1074/jbc.M807311200.
35. Sottocornola, B.; Gazzarrini, S.; Olivari, C.; Romani, G.; Valbuzzi, P.; Thiel, G.; Moroni, A. 14-3-3 Proteins Regulate the Potassium Channel KAT1 by Dual Modes. *Plant Biol.* **2008**, *10*, 231-236, doi:10.1111/j.1438-8677.2007.00028.x.
 36. Capera, J.; Serrano-Novillo, C.; Navarro-Pérez, M.; Cassinelli, S.; Felipe, A. The Potassium Channel Odyssey: Mechanisms of Traffic and Membrane Arrangement. *Int. J. Mol. Sci.* **2019**, *20*, doi:10.3390/ijms20030734.
 37. Miranda, M.; Bashi, E.; Vylkova, S.; Edgerton, M.; Slayman, C.; Rivetta, A. Conservation and Dispersion of Sequence and Function in Fungal TRK Potassium Transporters: Focus on *Candida albicans*. *FEMS Yeast Res.* **2009**, *9*, 278-292, doi:10.1111/j.1567-1364.2008.00471.x.
 38. Blom, N.; Gameltoft, S.; Brunak, S. Sequence and Structure-based Prediction of Eukaryotic Protein Phosphorylation Sites. *J. Mol. Biol.* **1999**, *294*, 1351-1362, doi:10.1006/jmbi.1999.3310.
 39. Madeira, F.; Tinti, M.; Murugesan, G.; Berrett, E.; Stafford, M.; Toth, R.; Cole, C.; MacKintosh, C.; Barton, G. 14-3-3-Pred: Improved Methods to Predict 14-3-3-binding Phosphopeptides. *Bioinformatics* **2015**, *31*, 2276-2283, doi:10.1093/bioinformatics/btv133.
 40. Zimmermannova, O.; Felcmanova, K.; Rosas-Santiago, P.; Papouskova, K.; Pantoja, O.; Sychrova, H. Erv14 Cargo Receptor Participates in Regulation of Plasma-membrane Potential, Intracellular pH and Potassium Homeostasis via its Interaction with K⁺-specific Transporters Trk1 and Tok1. *Biochim. Biophys. Acta* **2019**, *1866*, 1376-1388, doi:10.1016/j.bbamcr.2019.05.005.
 41. Eraso, P.; Mazon, M.; Portillo, F. Yeast Protein Kinase Ptk2 Localizes at the Plasma Membrane and Phosphorylates in vitro the C-terminal Peptide of the H⁺-ATPase. *Biochim. Biophys. Acta* **2006**, *1758*, 164-170, doi:10.1016/j.bbamem.2006.01.010.
 42. de Nadal, E.; Posas, F. The HOG Pathway and the Regulation of Osmoadaptive Responses in Yeast. *FEMS Yeast Res.* **2022**, *22*, doi:10.1093/femsyr/foac013.
 43. Taylor, I.; Wang, Y.; Seitz, K.; Baer, J.; Bennewitz, S.; Mooney, B.; Walker, J. Analysis of Phosphorylation of the Receptor-like Protein Kinase HAESA During Arabidopsis Floral Abscission. *PLoS One* **2016**, *11*, doi:10.1371/journal.pone.0147203.
 44. White, D.; Unwin, R.; Bidels, E.; Pierce, A.; Teng, H.; Muter, J.; Greystoke, B.; Somerville, T.; Griffiths, J.; Lovell, S.; et al. Phosphorylation of the Leukemic Oncoprotein EVI1 on Serine 196 Modulates DNA Binding, Transcriptional Repression and Transforming Ability. *PLoS One* **2013**, *8*, doi:10.1371/journal.pone.0066510.
 45. Jumper, J.; Evans, R.; Pritzel, A.; Green, T.; Figurnov, M.; Ronneberger, O.; Tunyasuvunakool, K.; Bates, R.; Zidek, A.; Potapenko, A.; et al. Highly Accurate Protein Structure Prediction with AlphaFold. *Nature* **2021**, *596*, 583-589, doi:10.1038/s41586-021-03819-2.
 46. Buchowiecka, A. Puzzling over Protein Cysteine Phosphorylation: Assessment of Proteomic Tools for S-phosphorylation Profiling. *Analyst.* **2014**, *139*, 4118-4123, doi:10.1039/c4an00724g.
 47. Vlastaridis, P.; Kyriakidou, P.; Chaliotis, A.; Van de Peer, Y.; Oliver, S.; Amoutzias, G. Estimating the Total Number of Phosphoproteins and Phosphorylation Sites in Eukaryotic Proteomes. *Gigascience* **2017**, *6*, 1-11, doi:10.1093/gigascience/giw015.
 48. Davidson, A. Mechanism of Coupling of Transport to Hydrolysis in Bacterial ATP-binding Cassette Transporters. *J. Bacteriol.* **2002**, *184*, 1225-1233, doi:10.1128/JB.184.5.1225-1233.2002.
 49. Levin, E.; Zhiu, M. Recent Progress on the Structure and Function of the TrkH/KtrB Ion Channel. *Curr. Opin. Struct. Biol.* **2014**, *27*, 95-101, doi:10.1016/j.sbi.2014.06.004.
 50. Chen, Z.; Cole, P. Synthetic Approaches to Protein Phosphorylation. *Curr. Opin. Chem. Biol.* **2015**, *28*, 115-122, doi:10.1016/j.cbpa.2015.07.001.

51. Rezaei-Ghaleh, N.; Amininasab, M.; Kumar, S.; Walter, J.; Zweckstetter, M. Phosphorylation Modifies the Molecular Stability of β -amyloid Deposits. *Nat. Commun.* **2016**, *7*, doi:10.1038/ncomms11359.
52. Geiler-Samerotte, K.; Dion, M.; Budnik, B.; Drummond, D. Misfolded Proteins Impose a Dosage-dependent Fitness Cost and Trigger a Cytosolic Unfolded Protein Response in Yeast. *PNAS* **2011**, *108*, 680-685, doi:10.1073/pnas.1017570108.
53. Wolozin, B.; Behl, C. Mechanisms of Neurodegenerative Disorders. *Arch. Neurol.* **2000**, *57*, 739-196, doi:10.1001/archneur.57.6.793.
54. Woerner, A.; Frottin, F.; Hornburg, D.; Feng, L.; Meissner, F.; Patra, M.; Tatzelt, J.; Mann, M.; Winklhofer, K.; FU, H.; et al. Cytoplasmic Protein Aggregates Interfere with Nucleocytoplasmic Transport of Protein and RNA. *Science* **2016**, *351*, 173-176, doi:10.1126/science.aad2033.
55. Hundal, H.; Taylor, P. Amino Acid Transceptors: Gate Keepers of Nutrient Exchange and Regulators of Nutrient Signaling. *Am. J. Physiol. Endocrinol. Metab.* **2009**, *296*, 603-613, doi:10.1152/ajpendo.91002.2008.
56. Steyfkens, F.; Zhang, Z.; Van Zeebroeck, G.; Thevelein, J. Multiple Transceptors for Macro- and Micro-nutrients Control Diverse Cellular Properties Through the PKA Pathway in Yeast: A Paradigm for the Rapidly Expanding World of Eukaryotic Nutrient Transceptors Up to Those in Human Cells. *Front. Pharmacol.* **2018**, *13*, doi:10.3389/fphar.2018.00191.
57. Yenush, L.; Mulet, J.; Arino, J.; Serrano, R. The Ppz Protein Phosphatases Are Key Regulators of K^+ and pH Homeostasis: Implications for Salt Tolerance, Cell Wall Integrity and Cell Cycle Progression. *EMBO J.* **2002**, *21*, 920-929, doi:10.1093/emboj/21.5.920.
58. Yenush, L.; Merchan, S.; Holmes, J.; Serrano, R. pH-responsive, Posttranslational Regulation of the Trk1 Potassium Transporter by the Type 1-related Ppz1 Phosphatase. *Mol. Cell. Biol.* **2005**, *25*, 8683-8692, doi:10.1128/MCB.25.19.8683-8692.2005.
59. Zhao, P.; Zhao, C.; Chen, D.; Yun, C.; Li, H.; Bai, L. Structure and Activation Mechanism of the Hexameric Plasma Membrane H^+ -ATPase. *Nat. Commun.* **2021**, *12*, doi:10.1038/s41467-021-26782-y.
60. Camoni, L.; Visconti, S.; Aducci, P.; Marra, M. From Plant Physiology to Pharmacology: Fusicoccin Leaves the Leaves. *Planta* **2019**, *249*, 49-57, doi:10.1007/s00425-018-3051-2.
61. Guldener, U.; Fielder, T.; Beinhauer, J.; Hegemann, J. A New Efficient Gene Disruption Cassette for Repeated Use in Budding Yeast. *Nucleic Acid Res.* **1996**, *24*, 2519-2524, doi:10.1093/nar/24.13.2519.
62. Crooks, G.; Hon, G.; Chandonia, J.; Brenner, S. WebLogo: A Sequence Logo Generator. *Genome Res.* **2004**, *14*, 1188-1190, doi:10.1101/gr.849004.
63. Varadi, M.; Anyango, S.; Deshpande, M.; Nair, S.; Natassia, C.; Yordanova, G.; Yuan, D.; Stroe, O.; Wood, G.; Laydon, A.; et al. AlphaFold Protein Structure Database: Massively Expanding the Structural Coverage of Protein-sequence Space with High-accuracy Models. *Nucleic Acid Res.* **2021**, *50*, 439-444, doi:10.1093/nar/gkab1061.
64. Goddard, T.; Huang, C.; Meng, E.; Pettersen, E.; Couch, G.; Morris, J.; Ferrin, T. UCSF ChimeraX: Meeting Modern Challenges in Visualization and Analysis. *Protein Sci.* **2018**, *27*, 14-25, doi:10.1002/pro.3235.
65. Veisova, D.; Rezabkova, L.; Stepanek, M.; Novotna, P.; Herman, P.; Vecer, J.; Obsil, T.; Obsilova, V. The C-terminal Segment of Yeast BMH Proteins Exhibits Different Structure Compared to Other 14-3-3 Protein Isoforms. *Biochemistry* **2010**, *49*, 3853-3861, doi:10.1021/bi100273k.
66. Pohl, P.; Joshi, R.; Petrvalska, O.; Obsil, T.; Obsilova, V. 14-3-3-protein Regulates Nedd4-2 by Modulating Interactions Between HECT and WW Domains. *Commun. Biol.* **2021**, *4*, doi:10.1038/s42003-021-02419-0.

Putative role of phosphorylation and interaction with 14-3-3 proteins in the regulation of activity of Trk1

Jakub Masaryk¹, Deepika Kale¹, Pavel Pohl³, Francisco J. Ruiz-Castilla², Veronika Obšilová³, José Ramos², Hana Sychrová¹

¹Laboratory of Membrane Transport, Institute of Physiology, Czech Academy of Sciences, 142 20 Prague 4, Czech Republic

²Department of Microbiology, University of Córdoba, 140 71 Córdoba, Spain

³Laboratory of Structural Biology of Signaling Proteins, Institute of Physiology- Division BIOCEV, Czech Academy of Sciences, 252 50 Vestec, Czech Republic

Supplementary material

Table S1. List of yeast strains

Name	Genotype	Reference
BYT12	<i>trk1Δ::loxP trk2Δ::loxP</i> , derived from strain BY4741	[67]
BYT12Δ <i>bmh1</i>	<i>bmh1Δ::loxP</i> , derived from BYT12	[68]
BYT12Δ <i>hog1</i>	<i>hog11Δ::loxP</i> , derived from BYT12	This study
BYT12Δ <i>snf1</i>	<i>snf1Δ::loxP</i> , derived from BYT12	This study
BYT12Δ <i>sky1</i>	<i>sky1Δ::loxP</i> , derived from BYT12	This study
BYT12Δ <i>ptk2</i>	<i>ptk2Δ::loxP</i> , derived from BYT12	This study
BYT12Δ <i>hal5</i>	<i>hal5Δ::loxP</i> , derived from BYT12	This study

67. Petrezselyova, S.; Zahradka, J.; Sychrova, H. *Saccharomyces cerevisiae* BY4741 and W303-1A Laboratory Strains Differ in Salt Tolerance. *Fungal Biol.* **2010**, *114*, 144-150, doi:10.1016/j.funbio.2009.11.002.
68. Zahradka, J.; van Heusden, G.; Sychrova, H. Yeast 14-3-3 Proteins Participate in the Regulation of Cell Cation Homeostasis via Interaction with Nha1 Alkali-metal-cation/proton Antiporter. *Biochim. Biophys. Acta.* **2012**, *1820*, 849-858, doi:10.1016/j.bbagen.2012.03.013.

Table S2. List of plasmids

Plasmid	Relevant feature	Reference
YCp352	<i>URA3</i> , CEN6ARS4	[8]
pCScTRK1	<i>ScTRK1</i> , <i>URA3</i> , CEN6ARS4	[8]
pGRU1ScTRK1	GFP-tagged <i>ScTRK1</i> , <i>URA3</i> , 2 μ origin	[40]
pCScTRK1-GFP	pGRU1ScTRK1-CEN6ARS4	[8]
<i>Plasmid pCScTRK1 bearing indicated substitutions in TRK1</i>		
pCScTRK1_S8A		This study
pCScTRK1_T155A		This study
pCScTRK1_S303A		This study
pCScTRK1_S414A		This study
pCScTRK1_S490A		This study
pCScTRK1_T491A		This study
pCScTRK1_T1196A		This study
pCScTRK1_S878A		This study
pCScTRK1_S887A		This study
pCScTRK1_S882A		This study
pCScTRK1_S882D		This study
pCScTRK1_S882C		This study
pCScTRK1_T900A		This study
pCScTRK1_T900D		This study
pCScTRK1_T900C		This study
pCScTRK1_S882A+T900A		This study
pCScTRK1_L881D		This study
<i>Plasmids pCScTRK1-GFP and pGRU1ScTRK1 bearing indicated substitutions in GFP-tagged TRK1</i>		
pGRU1ScTRK1_T155A		This study
pCScTRK1-GFP_S414A		This study
pGRU1ScTRK1_S882A		This study
pGRU1ScTRK1_S882D		This study
pGRU1ScTRK1_S882C		This study
pGRU1ScTRK1_T900A		This study
pGRU1ScTRK1_T900D		This study
pGRU1ScTRK1_T900C		This study
pGRU1ScTRK1_S882A+T900A		This study

TRK1 expressed under the control of weak and constitutive S. cerevisiae NHA1 promoter

8. Masaryk, J.; Sychrova, H. Yeast Trk1 Potassium Transporter Gradually Changes Its Affinity in Response to Both External and Internal Signals. *J. Fungi* **2022**, *8*, doi:10.3390/jof8050432.
40. Zimmermannova, O.; Felcmanova, K.; Rosas-Santiago, P.; Papouskova, K.; Pantoja, O.; Sychrova, H. Erv14 Cargo Receptor Participates in Regulation of Plasma-membrane Potential, Intracellular pH and Potassium Homeostasis via its Interaction with K⁺-specific Transporters Trk1 and Tok1. *Biochim. Biophys. Acta* **2019**, *1866*, 1376-1388, doi:10.1016/j.bbamcr.2019.05.005.

Table S3. List of oligonucleotides used for deletion of selected genes

Oligonucleotide	Sequence (5'-3')
<i>Oligonucleotides used for gene deletion</i>	
HAL5-KanMx-F1	ATGGGAGATGAGAAGCTTTCACGCCACACATCTTTGAAGATTTCGTACGCTGCAGGTCGAC
HAL5-KanMx-R1	TTGTATATCTTTATTTACTAACCTTGGTATGTAAGTGTCTGCATAGGCCACTAGTGGATCTG
PTK2-KanMx-F1	CCGTAGCAGTTTTTTACAGGTTAACCGATTGAATAAGATATTCGTACGCTGCAGGTCGAC
PTK2-KanMx-R1	ACTAAAGCATAAAAAGAGGGAATTAAGAAGTCCTAACGTCGCATAGGCCACTAGTGGATCTG
SKY1-KanMx-F1	GAGGTTGAAGAGATAGAGTAAAGAAGAAGTGTAGACATTATTCGTACGCTGCAGGTCGAC
SKY1-KanMx-R1	AGTAAAAGGCAAGGGCAAATAAAGGTATAAAGGTAATCAGCATAGGCCACTAGTGGATCTG
SNF1-KanMx-F1	GTAACAAGTTTTGCTACACTCCCTTAATAAAGTCAACATGTTTCGTACGCTGCAGGTCGAC
SNF1-KanMx-R1	AGGGAACCTCCATATCATTCTTTACGTTCCACCATCAATGCATAGGCCACTAGTGGATCTG
<i>Diagnostic oligonucleotides</i>	
Hal5-F1	CCCGGAAGAAGACATCAACT
Hal5-R1	GTATAGCGGTGATGAGGCAC
Hal5-F2	GAGCCATATGTGGCACCTGA
Hal5-R2	TGCTGTGTCTCCATATGCTC
Ptk2_F1	ATGCCGGAGCTGCAAGTACT
Ptk2_R1	GTACCTGTGCCAGAATATC
Ptk2_F2	TACTACACCAACACATAATG
Ptk2_R2	GATGTTGGTACTTGTAGCAG
Sky1-F1	TCGTTACGGACGAGCCTATA
Sky1-R1	CGATTGGATGGACACATGCG
Sky1-F2	GGATGATGACCATATTGCAC
Sky1-R2	TCTACTCTGAGCTGCTCATG
Snf1-F1	GCGTGATGATGGGACTCGAG
Snf1-R1	GGGTGTCTTAAGAGTCTCAG
Snf1-F2	TGGTATACGATCTCGCTCAT
Snf1-R2	TAACGCTCTGGAATTCAGTG
KanMX-F	CATTTGATGCTCGATGA
KanMX-R	CTCTGGCGCATCGGGC

Underlined: sequences complementary to the start and end of the deletion cassette KanMX

Table S4. List of oligonucleotides used for site-directed mutagenesis

Oligonucleotide	Sequence (5'-3')
ScTRK1_S8A_for	GAAGAACGATGGCTAGAGTGCCAC
ScTRK1_S8A_rev	GTGGGCACTCTAGCCATCGTTCTTC
ScTRK1_T155A_for	GAGAAGAACGAAAGCAATCTTAGAAAGGG
ScTRK1_T155A_rev	CCCTTTCTAAGATTGCTTTTCGTTCTTCTC
ScTRK1_S303A_for	CAAAAAGAAGGGGTGCAAGAGATATTAGCCC
ScTRK1_S303A_rev	GGGCTAATATCTCTTGCACCCCTTCTTTTGG
ScTRK1_S414A_for	CATAGATCAAATGCGGGCCCGATAGCC
ScTRK1_S414A_rev	GGCTATCGGGCCCGCATTTGATCTATG
ScTRK1_S490A_for	GAAGGCTTGCTACTGGTTC
ScTRK1_S490A_rev	GAACCAGTAGCAAGCCTTC
ScTRK1_T491A_for	GAAGGCTTTCTGCTGGTTCAATTGAG
ScTRK1_T491A_rev	CTCAATTGAACCAGCAGAAAGCCTTC
ScTRK1_T1196A_for	CAGGCTAGAACCAATGCAGAAGACCCAATGACG
ScTRK1_T1196A_rev	CGTCATTGGGTCTTCTGCATTGGTTCTAGCCTG
ScTRK1_S878A_for	GGATAATGTTTAAAATTGCTCCTGATTTATCACAGATG
ScTRK1_S878A_rev	CATCTGTGATAAATCAGGAGCAATTTTAAACATTATCC
ScTRK1_S887A_for	CAGATGAGAGAAGCTTTAGGTTTTTCTC
ScTRK1_S887A_rev	GAGAAAACCTAAAGCTTCTCTCATCTG
ScTRK1_S882A_for	CTCCTGATTTAGCACAGATGAGAGA
ScTRK1_S882A_rev	TCTCTCATCTGTGCTAAATCAGGAG
ScTRK1_S882D_for	CTCCTGATTTAGACCAGATGAGAGA
ScTRK1_S882D_rev	TCTCTCATCTGGTCTAAATCAGGAG
ScTRK1_S882C_for	CTCCTGATTTATGCCAGATGAGAGA
ScTRK1_S882C_rev	TCTCTCATCTGGCATAAATCAGGAG
ScTRK1_T900A_for	GTCGTTGTTTCGCCTTGCTATTTCC
ScTRK1_T900A_rev	GGAAATAGCAAGGCGAAACAACGAC
ScTRK1_T900D_for	GTCGTTGTTTCGACTTGCTATTTCC
ScTRK1_T900D_rev	GGAAATAGCAAGTCGAAACAACGAC
ScTRK1_T900C_for	GTCGTTGTTTCTGCTTGCTATTTCC
ScTRK1_T900C_rev	GGAAATAGCAAGCAGAAACAACGAC
ScTRK1_L881D_for	TCTCCTGATGATTCACAGATG
ScTRK1_L881D_rev	CATCTGTGAATCATCAGGAGA

Underlined: codons for substituting residue

Figure S1

Residue	Localization	Reference
Thr12	NTD	Holt (2009), Helbig (2010)
Ser15	NTD	Holt (2009)
Thr155	IL1	Swaney (2013)
Ser337	IL1	Swaney (2013)
Ser414	IL1	Holt (2009), Swaney (2013), Li (2007)
Thr450	IL1	Albuquerque (2008), Swaney (2013)
Ser576	IL1	Swaney (2013)
Thr592	IL1	Holt (2009), Swaney (2013), Li (2007)
Thr1143	CTD	Helbig (2010)
Ser1207	CTD	Helbig (2010)

Figure S1. List of putative phosphorylation sites of Trk1. Previously published residues are listed with their respective localizations (NTD- N-terminal domain, IL1- intracellular loop 1, CTD- C-terminal domain) and references.

Figure S2

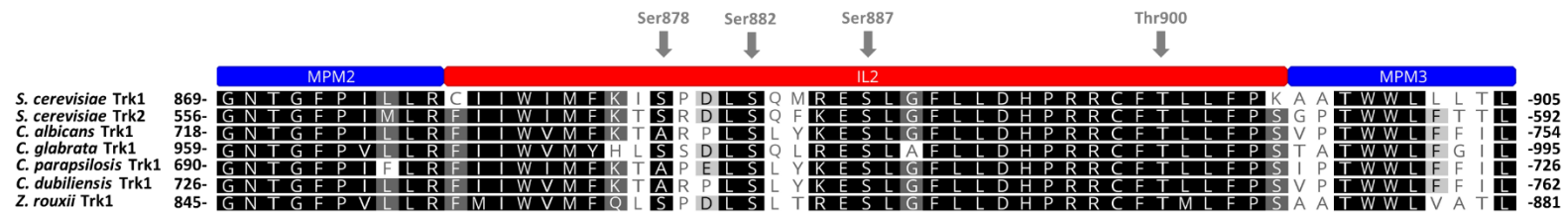


Figure S2. Alignment of sequences of IL2 of Trk1 from various yeast species. Sequences of Trk1 proteins from *Saccharomyces cerevisiae*, *Candida albicans*, *C. glabrata*, *C. parapsilosis*, *C. dubiliensis*, *Zygosaccharomyces rouxii* and Trk2 sequence from *S. cerevisiae* were aligned using Geneious prime version 2022.1.1. The alignment of parts of the sequences corresponding to IL2 (annotated in red) and short segments of domains MPM2 and MPM3 (annotated in blue) of each species is shown. Putative phosphorylation sites located within Trk1-IL2 from *S. cerevisiae* are highlighted with grey arrows.

Figure S3

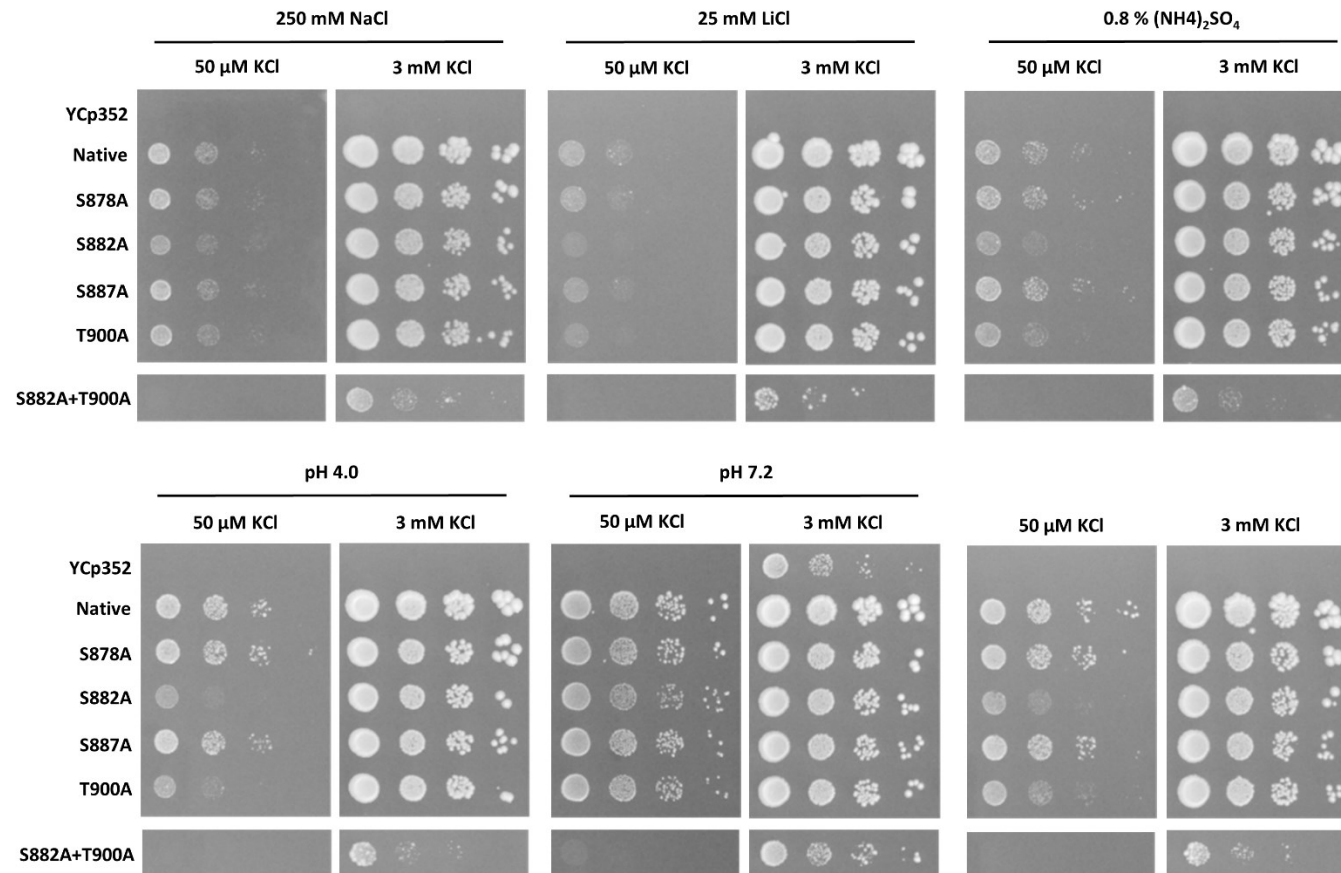


Figure S3. Growth of BYT12 cells carrying an empty vector and expressing native Trk1 or the mutated versions from pCScTRK1. Cells were grown on YNB-F plates with pH 5.8 (if not indicated otherwise), supplemented with indicated concentrations of KCl, NaCl, LiCl and (NH₄)₂SO₄. Pictures were captured after 7 days at 30 °C.

Figure S4

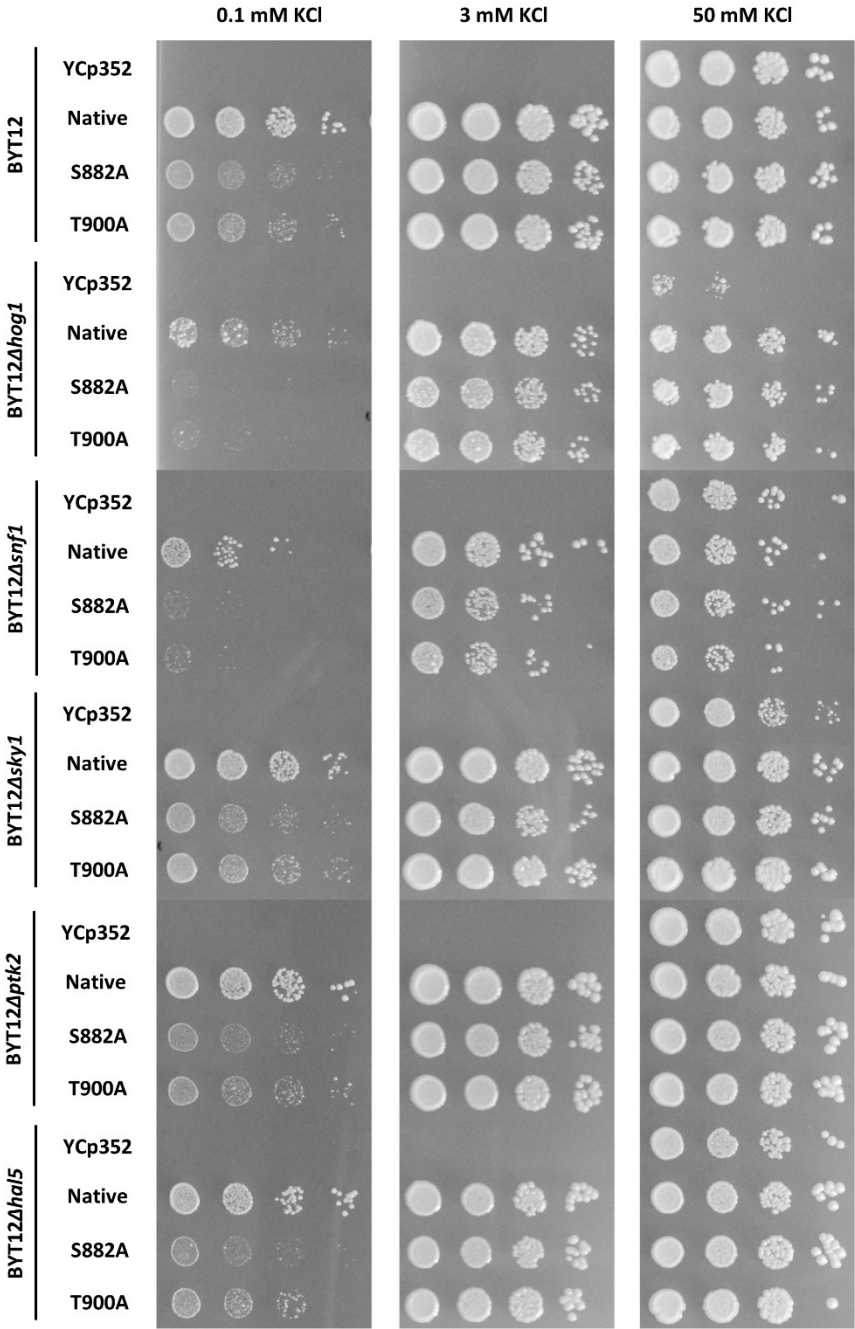


Figure S4. Growth of BYT12 cells and BYT12 cells with deletion of genes for selected kinases expressing native Trk1 and mutated version S882A and T900A. Cells were grown on YNB-F plates supplemented with the indicated concentration of KCl. Pictures were taken after 5 days at 30 °C.

Figure S5

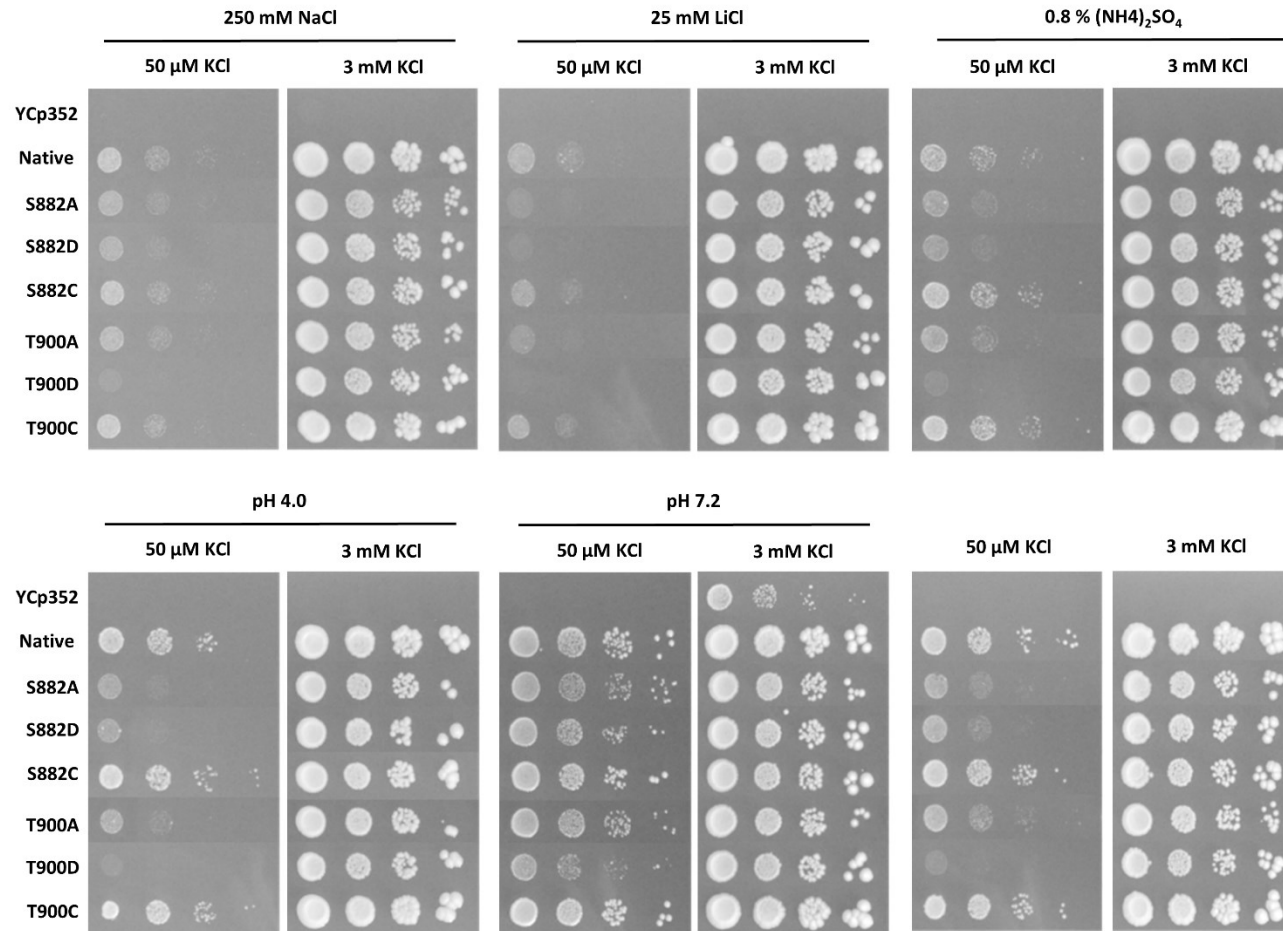


Figure S5. Growth of BYT12 cells carrying an empty vector and expressing native Trk1 or the mutated versions from pCScTRK1. Cells were grown on YNB-F plates with pH 5.8 (if not indicated otherwise), supplemented with the indicated concentrations of KCl, NaCl, LiCl and (NH₄)₂SO₄. Pictures were captured after 7 days at 30 °C.

Figure S6

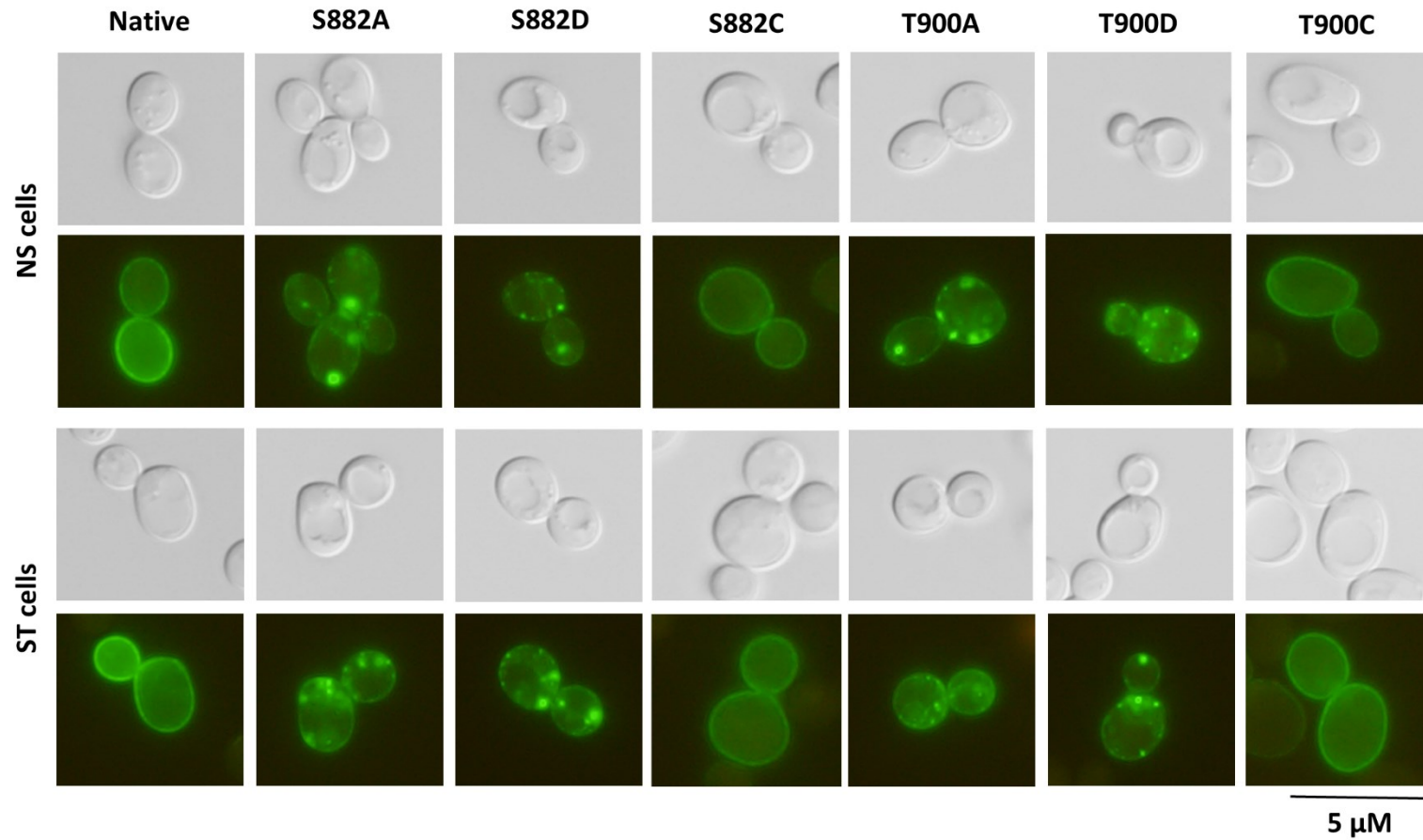


Figure S6. Subcellular localization of GFP-tagged native Trk1 and selected mutated versions in nonstarved (NS cells) and cells starved for potassium (ST cells). Cells were grown overnight on YNB supplemented with 100 mM KCl and observed under the microscope (NS cells) or additionally starved on YNB-F for 1 hour and then observed under the microscope (ST cells).

Figure S7

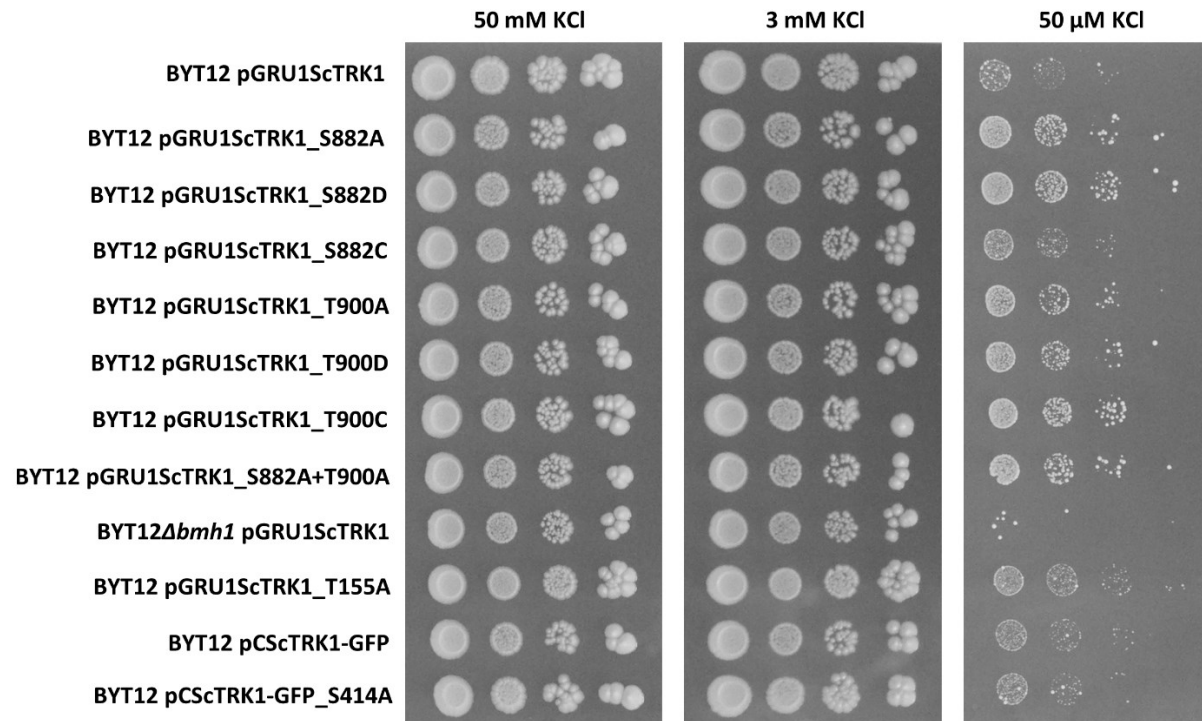


Figure S7. Growth of BYT12 and BYT12Δbmh1 cells expressing native Trk1 or the mutated versions from pGRU1ScTRK1 or pCScTRK1-GFP. Cells were grown on YNB-F plates with pH 5.8 supplemented with the indicated concentrations of KCl. Pictures were captured after 7 days at 30 °C.

Figure S8

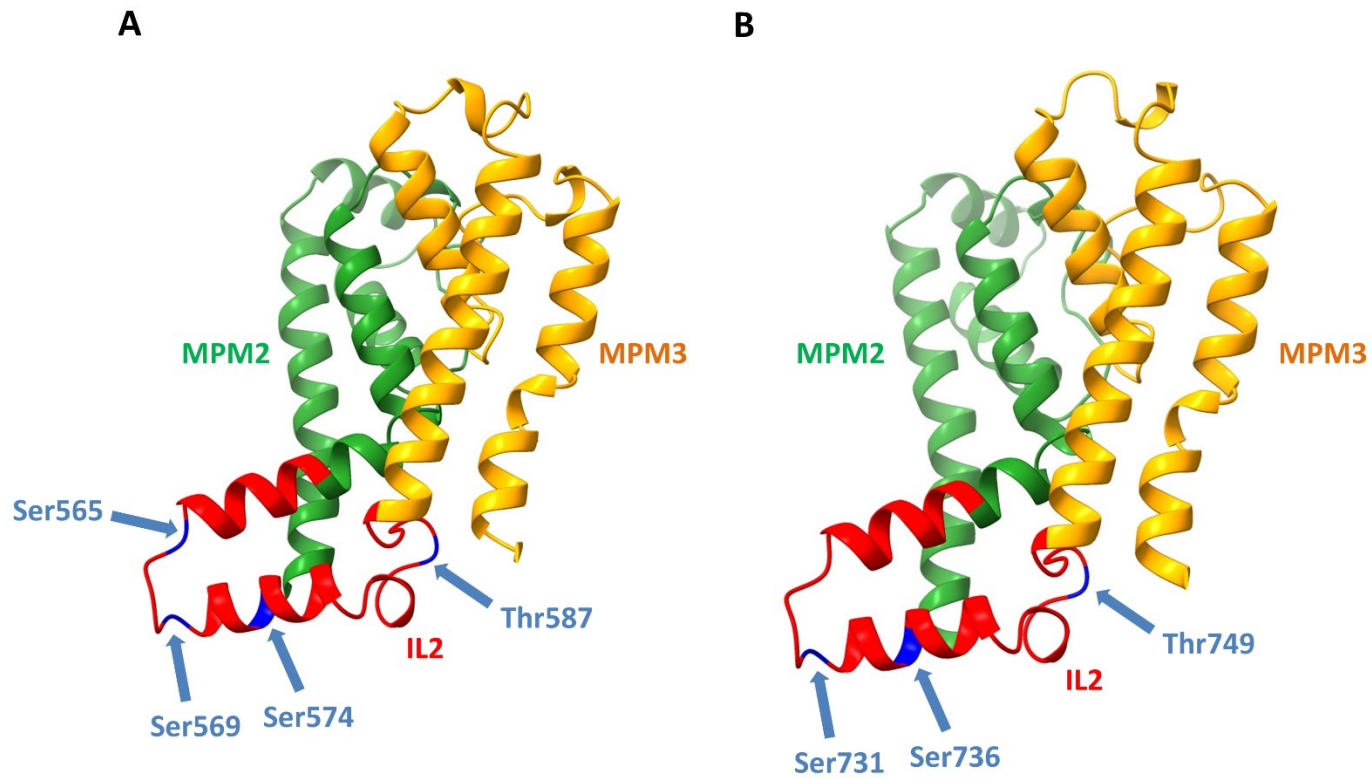


Figure S8. 3D model of proteins Trk2 from *S. cerevisiae* (A) and Trk1 from *C. albicans* (B). PDB files were obtained from the AlphaFold database (database numbers: P28584 for ScTrk2 and A0A1D8PTL7 for CaTrk1). For better clarity, only the MPM2 (green), MPM3 (yellow) and IL2 (red) domains are shown.

Figure S9

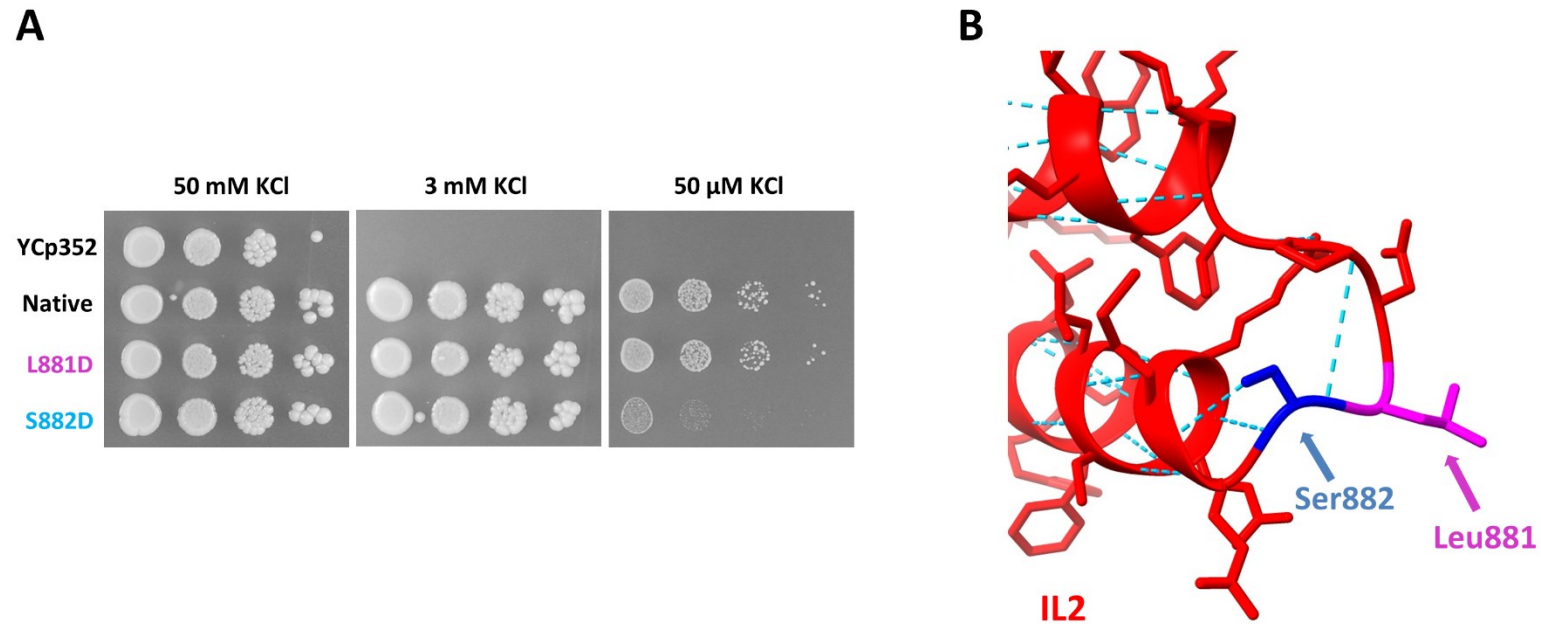


Figure S9. Effect of substitution L881D on the growth of BYT12 cells on various concentrations of potassium. (A) Growth of BYT12 cells carrying an empty vector (YCp352) or expressing native Trk1 and version S882D and L881D on YNB-F plates supplemented with indicated concentrations of KCl. Pictures were captured after 7 days at 30 °C. **(B)** Localization and orientation of residues Leu881 (purple) and Ser882 (blue) within 3D model of Trk1 from *S. cerevisiae* (PDB obtained from AlphaFold database, database number: P12685, only part of IL2 domain containing both Ser882 and Leu881 is shown). All hydrogen bonds predicted within the presented region are shown. 3D model visualized in ChimeraX version 1.1.

Figure S10

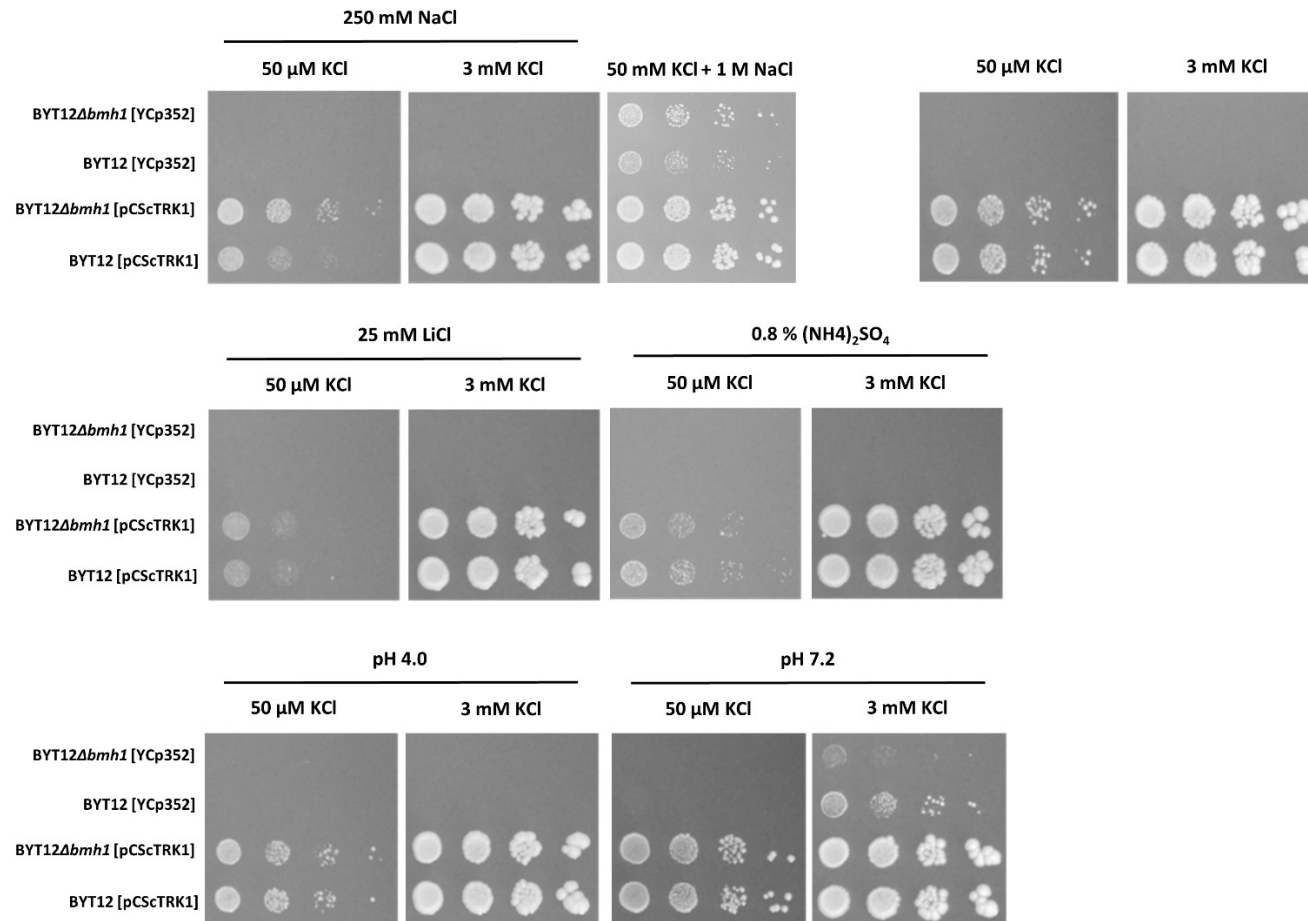


Figure S10. Growth of BYT12 and BYT12Δbmh1 cells carrying an empty vector and expressing native Trk1 from pCScTRK1. Cells were grown on YNB-F plates with pH 5.8 (if not indicated otherwise), supplemented with the indicated concentrations of KCl, NaCl, LiCl and (NH₄)₂SO₄. Pictures were captured after 7 days at 30 °C.

Figure S11

Residue	Localization	NetPhos 3.1 score	% of identity
Ser8	NTD	0.971	86
Thr155	IL1	0.950	100
Thr167	IL1	0.907	0
Ser303	IL1	0.996	43
Ser346	IL1	0.992	0
Ser414	IL1	0.923	43
Thr450	IL1	0.916	0
Ser490	IL1	0.998	43
Thr491	IL1	0.714	0
Thr592	IL1	0.754	29
Thr900	IL2	0.602	100
Thr1196	CTD	0.857	57
Thr1209	CTD	0.480	71
Thr1233	CTD	0.513	29

*all residues highly scored by three prediction methods (14-3-3-Pred)

residues selected for further analysis highlighted by **red

Figure S11. List of residues predicted by 14-3-3-Pred (all three algorithms) as potential residues for interaction with 14-3-3 proteins. Respective localizations (NTD- N-terminal domain, IL1- Intracellular loop1, IL2- Intracellular loop 2 and CTD- C-terminal domain), NetPhos 3.1 scores and identity are shown. Residues selected for further analysis are highlighted in red (selection based on NetPhos 3.1 score >0.6 and percent of identity >40%, values above threshold highlighted in green). Percent of identity calculated from the alignment of Trk1 sequences from species: *S. cerevisiae*, *C. albicans*, *C. glabrata*, *C. parapsilosis*, *C. dubiliensis*, *Z. rouxii* and Trk2 sequence from *S. cerevisiae* (see Material and methods).

Figure S12

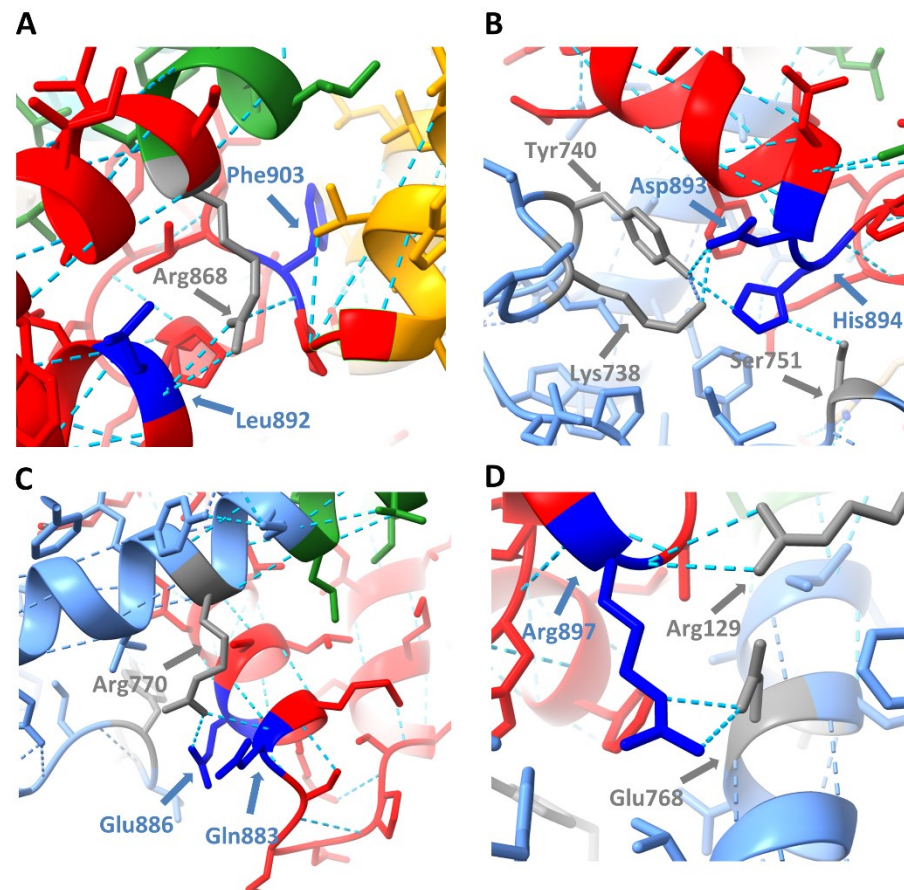


Figure S12. Predicted hydrogen bonds between IL2 and domains MPM2 or IL1. Domain MPM2 is highlighted in green, IL1 is highlighted in light blue and IL2 is highlighted in red. **(A)** Hydrogen bonds between Arg868 (MPM2) and Leu892 or Phe903 (both IL2). **(B)** Hydrogen bonds between Asp893 (IL2) and Lys738 or Tyr740 (both IL1) and His894 (IL2) and Tyr740 or Ser751 (both IL1). **(C)** Hydrogen bonds between Arg770 (terminal region of IL1) and Gln883 or Glu886 (both IL2). **(D)** Hydrogen bonds between Arg897 (IL2) and Arg129 or Glu768 (both IL1). All potential predicted hydrogen bonds are depicted (including mutually exclusive).

3.3 Minority potassium-uptake system Trk2 has a crucial role in yeast survival of glucose-induced cell death

Reference: Duskova, M.; Cmun, D.; Papouskova, K.; **Masaryk, J.**; Sychrova, H. Minority potassium-uptake system Trk2 has a crucial role in yeast survival of glucose-induced cell death. *Microbiology (Reading)* **2021**, *167*, doi: 10.1099/mic.0.001065. IF₂₀₂₁= 2.777

Summary: Glucose-induced cell death (GICD) is a phenomenon described as the apoptosis of yeast cells triggered by the presence of glucose in an environment lacking all other nutrients. When kept in pure water, stationary *S. cerevisiae* cells can survive up to several weeks, due to prior accumulation of reserve carbohydrates, however, when a small amount of glucose is added, cells undergo apoptosis with the presence of so-called apoptosis markers (e.g., DNA-degradation, production of ROS, fragmentation of nucleus etc.). Trk-transporters have been suggested to play a role in the survival of GICD, as their absence renders cells substantially more GICD-sensitive. As previous studies connecting Trk-transporters to the GICD were performed using strains lacking both Trk1 and Trk2, we focused our study on the individual contributions of Trk1, Trk2 and other potassium transporters to the survival of the GICD. Additionally, the role of these transporters in the survival of high-temperature stress and the link between potassium uptake and consumption of ATP was studied.

We confirmed that the presence of potassium-uptake systems is crucial for the ability of stationary cells to withstand environments lacking all the other nutrients except glucose. Surprisingly, we found not Trk1, but rather Trk2 to be a major player in the survival of the GICD. Moreover, our results showed significantly increased consumption of ATP and presumed de-regulation of the main cellular consumer of ATP, H⁺-ATPase Pma1 as a result of the absence of Trk2, thus suggesting the cause of increased susceptibility to GICD to be loss of cellular ATP and pointing to the possible link between Trk2 and Pma1.

The presented work provided new data regarding one of the secondary functions of Trk-transporters, involvement in the survival of the GICD. Additionally, as Trk1's paralog Trk2 has been shown to fulfil a marginal role in potassium uptake, our results expand on our knowledge about its physiological role. The results were published in *Microbiology (Reading)*.

Author's contribution: The author of the thesis contributed to the presented work by measurements of the internal potassium content of the individual strains.

Minority potassium-uptake system Trk2 has a crucial role in yeast survival of glucose-induced cell death

Michala Dušková, Denis Cmunť, Klára Papoušková, Jakub Masaryk and Hana Sychrová*

Abstract

The existence of programmed cell death in *Saccharomyces cerevisiae* has been reported for many years. Glucose induces the death of *S. cerevisiae* in the absence of additional nutrients within a few hours, and the absence of active potassium uptake makes cells highly sensitive to this process. *S. cerevisiae* cells possess two transporters, Trk1 and Trk2, which ensure a high intracellular concentration of potassium, necessary for many physiological processes. Trk1 is the major system responsible for potassium acquisition in growing and dividing cells. The contribution of Trk2 to potassium uptake in growing cells is almost negligible, but Trk2 becomes crucial for stationary cells for their survival of some stresses, e.g. anhydrobiosis. As a new finding, we show that both Trk systems contribute to the relative thermotolerance of *S. cerevisiae* BY4741. Our results also demonstrate that Trk2 is much more important for the cell survival of glucose-induced cell death than Trk1, and that stationary cells deficient in active potassium uptake lose their ATP stocks more rapidly than cells with functional Trk systems. This is probably due to the upregulated activity of plasma-membrane Pma1 H⁺-ATPase, and consequently, it is the reason why these cells die earlier than cells with functional active potassium uptake.

INTRODUCTION

Saccharomyces cerevisiae cells from a culture grown to the stationary phase can survive, when transferred to pure water, for several weeks. This is due to their large reserve stocks, mainly trehalose and glycogen, which help them to survive the starvation period [1]. On the other hand, if a small amount of some sugars, e.g. glucose, is added to the water during the starvation period, yeast cells start to die quite quickly. This phenomenon was named sugar-induced cell death (SICD) or glucose-induced cell death (GICD), respectively [2]. Sugar-induced death of stationary-phase yeast cells is characterized by several so-called apoptosis or programmed-cell-death markers, e.g. a rapid production of reactive oxygen species (ROS), RNA and DNA degradation, as well as nucleus fragmentation, cell shrinkage and membrane damage [2]. GICD exists also in exponentially growing cells, where it has more features of necrosis than apoptosis [3].

Besides the presence of sugar, other conditions were also shown to induce programmed cell death in *S. cerevisiae*, one of them being potassium starvation [4]. Potassium is a major cation in yeast cells, its concentration in *S. cerevisiae* cells is

usually 200–300 mM, depending on the growth conditions [5, 6], and it has multiple roles in cell physiology. Intracellular potassium not only contributes to compensating the surplus of negative charges inside the cells (e.g. those of nucleic acids or polyphosphates), but its high concentration is very important for cell turgor and thereby for cell division, as well as for osmotic stress survival. Even if the cells do not need to accumulate potassium, as they are not growing, they need a continuous influx and efflux of potassium across the plasma membrane, which participate in the regulation of membrane potential and Pma1 H⁺-ATPase activity, and thereby in the regulation of intracellular pH. The importance of potassium is also reflected in the fact that *S. cerevisiae* cells have more than ten different potassium transporters in their plasma membrane and in the membranes of organelles (reviewed in [5, 6]). At the plasma membrane, *S. cerevisiae* cells have two specific systems for K⁺ uptake (potassium-specific uniporters Trk1 and Trk2), and three transporters enabling potassium efflux. One of the efflux systems, the Tok1 channel, is potassium specific, whereas the other two exporters, Ena ATPases and the Nha1 antiporter, mediate the efflux of all alkali metal cations (reviewed in [5, 6]).

Received 29 January 2021; Accepted 21 May 2021; Published 25 June 2021

Author affiliations: ¹Laboratory of Membrane Transport, Institute of Physiology, Czech Academy of Sciences, Prague 4, Czech Republic.

***Correspondence:** Hana Sychrová, hana.sychrova@fgu.cas.cz

Keywords: GICD; potassium uptake; stationary cells; *Saccharomyces cerevisiae*; thermotolerance; ATP content.

Abbreviations: c.f.u., colony forming unit; GICD, glucose-induced cell death; ROS, reactive oxygen species.

†Present address: Dept. Oncology, Ludwig Institute for Cancer Research, University of Lausanne, Lausanne, Switzerland.

Two supplementary figures are available with the online version of this article.

Table 1. *Scerevisiae* strains used in this study

Strain	Genotype	Reference
BY4741	MATa <i>his3Δ1 leu2Δ0 met15Δ0 ura3Δ0</i>	EUROSCARF, Germany
BYT1	BY4741 <i>trk1Δ::loxP</i>	[9]
BYT2	BY4741 <i>trk2Δ::loxP</i>	[9]
BYT12	BY4741 <i>trk1Δ::loxP trk2Δ::loxP</i>	[14]
BYT3	BY4741 <i>tok1Δ::loxP</i>	[22]
BYT45	BY4741 <i>nha1Δ::loxP ena1-5Δ::kanMX</i>	[11]
BYT12345	BY4741 <i>trk1Δ::loxP trk2Δ::loxP tok1Δ::loxP nha1Δ::loxP ena1-5Δ::loxP</i>	[11]

Trk1 and Trk2 belong to the superfamily of K⁺ transporters (SKT), which, besides Trk systems of yeast species, contains potassium transporters from archaea, bacteria and plants. Yeast Trk transporters share to a great extent a similar structure. Their membrane part contains four highly conserved so-called MPM domains [7], and they mainly differ in the length and sequence of their hydrophilic parts [8]. The structures of *S. cerevisiae* Trk1 and Trk2 differ mainly in the length of their first intracellular loop, which is 647 amino-acid residues long in Trk1, and only 331 amino acids in Trk2. As for their physiological roles, Trk1 is the main potassium uptake system, whereas Trk2 contributes to potassium acquisition in growing cells to a much smaller extent [9]. On the other hand, Trk2 is indispensable if stationary cells are exposed to desiccation stress [10]. Together, Trk potassium uptake systems are very important for the maintenance of plasma-membrane potential and the regulation of intracellular pH, as their absence changes the activity of plasma membrane H⁺-ATPase [11].

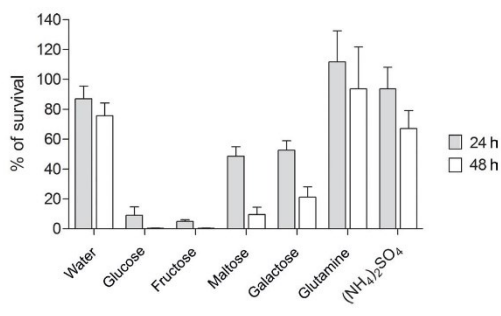


Fig. 1. Survival of BY4741 stationary cells in solutions containing various C or N sources. Cells were grown in YPD+100 mM KCl for 48 h and subsequently treated in water or in water containing various 2% carbon sources or nitrogen sources [0.5% (NH₄)₂SO₄ or 0.1% glutamine] at 37 °C for 24 and 48 h. Survival is expressed as a percentage of the number of colonies (c.f.u.) formed before treatment (100 %).

As for the induction of cell death, it was the function of Trk uptake systems, which was first described as being crucial for growing-cell survival in media with an extremely low potassium concentration, i.e. upon potassium deprivation. If the *TRK1* and *TRK2* genes were deleted, mutant cells exhibited programmed-cell-death markers to a much higher extent than the wild-type cells [4]. A role of potassium-uptake systems was also shown for stationary cells and their survival of GICD. The function of Trk1 and Trk2 was important for preventing GICD, as the double mutant lacking both Trk transporters was highly sensitive to incubation in 2% glucose at 37 °C [12]. On the other hand, the simultaneous absence of the three potassium-exporting systems resulted in a slightly higher tolerance of stationary-phase cells to GICD [12].

In this work we analysed tolerance/sensitivity to induced cell death in a series of mutants, derived from the BY4741 strain, differing in the presence or absence of plasma-membrane potassium importers and exporters. We studied in detail the individual contribution of Trk1 and Trk2 to cell survival of GICD (so far studied only with the double mutants [4, 12]) and examined a possibility of the connection between potassium influx and the consumption of ATP stocks in stationary-phase cells exposed to a glucose solution.

METHODS

Strains, media and growth conditions

The *S. cerevisiae* BY4741 strain (MATa *his3Δ1 leu2Δ met15Δ ura3Δ*; EUROSCARF) and its derivatives lacking various combinations of genes encoding potassium transporters (listed in Table 1) were used. Yeast strains were routinely grown in standard liquid YPD medium (YPD BROTH, Formedium) supplemented with 100 mM KCl in an orbital shaker at 160 r.p.m. at 30 °C. Solid YPD media (YPD AGAR, Formedium) were also supplemented with 100 mM KCl. KCl was added to support the growth of BYT1 and BYT12 strains, whose growth is inhibited at lower potassium concentrations due to the absence of Trk1 [9, 11].

Growth curves

In total, 10 ml of YPD medium supplemented with 100 mM KCl was inoculated with individual strains and the OD₆₀₀ of the culture was estimated at regular intervals for 72 h.

Induced cell death

To determine the effect of various compounds on long-term cell survival in water, cells were grown in 10 ml of YPD +100 mM KCl at 30 °C for 48 or 72 h. Cultures were washed twice with distilled water and resuspended in 10 ml of distilled water. Then, 0.5 ml of cell suspension was transferred to 9.5 ml of water alone, or water containing either 2% sugar or 0.5% (NH₄)₂SO₄ or 0.1% glutamine, and incubated at 30 or 37 °C. At the start (immediately after cell transfer) or after 18, 24 and 48 h, 100 μl aliquots of cell suspension were vortexed, transferred to 900 μl of distilled water, 2000-fold and 20 000-fold diluted, and 50 or 100 μl aliquots of diluted cell suspensions were plated on YPD in triplicate. The number of colonies

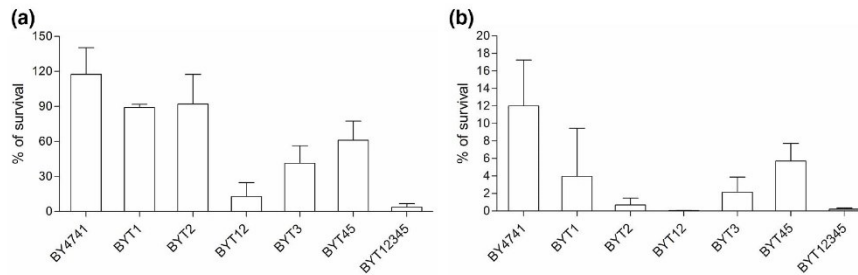


Fig. 2. Survival of BY4741 and its mutants lacking K^+ influx and efflux systems in 2% glucose. Cells were grown in YPD+100 mM KCl for 48 h and subsequently treated in water (a) or in water containing 2% glucose (b) at 37 °C for 24 h. Survival is expressed as a percentage of the number of colonies (c.f.u.) formed before treatment (100%).

(c.f.u.) was counted after 2 days of plate incubation at 30 °C. Each experiment (two parallels per strain and set of conditions) was repeated three times and the means \pm SD are shown.

ATP content

For the measurement of intracellular ATP, the same cultures and experimental set-up as described above were used. ATP was measured immediately after transfer to water or to water with 2% glucose (start) and after 18 h of incubation at 30 °C.

The reaction solution (BacTiter-Glo Reagent) was prepared according to the manufacturer's instructions (BacTiter-Glo Microbial Cell Viability Assay, Promega). For the construction of the calibration curve, ATP standard solutions (0, 0.05, 0.5, 5, 50, 500 nM) were diluted from a stock solution (Merck, 10 mM ATP in 50 mM HEPES). Then, 100 μ l aliquots of cell suspension was transferred to 96-well plates (Nunc-Immuno MicroWell 96-well polystyrene plates) and the same amount of reaction solution was added. The content of wells was briefly mixed on an orbital shaker, incubated at room temperature for 5 min, and then the luminescence was recorded (Cytation 3, BioTek Instruments). Standard solutions as well as blanks (100 μ l of standards, water or 2% glucose) were treated in the same way as samples with yeast cells. The presented data are means \pm SD of three biological replicates assayed in triplicate.

Fluorescence microscopy

Besides the estimation of c.f.u., dead cells were visualized with primuline under a fluorescence microscope. Cells (immediately after transfer to water or 2% glucose (start) or after incubation at 30 °C for 18 h) were stained with primuline (1 mg ml⁻¹ in water) for approx. 10 min. The fluorescence signal was observed under an Olympus BX53 microscope with an Olympus DP73 camera. A cool LED light source with 460 nm excitation and 515 nm emission was used to visualize primuline-stained cells. Nomarski optics was used for whole cell images. For the estimation of dead-cell number, the percentage of primuline stained cells in 200 cells visible in Nomarski optics was counted.

Glucose-induced acidification of cell surroundings

The activity of Pma1 ATPase was estimated by the acidification of external medium (water in our case) as described previously [13] with some modifications. Cells, grown in YPD+100 mM KCl at 30 °C for 48 h, were washed twice with distilled water, resuspended to OD₆₀₀=0.3 in water containing a pH indicator (0.01% bromocresol green sodium salt) and incubated at 30 or 37 °C, respectively. The changes in absorbance (A₅₉₅) of 100 μ l cell suspension were recorded in 96-well plates in an ELx808 Absorbance Microplate Reader (BioTek Instruments). After 60 min of incubation, 5 μ l of a 40% solution of glucose or 5 μ l of distilled water (control) were added, and the changes in absorbance were followed for another 180 min. The results were obtained from three biological replicates assayed in triplicate.

Potassium content measurement

To estimate intracellular potassium content, cells were grown in 10 ml of YPD+100 mM KCl at 30 °C for 48 h, washed with water and resuspended in water (OD₆₀₀~0.3). Three aliquots (1 ml) per strain suspension were withdrawn and harvested by filtration (Millipore filters, 0.8 μ m). Filters with cells were rapidly washed twice with 5 ml of 20 mM MgCl₂, acid extracted and potassium content in extracts was measured by atomic absorption.

RESULTS AND DISCUSSION

Both of the works that identified Trk-mediated potassium uptake into yeast cells as being crucial for cell survival of GICD used double mutants that lacked both Trk1 and Trk2 systems, and also differed from the corresponding parental strain W303 in their auxotrophies [4, 12]. We know that different levels of auxotrophies may influence the phenotypes of yeast strains grown in complete media, thus we decided to use an already available series of strains lacking one or multiple potassium transporting system(s) and that had the same auxotrophies as their parental strain BY4741 (Table 1).

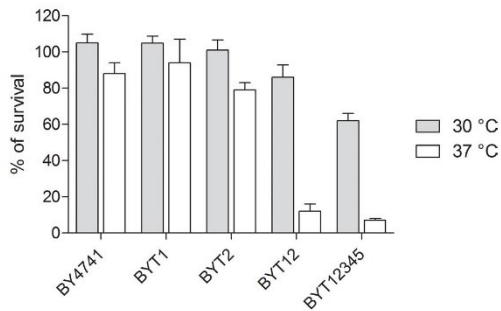


Fig. 3. Survival of BY4741 and its mutants lacking K^+ influx and efflux systems in water at 30 or 37 °C. Cells were grown in YPD+100 mM KCl for 48 h and subsequently incubated in water for 18 h. Survival is expressed as a percentage of the number of colonies (c.f.u.) formed before incubation in water (100%).

Viability of stationary-phase BY4741 cells is very sensitive to glucose and fructose

Since the *S. cerevisiae* W303 and BY4741 strains differ in their physiological parameters related to potassium homeostasis, such as membrane potential or salt tolerance [14], we first estimated whether BY4741 cells are subject to a similar sugar-induced cell death as the W303 cells. First, we tested the stationary-cell survival (estimated as c.f.u.) in water or 2% sugar solution after 24 or 48 h of incubation at 37 °C, in the same way as was done for the W303 cells [12]. Water alone did not cause a very significant harm to cells, as about 70% of cells were able to form colonies after 48 h of treatment in water at 37 °C (Fig. 1). Fig. 1 also shows that no BY4741 cells survived a 48 h incubation in 2% glucose or 2% fructose, and only a few of them (less than 10 or 5%, respectively) survived 24 h in these two sugar solutions. Only a very small portion of cells (about 10 or 20%) survived the 48 h treatment in 2% maltose or galactose (non-fermentable sugars), but about half of the cells survived a 24 h treatment with these two sugars (Fig. 1). These results suggested that cells are more susceptible to the presence of fermentable sugars, glucose and fructose, than to the presence of maltose or galactose. Further, we confirmed that the observed induced cell death is carbon-source dependent. We repeated the survival experiment with two different sources of nitrogen, glutamine and ammonium sulphate and found that the presence of none of them for 24 or 48 h led to a dramatic change in survival compared to water alone (Fig. 1).

In summary, these initial results confirmed the susceptibility of stationary-phase BY4741 cells to sugars, mainly fermentable, at 37 °C, and simultaneously showed that for observing possible differences among the strains, a 48 h incubation in the presence of sugars is too long. This is a difference with other genetic backgrounds, for which some surviving cells were visible even after 48 h in 2% glucose [2, 12].

BY4741 cells lacking the Trk2 transporter are the most susceptible to glucose induced cell death

To distinguish which potassium transporters contribute to BY4741 survival in 2% glucose, and how much, we used a series of six mutants differing in the presence/absence of potassium uptake (Trk1 and Trk2) and potassium efflux (Tok1, Nha1, Ena1-5) systems (Table 1). Fig. 2 shows the survival of stationary-phase cells incubated in water (a) or 2% glucose (b) for 24 h at 37 °C. In contrast to the results published for W303 and its mutants [12], we did not observe any improvement in survival when the cells were lacking the potassium-exporting Ena1-5 ATPases and Nha1 antiporter (BYT45) or the outward rectifying potassium channel Tok1 (BYT3). In fact, the BYT45 strain, which lacks both active exporters, was highly sensitive to glucose treatment, only 6% of cells survived in water with 2% glucose for 24 h, whereas around 60% of cells survived in water. The survival of BYT3 strain was even lower (Fig. 2b). From these results, we may conclude that the role of potassium exporters in glucose induced cell death differs between the W303 and BY4741 backgrounds.

On the other hand, it is evident in Fig. 2 that cells lacking both Trk1 and Trk2 transporters (BYT12) are extremely susceptible to incubation in 2% glucose, as almost none of them survived 24 h treatment (0.03% surviving, Fig. 2b), which is in agreement with published data for the W303 genetic background, where the mutant lacking both Trk systems was also much more susceptible than the wild type [2]. Also, the quintuple mutant lacking all potassium importers and exporters (BYT12345) was much more sensitive to glucose treatment than the strain lacking only potassium exporters (BYT45), which again highlights the role of active potassium import in the cell survival in 2% glucose.

Comparing the survival phenotypes for single mutants BYT1 (*trk1Δ*) and BYT2 (*trk2Δ*) revealed that it is the Trk2 system, which plays a more important role in GICD than the main uptake system Trk1. Only 0.7% of BYT2 cells survived the treatment, compared to roughly 4% of BYT1 cells. Nevertheless, both transporters contributed to cell survival, as only 0.03% of cells survived when the double mutant (BYT12; *trk1Δ trk2Δ*) was tested (Fig. 2b).

Absence of active potassium uptake renders BY4741 cells sensitive to high temperature

The results summarized in Fig. 2 showed an unexpected phenomenon, a worse survival of strains lacking both Trk systems compared to the other strains in pure water (Fig. 2a). As the treatment was performed at 37 °C (to have conditions similar to [2, 12]), which is already a high-temperature stress for *S. cerevisiae* cells, we compared the survival of wild-type BY4741, single and double mutants in pure water at 30 °C or at 37 °C. The obtained results revealed that cells need at least one active Trk system to survive in water at 37 °C. A significant difference was observable not only after 24 h of incubation (not shown) but after as little as 18 h (Fig. 3). Cells lacking both Trk transporters (strains BYT12 and BYT12345) had a greatly

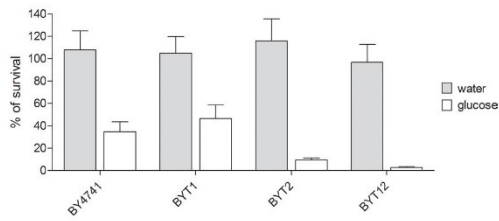


Fig. 4. Survival of BY4741 and its mutants lacking K^+ influx systems after an 18 h treatment in water or 2% glucose at 30 °C. Cells were grown in YPD+100 mM KCl for 48 h and subsequently incubated in water or 2% glucose at 30 °C for 18 h. Survival is expressed as a percentage of the number of colonies (c.f.u.) formed before treatment (100%).

reduced viability at 37 °C in water compared to the wild type or single mutants. As far as we know, this temperature-sensitive phenotype of cells lacking Trk1 and Trk2 uptake systems, suggesting the involvement of active potassium uptake in yeast thermotolerance, was observed for the first time.

Main role of Trk2 in cell survival of 2%-glucose treatment is visible even under mild conditions

Due to the results summarized in Figs 2 and 3, all subsequent survival experiments were performed at 30 °C to avoid the influence of thermosensitivity of strains lacking Trk systems. As shown in Fig. 4, the difference in cell survival in water or 2% glucose is already very clearly visible after 18 h at 30 °C. Under these relatively mild conditions, although the cell survival is higher compared to the original conditions (Fig. 2b, 2% glucose, 48 h, 37 °C) for all the tested strains, the main role of Trk2 for survival in 2% glucose is very clearly visible

(Fig. 4, white columns of strains BYT2 and BYT12 vs. white columns of BY4741 and BYT1). The presence of many dead cells in strains lacking Trk2 was further confirmed by primuline staining. As shown in Fig. 5, all strains had few dead cells after 18 h in water (6–13%); wild-type and BYT1 (*trk1Δ*) cultures had slightly higher amount of dead cells in 2% glucose (26 and 42%, respectively), but most BYT2 and BYT12 cells (88 and 92 %) were already dead after an 18 h treatment in 2% glucose at 30 °C.

It is worth noting, that we repeatedly observed a discrepancy between the values of OD_{600} and c.f.u. of the BYT2 and BYT12 cultures. These two cultures had lower OD_{600} and simultaneously higher c.f.u. at the end of growth in YPD with 100 mM KCl than the cultures of wild-type and BYT1 cells. It was the microscopic examination (Fig. 5) that helped us to understand this repeatedly observed discrepancy and revealed a new phenotype of cells lacking Trk2. We observed many clumps (up to ten cells) for the BYT2 and BYT12 strains, which explains the lower OD_{600} of the BYT2 and BYT12 cultures. Very often these clumps looked like they consisted of daughter cells, which started to bud before separating from the mother cell. Vortexing the cell suspensions prior to dilution and plating in c.f.u. assays helped to liberate the cells from clumps, i.e. increased the number of c.f.u. In summary, cells lacking the Trk2 transporter had difficulty completing the cell cycle at the level of cell separation (cf. Fig. 5, Nomarski, left panel).

Absence of Trk2 transporter changes the ATP content

One of the reasons for the yeast cell death after glucose exposure is the ATP exhaustion [15]. We measured the content of ATP in cell cultures at all the steps of our survival experiment. First, we estimated the amount of ATP in a culture grown under our standard conditions, i.e. 48 h in

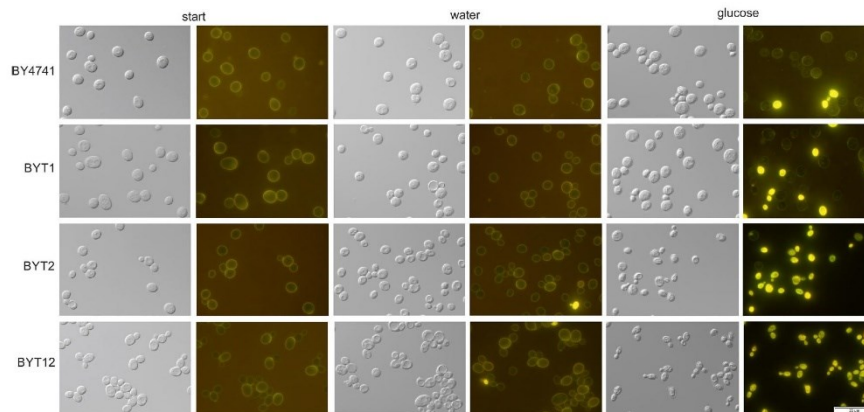


Fig. 5. Visualization of viable and nonviable cells by primuline staining. Cells were grown in YPD+100 mM KCl for 48 h (start) and subsequently incubated in water or 2% glucose at 30 °C for 18 h. Nomarski optics was used for whole cell pictures (left panels) and fluorescence microscopy for primuline staining (right panels).

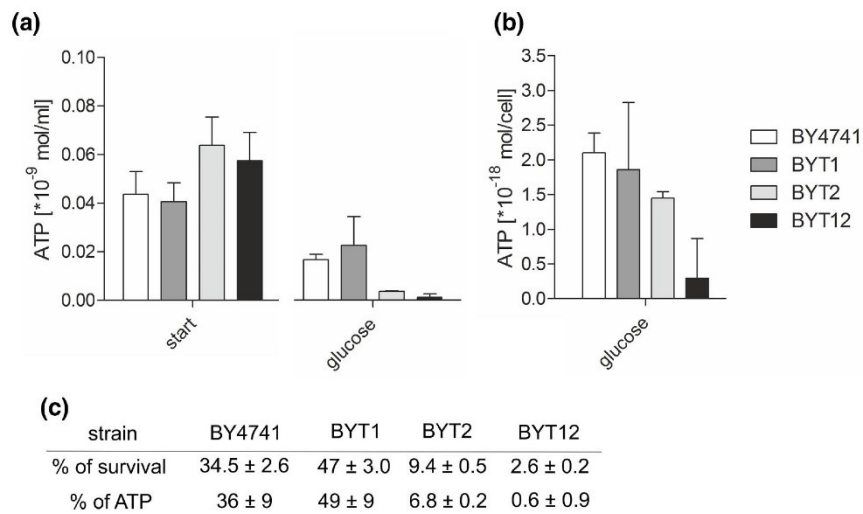


Fig. 6. ATP content in cultures and in one living cell of BY4741 and its mutants lacking K⁺ influx systems. Cells were grown in YPD+100 mM KCl for 48 h, transferred to 2% glucose and subsequently incubated in water or 2% glucose at 30 °C for 18 h. (a) ATP content in cells cultures. Samples were taken at the beginning of incubation (start) and after 18 h incubation (glucose). The amount of ATP in 1 ml of cell suspension (OD₆₀₀=1) is shown. (b) Amount of ATP in one living cell. (c) Comparison of cell survival and ATP content in cultures at the beginning (100 %) and after 18 h of incubation in 2% glucose.

YPD+100 mM KCl at 30 °C and after 18 h of incubation in water or 2% glucose at 30 °C. As shown in Fig. 6a, cultures of cells lacking the Trk2 transporter (BYT2 and BYT12) had a slightly higher amount of ATP than the wild type and cells lacking Trk1 after 48 h of growth. The 18 h incubation in water did not significantly change the amount of ATP in the cultures of all four strains (not shown), but all the cultures lost a substantial amount of ATP in 2% glucose. Cultures of BYT2 and BYT12 lost almost all of their ATP in 2% glucose (Fig. 6a), which is in agreement with the observed very high loss of viability.

Fig. S1 and the summary of the obtained results in Fig. 6c show a perfect correlation between the survival rate and ATP content in cultures of all four tested strains. When we recalculated the amount of ATP per living cell (a cell able to form a colony after 18 h of incubation in 2% glucose at), it was also evident that still living cells lacking both Trk transporters (BYT12) had the lowest amount of ATP (Fig. 6b). Also, the absence of only Trk2 in BYT2 cells resulted in a significantly diminished amount of ATP compared to the wild-type cells. These results confirmed the important role of Trk2 in the physiology of stationary cells and in their susceptibility to GICD.

One of the reasons why BYT2 and BYT12 cells have a higher amount of ATP at the end of a 48 h long growth might be that, despite the presence of 100 mM KCl in YPD, they did not reach the stationary phase of growth and are more

metabolically active than the wild-type and BYT1 cells, and thus more susceptible to GICD. To elucidate this possibility, we measured the growth of cultures of all 4 strains for 72 h (Fig. 7). The comparison of growth curves (Fig. 7) revealed that although the exponential phase of growth was similar for all four strains, i.e. the growth of BYT2 and BYT12 strains was not limited in YPD with 100 mM KCl, cultures of cells lacking Trk2 (BYT2) or both Trk1 and Trk2 (BYT12) did not reach as high OD₆₀₀ as the wild-type culture or the culture of cells lacking only Trk1 (BYT1). Nevertheless, it was evident that the OD₆₀₀ of all four cultures did not increase significantly after 35 h of growth, and thus the 48 h old cultures used in the above-described experiments contained stationary-phase cells. We also performed a survival test in water and 2% glucose with 72 h grown cells (Fig. S2), which revealed similar differences in survival among the strains compared to the survival of 48 h grown cells after an 18 h treatment in 2% glucose at 30 °C (Fig. 4).

Another reason for the observed differences in ATP content between the strains lacking/possessing Trk2 might be a difference in their potassium content. We estimated potassium content in stationary cells of all four strains and found that the wild-type and single mutants accumulated similar amounts of potassium (BY4741 423±18 [nmol/mg dry wt]; BYT1 409±10 [nmol/mg dry wt]; BYT2 410±23 [nmol/mg dry wt]). The double BYT12 mutant had an elevated intracellular concentration of potassium (556±24 [nmol/mg dry

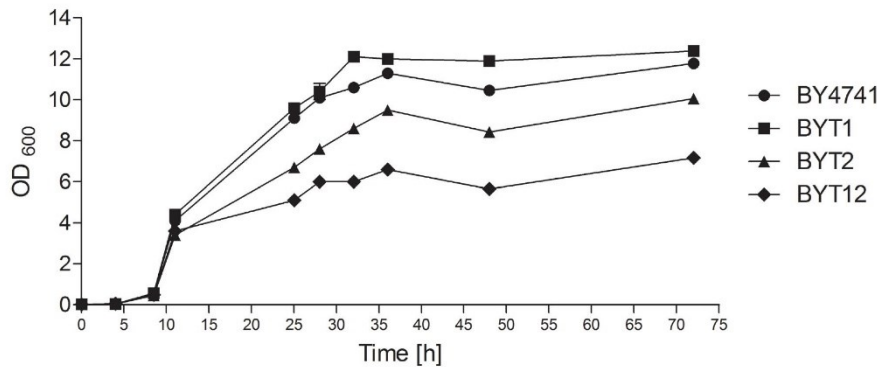


Fig. 7. Growth of BY4741 and its mutants lacking K⁺ influx systems in liquid YPD+100 mM KCl at 30 °C. OD₆₀₀ was measured at indicated time points. A representative result is shown.

wt]), which is in agreement with a higher potassium content in the exponentially growing BYT12 cells [11]. Obtained results show that (a) the presence of only one of the two Trk transporters is enough to ensure the 'normal' concentration of potassium in stationary cells and (b) the higher amount of ATP in BYT2 cells (Fig. 6a) is not accompanied with a higher amount of intracellular potassium.

The fact that cells without Trk2 lose more ATP when incubated in 2% glucose than cells with Trk2 led to the hypothesis that the activity of plasma-membrane H⁺-ATPase (Pma1) is deregulated in these cells, and its higher activity leads to an earlier consumption of intracellular ATP stocks in BYT2 and BYT12 cells than in the wild-type or BYT1 cells. To confirm this hypothesis, we monitored the glucose-induced acidification of cell environment, which is proportional to the activity of Pma1 H⁺-ATPase [16]. First preliminary comparison of the acidification rates of two strains (BY4741 and BYT12) incubated in water with those incubated in 2% glucose revealed that whereas the acidification rate observed for BY4741 cells in 2% glucose was about 3.8 times higher than in water, BYT12 cells acidified the external medium 6.8 times more quickly in 2% glucose than in water (results not shown). Table 2 summarizes the difference between the pH_{out} drop observed for each of the four strains in water and in 2%

Table 2. Extracellular pH drop in water cell suspensions 180 min after glucose addition

Strain	$\Delta\text{pH}_{\text{ex}} = \text{pH}_{\text{ex}}(\text{water}) - \text{pH}_{\text{ex}}(\text{glucose})$	
	30 °C	37 °C
BY4741	0.24±0.03	0.34±0.03
BYT1	0.25±0.01	0.36±0.03
BYT2	0.47±0.06	0.49±0.02
BYT12	0.40±0.01	0.48±0.03

glucose, and the dependence of this drop on the temperature in more detail. It is evident, that (a) the absence of Trk2 led to a significantly higher decrease in external pH (a higher pumping of protons out of the cells) compared to the two strains with functional Trk2 at both temperatures; and (b) all four strains extruded more protons at 37 °C, i.e. under temperature stress, than at 30 °C.

This final finding strongly supports our conclusion from the above-described experiments that stationary-phase cells lacking the Trk2 transporter are more sensitive to GICD due to the faster consumption of their ATP stocks caused by a higher activity of their Pma1 ATPase.

Altogether, our results showed four new pieces of knowledge related to yeast physiological parameters and/or GICD. First, the situation concerning GICD and potassium transporters in BY4741 cells is slightly different from the results described for the W303 background [12]. The difference observed in W303 and its mutants, i.e. cells lacking potassium importers being more susceptible, but cells lacking potassium exporters being more resistant to GICD, does not occur in BY4741. Our mutants lacking potassium exporters did not survive GICD better than the wild-type. Although their survival of GICD was much better than that of the cells lacking potassium importers, it was significantly worse than the survival of wild-type cells (Fig. 2). This difference between the two laboratory strains might be related to the overall differences in their physiological parameters, including membrane potential [14]. The GICD sensitivity of cells lacking Trk transporters is similar in both genetic backgrounds and might be related, to a hyperpolarization of their plasma membranes in the absence of active potassium uptake [9, 11].

Further, as a new phenotype, we show that mutants lacking Trk systems lose their viability more quickly in water at 37 °C than at 30 °C. How this relative thermosensitivity is connected to the function of active potassium importers remains to be

established. As the absence of Trk1 and Trk2 systems has a broad impact on gene expression [17] and on several crucial physiological parameters, including membrane potential and intracellular pH, we speculate that all these changes accompanying the absence of active potassium uptake may be reflected in the composition of the plasma membrane, one of the key parameters for thermotolerance [18, 19].

As the third, and main result, we would like to emphasize the role of Trk2 in GICD. Trk2 is not very active in growing cells and its role as a potassium transporter in *S. cerevisiae* was questioned for a long time (reviewed in [5]). Its contribution to potassium acquisition in growing cells is relatively small [9], nevertheless, its high contribution (much higher than that of Trk1) to yeast cell survival of desiccation and subsequent rehydration has been unambiguously shown [10]. Here we show that the presence of Trk2 is much more important for stationary cells exposed to 2% glucose than the absence of Trk1 (Figs 2 and 4). In summary, whereas Trk1 is more important for growing cells, Trk2 has its main role in the long-term survival of stationary cells.

Finally, we have shown that under GICD conditions, cells lacking active potassium uptake lose their intracellular ATP stocks more rapidly than cells with functional Trk1 and Trk2 systems (Fig. 6b). This rapid loss of ATP stocks is probably connected to a higher activity of plasma-membrane H⁺-ATPase in cells lacking potassium importers, which is observable as a higher acidification of the cell suspension upon addition of glucose (Table 2). Our explanation of the higher sensitivity of cells without potassium importers to GICD being a consequence of a more rapid consumption of ATP stocks by Pma1 is supported by earlier observations that mutants with a decreased activity of plasma-membrane H⁺-ATPase exhibit less cell death during GICD [12], and by the fact that glucose and fructose, which activate Pma1 more than maltose and galactose [20, 21], had the highest negative effect on cell survival in our study (Fig. 1).

Funding information

This work was supported by the Czech Science Foundation (GA ČR 20-04420S).

Acknowledgement

We thank P. Herynková for technical assistance and O. Zimmermannová for critical reading of the manuscript.

Conflicts of interest

The authors declare that there are no conflicts of interest.

References

- Granot D, Snyder M. Carbon source induces growth of stationary phase yeast-cells, independent of carbon source metabolism. *Yeast* 1993;9:465-479.
- Granot D, Levine A, Dor-Hefetz E. Sugar-induced apoptosis in yeast cells. *FEMS Yeast Res* 2003;4:7-13.
- Valiakmetov AY, Kuchin AV, Suzina NE, Zvonarev AN, Shepelyakovskaya AO, et al. Glucose causes primary necrosis in exponentially grown yeast *Saccharomyces cerevisiae*. *FEMS Yeast Res* 2019;19.
- Lauff DB, Santa-Maria GE. Potassium deprivation is sufficient to induce a cell death program in *Saccharomyces cerevisiae*. *FEMS Yeast Res* 2010;10:497-507.
- Arino J, Ramos J, Sychrova H. Alkali metal cation transport and homeostasis in yeasts. *Microbiol Mol Biol Rev* 2010;74:95-120.
- Arino J, Ramos J, Sychrova H. Monovalent cation transporters at the plasma membrane in yeasts. *Yeast* 2019;36:177-193.
- Durell SR, Guy HR. Structural models of the KtrB, TrkH, and Trk1.2 symporters based on the structure of the KcsA K(+) channel. *Biophys J* 1999;77:789-807.
- Elíčharova Heř et al. Potassium uptake systems of *Candida krusei*. *Yeast* 2019;36:439-448.
- Petrezselyova S, Ramos J, Sychrova H. Trk2 transporter is a relevant player in K⁺ supply and plasma-membrane potential control in *Saccharomyces cerevisiae*. *Folia Microbiol* 2011;56:23-28.
- Borovikova D, Herynkova P, Rapoport A, Sychrova H, et al. Potassium uptake system Trk2 is crucial for yeast cell viability during anhydrobiosis. *FEMS Microbiol Lett* 2014;350:28-33.
- Navarrete C, Petrezselyová S, Barreto L, Martínez JL, Zahrádka J, et al. Lack of main K⁺ uptake systems in *Saccharomyces cerevisiae* cells affects yeast performance in both potassium-sufficient and potassium-limiting conditions. *FEMS Yeast Res* 2010;10:508-517.
- Hoerichs FA, Perez-Valle J, Montesinos C, Mulet JM, Planes MD, et al. The role of K(+) and H(+) transport systems during glucose- and H(2)O(2)-induced cell death in *Saccharomyces cerevisiae*. *Yeast* 2010;27:713-725.
- Maresova L, Sychrova H. Applications of a microplate reader in yeast physiology research. *Biotechniques* 2007;43:667-672.
- Petrezselyova S, Zahrádka J, Sychrova H. *Saccharomyces cerevisiae* BY4741 and W303-1A laboratory strains differ in salt tolerance. *Fungal Biol* 2010;114:144-150.
- de Alteriis E, Carteni F, Parascandola P, Serpa J, Mazzoleni S, et al. Revisiting the Crabtree/warburg effect in a dynamic perspective: A fitness advantage against sugar-induced cell death. *Cell Cycle* 2018;17:688-701.
- Serrano R. *In vivo* glucose activation of the yeast plasma membrane ATPase. *FEBS Lett* 1983;156:11-14.
- Barreto L, Canadell D, Petrezselyová S, Navarrete C, Maresová L, et al. A genomewide screen for tolerance to cationic drugs reveals genes important for potassium homeostasis in *Saccharomyces cerevisiae*. *Eukaryot Cell* 2011;10:1241-1250.
- Caspeta L. Biofuels. Altered sterol composition renders yeast thermotolerant. *Science* 2014;346:75-78.
- Godinho CP, Costa R, Sá-Correia I. The ABC transporter Pdr18 is required for yeast thermotolerance due to its role in ergosterol transport and plasma membrane properties. *Environ Microbiol* 2021;23:69-80.
- Souza MAA, Tropic MJ, Brandao RL. New aspects of the glucose activation of the H(+)-ATPase in the yeast *Saccharomyces cerevisiae*. *Microbiol SGM* 2001;147:2849-2855.
- Sychrova H, Kotyk A. Conditions of activation of yeast plasma membrane ATPase. *FEBS Lett* 1985;183:21-24.
- Zahrádka J, Sychrova H. Plasma-membrane hyperpolarization diminishes the cation efflux via Nha1 antiporter and Ena ATPase under potassium-limiting conditions. *FEMS Yeast Res* 2012;12:439-446.

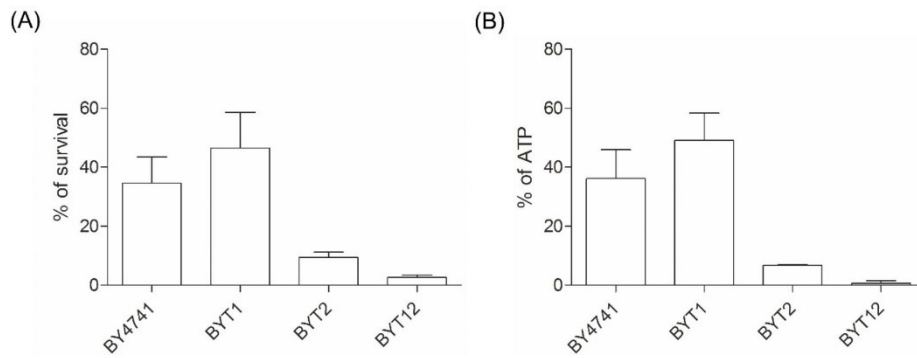
Edited by: J. Cavet and H. Martin

**Minority potassium-uptake system Trk2 has crucial role in yeast survival of
glucose-induced cell death**

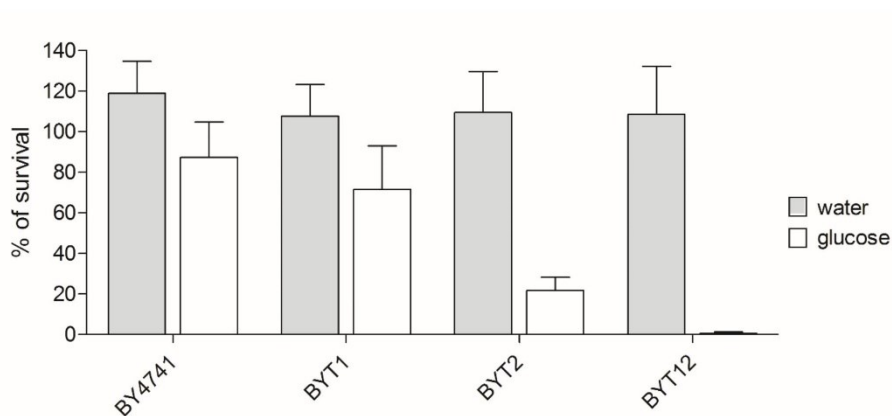
Michala Dušková, Denis Cmunt[†], Klára Papoušková, Jakub Masaryk, Hana
Sychrová*

*Laboratory of Membrane Transport, Institute of Physiology, Czech Academy of Sciences,
Prague 4, Czech Republic*

Supplementary Figure 1. Survival of BY4741 and its mutants lacking K⁺ influx and efflux systems in 2% glucose and their ATP content. Cells were grown in YPD + 100 mM KCl for 48 hours and subsequently treated in 2% glucose at 30 °C for 18 hours. (A), Survival is expressed as a percentage of the number of colonies (CFU) formed before treatment. (B) Amount of intracellular ATP in the cultures. 100 % represent amount of ATP in cultures before the 2% glucose treatment.



Supplementary Figure 2. Survival of BY4741 and its mutants lacking K⁺ influx and efflux systems in 2% glucose. Cells were grown in YPD + 100 mM KCl for 72 hours and subsequently treated in water or in water containing 2% glucose at 30 °C for 18 hours. Survival is expressed as a percentage of the number of colonies (CFU) formed before treatment.



3.4 Potassium-uptake systems in *Kluyveromyces marxianus*

Summary: In the last part of the presented dissertation thesis, we focused on the characterisation of potassium uptake systems in non-conventional yeast species *Kluyveromyces marxianus*. Species *K. marxianus* represents an attractive yeast for utilization in biotechnological production. As elevated uptake of potassium has been shown to be beneficial in the survival of various stresses encountered throughout prolonged fermentation, detailed knowledge of fundamental aspects of potassium homeostasis in relevant species might bring enhancement of the efficiency of various biotechnological processes. The genome of *K. marxianus* presumably encodes two, previously uncharacterised potassium uptake systems: uniporter Trk1 and K⁺-H⁺ symporter Hak1. The main goal of this section of the thesis was the characterisation of both Trk1 and Hak1 in terms of their individual contribution to potassium uptake in *K. marxianus*, as well as their contribution to the survival of various external stresses.

We employed variations of methods CRISPR-Cas9 and Golden-Gate assembly developed and optimized at University College Cork to construct *K. marxianus* strains lacking *TRK1* and/or *HAK1* genes. Growth phenotypes of resulting mutant strains were analysed. We found both Trk1 and Hak1 to be able to provide cells with a sufficient amount of potassium under potassium non-limiting conditions, however, when external potassium was scarce, transporter Hak1 appeared to be dominant. Additionally, we observed different growth rates of individual mutants upon exposure to various external stresses.

Mutant strains were constructed during an internship at University College Cork under the supervision of John Morrissey. Acquired theoretical and practical skills were transferred by the author of the thesis to the Laboratory of Membrane Transport, Institute of Physiology for future use. Obtained strains and results from their basic characterisation will serve as a base for a thorough study focused on potassium-uptake systems and potassium homeostasis in *K. marxianus*. Characterization of potassium uptake systems in *K. marxianus* will be a joint effort of three departments: Laboratory of Membrane Transport, Czech Academy of Sciences; School of Microbiology, University College Cork and Department of Microbiology, University of Córdoba.

Author's contribution: Mutant strains were constructed and basic characterisation of growth phenotypes was performed by the author of the thesis. Mutant strains will be further characterised by the author of the thesis and by a group of José Ramos from the University of Córdoba. Final results are expected to be published.

3.4.1 Introduction

Due to various favourable traits (discussed in more detail in section 1.8) species *Kluyveromyces marxianus*, is currently one of the most promising, non-conventional, yeast regarding applications in food and environmental biotechnology and also potential cell factory for the production of valuable metabolites [176]. Despite its biotechnological relevancy, fundamental physiological processes, including potassium uptake and homeostasis, are largely unknown for they have not been subjected to a proper study. The availability of whole-genome sequences from various strains, emerging in recent years [39,177], provides an excellent basis for such basic research. Here we present a short study aimed at the identification and basic characterisation of two potassium-uptake systems of *K. marxianus*, Trk1 and Hak1. As mentioned before, uniporter Trk1 is considered a key potassium uptake system, expressed in all yeast, while K⁺-H⁺ symporter Hak1 has been observed in certain species, being expressed mainly under specific conditions. In order to study these two potassium uptake systems, we constructed a series of deletion mutants, employing a variation of the CRISPR-Cas9 method designed specifically for use in *K. marxianus* [178].

3.4.2 Material and methods

3.4.2.1 Deletion of *TRK1* and *HAK1* in *K. marxianus* using CRISPR-Cas9

We used strain NBRC 1777 with deletion of *LIG4* (section 3.4.2.1, Tab. 1), rendering the strain deficient in non-homologous end-joining, improving the effectiveness of deletion using CRISPR-Cas9 and homologous repair fragments. Both *TRK1* and *HAK1* were deleted using CRISPR-Cas9 as described in Rajkumar et. al. [178]. ORFs were identified and gRNA oligos design was based on the results of whole genome sequencing of *K. marxianus* NBRC 1777 [39]. We designed one pair of repair fragments (section 3.4.2.1, Tab. 2) and four pairs of gRNA oligos (section 3.4.2.1, Tab. 3) for each gene to be deleted. Respective pairs of gRNA oligos were used individually, all designed gRNAs were effective in the deletion of selected genes.

gRNAs were expressed from plasmid pUCC001 [179]. Proper integration of each pair of gRNA oligos into the plasmid was verified by PCR, as described in Rajkumar et. al. [178], using respective forward gRNA oligo (section 3.4.2.1, Tab. 3) and oligo Bsa-R (section 3.4.2.1, Tab. 4).

Table 1. List of yeast strains

Genotype/Name	Strain	Genotype
<i>TRK1HAK1</i> (WT)	<i>K. marxianus</i> NBRC 1777	<i>lig4Δ</i>
<i>trk1hak1</i>	<i>K. marxianus</i> NBRC 1777	<i>lig4Δ trk1Δ hak1Δ</i>
<i>TRK1hak1</i>	<i>K. marxianus</i> NBRC 1777	<i>lig4Δ hak1Δ</i>
<i>trk1HAK1</i>	<i>K. marxianus</i> NBRC 1777	<i>lig4Δ trk1Δ</i>

Table 2. List of repair fragments

Name	Sequence 5'-3'
TRK1_RF_F	GCCACAAACTTCATCCTATTGCAAGTTTAATATGCCCGAACTTTATTGCATTTC ACTATTTTTATATTATAGGGTTTTTCGATATTAGGCAGTATTAAGAAGAGATTCAT
TRK1_RF_R	AATCAGTAAAAGCCACCATGTTGCTGCCTTTGGGAAAAGCATAGTGAAACAACGC CGTGGATGATCCAATAAAAATCCCAATGAATCTTCTTAATACTGCCTAATATC
HAK1_RF_F	TTGCTAATATAAGTACAAGCATAGTATCAGCAGTATCGACGCCCAAAACAGACTT TTTTATTACCTATTAGCAGCAACCCTTGGCCTAAATGAGCATGTCGGTATTGCTG
HAK1_RF_R	CCAAGCACCATGTGGCACCTTGAGCAAGTTAGCACCGATCAAACAGCACTCGAGG GAACCGAACACGCACAAGAAGAGCACAGCAATACCGACATGCTCATTTAGGCCAA

Table 3. List of gRNA oligos

Name	Sequence 5'-3'
TRK1_gRNA_1_F	CGTCTGAGATGGTGAATAGAGACG
TRK1_gRNA_1_R	AAACCGTCTCTATTCACCATCTCA
TRK1_gRNA_2_F	CGTCTGTGAAAAGTCCTGCAGAAA
TRK1_gRNA_2_R	AACTTTCTGCAGGACTTTTACA
TRK1_gRNA_3_F	CGTCAGATGGGCATGATGCTGATA
TRK1_gRNA_3_R	AAACTATCAGCATCATGCCATCT
TRK1_gRNA_4_F	CGTCCTGATGGTATCAATCCGACT
TRK1_gRNA_4_R	AAACAGTCGGATTGATACCATCAG
HAK1_gRNA_1_F	CGTCTGCCACGTCGCCATTGTATA
HAK1_gRNA_1_R	AAACTATACAATGGCGACGTGGCA
HAK1_gRNA_2_F	CGTCAAGAGCTTCAGAAAGTGGGT
HAK1_gRNA_2_R	AAACACCCACTTTCTGAAGCTCTT
HAK1_gRNA_3_F	CGTCATTGTCCTATTGGTTATCGG
HAK1_gRNA_3_R	AAACCCGATAACCAATAGGACAAT
HAK1_gRNA_4_F	CGTCAGAGCGGTCAAGGATTCTAC
HAK1_gRNA_4_R	AAACGTAGAATCCTTGACCGCTCT

Proper deletion of selected genes was verified by PCR, as described in Rajkumar et. al. [178], using primers listed in Table 4 (section 3.4.2.1).

Table 4. List of PCR oligonucleotides

Name	Sequence 5'-3'
TRK1_chk_F	TTACAGGAAGACGTTAGG
TRK1_chk_R	ACAGAGGTATCTAAATCC
HAK1_chk_F	TTCTCTCGTGATAGAAGG
HAK1_chk_R	GTCATCATCATCATCACC
Bsa-R	ACACGCGTTTGTACAGAAAAAAGAAAAATTTGA

The resulting mutant strains are listed in Table 1 (section 3.4.2.1).

3.4.2.2 Media and growth tests

The growth of yeast cells was tested on solid media with 2% agar. Cells were pregrown on YPD (2% peptone, 1% yeast extract, 2% glucose) plates at 30 °C, collected and resuspended in sterile water to OD₆₀₀ 0.6. Three additional 10-fold dilutions were prepared and 3 µL were spotted plates. We used YNB-F (0.17% YNB-F, 2% glucose, containing approximately 15 µM KCl) plates supplemented with indicated concentrations of KCl, NaCl, LiCl, (NH₄)₂SO₄, Proline or Hygromycin B. If not indicated otherwise, plates contained 0.4% (NH₄)₂SO₄ and the pH was adjusted to 5.8., the pH of the plates was adjusted with either NH₄OH (plates with pH 5.8 or 7.2) or diluted HCl (plates with pH 3.5). Plates with pH 7.2 were buffered with 20 mM MOPS buffer. Media were sterilized by autoclaving. Hygromycin was added to the media after sterilization. Yeast cells were incubated at 30 °C, photos were captured after 3 days. Representative results of at least three repetitions are shown.

3.4.3 Results

To elucidate the individual contribution of both Trk1 and Hak1 to the uptake of potassium, growth on YNB-F plates supplemented with various potassium concentrations was first tested. As seen in Figure 7 (section 3.4.3), growth of WT and strain *trk1HAK1* was comparable and detectable on all tested external potassium concentrations, granted it diminished with decreasing potassium levels. Strain *TRK1hak1* grew comparably to both WT and *trk1HAK1* on external potassium chloride concentrations 2.5 mM and above, however, its growth rate was significantly decreased on external potassium chloride 1 mM and below, with almost complete inhibition on external potassium chloride concentration below 0.2 mM (section 3.4.3, Fig. 7). We did not detect any growth for double mutant *trk1hak1* on plates supplemented with potassium concentration bellow 25 mM (section 3.4.3, Fig. 7),

confirming a key role of both Trk1 and Hak1 in the facilitation of active uptake of potassium. Altogether, these results suggested a crucial role of Hak1 in the acquisition of potassium when external potassium levels were very low and the presumed role of Trk1 under conditions of external potassium concentration in millimolar ranges.

Trk1 in *S. cerevisiae* has been suggested to also be able to facilitate the uptake of ammonium ions [45]. We, therefore, also tested the growth of mutant strains under the elevated external concentration of ammonium sulphate (0.8% as opposed to standard 0.4%) and on plates supplemented with an alternative nitrogen source, proline. The elevated external concentration of ammonium sulphate, in fact, had a negative effect on strains expressing Trk1, *TRK1hak1* and to a smaller extent also on WT, as seen on plates combining 1 mM potassium chloride and 0.8% ammonium sulphate compared to standard 0.4% of ammonium sulphate (section 3.4.3, Fig. 8). We also saw a general negative effect of 0.8% ammonium sulphate on all strains on plates supplemented with 0.2 mM potassium chloride, however, under these 'low-potassium' conditions, the cells are likely hyperpolarized and thus non-specific uptake of positively charged ammonium ions might be promoted. When the growth of strains on plates supplemented with proline as a source of nitrogen was tested, we saw the most pronounced improvement of growth of strain *TRK1hak1* (section 3.4.3, Fig. 8), further supporting the notion that Trk1-mediated potassium might be, to some degree, competitively inhibited by a presence of ammonium ions in the media.

As functions of both Trk1 and Hak1 have been previously shown to be dependent on external pH [70], especially in the case of Hak1, since it presumably functions as a H^+K^+ symporter, thus depends on the existence of the proton gradient, we tested the growth of mutant strains also on plates with various external pH values supplemented with four selected concentrations of potassium. As seen in Figure 9 (section 3.4.3), however, we only detected the effect of low pH (3.5) on double mutant *trk1hak1* and none on remaining mutant strains or WT. Regarding the high pH (7.2), we only observed a general improvement in the growth of all four strains, including double mutant strain *trk1hak1*, thus no specific effect on the function of Trk1 nor Hak1 transporters (section 3.4.3, Fig. 9). These results were contrary to the previously published dependence of Trk1 on neutral or high external pH and Hak1 on low external pH, albeit these results were obtained from a study of a different species [70].

Hygromycin B is a cationic drug able to enter the cells proportionally to membrane potential, thus being significantly more toxic in hyperpolarized cells. As internal potassium is one of the key determinants of membrane potential and also the absence of Trk1 has been previously shown to lead to hyperpolarization [4], we decided to test the effects of the presence of Hygromycin B on

constructed mutant strains. According to the obtained results, the presence of Hygromycin B seemed to be especially toxic in strain *trk1HAK1*, lacking Trk1, for which we detected diminished growth on all tested external concentrations of potassium combined with Hygromycin B, compared to a WT (section 3.4.3, Fig. 10). Surprisingly, Hygromycin seemed to have a more negative effect on strain *trk1HAK1* in combination with 1 mM and 5mM concentration of external potassium chloride, inhibiting growth completely, compared to 0.2 mM external potassium chloride, on which the cells were able to grow (section 3.4.3, Fig. 10). We also saw a negative effect of Hygromycin B on WT and strain *TRK1hak1*, however only if the external potassium was low and cells thus might have been partially hyperpolarized (section 3.4.3, Fig. 10). Taken all together, these results confirmed the importance of both internal potassium and presence of Trk1 for maintenance of proper membrane potential.

As SKT proteins, a group of potassium-uptake systems, including Trk1, have been shown to be able, to a lesser extent, to facilitate the uptake of other small ions, such as lithium and sodium [13], therefore, we also tested the growth of mutant strains in presence of these two cations. The presence of sodium had no effect on any of the tested strains (section 3.4.3, Fig. 11), however, we detected significant inhibition of growth in presence of lithium in strains WT and *trk1HAK1*, hence strains expressing Hak1. This negative effect was seen on plates combining 25 mM lithium chloride with 1 mM and 0.2 mM potassium chloride. Additionally, the presence of lithium also negatively influenced the growth of double mutant *trk1hak1* (section 3.4.3, Fig. 11). These results did not confirm the ability of Trk1 to be able to transport lithium and sodium, however, they suggested the possibility of uptake of lithium being facilitated by Hak1, although additional experimental work is necessary to confirm this notion.

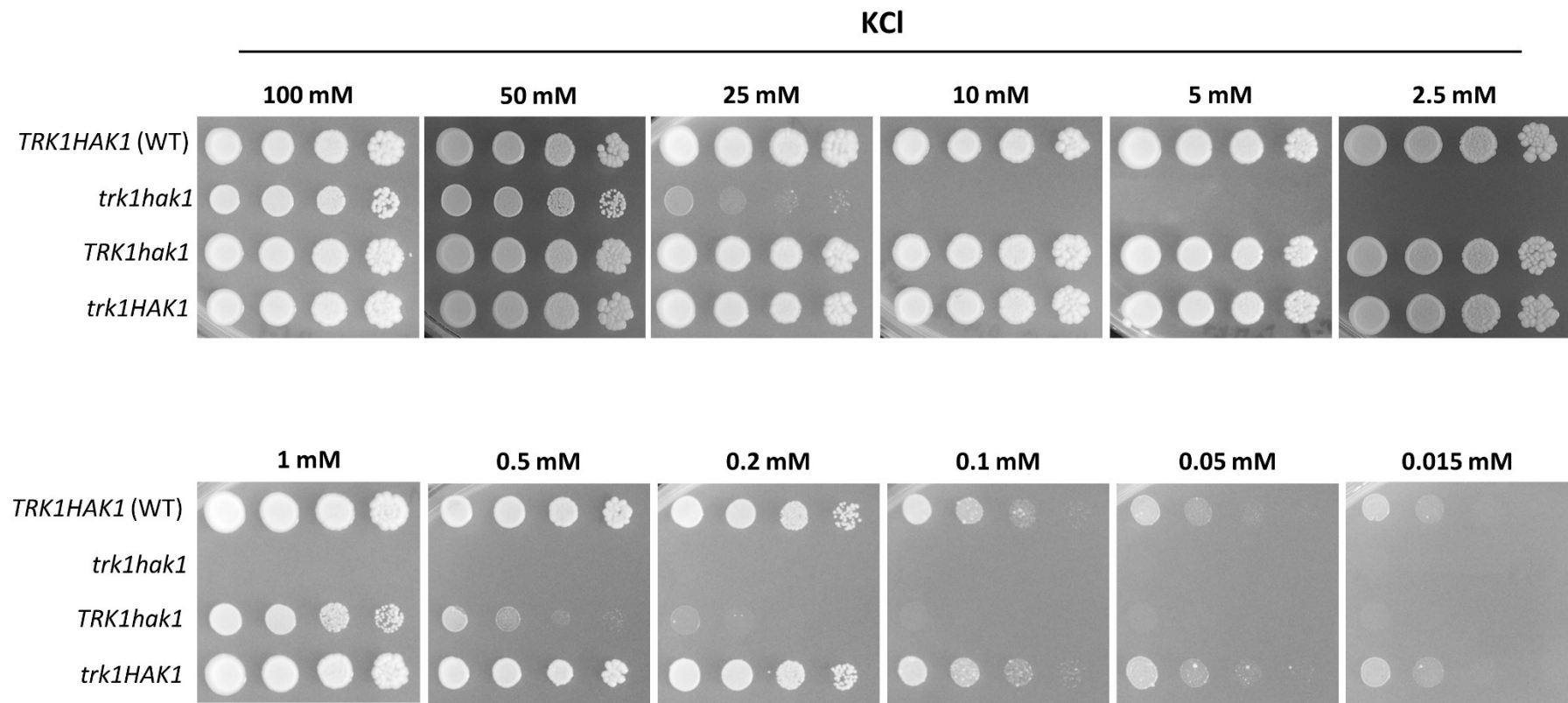


Figure 7. Growth of *K. marxianus* WT and mutant strains with a deletion in *TRK1* and/or *HAK1* on various external concentrations of potassium. Cells were grown on YNB-F plates (0.4% ammonium sulphate) supplemented with indicated concentrations of potassium chloride (KCl). Pictures were captured after 3 days at 30 °C.

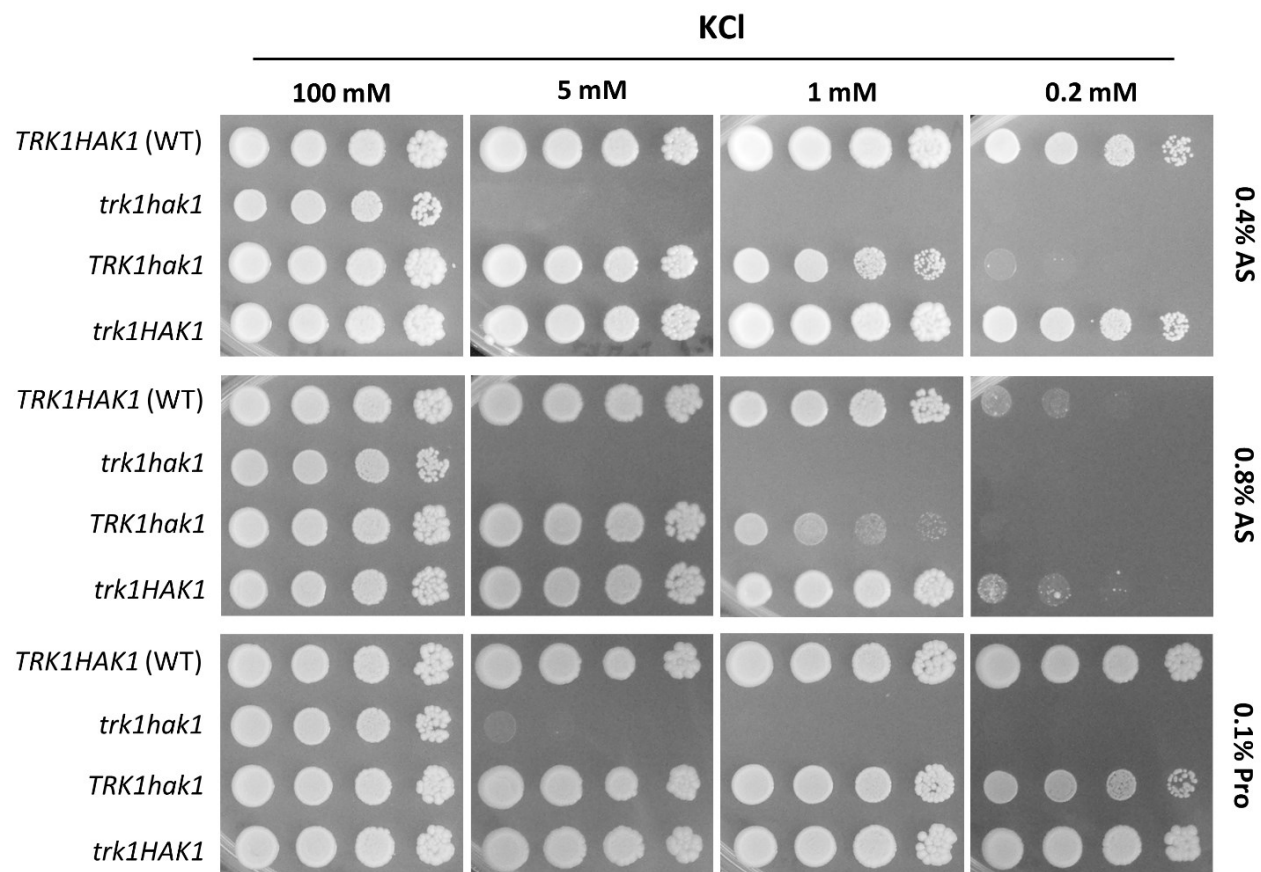


Figure 8. Growth of *K. marxianus* WT and mutant strains with a deletion in *TRK1* and/or *HAK1* on the elevated external concentration of ammonium sulphate and proline. Cells were grown on YNB-F supplemented with indicated concentrations of potassium chloride (KCl), ammonium sulphate (AS) or proline (Pro). Pictures were captured after 3 days at 30 °C.

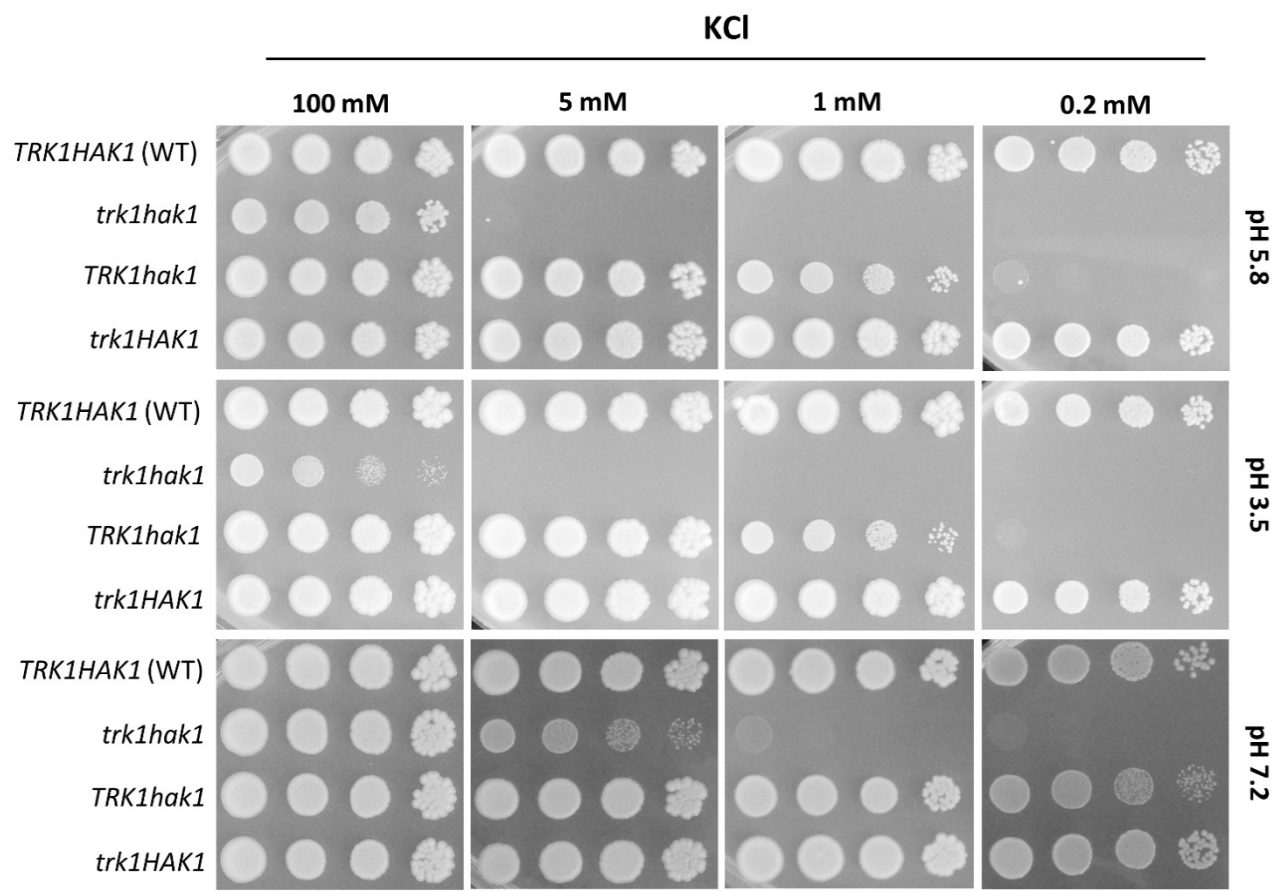


Figure 9. Growth of *K. marxianus* WT and mutant strains with a deletion in *TRK1* and/or *HAK1* on various external pH. Cells were grown on YNB-F (0.4% ammonium sulphate) supplemented with indicated concentrations of potassium chloride (KCl). pH was adjusted to standard 5.8, low 3.5 or high 7.2 Pictures were captured after 3 days at 30 °C.

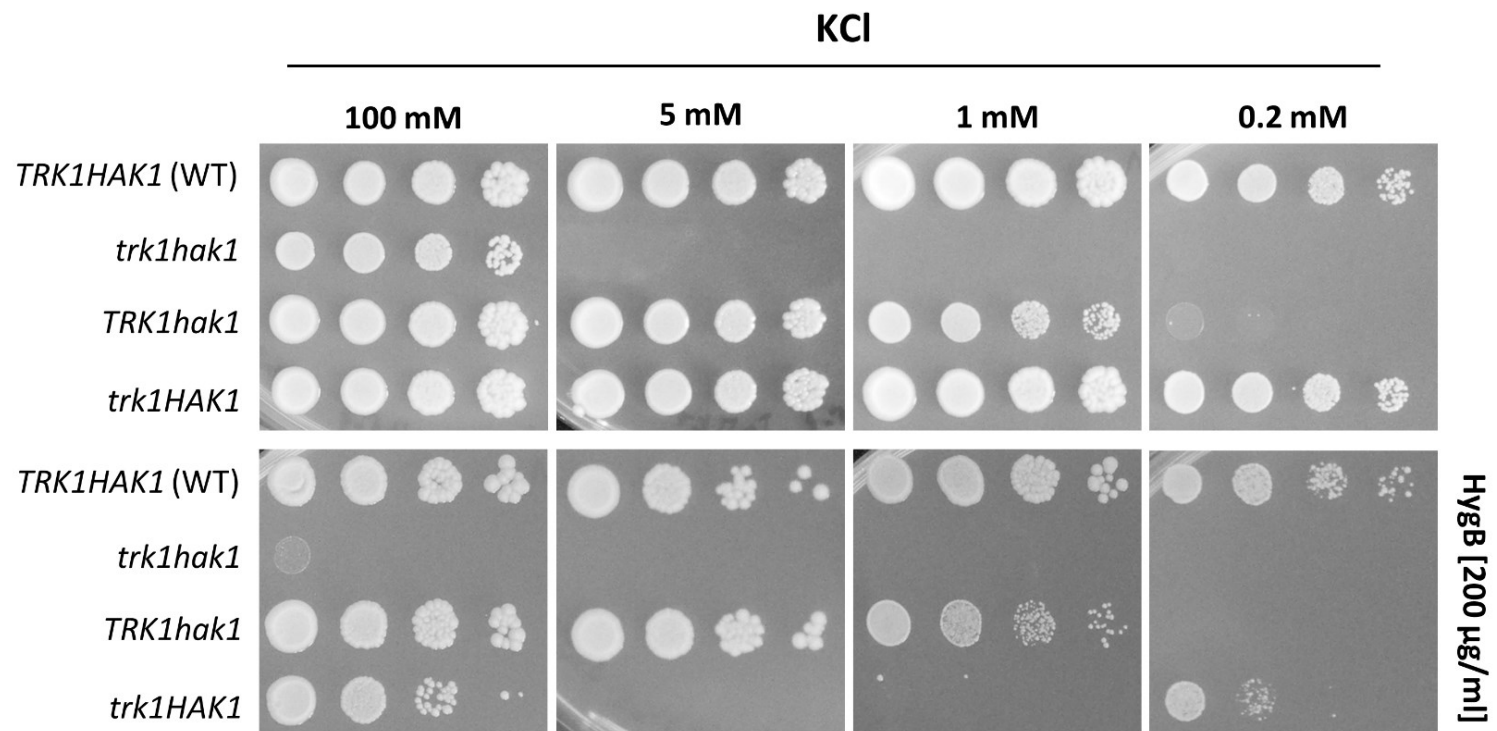


Figure 10. Growth of *K. marxianus* WT and mutant strains with a deletion in *TRK1* and/or *HAK1* in presence of Hygromycin B. Cells were grown on YNB-F (0.4% ammonium sulphate) supplemented with indicated concentrations of potassium chloride (KCl) and Hygromycin B. Pictures were captured after 3 days at 30 °C.

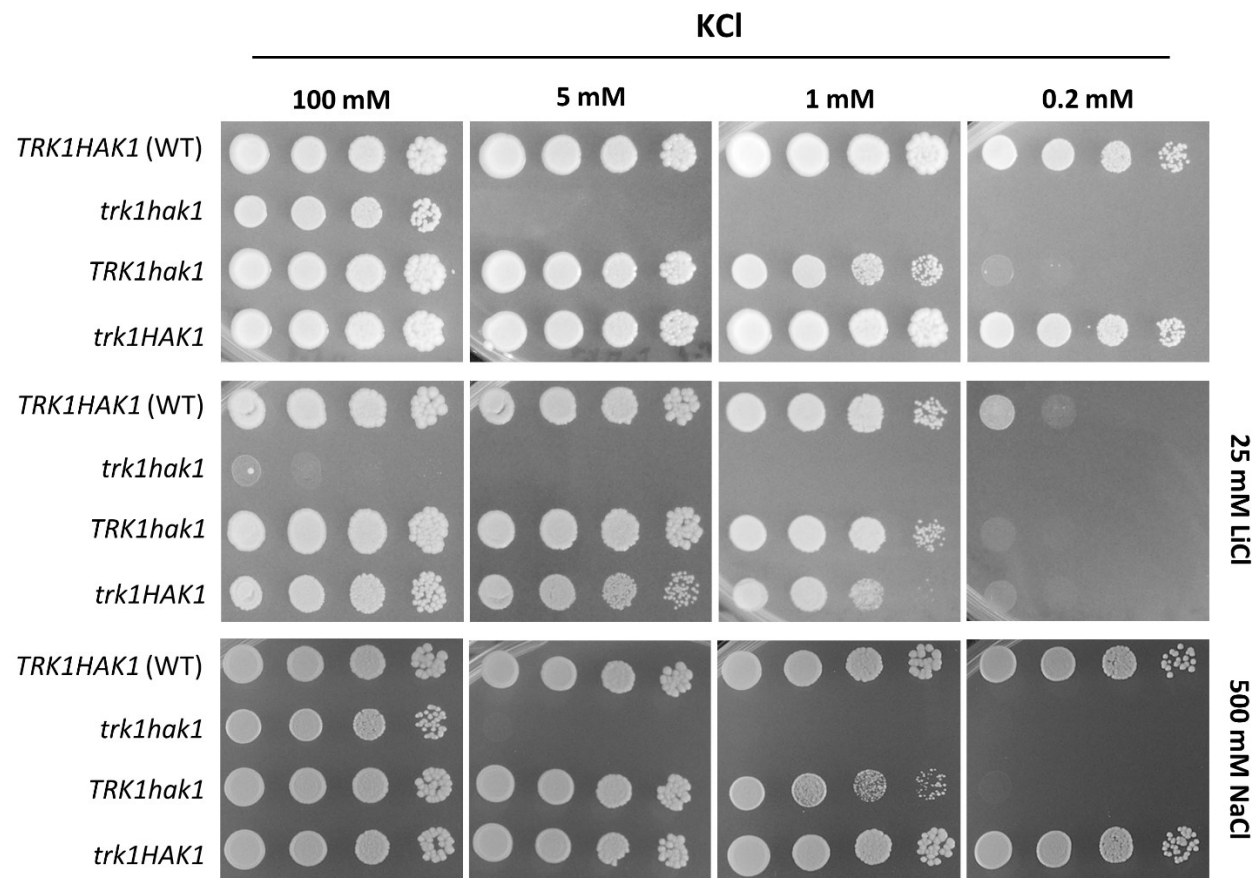


Figure 11. Growth of *K. marxianus* WT and mutant strains with a deletion in *TRK1* and/or *HAK1* in presence of sodium and lithium ions. Cells were grown on YNB-F (0.4% ammonium sulphate) supplemented with indicated concentrations of potassium chloride (KCl), lithium chloride (LiCl) and sodium chloride (NaCl). Pictures were captured after 3 days at 30 °C.

4. Discussion

The presented thesis aimed to enhance the knowledge of various aspects of functionality and regulation of Trk1 in *S. cerevisiae* and the basic characterization of potassium-uptake systems in non-conventional yeast *K. marxianus*. As mentioned before, the uptake of potassium has been connected to both virulence of pathogenic yeast species and the effectiveness of fermentation and survival of stress encountered throughout the biotechnological processes. Even though results presented here would fall into the category of basic research, knowledge of fundamental processes of potassium acquisition and homeostasis might, in future, lead to either exploitation of defects in potassium homeostasis in order to design effective antifungal therapy or improvement of potassium import with the aim to increase the effectiveness of biotechnological production.

4.1 Regulation and putative mechanism of changes in affinity and maximum velocity of Trk1-mediated uptake

The first part of the thesis focused on the ability of Trk1 to modify its capacity for uptake by switching between low- and high-affinity modes as a reaction to changes in the availability of external potassium. This ability, even though distinctive, is not unique to protein Trk1 and has been previously documented in other transporters such as Kup1 and Nrt1.1 in plants [180,181] or several hexose and pentose transporters in yeast [182-184]. By virtue of this ability, Trk1 and other aforementioned proteins not only provide cells with their respective substrates but also participate in fine-tuning of uptake and thus in overall cellular homeostasis under constantly changing external conditions. The general pattern of affinity-switch can be summarized by a substantial increase in affinity and a simultaneous decrease in maximum velocity as a reaction to a significant reduction in the external availability of a substrate [185]. Even though the decrease in maximum velocity seems counter-intuitive under conditions of limiting concentration of substrate, it is most likely a natural result of a stronger bond between the high-affinity binding site and substrate. Moreover, under conditions of low external concentration of substrate, it is probably more desirable for the cells to employ transporters with high affinity and low maximum velocity rather than high maximum velocity and low affinity, for under conditions of limiting substrate availability, the uptake would not be saturated and thus the maximum velocity would likely have a less pronounced effect on overall uptake of the particular compound.

The most thorough study of affinity-switch to date was performed on a plant nitrate importer Nrt1.1. Upon a sharp decrease in the external availability of nitrate, the Nrt1.1 transporter is phosphorylated on residue Thr101 leading to an above-mentioned significant increase in affinity and at the same time decrease in maximum velocity [181,186]. According to Tsay et. al. [187], phosphorylation of Thr101 leads to the dissociation of Nrt1.1 dimers to monomers and consequently to increased structural flexibility which results in increased affinity and decreased maximum velocity, thus the effective mechanism of affinity-switch in Nrt1.1 can be summarized as a structural change as a result of phosphorylation.

As mentioned above, the ability to perform an affinity switch is not unique to Trk1, however, according to our results, the Trk1 derives from the general pattern in two significant ways. First, as opposed to the general pattern and aforementioned transporters, the increase in affinity in Trk1 was in fact accompanied by an increase in maximum velocity, with V_{max} in the designated high-affinity state being almost double of V_{max} in the low-affinity state. We did not however consider this a novel mechanism of affinity-switch, but rather a combination of two separate mechanisms of affinity-switch and independent increase in maximum velocity, both being a reaction to potassium limitations. The separateness of these two processes was supported mainly by the discrepancy in changes of both affinity and maximum velocity with prolonged starvation, with affinity being at its peak after about 45-60 minutes with subsequent decrease and V_{max} rising continuously up to 5 hours of potassium-limiting conditions. Since the maximum velocity directly correlates with the number of active transporters in the membrane, we hypothesized that the increase in V_{max} of Trk1-mediated uptake under potassium starvation might have been a result of three potential mechanisms, presumably promoted under potassium limitations: stimulation of expression of *TRK1*, increase in the rate of transition through later stages of the secretory pathway [188] or simply an activation of inactive Trk1 proteins in the plasma membrane. Since Trk1 has been previously shown to be expressed on a stable level and independently of external conditions, including potassium limitations [57] and we did not observe retention of a significant portion of Trk1 proteins in later stages of the secretory pathway under potassium non-limiting conditions, we consider activation of inactive portion of Trk1 in the plasma membrane as the most likely mechanism of increase in V_{max} of Trk1-mediated potassium uptake under potassium starvation. Considering an option of the separateness of changes in affinity and maximum velocity in Trk1, the actual mechanism of affinity-switch in Trk1 might, in fact, be similar to the general pattern of increase in affinity accompanied by a decrease in maximum velocity with the reduction of V_{max} simply being masked by above-mentioned activation of a substantial portion of inactive transporters in the plasma membrane.

The second derivation of Trk1 from the general pattern of the affinity switch were the actual changes in affinity resulting from a decrease in the availability of potassium. While in all the documented cases, the affinity simply switches between low- and high-affinity states, the concept originally considered being also the case of Trk1, according to our results, the Trk1 did not switch but rather was able to precisely adjust its K_T according to availability of potassium, increasing the affinity with the decrease in the external concentration of potassium. Interestingly, in the case of changes in external potassium concentration, maximum velocity followed the same trend as affinity. We consider the precise adjustment of affinity according to the availability of substrate to be a novel mechanism among yeast membrane transporters.

To put the derivations of Trk1 from the general pattern of affinity-switch into an evolutionary perspective, we must consider the existence of threshold concentration upon which the affinity-switch presumably occurs. In the case of transporters, such as Nrt1.1, when the external concentration of nitrate decreases to a certain level, that potentially being a result of even very small fluctuations in its availability if the external concentration is close to the above-mentioned threshold, Nrt1.1 transporter switches directly to high-affinity state [185]. However, it is still imperative for the cells to avoid a sudden and dramatic increase in the uptake of nitrate, for such changes might result in overall disruption in nitrate homeostasis, especially when the external concentration is not limiting but rather slightly above the putative threshold. The designated 'back-pedal' in this case, most likely represents the aforementioned decrease in maximum velocity that accompanies the switch to a high-affinity state and prevents sudden excessive uptake of nitrate. Since, in the case of Trk1, transition to a high-affinity state is accompanied by an increase in maximum velocity, rather than its decrease, it would have been potentially harmful to the cells, had the Trk1 functioned by switching between only low- and high-affinity states, for very small shifts in the availability of external potassium could potentially lead to a substantial elevation in its uptake due to simultaneous and substantial increase in both affinity and maximum velocity and inevitably to disruption of overall potassium homeostasis. Herein most likely lies the evolutionary advantage of developing a transporter able to adjust its affinity gradually rather than by abrupt increase, for this adjustment can also be accompanied by an elevation in maximum velocity of substrate uptake.

Another, hitherto, obscure aspect of adjustments of both affinity and maximum velocity of Trk1 is the actual signal driving these changes. With exception of a few articles considering internal potassium [56] or even the presence of toxic ions, such as sodium [43], the majority of data suggested the external potassium levels as a dominant force in the regulation of kinetic parameters of Trk1. However, according to our results, both internal potassium concentration and membrane potential seemed to be more likely candidates. Moreover, judging exclusively by correlation with changes in K_T

and V_{max} , membrane potential appeared to be a dominant signal. It is important to note that our results are not opposing the previously published data regarding Trk1 reacting to alternations in external potassium concentration by changing its kinetic parameters, quite the contrary. Since both changes in internal potassium content and membrane potential are to a large degree a direct consequence of shifts in external potassium concentration, the notion of either internal potassium content or membrane potential being the actual signal promoting changes in K_T and V_{max} is a mere expansion of the original concept, suggesting potential mediators responsible for transferring the changes in external potassium into the adjustment of the overall capacity of Trk1-mediated uptake.

The possibility of membrane potential being involved in the regulation of kinetic parameters of Trk1 also indirectly confirmed previously observed functional connection between Trk1 and H^+ -ATPase Pma1, proton-pump responsible i. a. for creation and maintenance of membrane potential. The putative interplay between Trk1 and Pma1 could be summarised as a need for balancing the export of protons by the import of potassium in order to maintain proper membrane potential [41,189]. Additionally, the transport activities of Trk1 and Pma1 have been observed to be mutually dependent, It is, therefore, possible that elevated activity of Pma1 and consequently hyperpolarization of plasma membrane could lead to an increase in the overall capacity of Trk1-mediated uptake and inevitably to an increase in the import of potassium. Changes in membrane potential would thus represent a missing link connecting the increase in activity of Pma1 to stimulation of Trk1-mediated potassium uptake. Additionally, a such mechanism also offers a possibility for self-regulating negative feedback. Since elevated potassium uptake leads to depolarization of the plasma membrane this could, in turn, result in a gradual decrease in the uptake capacity of Trk1.

Additional data regarding Trk1-mediated affinity-switch was provided by the work of Haro et. al. [60] in which random mutagenesis combined with selection for mutants unable to grow under potassium limitations yielded a Trk1 mutant with substitution L949P as being unable to switch to a high-affinity state. According to a current structural model of Trk1, Leu949 is located approximately in the middle of the third P-helix, a subdomain responsible mainly for the conformation and structural integrity of the selectivity filter [27]. As the presence of proline is known to be able to disrupt helices by breaking the succession of hydrogen bonds [190], we hypothesized that its introduction into P-helix, for instance in form of substitution L949P, might lead to conformational changes affecting not only particular P-helix itself, but rather the entire region of selectivity filter and potassium-binding site. In order to disclose, in more detail, the effects of disruption of P-helices on the activity of Trk1 and its ability to adjust its kinetic parameters as a reaction to potassium

limitations we constructed four versions of Trk1, each carrying a proline in an analogous position within one of the P-helices (substitutions L81P, F820P, L949P and L115P).

The most striking effect of two of the introduced substitutions, F820P and L949P, was the absence of disruption of Trk1-mediated potassium uptake per se, but rather specific prevention of a complete transition to the high-affinity state, suggesting the possibility, that increase in affinity in Trk1 includes conformational change including the region of the potassium-binding site and selectivity filter and that this putative conformational change is prevented by disruptions of P-helices resulting from substitutions F820P and L949P. One of the key structural differences between channel KcsA and SKT-proteins, including Trk1, is the selectivity filter (section 1.3, Fig. 3). In SKT proteins the so-called signature sequence of selectivity filter deviates from standard TVGYG, present in KcsA [23], leading to a reduction in a total number of potassium-binding sites from 4 to 1 and consequently to a lesser degree of selectivity and elevated structural flexibility of the whole region [29,30]. It is thus conceivable, that this difference allows certain conformational changes in SKT-proteins that would not be possible in KcsA channels and that in Trk1 these changes, likely gradual and dependent on before-mentioned signals, could be a part of the effective mechanism of affinity adjustment. We also introduced proline into P-helices 1 and 4 in form of substitutions L81P and L115P. However, these individual substitutions led to a substantial mis localization of Trk1, possibly due to structural defects caused by a disruption of a number of non-covalent interactions predicted between domains MPM1 and MPM4 [27]. It is possible, however, that had they not disrupted crucial non-covalent interactions and consequently overall conformation of Trk1, these two substitutions would have had an effect similar to that of substitutions F820P and L949P.

Considering the possibility of conformational change of Trk1 being an effective mechanism of adjustment of affinity, it is appropriate to propose a putative role of both internal potassium content and membrane potential in this ostensible process. One of the possibilities for the involvement of internal potassium concentration is the existence of proteins containing intracellular potassium-binding domains able to bind potassium with a frequency proportional to its intracellular concentration and thus promote conformational changes resulting in changes in the activity of the particular protein. Similar potassium-binding proteins have been previously described in bacteria [191]. Such proteins could potentially be a part of a signalling cascade resulting in the phosphorylation of transporters, small regulatory proteins able to interact with Trk1 or possibly even a subdomain of Trk1-itself. However, this mechanism is unlikely to be involved in yeast. According to Herrera et. al. [81], potassium starvation leads to loss of internal potassium in *S. cerevisiae*, presumably by export from the cytoplasm, nonetheless, the actual levels of potassium in cytoplasm remain relatively stable because they are being constantly supplemented from vacuoles. According

to this dynamic, the presumed potassium-binding proteins would, in fact, be unable to react to potassium starvation for they would be constantly exposed to a similar amount of cytoplasmic potassium. The stable level of potassium present in the cytoplasm upon potassium starvation also indirectly disproves the key role of internal potassium content in the regulation of the capacity of Trk1-mediated uptake. The putative effect of membrane potential on conformation and consequently activity of proteins has been previously described for a number of bacterial membrane proteins including transporters [192,193]. To our knowledge, a similar mechanism has not been described in yeast however, membrane potential has been shown to affect the structure of plasma membrane microdomains [194]. It is hence possible that changes in membrane potential resulting from limited availability of external potassium affect the overall capacity of Trk1-mediated potassium uptake either by directly altering its conformation or through reorganization of plasma membrane domains.

Even though according to the results presented here, Trk1 most likely adjusted rather than switched its affinity, it is still conceivable that a simple switch between low- and high-affinity states occurred and that the results suggesting the adjustment merely arose from a limitation of our experimental procedures. Since data from measurements of Trk1-mediated uptake and estimation of kinetic parameters were obtained from measurements on the level of the whole cell, rather than a single protein, it is possible that Trk1, upon exposure to different, external potassium concentrations, in fact, switched directly to high-affinity state but this switch occurred only in a certain portion of the total amount of active proteins and this portion was directly proportional to the availability of potassium. Such a mechanism, in which only a subset of Trk1 proteins transitioned to a high-affinity state could, in theory, produce results as we present here, hence a gradual increase in uptake capacity as a reaction to a decrease in external potassium.

In Nrt1.1, the best studied of the before-mentioned examples of proteins capable of affinity-switch is promoted by phosphorylation of a single residue, Thr101 [185]. While we cannot exclude phosphorylation being involved in the regulation of kinetic parameters of Trk1-mediated uptake as well, it is unlikely to work in a fashion similar to Nrt1.1 considering the putative different nature of changes in affinity, hence adjustment as opposed to the switch. Affinity being adjusted gradually could in theory be achieved by phosphorylation of multiple residues as a reaction to a decrease in the availability of potassium, each increasing the affinity partially, rather than completely. Alternatively, considering the above-mentioned possibility of affinity-switch occurring in a specific portion of active Trk1 proteins, the involvement of a single phosphorylated residue is feasible. Knowledge about the regulation of Trk1 through phosphorylation or possible involvement of specific

kinases and signalling pathways able to sense changes in potassium homeostasis is, however, so far, very limited.

4.2 Putative role of phosphorylation and interaction with 14-3-3 proteins in the regulation of activity of Trk1

As mentioned above, there is a substantial scarcity of data regarding the regulation of Trk1 through phosphorylation. Beyond several phosphoproteomic studies aimed at the identification of changes in the entire phosphoproteome under specific conditions, essentially no studies identifying putative phosphorylation sites and disclosing their role in the regulation of Trk1 are currently available. The second part of the presented thesis, therefore, focused on the identification of potential phosphorylation sites with the goal of distinguishing specific conditions upon which the presumed site would be phosphorylated, effects of this potential phosphorylation on the function of Trk1 and connection to a specific set of kinases previously suggested to be involved in the regulation of Trk1 and overall potassium homeostasis.

Initially, our study was limited to a specific segment of Trk1, the second intracellular loop. Due to its highly defined structure and the remarkable degree of sequence conservation, compared to other intracellular segments of Trk1, the second intracellular loop most likely fulfils a crucial role in the overall function of Trk1. Apart from harbouring potential phosphorylation sites, there are several possibilities regarding the involvement of internal segments in the regulation and function of plasma membrane proteins, most notably: interaction with other proteins, either during transition through the secretory pathway [188] or proteins with regulatory effect on given transporter [195] or interaction with macromolecules, such as ATP [196]. Additionally, this segment in Trk1 might simply fulfil a crucial structural function, a notion supported by a model generated by AlphaFold, in which several non-covalent interactions with other subdomains of Trk1 were predicted. These interactions could potentially participate in the determination of the overall conformation of Trk1 and their alternations, due to phosphorylation/dephosphorylation, could presumably lead to larger conformational changes of Trk1 with substantial consequences on its function, thus representing a potential regulatory mechanism.

We identified two potential phosphorylation sites within the sequence of the second intracellular loop: Ser882 and Thr900. As the abolition of the potential for phosphorylation of these residues led to a decrease in Trk1-mediated uptake, phosphorylation of these residues would most likely have a stimulatory effect on Trk1. It is important to note, that the presumed absence of

phosphorylation of either Ser882 or Thr900 did not inactivate Trk1-mediated uptake completely, but rather led to its partial diminishment, suggesting that these two residues might be a part of a larger set of phosphorylation sites responsible for activation of Trk1 or alternatively being a sites, phosphorylation of which could be responsible for the enhancement of the basal activity of Trk1 under specific conditions, such as potassium limitations. In this context, it is appropriate to consider the possibility of both Ser882 and Thr900 to be a part of the before-mentioned set of phosphorylation sites responsible for the gradual increase in affinity upon the decrease in external potassium availability, as according to our results, the individual substitution of both of these residues for non-phosphorylatable cysteine, led to partially diminished affinity in designated high-affinity state.

Interestingly, according to a structural model, side chains of both of these residues in a non-phosphorylated state, might participate in the creation of hydrogen bonds. In the case of Ser882, the hydrogen bond is presumably formed with Met884, another residue of the second intracellular loop, suggesting the importance in maintaining the proper conformation of the second intracellular loop itself. The side chain of Thr900 potentially forms a hydrogen bond with His122, part of the second transmembrane helix of the MPM1 domain, i.e., a non-covalent interaction with a potential impact on the conformation of a large portion of Trk1. It is possible that the addition of the phosphate group to any of these side chains might potentially lead to the reorganisation of existing or the creation of novel non-covalent interactions and consequently to alternations in the conformation and function of Trk1. A similar mechanism of alternations in non-covalent interactions upon the addition of a phosphate group has been previously described in B-amyloid peptides [197].

It is important to note that our results did not irrefutably confirm the phosphorylation occurring at residues Ser882 and Thr900, even though much of the circumstantial evidence seemed to agree with this notion. To obtain definitive proof, future experimental work regarding Trk1 and phosphorylation on specific residues would inevitably have to resort to one of many methods aimed at the determination of the phosphorylation status of a single protein or peptide.

Our study was also aimed at establishing a potential involvement of 14-3-3 proteins in the regulation of Trk1. In *S. cerevisiae*, 14-3-3 proteins are encoded by *BMH1* and *BMH2* [134]. Initial estimation of the effects of the absence of 14-3-3 proteins on potassium homeostasis was complicated by the fact that combined deletion of both *BMH1* and *BMH2* has been shown to be lethal in most strains [155] and therefore strain lacking only *BMH1*, hence strain with a substantial decrease in expression of 14-3-3 proteins was used. Despite the presence of *Bmh2* however, we were able to detect effects of the absence of *Bmh1* directly connected to both potassium

homeostasis and Trk1, establishing putative involvement of 14-3-3 proteins in the regulation of the function of Trk1. Moreover, according to our results, this interaction would most likely lead to stimulation of the activity of Trk1, especially under conditions where external potassium was limited.

Attempt to identify specific sites responsible for interaction with 14-3-3 proteins provided three such residues: Thr155, Ser414 and the before-mentioned Thr900. Both Thr155 and Ser414 were previously identified in a few of the phosphoproteomic studies [198-200] and thus, our results merely provide additional information regarding the potential mechanism of their contribution to the regulation of Trk1. Residue Thr900 was first identified and analysed in this study. Additionally, for residue Thr900, we proved direct interaction with both Bmh1 and Bmh2 *in vitro*. Thus, based on our data, we can strongly argue in favour of the involvement of 14-3-3 proteins in the regulation of Trk1, by interacting with specific sites, with a presumed positive regulatory effect on Trk1.

There are multiple mechanisms by which 14-3-3 proteins can participate in the regulation of membrane proteins, e.g., facilitation of interaction with other proteins or alternations in conformation with effect on the functionality of target protein [137,139]. None of these mechanisms, however, could be directly confirmed by our results. Probably the most notable mechanism of 14-3-3 protein-mediated regulation of membrane proteins, confirmed by several studies, is a promotion of transition through the secretory pathway by binding to a specific site and occluding so-called ER-retention signals, such as di-arginine motif [201-203]. Even though such a di-arginine motif is located close to both Thr155 and Thr900, this mechanism is unlikely to be involved in the case of Trk1 since we did not observe retention of Trk1 in the secretory pathway either in a strain lacking *BMH1* or in strains expressing Trk1 with substitutions in either Thr155 or Thr900.

Antiporter Nha1 is one of the main cellular exporters of potassium, crucial for the maintenance of potassium homeostasis, especially under conditions of abundance of external potassium [1]. However, under low external potassium concentrations, the activity of Nha1 needs to be limited, in order to ensure sufficient intracellular potassium content. In theory, it could be beneficial for the cells to possess a means of a regulatory interplay between Trk1 and Nha1, that would, under potassium limitations, be able to simultaneously stimulate the activity of Trk1 and thus import of potassium and attenuate its Nha1-mediated export. As 14-3-3 proteins have been shown to negatively regulate Nha1 [106] and our results suggested the possibility of 14-3-3 proteins stimulating the activity of Trk1, these proteins could, in fact, represent such a regulatory connection.

Additionally, there is also a certain, so far, experimentally unsupported, likelihood of 14-3-3 proteins being involved in the before-mentioned simultaneous stimulation of activities of both Trk1 and Pma1. Pma1 ATPase has been shown to be regulated by C-terminal end-mediated autoinhibition

suppressed by phosphorylation [127]. A strikingly similar mechanism has been described for plant H⁺-ATPase, although in the case of plant-ATPase, the involvement of 14-3-3 proteins in the suppression of autoinhibition has also been confirmed [204,205]. Even though the association of yeast H⁺-ATPase Pma1 with 14-3-3 proteins has not been established yet, according to 14-3-3-Pred software, this protein contains a putative site for interaction with Bmh-proteins (Thr912) on its C-terminal end, albeit predicted only by one out of three used algorithms. However, plant H⁺-ATPase does not contain a canonical recognition sequence for interaction with 14-3-3 proteins on its C-terminal end at all and yet, this section of protein is able to interact with 14-3-3 proteins [205]. It is therefore possible that 14-3-3 proteins upregulate the activity of yeast H⁺-ATPase Pma1 by suppressing the autoinhibition as well. Bmh1 and Bmh2 proteins could thus represent a regulatory link connecting these three major players responsible for potassium homeostasis. For instance, under conditions of potassium limitation, association with 14-3-3 proteins could presumably lead to stimulation of acquisition of potassium through Trk1, balancing of membrane potential by activating Pma1 and retainment of acquired potassium through inactivation of Nha1. Data establishing the potential involvement of 14-3-3 proteins in the regulation of Trk1, thus, on top of suggesting a novel mechanism of regulation of potassium uptake in *S. cerevisiae*, also reinforced the topic recurring throughout our work and that is the functional connection of Trk1 to other membrane transporters, involved in overall ion homeostasis.

4.3 Role of Trk-transporters in the survival of glucose-induced cell death and high-temperature

Glucose-induced cell death (GICD) is a phenomenon characterised by programmed cell death triggered by glucose in absence of additional nutrients [206]. The probable cause of cell death upon exposure to glucose as a sole nutrient is an initiation of processes leading to the cellular division that can not be completed due to a lack of other essential nutrients, leading to depletion of ATP [207] and inevitably to loss of viability of treated cells. Both Trk-transporters have been shown to be crucial for the survival of GICD [49], however individual contributions of Trk1 and Trk2 have never been disclosed.

We found transporter Trk2 to play a key role in the survival of stationary cells upon exposure to glucose since strains lacking this transporter exhibited significantly decreased survival, compared to both wild-type and a strain lacking the Trk1 transporter. According to our results, the probable source of this decrease in survival of GICD in strains lacking Trk2, was the up-regulation of Pma1 and

consequently elevated consumption of ATP, again pointing to a functional connection between Pma1 and Trk-proteins. However, this connection seemed to be contrary to previously shown simultaneous activation of Trk1 and Pma1, for our result suggested up-regulation of Pma1 as a consequence of the absence of Trk2, rather than its inhibition. Even though the precise nature of the connection between the lack of Trk2 and up-regulation of Pma1 and its consequences on the survival of GICD remains largely unknown, our data provided additional possibilities regarding, so far mostly obscure, the physiological role of Trk2.

Additionally, cells lacking potassium-uptake systems Trk1 and Trk2 were susceptible to high temperature. As a sufficient amount of intracellular potassium has been shown to be crucial for the survival of various stresses [208], increased susceptibility to high temperature was, in fact, not surprising. However, the exact link between a lack of potassium uptake systems and elevated susceptibility to stress under our conditions is difficult to disclose for two main reasons. First, after 48 hours of incubation on YPD supplemented with 100 mM potassium chloride both the wild-type strain and strains lacking Trk-proteins exhibited similar potassium content, hence different intracellular concentrations of potassium at the beginning of testing are improbable. Additionally, as susceptibility to high temperatures was tested after incubation in water, differences in uptake of potassium are unlikely the cause of changes in thermotolerance, for potassium content in deionized water is extremely low. Therefore, if we consider differences in potassium homeostasis to be a cause of dissimilarities in susceptibility to high temperature among the strains, as a result of lack of Trk-proteins, it would most likely be an either different rate of loss of internal potassium upon incubation in water or unfavourable alternation in intracellular distribution of potassium.

4.4 Potassium-uptake systems in *Kluyveromyces marxianus*

In order to translate our theoretical and practical knowledge from the study of potassium uptake in *S. cerevisiae* into use that could, in theory, reach beyond basic research, we decided to attempt a characterisation of potassium uptake systems also in biotechnologically attractive species *Kluyveromyces marxianus*. Since improved uptake of potassium has been previously shown to enhance biotechnological production, any fundamental knowledge regarding potassium uptake in *K. marxianus* might potentially lead to its increased effectiveness in various biotechnological processes.

According to the results of whole-genome sequencing, the genome of *K. marxianus* encodes two potassium-uptake systems: uniporter Trk1 and K⁺-H⁺ symporter Hak1. Similar Trk1-Hak1 tandem of transporters have been previously described in a few yeast species such as *Schwanniomyces*

occidentalis [70], *Hansenula polymorpha* [36] and *Neurospora crassa* [59]. The common and recurring theme, concerning these two transporters, seemed to be their different expression profiles resulting from variations in external potassium concentrations. Trk1 has been shown in all three species, to be expressed constitutively and on a very low, almost undetectable level, while expression of Hak1 appeared to be negligible under high external potassium and was substantially stimulated under potassium-limiting conditions. Besides a low level of expression, Hak1 was also shown to undergo endocytosis under high external potassium concentration [36]. Additionally, Hak1 exhibited a substantially higher affinity for uptake, compared to Trk1 [36], underlining its importance specifically under conditions when external potassium is scarce. Taken all together, available results suggest an interesting dynamic of the interplay between these two transporters. Trk1, due to either its low level of expression or overall low capacity for uptake of potassium, would likely be the dominant uptake system specifically under higher external concentrations of potassium, since under these conditions Hak1 is expressed on a very low level and also being endocytosed. However, due to its strongly stimulated expression under potassium starvation and high affinity for potassium uptake, Hak1 likely fulfils a major role in potassium uptake specifically under conditions of severe potassium limitations.

Our results were, to a large degree, in line with the above-mentioned concept, confirming the dominant role of Hak1 under low external potassium concentrations. Contrary to the before-mentioned results, in the case of *K. marxianus*, Hak1 was presumably also expressed in presence of high external potassium, since strain *trk1HAK1* also grew well on external potassium concentrations in millimolar ranges. However, this expression might have been triggered specifically by the absence of Trk1, a mechanism previously confirmed in *N. crassa* [59]. It is thus possible, that in presence of Trk1, the expression profile of Hak1, under various external concentrations of potassium, would be different.

Since strain *trk1hak1*, lacking both presumed potassium-uptake systems, was unable to grow on external potassium concentration below 25 mM, we presumed that Trk1 and Hak1 are really the only transporters, in *K. marxianus*, able to facilitate active uptake of potassium.

We also detected a possibility of Trk1 of *K. marxianus* being able to facilitate the uptake of ammonium, as we observed the strain *TRK1hak1* to be especially sensitive to elevated concentrations of ammonium sulphate. When an alternative source of nitrogen, proline, was used, we actually noted a diminished difference between the growth of wild-type and strain *TRK1hak1*, suggesting that the Trk1-mediated uptake was, presumably, competitively inhibited by the presence of ammonium ions. The ability of Trk1 to be able to mediate the uptake of ammonium has been proposed also in *S. cerevisiae* [45]. Considering the possibility of competitive inhibition of Trk1-

mediated potassium uptake by ammonium, it is possible, that diminished growth of strain *TRK1hak1* on low potassium concentrations, compared to wild-type and *trk1HAK1*, was partially caused by this presumed competitive inhibition rather than exclusively by lower capacity for uptake of potassium.

Contrary to previously published data regarding Trk1 and Hak1 in a few other species, we did not detect significant effects of low nor high pH on the functionality of any of these transporters. Especially surprising was the lack of effect of high pH on Hak1, as Hak1 presumably functions as a symporter of H^+K^+ and we would, thus, expect a lack of proton gradient to have a negative impact on Hak1-mediated uptake. There are, however, two possible explanations. First, we observed an overall increase in the growth rate of all tested strains on high pH, so the negative effect of high pH on Hak1 might have simply been overshadowed by this general positive effect. Alternatively, *K. marxianus* might possess a very effective H^+ -ATPase, able to create a strong proton gradient close to the plasma membrane and thus maintain proper Hak1-mediated potassium uptake even under conditions of high pH.

Putative involvement of Trk1, in the regulation of membrane potential, was also supported by our results, since the strain lacking Trk1 was especially sensitive to the presence of the cationic drug Hygromycin B and was thus presumably hyperpolarized. The connection of Trk1 to the regulation of membrane potential was already established in *S. cerevisiae* [4]. Surprisingly, however, strain *trk1HAK1* was more sensitive to Hygromycin B in presence of external potassium concentration in millimolar ranges a less sensitive on plates containing a micromolar concentration of potassium. A possible explanation for this phenomenon might be a putative strong stimulation of expression of Hak1 on low external potassium and consequently elevation of uptake of potassium leading to a partial suppression of the negative effect of Hygromycin B. However, as we did not detect overall better growth of *trk1HAK1* strain on micromolar potassium, compared to its growth on millimolar potassium, in absence of Hygromycin B, this explanation is not sufficient and would be conceivable only if the presence of stress, in the form Hygromycin B, further stimulated expression of Hak1 and thus increased uptake of potassium.

We also tested the effects of the presence of Na^+ and Li^+ on the growth of mutant strains. We did not observe any effect of Na^+ , however, we detected a strong inhibitory effect of Li^+ specifically on strains expressing Hak1, i.e., wild-type and mutant strain *trk1HAK1*, suggesting an ability of Hak1 to facilitate uptake of Li^+ ions. A possible explanation in strain *trk1HAK1* could be a hyperpolarization as a consequence of lack of Trk1, leading to elevated non-specific uptake of positively charged Li^+ , however, as we have also seen a similar effect in the wild-type, in which membrane potential is presumably unaffected, this explanation is unlikely. The ability of Hak1 to mediate the uptake of Li^+ ,

to our knowledge, has not been observed before and its confirmation would require additional experimental work.

Obtained results produced a basic characterisation of two potassium-uptake systems, Trk1 and Hak1, thus providing a good starting point for their detailed study and potential utilization in increasing the biotechnological relevance of *Kluyveromyces marxianus*.

5. Conclusions

The presented thesis focused on the study of Trk1, one of the key players in potassium uptake and homeostasis in yeast. Obtained results expanded our knowledge regarding Trk1 in four main areas, as listed in the aims of the thesis. The main results can be summarised as follows:

- We supplemented the original concept of ‘affinity-switch’ by proving the ability of Trk1 to precisely adjust its kinetic parameters according to the availability of potassium. Additionally, we identified novel putative signals: internal potassium content and membrane potential, presumably involved in governing the changes in both affinity and maximum velocity of Trk1. Our results also pointed to a putative role of P-helices in the adjustment of the affinity of Trk1. Results obtained in this section of the thesis were published in the *Journal of Fungi*.
- In the second section of the thesis, we analysed four and identified two novel phosphorylation sites within the highly conserved region of the second intracellular loop: Ser882 and Thr900. Based on the model and experimental results we also confirmed the putative structural role of the second intracellular loop. Additionally, our data supported the involvement of 14-3-3 proteins in the regulation of both Trk1 and overall potassium homeostasis and also identified three potential binding sites for 14-3-3 proteins: Thr155, Ser414 and Thr900. Obtained results are presented as a near-final version of a manuscript.
- Study of the connection between the Trk-proteins and GICD confirmed the involvement of both Trk1 and Trk2 in the survival of GICD with Trk2 fulfilling a dominant role. Additionally, a functional connection between the main H⁺-ATPase and Trk2 with crucial consequences on the survival of GICD was established. Obtained results were published in *Microbiology*.
- In order to characterise the potassium-uptake systems in non-conventional species *Kluyveromyces marxianus*, we successfully employed CRISP-Cas9 and Golden-Gate assembly methods and confirmed Trk1 and Hak1 as the main potassium importers in this yeast species. Additionally, our results suggested the Hak1 protein to be a dominant potassium-uptake system under low external potassium concentration, with Trk1, under such conditions, contributing only marginally.

6. References

1. Arino, J.; Ramos, J.; Sychrova, H. Alkali Metal Cation Transport and Homeostasis in Yeasts. *Microbiol. Mol. Biol. Rev.* **2010**, *74*, 95-120, doi:10.1128/MMBR.00042-09.
2. Benito, B.; Moreno, E.; Lagunas, R. Half-life of the plasma membrane ATPase and its activating system in resting yeast cells. *Biochim. Biophys. Acta* **1991**, *1063*, 265-268, doi:10.1016/0005-2736(91)90381-H.
3. Herrera, R.; Alvarez, M.; Gelis, S.; Kodedova, M.; Sychrova, H.; Kschischo, M.; Ramos, J. Role of *Saccharomyces cerevisiae* Trk1 in stabilization of intracellular potassium content upon changes in external potassium levels. *Biochim. Biophys. Acta* **2014**, *1838*, 127-133, doi:10.1016/j.bbamem.2013.08.022.
4. Navarrete, C.; Petrezselyova, S.; Barreto, L.; Martinez, J.; Zahradka, J.; Arino, J.; Sychrova, H.; Ramos, J. Lack of main K⁺ uptake systems in *Saccharomyces cerevisiae* cells affects yeast performance in both potassium-sufficient and potassium-limiting conditions. *FEMS Yeast Res.* **2010**, *10*, 508-517, doi:10.1111/j.1567-1364.2010.00630.x.
5. Razov, A.; Khusainov, I.; El Omari, K.; Duman, R.; Mykhaylyk, V.; Yusupov, M.; Westhof, E.; Wagner, A.; Yusupova, G. Importance of potassium ions for ribosome structure and function revealed by long-wavelength X-ray diffraction. *Nat. Commun.* **2019**, *10*, doi:10.1038/s41467-019-10409-4.
6. Bostian, K.; Betts, G. Rapid purification and properties of potassium-activated aldehyde dehydrogenase from *Saccharomyces cerevisiae*. *Biochem. J.* **1978**, *173*, 773-786, doi:10.1042/bj1730773.
7. Turner, J.; Ewald, J.; Skotheim, J. Cell size control in yeast. *Curr. Biol.* **2012**, *22*, 350-359, doi:10.1016/j.cub.2012.02.041.
8. Lam, F.; Ghaderi, A.; Fink, G.; Stephanopoulos, G. Engineering alcohol tolerance in yeast. *Science* **2014**, *346*, 71-75, doi:10.1126/science.1257859.
9. Xu, X.; Williams, T.; Divne, C.; Pretorius, I.; Paulsen, I. Evolutionary engineering in *Saccharomyces cerevisiae* a TRK1-dependent potassium influx mechanism for propionic acid tolerance. *Biotechnol. Biofuel.* **2019**, *12*, doi:10.1186/s13068-019-1427-6.
10. Barreto, L.; Canadell, D.; Valverde-Saubi, D.; Casamayor, A.; Arino, J. The short-term response of yeast to potassium starvation. *Environ. Microbiol.* **2012**, *14*, 3026-3042, doi:10.1111/j.1462-2920.2012.02887.x.
11. Rangarajan, N.; Kapoor, I.; Li, S.; Drossopoulos, P.; White, K.; Madden, Y.; Dohlman, H. Potassium starvation induces autophagy in yeast. *J. Biol. Chem.* **2020**, *295*, 14189-14202, doi:10.1074/jbc.RA120.014687.
12. Durell, S.; Hao, Y.; Nakamura, T.; Bakker, E.; Guy, H. Evolutionary relationship between K(+) channels and symporters. *Biophys. J.* **1999**, *77*, 775-788, doi:10.1016/S0006-3495(99)76931-6.
13. Levin, E.; Zhiu, M. Recent Progress on the Structure and Function of the TrkH/KtrB Ion Channel. *Curr. Opin. Struct. Biol.* **2014**, *27*, 95-101, doi:10.1016/j.sbi.2014.06.004.
14. Greie, J. The KdpFABC complex from *Escherichia coli*: A chimeric K⁺ transporter merging ion pumps with ion channels. *Eur. J. Cell Biol.* **2011**, *90*, 705-710, doi:10.1016/j.ejcb.2011.04.011.
15. Diskowski, M.; Mikusevic, V.; Stock, C.; Hanelt, I. Functional diversity of the superfamily of K⁺ transporters to meet various requirements. *Biol. Chem.* **2015**, *396*, 1003-1014, doi:10.1515/hsz-2015-0123.
16. Cao, Y.; Jin, X.; Huang, H.; Derebe, M.; Levin, E.; Kabaleeswaran, V.; Pan, Y.; Punta, M.; Love, J.; Weng, J.; et al. Crystal structure of a potassium ion transporter, TrkH. *Nature* **2011**, *471*, 336-340, doi:10.1038/nature09731.
17. Vieira-Pires, R.; Szollosi, A.; Morais-Cabral, J. The structure of the KtrAB potassium transporter. *Nature* **2013**, *496*, 323-328.

18. Huang, C.; Pedersen, B.; Stokes, D. Crystal Structure of the Potassium Importing KdpFABC Membrane Complex. *Nature* **2017**, *546*, 681-685, doi:10.1038/nature22970.
19. Ali, A.; Maggio, A.; Bressan, R.; Yun, D. Role and Functional Differences of HKT1-Type Transporters in Plants under Salt Stress. *Int. J. Mol. Sci.* **2019**, *20*, doi:10.3390/ijms20051059.
20. Waters, S.; Gilliham, M.; Hrmova, M. Plant High-Affinity Potassium (HKT) Transporters Involved in Salinity Tolerance: Structural Insights to Probe Differences in Ion Selectivity. *Int. J. Mol. Sci.* **2013**, *14*, 7660-7680, doi:10.3390/ijms14047660.
21. Horie, T.; Hauser, F.; Schroeder, J. HKT transporter-mediated salinity resistance mechanisms in Arabidopsis and monocot crop plants. *Trends Plant Sci.* **2009**, *14*, 660-668, doi:10.1016/j.tplants.2009.08.009.
22. Durell, S.; Guy, H. Structural models of the KtrB, TrkH, and Trk1,2 symporters based on the structure of the KcsA K(+) channel. *Biophys. J.* **1999**, *77*, 789-807, doi:10.1016/S0006-3495(99)76932-8.
23. Doyle, D.; Morais, C.; Pfuetzner, R.; Kuo, A.; Gulbis, J.; Cohen, S.; Chait, B.; MacKinnon, R. The structure of the potassium channel: molecular basis of K⁺ conduction and selectivity. *Science* **1998**, *280*, 69-77, doi:10.1126/science.280.5360.69.
24. Zhou, Y.; MacKinnon, R. The Occupancy of Ions in the K1 Selectivity Filter: Charge Balance and Coupling of Ion Binding to a Protein Conformational Change Underlie High Conduction Rates. *J. Mol. Biol.* **2003**, *333*, 965-975, doi:10.1016/j.jmb.2003.09.022.
25. Zhou, M.; Morais-Cabral, J.; Mann, S.; MacKinnon, R. Potassium channel receptor site for the inactivation gate and quaternary amine inhibitors. *Nature* **2001**, *411*, 657-661, doi:10.1038/35079500.
26. Zhou, M.; MacKinnon, R. A Mutant KcsA K1 Channel with Altered Conduction Properties and Selectivity Filter Ion Distribution. *J. Mol. Biol.* **2004**, *338*, doi:10.1016/j.jmb.2004.03.020.
27. Zayats, V.; Stockner, T.; Pandey, S.; Wortz, K.; Ettrich, R.; Ludwig, J. A Refined Atomic Scale Model of the *Saccharomyces cerevisiae* K⁺-translocation Protein Trk1p Combined With Experimental Evidence Confirms the Role of Selectivity Filter Glycines and Other Key Residues. *Biochim. Biophys. Acta* **2015**, *1848*, 1183-1195, doi:10.1016/j.bbamem.2015.02.007.
28. Kale, D.; Spurny, P.; Shamayeva, K.; Spurna, K.; Kahoun, D.; Ganser, D.; Zayats, V.; Ludwig, J. The *S. cerevisiae* Cation Translocation Protein Trk1 is Functional Without Its "Long Hydrophilic Loop" But LHL Regulates Cation Translocation Activity and Selectivity. *Biochim. Biophys. Acta* **2019**, *1861*, 1476-1488, doi:10.1016/j.bbamem.2019.06.010.
29. Mikusevic, V.; Schrecker, M.; Kolesova, N.; Patino-Ruiz, M.; Fendler, K.; Hanelt, I. A channel profile report of the unusual K⁺ channel KtrB. *J. Gen. Physiol.* **2019**, *151*, 1357-1368, doi:10.1085/jgp.201912384.
30. Hanelt, I.; Tholema, N.; Kroning, N.; Vor der Bruggen, M.; Wunnicke, D.; Bakker, E. KtrB, a member of the superfamily of K⁺ transporters. *Eur. J. Cell Biol.* **2011**, *90*, 696-704, doi:10.1016/j.ejcb.2011.04.010.
31. Derebe, M.; Sauer, D.; Zeng, W.; Alam, A.; Shi, N.; Jiang, Y. Tuning the ion selectivity of tetrameric cation channels by changing the number of ion binding sites. *Proc. Natl. Acad. Sci. USA* **2011**, *108*, 598-602, doi:10.1073/pnas.1013636108.
32. Sauer, D.; Zeng, W.; Canty, J.; Lam, Y.; Jiang, Y. Sodium and potassium competition in potassium-selective and non-selective channels. *Nat. Commun.* **2013**, *2721*, doi:10.1038/ncomms3721.
33. Ramos, J.; Contreras, P.; Rodriguez-Navarro, A. A potassium transport mutant of *Saccharomyces cerevisiae*. *Archives of Microbiology* **1985**, *143*, 88-93.
34. Gaber, R.; Styles, C.; Fink, G. TRK1 Encodes a Plasma Membrane Protein Required for High-affinity Potassium Transport in *Saccharomyces cerevisiae*. *Mol. Cell. Biol.* **1988**, *8*, 2848-2859, doi:10.1128/mcb.8.7.2848-2859.1988.

35. Martinez, J.; Sychrova, H.; Ramos, J. Monovalent cations regulate expression and activity of the Hak1 potassium transporter in *Debaryomyces hansenii*. *Fungal Genet. Biol.* **2011**, *48*, 177-184, doi:10.1016/j.fgb.2010.06.013.
36. Cabrera, E.; Alvarez, M.; Martin, Y.; Siverio, J.; Ramos, J. K⁺ uptake systems in the yeast *Hansenula polymorpha*. Transcriptional and post-translational mechanisms involved in high-affinity K⁺ transporter regulation. *Fungal Genet. Biol.* **2012**, *49*, 755-763, doi:10.1016/j.fgb.2012.06.008.
37. Llopis-Torregrosa, V.; Husekova, B.; Sychrova, H. Potassium uptake mediated by Trk1 is crucial for *Candida Glabrata* growth and fitness. *PLoS One* **2016**, *11*, 1-18, doi:10.1371/journal.pone.0153374.
38. Elicharova, H.; Husekova, B.; Sychrova, H. Three *Candida albicans* potassium uptake systems differ in their ability to provide *Saccharomyces cerevisiae* *trk1trk2* mutants with necessary potassium. *FEMS Yeast Res.* **2016**, *16*, 1-10, doi:10.1093/femsyr/fow039.
39. Inokuma, K.; Ishii, J.; Hara, K.; Mochizuki, M.; Hasunama, T.; Kondo, A. Complete Genome Sequence of *Kluyveromyces marxianus* NBRC1777, a Nonconventional Thermotolerant Yeast. *Genome Announc.* **2015**, *3*, doi:10.1128/genomeA.00389-15.
40. Ko, C.; Gaber, R. *TRK1* and *TRK2* Encode Structurally Related K⁺ Transporters in *Saccharomyces cerevisiae*. *Mol. Cell. Biol.* **1991**, *11*, 4266-4273, doi:10.1128/mcb.11.8.4266.
41. Yenush, L.; Merchan, S.; Holmes, J.; Serrano, R. pH-Responsive, Posttranslational Regulation of the Trk1 Potassium Transporter by the Type 1-Related Ppz1 Phosphatase. *Mol. Cell. Biol.* **2005**, *25*, 8683-8692, doi:10.1128/MCB.25.19.8683-8692.2005.
42. Rivetta, A.; Slayman, C.; Kuroda, T. Quantitative Modeling of Chloride Conductance in Yeast TRK Potassium Transporters. *Biophys. J.* **2005**, *89*, 2412-2426, doi:10.1529/biophysj.105.066712.
43. Ramos, J.; Haro, R.; Rodriguez-Navarro, A. Regulation of potassium fluxes in *Saccharomyces cerevisiae*. *Biochim. Biophys. Acta* **1990**, *1029*, 211-217, doi:10.1016/0005-2736(90)90156-I.
44. Rodriguez-Navarro, A. Potassium transport in fungi and plants. *Biochim. Biophys. Acta* **2000**, *1469*, 1-30, doi:10.1016/s0304-4157(99)00013-1.
45. Reisser, C.; Dick, C.; Kruglyak, L.; Botstein, D.; Schacherer, J.; Hess, D. Genetic Basis of Ammonium Toxicity Resistance in a Sake Strain of Yeast: A Mendelian Case. *G3 (Bethesda)* **2013**, *3*, 733-740, doi:10.1534/g3.113.005884.
46. Madrid, R.; Gomez, M.; Ramos, J.; Rodriguez-Navarro, A. Ectopic potassium uptake in *trk1trk2* mutants of *Saccharomyces cerevisiae* correlates with a highly hyperpolarized membrane potential. *J. Biol. Chem.* **1998**, *273*, 14838-14844, doi:10.1074/jbc.273.24.14838.
47. Zimmermannova, O.; Felcmanova, K.; Rosas-Santiago, P.; Papouskova, K.; Pantoja, O.; Sychrova, H. Erv14 Cargo Receptor Participates in Regulation of Plasma-membrane Potential, Intracellular pH and Potassium Homeostasis via its Interaction with K⁺-specific Transporters Trk1 and Tok1. *Biochim. Biophys. Acta* **2019**, *1866*, 1376-1388, doi:10.1016/j.bbamcr.2019.05.005.
48. Rivetta, A.; Kuroda, T.; Slayman, C. Anion currents in yeast K⁺ transporters (TRK) characterize a structural homologue of ligand-gated ion channels. *Pflugers Arch.* **2011**, *462*, 315-330, doi:10.1007/s00424-011-0959-9.
49. Hoerberichts, F.; Perez-Valle, J.; Montesinos, C.; Mulet, J.; Planes, M.; Hueso, G.; Yenush, L.; Sharma, S.; Serrano, R. The role of K(+) and H(+) transport systems during glucose- and H(2)O(2)-induced cell death in *Saccharomyces cerevisiae*. *Yeast* **2010**, *27*, 713-725, doi:10.1002/yea.1767.
50. Ramos, J.; Alijo, R.; Haro, R.; Rodriguez-Navarro, A. TRK2 is not a low-affinity potassium transporter in *Saccharomyces cerevisiae*. *J. Bacteriol.* **1994**, *176*, 249-252, doi:10.1128/jb.176.1.249-252.1994.
51. Petrezselyova, S.; Ramos, J.; Sychrova, H. Trk2 Transporter is a Relevant Player in K⁺ Supply and Plasma-membrane Potential Control in *Saccharomyces cerevisiae*. *Folia Microbiol.* **2011**, *56*, 23-28, doi:10.1007/s12223-011-0009-1.

52. Boroviova, D.; Herynkova, P.; Rapoport, A.; Sychrova, H. Potassium uptake system Trk2 is crucial for yeast cell viability during anhydrobiosis. *FEMS Microbiol. Lett.* **2013**, *350*, 28-33, doi:10.1111/1574-6968.12344.
53. Miranda, M.; Bashi, E.; Vylkova, S.; Edgerton, M.; Slayman, C.; Rivetta, A. Conservation and Dispersion of Sequence and Function in Fungal TRK Potassium Transporters: Focus on *Candida albicans*. *FEMS Yeast Res.* **2009**, *9*, 278-292, doi:10.1111/j.1567-1364.2008.00471.x.
54. Haro, R.; Rodriguez-Navarro, A. Functional analysis of the M2D helix of the TRK1 potassium transporter of *Saccharomyces cerevisiae*. *Biochim. Biophys. Acta* **2003**, *1613*, 1-6, doi:10.1016/S0005-2736(03)00132-9.
55. Rodriguez-Navarro, A.; Ramos, J. Dual system for potassium transport in *Saccharomyces cerevisiae*. *J. Bacteriol.* **1984**, *159*, 940-945.
56. Ramos, J.; Rodriguez-Navarro, A. Regulation and interconversion of the potassium transport systems of *Saccharomyces cerevisiae* as revealed by rubidium transport. *Eur. J. Biochem.* **1986**, *154*, 307-311, doi:10.1111/j.1432-1033.1986.tb09398.x.
57. Ruiz-Castilla, F.; Bieber, J.; Caro, G.; Michan, C.; Sychrova, H.; Ramos, J. Regulation and Activity of CaTrk1, CaAcu1 and CaHak1, the Three Plasma Membrane Potassium Transporters in *Candida albicans*. *Biochim. Biophys. Acta* **2021**, *1863*, doi:10.1016/j.bbamem.2020.183486.
58. Haro, R.; Sainz, L.; Rubio, F.; Rodriguez-Navarro, A. Cloning of two genes encoding potassium transporters in *Neurospora crassa* and expression of the corresponding cDNAs in *Saccharomyces cerevisiae*. *Mol. Microbiol.* **1999**, *31*, 511-520, doi: 10.1046/j.1365-2958.1999.01192.x.
59. Rivetta, A.; Allen, K.; Slayman, C.; Slayman, C. Coordination of K⁺ Transporters in *Neurospora*: TRK1 Is Scarce and Constitutive, while HAK1 Is Abundant and Highly Regulated. *Eukaryot. Cell* **2013**, *12*, 684-696, doi:10.1128/EC.00017-13.
60. Haro, R.; Rodriguez-Navarro, A. Molecular analysis of the mechanism of potassium uptake through the TRK1 transporter of *Saccharomyces cerevisiae*. *Biochim. Biophys. Acta* **2002**, *1564*, 114-122, doi:10.1016/s0005-2736(02)00408-x.
61. Mulet, J.; Leuebe, M.; Kron, S.; Rios, G.; Fink, G.; Serrano, R. A Novel Mechanism of Ion Homeostasis and Salt Tolerance in Yeast: the Hal4 and Hal5 Protein Kinases Modulate the Trk1-Trk2 Potassium Transporter. *Mol. Cell Biol.* **1999**, *19*, 3328-3327, doi:10.1128/MCB.19.5.3328.
62. Perez-Valle, J.; Jenkins, H.; Merchan, S.; Montiel, V.; Ramos, J.; Sharma, S.; Serrano, S.; Yenush, L. Key Role for Intracellular K⁺ and Protein Kinases Sat4/Hal4 and Hal5 in the Plasma Membrane Stabilization of Yeast Nutrient Transporters. *Mol. Cell Biol.* **2007**, *27*, 5725-5736, doi:10.1128/MCB.01375-06.
63. Forment, J.; Mulet, J.; Vicente, O.; Serrano, R. The Yeast SR Protein Kinase Sky1p Modulates Salt Tolerance, Membrane Potential and the Trk1,2 Potassium Transporter. *Biochim. Biophys. Acta* **2002**, *1565*, 36-40, doi:10.1016/s0005-2736(02)00503-5.
64. Portillo, F.; Mulet, J.; Serrano, R. A Role for the Non-phosphorylated Form of Yeast Snf1: Tolerance to Toxic Cations and Activation of Potassium Transport. *FEBS Lett.* **2005**, *579*, 512-516, doi:10.1016/j.febslet.2004.12.019.
65. Mendoza, I.; Rubio, F.; Rodriguez-Navarro, A.; Pardo, J. The Protein Phosphatase Calcineurin Is Essential for NaCl Tolerance of *Saccharomyces cerevisiae*. *J. Biol. Chem.* **1994**, *269*, 8792-8796, doi:10.1016/S0021-9258(17)37038-2.
66. Marquina, M.; Gonzalez, A.; Barreto, L.; Gelis, S.; Munoz, I.; Ruiz, A.; Alvarez, M.; Ramos, J.; Arino, J. Modulation of Yeast Alkaline Cation Tolerance by Ypi1 Requires Calcineurin. *Genetics* **2012**, *190*, 1355-1364, doi:10.1534/genetics.112.138370.
67. Casado, C.; Yenush, L.; Melero, C.; Ruiz, M.; Serrano, R.; Perez-Valle, J.; Arino, J.; Ramos, J. Regulation of Trk-Dependent Potassium Transport by the Calcineurin Pathway Involves the Hal5 Kinase. *FEBS Lett.* **2010**, *584*, 2415-2420, doi:10.1016/j.febslet.2010.04.042.
68. Henriques, S.; Mira, N.; Sa-Correia, I. Genome-wide search for candidate genes for yeast robustness improvement against formic acid reveals novel susceptibility (Trk1 and positive

- regulators) and resistance (Haa1-regulon) determinants. *Biotechnol. Biofuels* **2017**, *10*, doi:10.1186/s13068-017-0781-5.
69. Llopis-Torregrosa, V.; Vaz, C.; Monteoliva, R.; Ryman, K.; Engstrom, Y.; Gacser, A.; Gil, C.; Lungdahl, P.; Sychrova, H. Trk1-mediated potassium uptake contributes to cell-surface properties and virulence of *Candida glabrata*. *Sci. Rep.* **2019**, *9*, doi:10.1038/s41598-019-43912-1.
 70. Banuelos, M.; Madrid, R.; Rodriguez-Navarro, A. Individual functions of the HAK and TRK potassium transporters of *Schwanniomyces occidentalis*. *Mol. Microbiol.* **2002**, *37*, 671-679, doi:10.1046/j.1365-2958.2000.02040.x.
 71. Ruiz-Castilla, F.; Rodriguez-Castro, E.; Michan, C.; Ramos, J. The Potassium Transporter Hak1 in *Candida Albicans*, Regulation and Physiological Effects at Limiting Potassium and under Acidic Conditions. *J. Fungi* **2021**, *7*, doi:10.3390/jof7050362
 72. Benito, B.; Garciadeblas, B.; Schreier, P.; Rodriguez-Navarro, A. Novel P-type ATPases mediate high-affinity potassium or sodium uptake in fungi. *Eukaryot. Cell* **2004**, *3*, 359-368, doi:10.1128/EC.3.2.359-368.2004.
 73. Wright, M.; Ramos, J.; Gomez, M.; Moulder, K.; Scherrer, M.; Munson, G.; Gaber, R. Potassium Transport by Amino Acid Permeases in *Saccharomyces cerevisiae*. *J. Biol. Chem.* **1997**, *272*, 13647-13652, doi:10.1074/jbc.272.21.13647.
 74. Ko, C.; Liang, H.; Gaber, R. Roles of multiple glucose transporters in *Saccharomyces cerevisiae*. *Mol. Cell. Biol.* **1993**, *13*, 638-348, doi:10.1128/mcb.13.1.638.
 75. Bihler, H.; Slayman, C.; Bertl, A. NSC1: a novel high-current inward rectifier for cations in the plasma membrane of *Saccharomyces cerevisiae*. *FEBS Lett.* **1998**, *432*, 59-64, doi:10.1016/s0014-5793(98)00832-1.
 76. Wilson, Z.; Scott, A.; Dowell, R.; Odorizzi, G. PI(3,5)P2 controls vacuole potassium transport to support cellular osmoregulation. *Mol. Biol. Cell.* **2018**, *29*, 1718-1731, doi:10.1091/mbc.E18-01-0015.
 77. Sasikumar, A.; Killiea, D.; Kennedy, B.; Brem, R. Potassium Restriction Boosts Vacuolar Acidity and Extends Lifespan in Yeast. *Exp. Gerontol.* **2019**, *120*, 101-106, doi:10.1016/j.exger.2019.02.001.
 78. Cagnac, O.; Leterrier, M.; Yeager, M.; Blumwald, E. Identification and Characterization of Vnx1p, a Novel Type of Vacuolar Monovalent Cation/H⁺ Antiporter of *Saccharomyces cerevisiae*. *J. Biol. Chem.* **2007**, *282*, 24284-24293, doi:10.1074/jbc.M703116200.
 79. Zhang, F.; Bian, J.; Chen, X.; Huang, J.; Smith, N.; Lu, W.; Xu, Y.; Lee, J.; Wu, X. Roles for intracellular cation transporters in respiratory growth of yeast. *Metallomics* **2019**, *11*, 1667-1678, doi:10.1039/c9mt00145j.
 80. Garlid, K.; Paucek, P. Mitochondrial potassium transport: the K⁺ cycle. *Biochim. Biophys. Acta* **2003**, *1606*, doi:10.1016/S0005-2728(03)00108-7.
 81. Herrera, R.; Alvarez, M.; Gelis, S.; Ramos, J. Subcellular potassium and sodium distribution in *Saccharomyces cerevisiae* wild-type and vacuolar mutants. *Biochem. J.* **2013**, *454*, 525-532, doi:10.1042/BJ20130143.
 82. Job, G.; Brugger, C.; Xu, T.; Lowe, B.; Pfister, Y.; Qu, C.; Shanker, S.; Sanz, J.; Partridge, J.; Schlach, T. SHREC Silences Heterochromatin via Distinct Remodeling and Deacetylation Modules. *Mol. Cell.* **2016**, *62*, 207-221, doi:10.1016/j.molcel.2016.03.016.
 83. Strick, R.; Strissel, P.; Gavrilov, K.; Levi-Setti, R. Cation–chromatin binding as shown by ion microscopy is essential for the structural integrity of chromosomes. *J. Cell Biol.* **2001**, *155*, 899-910, doi:10.1083/jcb.200105026.
 84. Yenush, L. Potassium and sodium transport in yeast. *Adv. Exp. Med. Biol.* **2016**, *892*, 187-228, doi:10.1007/978-3-319-25304-6_8.
 85. Yenush, L.; Mulet, J.; Arino, J.; Serrano, R. The Ppz Protein Phosphatases Are Key Regulators of K⁺ and pH Homeostasis: Implications for Salt Tolerance, Cell Wall Integrity and Cell Cycle Progression. *EMBO J.* **2002**, *21*, 920-929, doi:10.1093/emboj/21.5.920.

86. Cagnac, O.; Sranda-Sicilia, M.; Letierrier, M.; Rodriguez-Rosales, M.; Venema, K. Vacuolar Cation/H⁺ Antiporters of *Saccharomyces cerevisiae*. *J. Biol. Chem.* **2010**, *285*, 33914-33922, doi:10.1074/jbc.M110.116590.
87. Petrezselyova, S.; Kinclova-Zimmermannova, O.; Sychrova, H. Vhc1, a novel transporter belonging to the family of electroneutral cation-Cl(-) cotransporters, participates in the regulation of cation content and morphology of *Saccharomyces cerevisiae* vacuoles. *Biochim. Biophys. Acta* **2013**, *1828*, 623-631, doi:10.1016/j.bbamem.2012.09.019.
88. Peng, L.; Du, J.; Zhang, R.; Zhu, N.; Zhao, H.; Zhao, Q.; Yu, Q.; Li, M. The Transient Receptor Potential Channel Yvc1 Deletion Recovers the Growth Defect of Calcineurin Mutant Under Endoplasmic Reticulum Stress in *Candida albicans*. *Front. Microbiol.* **2021**, *12*, doi:10.3389/fmicb.2021.752670.
89. Zahran, N.; Hofmann, J.; Ho, S.; Thomas, L. Yvc1p and the Hyperosmotic Shock Response in *Saccharomyces cerevisiae*. *Biophys. J.* **2012**, *102*, doi:10.1016/j.bpj.2011.11.1892.
90. Qiu, Q.; Fratti, R. The Na⁺/H⁺ exchanger Nhx1p regulates the initiation of *Saccharomyces cerevisiae* vacuole fusion. *J. Cell Sci.* **2010**, *123*, 3266-3275, doi:10.1242/jcs.067637.
91. Brett, C.; Tukaye, D.; Mukhrjee, S.; Rao, R. The Yeast Endosomal Na⁺(K⁺)/H⁺ Exchanger Nhx1 Regulates Cellular pH to Control Vesicle Trafficking. *Mol. Cell Biol.* **2005**, *16*, 1396-1405, doi:10.1091/mbc.E04-11-0999.
92. Qiu, Q. V-ATPase, ScNhx1p and yeast vacuole fusion. *J. Genet. Genomics* **2012**, *39*, 167-171, doi:10.1016/j.jgg.2012.02.001.
93. Maresova, L.; Sychrova, H. Physiological characterization of *Saccharomyces cerevisiae kha1* deletion mutants. *Mol. Microbiol.* **2004**, *55*, 588-600, doi:10.1111/j.1365-2958.2004.04410.x.
94. Maresova, L.; Sychrova, H. Genetic interactions among the Arl1 GTPase and intracellular Na⁺/H⁺ antiporters in pH homeostasis and cation detoxification. *FEMS Yeast Res.* **2010**, *10*, 802-811, doi:10.1111/j.1567-1364.2010.00661.x.
95. Nowikovsky, K.; Devenish, R.; Froschauer, E.; Schweyen, R. Determination of yeast mitochondrial KHE activity, osmotic swelling and mitophagy. *Methods Enzymol.* **2009**, *457*, 305-317, doi:10.1016/S0076-6879(09)05017-4.
96. Zotova, L.; Aleschko, M.; Sponder, G.; Baumgartner, R.; Reipert, S.; Prinz, M.; Schweyen, R.; Nowikovsky, K. Novel Components of an Active Mitochondrial K⁺/H⁺ Exchange. *J. Biol. Chem.* **2010**, *285*, 14399-14414, doi:10.1074/jbc.M109.059956.
97. Dutta, D.; Fliegel, L. Structure and function of yeast and fungal Na⁺ /H⁺ antiporters. *IUBMB Life* **2018**, *70*, 23-31, doi:10.1002/iub.1701.
98. Prior, C.; Potier, S.; Souciet, J.; Sychrova, H. Characterization of the *NHA1* gene encoding a Na⁺/H⁺-antiporter of the yeast *Saccharomyces cerevisiae*. *FEBS Lett.* **1996**, *387*, 89-93, doi:10.1016/0014-5793(96)00470-X.
99. Kinclova-Zimmermannova, O.; Gaskova, D.; Sychrova, H. The Na⁺,K⁺/H⁺-antiporter Nha1 influences the plasma membrane potential of *Saccharomyces cerevisiae*. *FEMS Yeast Res.* **2006**, *6*, 792-800, doi:10.1111/j.1567-1364.2006.00062.x.
100. Kinclova, o.; Ramos, J.; Potier, S.; Sychrova, H. Functional study of the *Saccharomyces cerevisiae* Nha1p C-terminus. *Mol. Microbiol.* **2001**, *40*, 656-668, doi:10.1046/j.1365-2958.2001.02412.x.
101. Sychrova, H.; Pena, J. Involvement of Nha1 antiporter in regulation of intracellular pH in *Saccharomyces cerevisiae*. *FEMS Microbiol. Lett.* **1999**, *171*, 167-172, doi:10.1111/j.1574-6968.1999.tb13428.x.
102. Banuelos, M.; Sychrova, H.; Bleykasten-Grosshans, C.; Souciet, J.; Potier, S. The Nha1 antiporter of *Saccharomyces cerevisiae* mediates sodium and potassium efflux. *Microbiology (Reading)* **1998**, *144*, 2749-2758, doi:10.1099/00221287-144-10-2749.
103. Proft, M.; Struhl, K. MAP kinase-mediated stress relief that precedes and regulates the timing of transcriptional induction. *Cell* **2004**, *118*, 351-361, doi:10.1016/j.cell.2004.07.016.

104. Kinclova-Zimmermannova, O.; Sychrova, H. Functional study of the Nha1p C-terminus: involvement in cell response to changes in external osmolarity. *Curr. Gen.* **2006**, *49*, 229-236, doi:10.1007/s00294-005-0050-1.
105. Zahradka, J.; van Heusden, G.; Sychrova, H. Yeast 14-3-3 Proteins Participate in the Regulation of Cell Cation Homeostasis via Interaction with Nha1 Alkali-metal-cation/proton Antiporter. *Biochim. Biophys. Acta.* **2012**, *1820*, 849-858, doi:10.1016/j.bbagen.2012.03.013.
106. Smidova, A.; Stankova, K.; Petrvalska, O.; Lazar, J.; Sychrova, H.; Obsil, T.; Zimmermannova, O.; Obsilova, V. The Activity of *Saccharomyces cerevisiae* Na⁺, K⁺/H⁺ Antiporter Nha1 Is Negatively Regulated by 14-3-3 Protein Binding at Serine 481. *Biochim. Biophys. Acta* **2019**, *1866*, doi:10.1016/j.bbamcr.2019.118534.
107. Rosas-Santiago, P.; Zimmermannova, O.; Vera-Estrella, R.; Sychrova, H.; Pantoja, O. Erv14 cargo receptor participates in yeast salt tolerance via its interaction with the plasma-membrane Nha1 cation/proton antiporter. *Biochim. Biophys. Acta* **2016**, *1858*, 67-74, doi:10.1016/j.bbamem.2015.09.024.
108. Benito, B.; Garciadoblas, B.; Rodriguez-Navarro, A. Potassium- or sodium-efflux ATPase, a key enzyme in the evolution of fungi. *Microbiology (Reading)* **2002**, *148*, 933-941, doi:10.1099/00221287-148-4-933.
109. Petrezselyova, S.; Lopez-Malo, M.; Canadell, D.; Roque, A.; Serra-Cardona, A.; Marques, M.; Vilaprinyo, E.; Alves, R.; Yenush, L.; Arino, J. Regulation of the Na⁺/K⁺-ATPase Ena1 Expression by Calcineurin/Crz1 under High pH Stress: A Quantitative Study. *PLoS One* **2016**, *11*, doi:10.1371/journal.pone.0158424.
110. Thewes, S. Calcineurin-Crz1 signaling in lower eukaryotes. *Eukaryot. Cell* **2014**, *13*, 694-705, doi:10.1128/EC.00038-14.
111. Lamb, T.; Mitchell, A. The Transcription Factor Rim101p Governs Ion Tolerance and Cell Differentiation by Direct Repression of the Regulatory Genes *NRG1* and *SMP1* in *Saccharomyces cerevisiae*. *Mol. Cell. Biol.* **2003**, *23*, 677-686, doi:10.1128/MCB.23.2.677-686.2003.
112. Ruiz, A.; Yenush, L.; Arino, J. Regulation of ENA1 Na⁺-ATPase Gene Expression by the Ppz1 Protein Phosphatase Is Mediated by the Calcineurin Pathway. *Eukaryot. Cell* **2003**, *2*, 937-948, doi:10.1128/EC.2.5.937-948.2003.
113. Proft, M.; Serrano, R. Repressors and Upstream Repressing Sequences of the Stress-Regulated *ENA1* Gene in *Saccharomyces cerevisiae*: bZIP Protein Sko1p Confers HOG-Dependent Osmotic Regulation. *Mol. Cell. Biol.* **1999**, *19*, 537-546, doi:10.1128/mcb.19.1.537.
114. Crespo, J.; Daicho, K.; Ushimaru, T.; Hall, M. The GATA Transcription Factors GLN3 and GAT1 Link TOR to Salt Stress in *Saccharomyces cerevisiae*. *J. Biol. Chem.* **2001**, *276*, 34441-34444, doi:10.1074/jbc.M103601200.
115. Manville, W.; Corran, A.; Lewis, A. TOK1 Potassium Channels in Phytopathogenic Fungi. *Biophys. J.* **2015**, *108*, doi:10.1016/j.bpj.2014.11.3201.
116. Loukin, S.; Saimi, Y. K(+)-dependent composite gating of the yeast K(+) channel, Tok1. *Biophys. J.* **1999**, *77*, 3060-3070, doi:10.1016/S0006-3495(99)77137-7.
117. Fairman, C.; Zhou, X.; Kung, C. Potassium uptake through the TOK1 K⁺ channel in the budding yeast. *J. Membr. Biol.* **1999**, *168*, 149-157, doi:10.1007/s002329900505.
118. Loukin, S.; Saimi, Y. Carboxyl tail prevents yeast K(+) channel closure: proposal of an integrated model of TOK1 gating. *Biophys. J.* **2002**, *82*, 781-792, doi:10.1016/S0006-3495(02)75440-4.
119. Meena, R.; Thakur, S.; Chakrabati, A. Regulation of *Saccharomyces cerevisiae* Plasma membrane H(+)-ATPase (Pma1) by Dextrose and Hsp30 during Exposure to Thermal Stress. *Indian J. Microbiol.* **2011**, *51*, 153-158, doi:10.1007/s12088-011-0137-y.
120. Kuhlbrandt, W.; Zeelen, J.; Dietrich, J. Structure, mechanism, and regulation of the *Neurospora* plasma membrane H⁺-ATPase. *Science* **2002**, *297*, 1692-1696, doi:10.1126/science.1072574.

121. Supply, P.; Wach, A.; Goffeau, A. Enzymatic properties of the Pma2 plasma membrane-bound H(+)-ATPase of *Saccharomyces cerevisiae*. *J. Biol. Chem.* **1993**, *268*, 19753-19759, doi:10.1016/S0021-9258(19)36578-0.
122. Bianchi, F.; van't Klooster, J.; Ruiz, S.; Poolman, B. Regulation of Amino Acid Transport in *Saccharomyces cerevisiae*. *Microbiol. Mol. Biol. Rev.* **2019**, *83*, doi:10.1128/MMBR.00024-19.
123. Ghillebert, R.; Swinnen, E.; De Snijder, P.; Smets, B.; Winderickx, J. Differential roles for the low-affinity phosphate transporters Pho87 and Pho90 in *Saccharomyces cerevisiae*. *Biochem. J.* **2011**, *434*, doi:10.1042/BJ20101118.
124. Goossens, A.; de la Fuente, N.; Forment, J.; Serrano, R.; Portillo, F. Regulation of Yeast H⁺-ATPase by Protein Kinases Belonging to a Family Dedicated to Activation of Plasma Membrane Transporters. *Mol. Cell. Biol.* **2000**, *20*, 7654-7661, doi:10.1128/mcb.20.20.7654-7661.2000.
125. Lecchi, S.; Allen, K.; Pardo, J.; Mason, A.; Slayman, C. Conformational changes of yeast plasma membrane H(+)-ATPase during activation by glucose: role of threonine-912 in the carboxy-terminal tail. *Biochemistry* **2005**, *44*, 16624-16632, doi:10.1021/bi051555f.
126. Mazon, M.; Eraso, P.; Portillo, F. Specific phosphoantibodies reveal two phosphorylation sites in yeast Pma1 in response to glucose. *FEMS Yeast. Res.* **2015**, *15*, doi:10.1093/femsyr/fov030.
127. Zhao, P.; Zhao, C.; Chen, D.; Yun, C.; Li, H.; Bai, L. Structure and Activation Mechanism of the Hexameric Plasma Membrane H⁺-ATPase. *Nature Comm.* **2021**, *12*, doi:10.1038/s41467-021-26782-y.
128. Kane, P. The long physiological reach of the yeast vacuolar H⁺-ATPase. *J. Bioenerg. Biomembr.* **2007**, *39*, 415-421, doi:10.1007/s10863-007-9112-z.
129. Kane, P.; Smardon, A. Assembly and regulation of the yeast vacuolar H⁺-ATPase. *J. Bioenerg. Biomembr.* **2003**, *35*, 313-321, doi:10.1023/a:1025724814656.
130. Parra, K.; Kane, P. Reversible association between the V₁ and V₀ domains of yeast vacuolar H⁺-ATPase is an unconventional glucose-induced effect. *Mol. Cell. Biol.* **1998**, *18*, 7064-7074, doi:10.1128/MCB.18.12.7064.
131. Hecht, K.; O'Donnell, A.; Brodsky, J. The proteolytic landscape of the yeast vacuole. *Cell Logist.* **2014**, *4*, doi:10.4161/cl.28023.
132. Madeira, F.; Tinti, M.; Murugesan, G.; Berrett, E.; Stafford, M.; Toth, R.; Cole, C.; MacKintosh, C.; Barton, G. 14-3-3-Pred: Improved Methods to Predict 14-3-3-binding Phosphopeptides. *Bioinformatics* **2015**, *31*, 2276-2283, doi:10.1093/bioinformatics/btv133.
133. Emery, A.; Hardwick, B.; Crooks, A.; Mitech, N.; Watt, P.; Mithra, C.; Kumar, V.; Giridharan, S.; Sadasivam, G.; Mathivanan, S.; et al. Target identification for small-molecule discovery in the FOXO3a tumor-suppressor pathway using a biodiverse peptide library. *Cell Chem. Biol.* **2021**, *28*, 1602-1615, doi:10.1016/j.chembiol.2021.05.009.
134. van Heusden, G. 14-3-3 Proteins: Insights From Genome-wide Studies in Yeast. *Genomics* **2009**, *94*, 287-293, doi:10.1016/j.ygeno.2009.07.004.
135. De, S.; Marcikiewitz, J.; Vijayaraghavan, S.; Kline, D. Expression of 14-3-3 protein isoforms in mouse oocytes, eggs and ovarian follicular development. *BMC Res. Notes* **2012**, *5*, doi:10.1186/1756-0500-5-57.
136. Denison, F.; Paul, A.; Zupanska, A.; Ferl, R. 14-3-3 proteins in plant physiology. *Semin. Cell Dev. Biol.* **2011**, *22*, 720-727, doi:10.1016/j.semcdb.2011.08.006.
137. Dougherty, M.; Morrison, M. Unlocking the code of 14-3-3. *J. Cell Sci.* **2004**, *117*, 1875-1884, doi:10.1242/jcs.01171.
138. Fu, H.; Coburn, J.; Collier, R. The eukaryotic host factor that activates exoenzyme S of *Pseudomonas aeruginosa* is a member of the 14-3-3 protein family. *Proc. Natl. Acad. Sci. USA* **1993**, *90*, 2320-2324, doi:10.1073/pnas.90.6.2320.
139. Bridges, D.; Moorhead, G. 14-3-3 Proteins: a Number of Functions For a Numbered Protein. *Sci. STKE* **2004**, doi:10.1126/stke.2962005re10.

140. Xiao, B.; Smerdon, S.; Jones, D.; Dodson, G.; Soneji, Y.; Aitken, A.; Gamblin, S. Structure of a 14-3-3 protein and implications for coordination of multiple signalling pathways. *Nature* **1995**, *376*, 188-191, doi:10.1038/376188a0.
141. Liu, D.; Bienkowska, J.; Petosa, C.; Collier, R.; Fu, H.; Liddington, R. Crystal structure of the zeta isoform of the 14-3-3 protein. *Nature* **1995**, *376*, 191-194, doi:10.1038/376191a0.
142. Obsil, T.; Obsilova, V. Structural basis of 14-3-3 protein functions. *Semin. Cell Dev. Biol.* **2011**, *22*, 663-672, doi:10.1016/j.semcdb.2011.09.001.
143. Brunet, A.; Bonni, A.; Zigmond, M.; Lin, M.; Juo, P.; Hu, L.; Anderson, M.; Arden, K.; Blenis, J.; Greenberg, M. Akt promotes cell survival by phosphorylating and inhibiting a Forkhead transcription factor. *Cell* **1999**, *96*, 857-868, doi:10.1016/s0092-8674(00)80595-4.
144. Obsil, T.; Ghirlando, R.; Anderson, D.; Hickamn, A.; Dyda, F. Two 14-3-3 binding motifs are required for stable association of Forkhead transcription factor FOXO4 with 14-3-3 proteins and inhibition of DNA binding. *Biochemistry* **2003**, *42*, 15264-15272, doi:10.1021/bi0352724.
145. Rajagopalan, S.; Jaulent, A.; Wells, M.; Veprintsev, D.; Fersht, A. 14-3-3 activation of DNA binding of p53 by enhancing its association into tetramers. *Nucleic Acids Res.* **2008**, *36*, 5983-5991, doi:10.1093/nar/gkn598.
146. Berruti, G. A novel rap1/B-Raf/14-3-3 theta protein complex is formed in vivo during the morphogenetic differentiation of postmeiotic male germ cells. *Exp. Cell. Res.* **2000**, *257*, 172-179, doi:10.1006/excr.2000.4877.
147. Shen, Y.; Godlewski, J.; Bronisz, A.; Zhu, J.; Comb, M.; Avruch, J.; Tzivion, G. Significance of 14-3-3 self-dimerization for phosphorylation-dependent target binding. *Mol. Biol. Cell.* **2003**, *14*, 4721-4733, doi:10.1091/mbc.e02-12-0821.
148. Stevers, L.; Sijbesma, E.; Botta, M.; MacKintosh, C.; Obsil, T.; Landrieu, I.; Cau, Y.; Wilson, A.; Karawajczyk, A.; Eickhoff, J.; et al. Modulators of 14-3-3 Protein-Protein Interactions. *J. Med. Chem.* **2018**, *61*, 3755-3778, doi:10.1021/acs.jmedchem.7b00574.
149. Heverin, M.; Brennan, G.; Koehler, C.; Treumann, A.; Henshall, D. Proteomic analysis of 14-3-3 zeta binding proteins in the mouse hippocampus. *Int. J. Physiol. Pathophysiol. Pharmacol.* **2012**, *4*, 74-83.
150. Mugabo, Y.; Sadeghi, M.; Fang, N.; Mayor, T.; Lim, G. Elucidation of the 14-3-3ζ interactome reveals critical roles of RNA-splicing factors during adipogenesis. *J. Biol. Chem.* **2018**, *293*, 6736-6750, doi:10.1074/jbc.M117.816272.
151. Kleppe, R.; Martinez, A.; Doskeland, S.; Haavik, J. The 14-3-3 proteins in regulation of cellular metabolism. *Semin. Cell Dev. Biol.* **2011**, *22*, 713-719, doi:10.1016/j.semcdb.2011.08.008.
152. van Hemert, M.; Steensma, H.; van Heusden, G. 14-3-3 proteins: key regulators of cell division, signalling and apoptosis. *Bioessays* **2001**, *23*, 936-946, doi:10.1002/bies.1134.
153. Toyo-oka, K.; Wachi, T.; Hunt, R.; Baraban, S.; Taya, S.; Ramshaw, H.; Kaibuchi, K.; Schwartz, Q.; Lopez, A.; Wynshaw-Boris, A. 14-3-3ε and ζ Regulate Neurogenesis and Differentiation of Neuronal Progenitor Cells in the Developing Brain. *J. Neurosci.* **2014**, *34*, 12168-12181, doi:10.1523/JNEUROSCI.2513-13.2014.
154. Clapp, C.; Portt, L.; Houry, C.; Sheibani, S.; Norman, G.; Ebner, P.; Eid, R.; Vali, H.; Mandato, C.; Madeo, F.; et al. 14-3-3 Protects against stress-induced apoptosis. *Cell. Death. Dis.* **2012**, *3*, doi:10.1038/cddis.2012.90.
155. Bruckmann, A.; Steensma, H.; de Mattos, M.; van Heusden, G. Regulation of Transcription by *Saccharomyces cerevisiae* 14-3-3 Proteins. *Biochem. J.* **2004**, *382*, 867-875, doi:10.1042/BJ20031885.
156. Kakiuchi, K.; Yamauchi, Y.; Taoka, M.; Iwago, M.; Fujita, T.; Ito, T.; Song, S.; Isobe, T.; Ichimura, T. Proteomic Analysis of in Vivo 14-3-3 Interactions in the Yeast *Saccharomyces cerevisiae*. *Biochemistry* **2007**, *46*, 7781-7792, doi:10.1021/bi700501t.
157. van Heusden, G.; Steensma, H. Yeast 14-3-3 Proteins. *Yeast* **2006**, *23*, 159-171, doi:10.1002/yea.1338.
158. Lane, M.; Morrissey, J. *Kluyveromyces marxianus*: A yeast emerging from its sister's shadow. *Fungal Biology Reviews* **2010**, *24*, 17-26, doi:10.1016/j.fbr.2010.01.001.

159. Ortiz-Merino, R.; Varela, J.; Coughlan, A.; Hoshida, H.; da Silveira, W.; Wilde, C.; Kuijpers, N.; Geertman, J.; Wolfe, K.; Morrissey, J. Ploidy Variation in *Kluyveromyces marxianus* Separates Dairy and Non-dairy Isolates. *Front. Genet.* **2018**, *9*, doi:10.3389/fgene.2018.00094.
160. Rocha, S.; Abrahao-Neto, J.; Gombert, A. Physiological diversity within the *Kluyveromyces marxianus* species. *Antonie Van Leeuwenhoek.* **2011**, *100*, 619-630, doi:10.1007/s10482-011-9617-7.
161. Lertwattanasakul, N.; Kosaka, T.; Hosoyama, A.; Suzuki, Y.; Rodrussamee, N.; Matsutani, M.; Fujimoto, N.; Tsuchikane, K.; Limtong, S.; Fujita, N.; et al. Genetic basis of the highly efficient yeast *Kluyveromyces marxianus*: complete genome sequence and transcriptome analyses. *Biotechnol. Biofuels* **2015**, *8*, doi:10.1186/s13068-015-0227-x.
162. Sakihama, Y.; Hidese, R.; Hasunuma, T.; Kondo, A. Increased flux in acetyl-CoA synthetic pathway and TCA cycle of *Kluyveromyces marxianus* under respiratory conditions. *Sci. Rep.* **2019**, *9*, doi:10.1038/s41598-019-41863-1.
163. Groeneveld, P.; Stouthamer, A.; Westerhoff, H. Super life – how and why ‘cell selection’ leads to the fastest-growing eukaryote. *The FEBS J.* **2008**, *276*, 254-270, doi:10.1111/j.1742-4658.2008.06778.x.
164. Banat, I.; Nigam, P.; Marchant, R. Isolation of thermotolerant, fermentative yeasts growing at 52°C and producing ethanol at 45°C and 50°C. *World J. Microbiol. Biotechnol.* **1992**, *8*, 259-263, doi:10.1007/BF01201874.
165. Marcisauskas, S.; Ji, B.; Nielsen, J. Reconstruction and analysis of a *Kluyveromyces marxianus* genome-scale metabolic model. *BMC Bioinformatics* **2019**, *20*, doi:10.1186/s12859-019-3134-5.
166. Zhou, J.; Zhu, P.; Hu, X.; Lu, H.; Yu, Y. Improved secretory expression of lignocellulolytic enzymes in *Kluyveromyces marxianus* by promoter and signal sequence engineering. *Biotechnol. Biofuels* **2018**, *11*, doi:10.1186/s13068-018-1232-7.
167. Oda, Y.; Nakamura, K. Production of ethanol from the mixture of beet molasses and cheese whey by a 2-deoxyglucose-resistant mutant of *Kluyveromyces marxianus*. *FEMS Yeast Res.* **2009**, *9*, 742-748, doi:10.1111/j.1567-1364.2009.00519.x.
168. Mo, W.; Wang, M.; Zhan, R.; Yu, Y.; He, Y.; Lu, H. *Kluyveromyces marxianus* developing ethanol tolerance during adaptive evolution with significant improvements of multiple pathways. *Biotechnol. Biofuels* **2019**, *12*, doi:10.1186/s13068-019-1393-z.
169. da Silveira, F.; de Oliviera Soares, D.; Bang, K.; Balbino, T.; de Moura Ferreira, M.; Diniz, R.; de Lima, L.; Brandao, M.; Villas-Boas, S.; de Silveira, W. Assessment of ethanol tolerance of *Kluyveromyces marxianus* CCT 7735 selected by adaptive laboratory evolution. *Appl. Microbiol. Biotechnol.* **2020**, *104*, 7483-7494, doi:10.1007/s00253-020-10768-9.
170. Vasallo, M.; Puppo, M.; Palazolo, G.; Otero, M.; Beress, L.; Wagner, J. Cell wall proteins of *Kluyveromyces fragilis*: Surface and emulsifying properties. *LWT- Food Science and Technology* **2006**, *39*, 729-739, doi:10.1016/j.lwt.2005.06.003.
171. Morrissey, J.; Etschmann, M.; Schrader, J.; de Billerbeck, G. Cell factory applications of the yeast *Kluyveromyces marxianus* for the biotechnological production of natural flavour and fragrance molecules. *Yeast* **2015**, *32*, 3-16, doi:10.1002/yea.3054.
172. Meehan, C.; Banat, I.; McMullan, G.; Nigam, P.; Smyth, F.; Marchant, R. Decolorization of Remazol Black-B using a thermotolerant yeast, *Kluyveromyces marxianus* IMB3. *Environ. Int.* **2000**, *26*, 75-79, doi:10.1016/s0160-4120(00)00084-2.
173. Pal, R.; Teweri, S.; Rai, J. Metals sorption from aqueous solutions by *Kluyveromyces marxianus*: process optimization, equilibrium modeling and chemical characterization. *Biotechnol. J.* **2009**, *4*, 1471-1478.
174. Hang, D.; Woodams, E.; Hang, L. Utilization of corn silage juice by *Kluyveromyces marxianus*. *Biores. Techn.* **2003**, *86*, 305-307, doi:10.1016/S0960-8524(02)00170-0.
175. Kadar, Z.; Reczey, K.; Szengyel, Z. Simultaneous saccharification and fermentation (SSF) of industrial wastes for the production of ethanol. *Industrial Crops and Products* **2004**, *20*, 103-110, doi:10.1016/j.indcrop.2003.12.015.

176. Karim, A.; Gerliani, N.; Alder, M. *Kluyveromyces marxianus*: An emerging yeast cell factory for applications in food and biotechnology. *Int. J. Food Microbiol.* **2020**, *333*, doi:10.1016/j.ijfoodmicro.2020.108818.
177. Jeong, H.; Lee, D.; Kim, S.; Kim, H.; Lee, K.; Song, J.; Kim, B.; Sung, B.; Park, J.; Sohn, J.; et al. Genome Sequence of the Thermotolerant Yeast *Kluyveromyces marxianus* var. *marxianus* KCTC 17555. *Eukaryot. Cell* **2012**, *11*, 1584-1585, doi:10.1128/EC.00260-12.
178. Rajkumar, A.; Morrissey, J. Protocols for marker-free gene knock-out and knock-down in *Kluyveromyces marxianus* using CRISPR/Cas9. *FEMS Yeast Res.* **2022**, *22*, doi:10.1093/femsyr/foab067.
179. Rajkumar, A.; Varela, J.; Juergens, H.; Daran, J.; Morrissey, J. Biological Parts for *Kluyveromyces marxianus* Synthetic Biology. *Front. Bioeng. Biotechnol.* **2019**, *7*, doi:10.3389/fbioe.2019.00097.
180. Fu, H.; Luan, S. AtKUP1: A Dual-Affinity K⁺ Transporter from Arabidopsis. *Plant Cell.* **1998**, *10*, 63-73, doi:10.1105/tpc.10.1.63.
181. Sun, J.; Zheng, N. Molecular Mechanism Underlying the Plant NRT1.1 Dual-Affinity Nitrate Transporter. *Front. Physiol.* **2015**, *6*, doi:10.3389/fphys.2015.00386.
182. Reifengerger, E.; Boles, E.; Ciriacy, M. Kinetic characterization of individual hexose transporters of *Saccharomyces cerevisiae* and their relation to the triggering mechanisms of glucose repression. *Eur. J. Biochem.* **1997**, *245*, doi:10.1111/j.1432-1033.1997.00324.x.
183. Pacheco, A.; Donzella, L.; Hernandez-Lopez, M.; Almeida, M.; Prieto, J.; Randez-Gil, F.; Morrissey, J.; Sousa, M. Hexose transport in *Torulaspora delbrueckii*: identification of Igt1, a new dual-affinity transporter. *FEMS Yeast Res.* **2020**, *20*, doi:10.1093/femsyr/foaa004.
184. Donzella, L.; Varela, J.; Sousa, M.; Morrissey, J. Identification of novel pentose transporters in *Kluyveromyces marxianus* using a new screening platform. *FEMS Yeast Res.* **2021**, *21*, doi:10.1093/femsyr/foab026.
185. Liu, K.; Tsay, Y. Switching between the two action modes of the dual-affinity nitrate transporter CHL1 by phosphorylation. *EMBO J.* **2003**, *22*, 1005-1013, doi:10.1093/emboj/cdg118.
186. Parker, J.; Newstead, S. Molecular basis of nitrate uptake by the plant nitrate transporter NRT1.1. *Nature* **2014**, *507*, 68-72, doi:10.1038/nature13116.
187. Tsay, Y. How to switch affinity. *Nature.* **2014**, *507*, 44-45.
188. Capera, J.; Serrano-Novillo, C.; Navarro-Pérez, M.; Cassinelli, S.; Felipe, A. The Potassium Channel Odyssey: Mechanisms of Traffic and Membrane Arrangement. *Int. J. Mol. Sci.* **2019**, *20*, doi:10.3390/ijms20030734.
189. Martinez-Munoz, G.; Kane, P. Vacuolar and Plasma Membrane Proton Pumps Collaborate to Achieve Cytosolic pH Homeostasis in Yeast. *J. Biol. Chem.* **2008**, *283*, 20309-20319, doi:10.1074/jbc.M710470200.
190. Yun, R.; Anderson, A.; Hermans, J. Proline in alpha-helix: stability and conformation studied by dynamics simulation. *Proteins* **1991**, *10*, 219-228, doi:10.1002/prot.340100306.
191. Ashraf, K.; Josts, I.; Moshbahi, K.; Kelly, S.; Byron, O.; Smith, B.; Walker, D. The Potassium Binding Protein Kbp Is a Cytoplasmic Potassium Sensor. *Structure* **2016**, *24*, 741-749, doi:10.1016/j.str.2016.03.017.
192. Rubino, F.; Kumar, S.; Ruiz, N.; Walker, S.; Kahne, D. Membrane Potential Is Required for MurJ Function. *J. Am. Chem. Soc.* **2018**, *140*, 4481-4484, doi:10.1021/jacs.8b00942.
193. Zhang, X.; Hang, L. Interplay between the electrostatic membrane potential and conformational changes in membrane proteins. *Protein Sci.* **2019**, *28*, 502-512, doi:10.1002/pro.3563.
194. Herman, P.; Vecer, J.; Opekarova, M.; Vesela, P.; Janickova, I.; Zahumensky, J.; Malinsky, J. Depolarization affects the lateral microdomain structure of yeast plasma membrane. *FEBS J.* **2015**, *282*, 419-434, doi:10.1111/febs.13156.

195. Diskowski, M.; Mehdipour, A.; Wunnicke, D.; Mills, D.; Mikusevic, V.; Barland, N.; Hoffmann, J.; Morgner, N.; Steinhoff, H.; Hummer, G.; et al. Helical Jackknives Control the Gates of the Double-Pore K⁺ Uptake System KtrAB. *Elife* **2017**, *6*, doi:10.7554/eLife.24303.
196. Davidson, A. Mechanism of Coupling of Transport to Hydrolysis in Bacterial ATP-binding Cassette Transporters. *J. Bacteriol.* **2002**, *184*, 1225-1233, doi:10.1128/JB.184.5.1225-1233.2002.
197. Rezaei-Ghaleh, N.; Amininasab, M.; Kumar, S.; Walter, J.; Zweckstetter, M. Phosphorylation Modifies the Molecular Stability of β -amyloid Deposits. *Nat. Commun.* **2016**, *7*, doi:10.1038/ncomms11359.
198. Li, X.; Gerber, S.; Rudner, A.; Beausoleil, S.; Haas, W.; Villén, J.; Elias, J.; Gygi, S. Large-scale Phosphorylation Analysis of Alpha-factor-arrested *Saccharomyces cerevisiae*. *J. Proteome Res.* **2007**, *6*, 1190-1197, doi:10.1021/pr060559j.
199. Holt, L.; Tuch, B.; Vilén, J.; Johnson, A.; Gygi, S.; Morgan, D. Global Analysis of Cdk1 Substrate Phosphorylation Sites Provides Insights Into Evolution. *Science* **2009**, *325*, 1682-1686, doi:10.1126/science.1172867.
200. Swaney, D.; Beltrao, P.; Starita, L.; Guo, A.; Rush, J.; Fields, S.; Krogan, L.; Vilén, J. Global Analysis of Phosphorylation and Ubiquitylation Cross-talk in Protein Degradation. *Nat. Methods* **2013**, *10*, 676-682, doi:10.1038/nmeth.2519.
201. O'Kelly, I.; Butler, M.; Zilberberg, N.; Goldstein, S. Forward transport. 14-3-3 binding overcomes retention in endoplasmic reticulum by dibasic signals. *Cell* **2002**, *111*, 577-588, doi:10.1016/s0092-8674(02)01040-1.
202. Yuan, H.; Michelsen, K.; Schwappach, B. 14-3-3 Dimers Probe the Assembly Status of Multimeric Membrane Proteins. *Curr. Biol.* **2003**, *13*, 639-646, doi:10.1016/s0960-9822(03)00208-2.
203. Okamoto, Y.; Shikano, S. Phosphorylation-dependent C-terminal binding of 14-3-3 proteins promotes cell surface expression of HIV co-receptor GPR15. *J. Biol. Chem.* **2011**, *286*, 7171-7181, doi:10.1074/jbc.M110.199695.
204. Duby, G.; Poreba, W.; Piotrowiak, D.; Bobik, K.; Derua, R.; Waelkens, E.; Boutry, M. Activation of Plant Plasma Membrane H⁺-ATPase by 14-3-3 Proteins Is Negatively Controlled by Two Phosphorylation Sites Within the H⁺-ATPase C-terminal Region. *J. Biol. Chem.* **2009**, *284*, 4213-4221, doi:10.1074/jbc.M807311200.
205. Camoni, L.; Visconti, S.; Aducci, P.; Marra, M. From Plant Physiology to Pharmacology: Fusicocin Leaves the Leaves. *Planta* **2019**, *249*, 49-57, doi:10.1007/s00425-018-3051-2.
206. Granot, D.; Snyder, M. Glucose induces cAMP-independent growth-related changes in stationary-phase cells of *Saccharomyces cerevisiae*. *Proc. Natl. Acad. Sci. USA* **1991**, *88*, 5724-5728, doi:10.1073/pnas.88.13.5724.
207. de Alteriis, E.; Carteni, F.; Parascandola, P.; Serpa, J.; Mazzoleni, S. Revisiting the Crabtree/Warburg effect in a dynamic perspective: a fitness advantage against sugar-induced cell death. *Cell Cycle* **2018**, *17*, 688-701, doi:10.1080/15384101.2018.1442622.
208. Arino, J.; Ramos, J.; Sychrova, H. Monovalent Cation Transporters at the Plasma Membrane in Yeasts. *Yeast* **2019**, *36*, 177-193, doi:10.1002/yea.3355.